ISSN 1854-6250

APEM journal

# Advances in Production Engineering & Management

Volume 17 | Number 4 | December 2022

University of Maribor

Published by CPE
apem-journal.org

# Advances in Production Engineering & Management

## Identification Statement

APEM journal

ISSN 1854-6250 | Abbreviated key title: **Adv produc engineer manag** | Start year: 2006
ISSN 1855-6531 (on-line)

Published quarterly by **Chair of Production Engineering (CPE)**, **University of Maribor**
Smetanova ulica 17, SI – 2000 Maribor, Slovenia, European Union (EU)

Phone: 00386 2 2207522, Fax: 00386 2 2207990
Language of text: English

APEM homepage: apem-journal.org
University homepage: www.um.si

University of Maribor

## APEM Editorial



OPEN ACCESS

**Subsidizer:** The journal is subsidized by Slovenian Research Agency



*Advances in Production Engineering & Management* is indexed and abstracted in the **WEB OF SCIENCE** (maintained by **Clarivate Analytics**): **Science Citation Index Expanded**, **Journal Citation Reports** – Science Edition, **Current Contents** – Engineering, Computing and Technology • **Scopus** (maintained by **Elsevier**) • **Inspec** • **EBSCO**: Academic Search Alumni Edition, Academic Search Complete, Academic Search Elite, Academic Search Premier, Engineering Source, Sales & Marketing Source, TOC Premier • **ProQuest**: CSA Engineering Research Database – Cambridge Scientific Abstracts, Materials Business File, Materials Research Database, Mechanical & Transportation Engineering Abstracts, ProQuest SciTech Collection • **TEMA** (**DOMA**) • The journal is listed in **Ulrich's** Periodicals Directory and **Cabell's** Directory

University of Maribor
Chair of Production Engineering (CPE)

# Advances in Production Engineering & Management

Volume 17 | Number 4 | December 2022 | pp 397–516

## Contents



Journal homepage: apem-journal.org

ISSN 1854-6250 (print)
ISSN 1855-6531 (on-line)

Published by CPE, University of Maribor.

## Scope and topics

*Advances in Production Engineering & Management* (*APEM journal*) is an interdisciplinary refereed international academic journal published quarterly by the *Chair of Production Engineering* at the *University of Maribor*. The main goal of the *APEM journal* is to present original, high quality, theoretical and application-oriented research developments in all areas of production engineering and production management to a broad audience of academics and practitioners. In order to bridge the gap between theory and practice, applications based on advanced theory and case studies are particularly welcome. For theoretical papers, their originality and research contributions are the main factors in the evaluation process. General approaches, formalisms, algorithms or techniques should be illustrated with significant applications that demonstrate their applicability to real-world problems. Although the *APEM journal* main goal is to publish original research papers, review articles and professional papers are occasionally published.

Fields of interest include, but are not limited to:

Additive Manufacturing Processes
Advanced Production Technologies
Artificial Intelligence in Production
Assembly Systems
Automation
Big Data in Production
Block Chain in Manufacturing
Computer-Integrated Manufacturing
Cutting and Forming Processes
Decision Support Systems
Deep Learning in Manufacturing
Discrete Systems and Methodology
e-Manufacturing
Evolutionary Computation in Production
Fuzzy Systems
Human Factor Engineering, Ergonomics
Industrial Engineering
Industrial Processes
Industrial Robotics
Intelligent Manufacturing Systems
Joining Processes
Knowledge Management
Logistics in Production
Machine Learning in Production
Machine-to-Machine Economy
Machine Tools
Machining Systems
Manufacturing Systems
Materials Science, Multidisciplinary
Mechanical Engineering
Mechatronics
Metrology in Production
Modelling and Simulation
Numerical Techniques
Operations Research
Operations Planning, Scheduling and Control
Optimisation Techniques
Project Management
Quality Management
Risk and Uncertainty
Self-Organizing Systems
Smart Manufacturing
Statistical Methods
Supply Chain Management
Virtual Reality in Production

APEM journal
**Advances in Production Engineering & Management** **ISSN 1854-6250**
Volume 17 | Number 4 | December 2022 | pp 401–412 Journal home: apem-journal.org
https://doi.org/10.14743/apem2022.4.444 Original scientific paper

# Verification of intelligent scheduling based on deep reinforcement learning for distributed workshops via discrete event simulation

**Yang, S.L.[a], Wang, J.Y.[b,c,*], Xin, L.M.[d], Xu, Z.G.[b,c,*]**

[a]School of Mechanical Engineering, University of Shanghai for Science and Technology, Shanghai, P.R. China
[b]Shenyang Institute of Automation, Chinese Academy of Sciences, Shenyang, P.R. China
[c]Institutes for Robotics and Intelligent Manufacturing, Chinese Academy of Sciences, Shenyang, P.R. China
[d]School of Computer Engineering and Science, Shanghai University, Shanghai, P.R. China

**A B S T R A C T**

Production scheduling, which directly influences the completion time and throughput of workshops, has received extensive research. However, due to the high cost of real-world production verification, most literature did not verify the optimized scheduling scheme in real-world workshops. This paper studied the verification of scheduling schemes and environments, using a discrete event simulation (DES) platform. The aim of this study is to provide an efficient way to verify the correctness of scheduling environments established by programming languages and scheduling results obtained by intelligent algorithms. The system architecture of scheduling verification based on DES is established. The modelling approach via DES is proposed by designing parametric workshop generation, flexible production control, and real-time data processing. The popular distributed permutation flowshop scheduling problem is selected as a case study, where the optimal scheduling scheme obtained by a deep reinforcement learning algorithm is fed into the production simulation model in Plant Simulation software. The experiment results show that the proposed scheduling verification approach can validate the scheduling scheme and environment effectively. The utilization and Gantt charts clearly show the performance of scheduling schemes. This work can help to verify the scheduling schemes and programmed scheduling environment efficiently without costly real-world validation.

**A R T I C L E I N F O**

*Keywords:*
Production scheduling;
Distributed flowshop scheduling;
Discrete event simulation (DES);
Deep reinforcement learning;
Production simulation;
Modelling;
Scheduling verification;
Plant Simulation software

**Corresponding author:*
jywang@sia.cn
(Wang, J.Y.)
zgxu@sia.cn
(Xu, Z.G.)

*Article history:*
Received 14 November 2022
Revised 12 December 2022
Accepted 15 December 2022



## 1. Introduction

Production scheduling is an important problem for real-world manufacturers. Effective scheduling schemes can help to reduce production costs, decrease completion time, and increase throughput. For several decades, production scheduling has received extensive research interest. For example, only for the permutation flowshop scheduling problem, more than 100 kinds of heuristic and meta-heuristic algorithms have been proposed according to the reviews of Fernandez-Viagas *et al*. [1].

Under the globalized economy, companies tend to establish production bases in different regions to fulfill the production requirement of customers distributed in different areas. Under distributed manufacturing, the distributed permutation flowshop scheduling problem (DPFSP) was proposed by Naderi, Ruiz [2]. In the DPFSP, a set of factories are distributed in different regions. A set of jobs can be processed in one of the factories. The optimization problem is to minimize the total completion time of all jobs by properly assigning jobs to factories and scheduling jobs in each factory. The DPFSP has been solved by several kinds of intelligent algorithms, such as iterated greedy algorithm [3], artificial bee colony algorithm [4], cooperative memetic algorithm [5], etc. Some realistic characteristics have been considered in the DPFSP, such as sequence-dependent setup times[6, 7], blocking constraint [8, 9], no-wait constraint [10], no-idle constraint [11], hybrid flowshop [12], batch delivery [13], etc.

Most product scheduling is optimized by intelligent algorithms. Usually, intelligent algorithms are written in programming languages, such as C++, Java, MATLAB, Python, etc. At the same time, the production environment for simulating and optimizing the scheduling scheme is also programmed using programming languages. Although the scheduling scheme can be optimized through the programmed scheduling simulation environment, the correctness of the scheduling simulation environment and scheduling scheme remains a problem. Since the verification for an optimized scheduling scheme is crucial for implementation in real-world factories, the verification for the simulation environment and scheduling schemes should be performed.

In current literature, only very few studies applied proposed scheduling models and algorithms to real production workshops, such as applied to the manufacturing execution system (MES) of a real factory. A few studies only used real-world data as production instances. However, most literature did not apply the scheduling algorithms and methods to real-world production cases. For the scheduling application in real-world production, Zhou *et al.* [14] studied the multi-objective flexible job shop scheduling problem using multi-agent-based hyper-heuristics and applied the proposed methods and algorithms to an aero-engine blade manufacturing plant. For the usage of real-world data, Jiang *et al.* [15] studied a real case scheduling problem for aerospace industry components in a flexible job shop. Li *et al.* [16] solved the welding shop scheduling problem using a discrete artificial bee colony algorithm and applied the algorithm in a real-world girder welding shop. Yankai *et al.* [17] studied the hybrid flowshop scheduling problem, in which numerical experiments are carried out based on real-world cases in a hot-rolling workshop. Wang *et al.* [18] studied the energy-aware welding shop scheduling problem using a decomposition-based multi-objective evolutionary algorithm and applied the proposed algorithm to a real-world case. Schumacher, Buchholz [19] studied the hybrid flow shop scheduling problem under uncertainty and applied the proposed methods to a real-world production case. Ojstersek *et al.* [20] studied the multi-objective scheduling problem of flexible job shops using a real-world manufacturing dataset.

Although some literature used real-world data for problem-solving, most scheduling literature did not verify the correctness of scheduling simulation and scheduling results. The reasons may be as follows. Firstly, the implementation of production scheduling in a real-world workshop costs too much with a lot of production resources required. In addition, some researchers do not have suitable industrial cooperation for validation or lack a production line in the laboratory for proper production validation. With the development of simulation software, discrete event simulation (DES) servers as an efficient tool for production optimization and validation.

The Plant Simulation software is one of the widely used production simulation platforms. Some researchers used the Plant Simulation to optimize production processes and validate the production scenarios. Yang *et al.* [21] proposed a modelling method for workshop modelling in Plant Simulation and optimized the production configurations of an assembly shop. Xu *et al.* [22] studied the optimization problem of multi-stage production scheduling. Wang *et al.* [23] studied the reliability allocation method for a production system using Plant Simulation. Pekarcikova *et al.* [24] studied the simulation testing of the E-Kanban to improve the efficiency of logistics processes. Yang *et al.* [25] optimized the assembly transport optimization problem in a reconfigurable flow shop. Pekarcikova *et al.* [26] studied the bottleneck problem in the logistics flow of a manufacturing company using Plant Simulation software. Li *et al.* [27] dealt with the bottleneck identification and alleviation in a blocked serial production line via Plant Simulation. Jurczyk-Bunkowska [28] studied the tactical manufacturing capacity planning of a medium-sized production enterprise by Plant Simulation. Gregor *et al*. [29] verified the routes of an automated guided vehicle using Plant Simulation. Li *et al*. [30] studied resource allocation in a production logistics system using Plant Simulation software. Gola *et al*. [31] used the Plant Simulation software to identify the bottlenecks in a reconfigurable manufacturing system.

In addition to optimizing and verifying the production process, Plant Simulation software has also been used to optimize some scheduling problems by using the built-in intelligent algorithm packages. Xu *et al*. [22] optimized a multi-stage production scheduling problem of an automated production system by using Plant Simulation software. Istokovic *et al*. [32] determined the order and size of production batches in a flow shop using the genetic algorithm optimization tool of Plant Simulation. Ferro *et al*. [33] used Plant Simulation to optimize the production planning of the textile industry.

From the above literature review, we can know that the verification of the scheduling scheme has not received adequate research, and Plant Simulation software has been used to optimize and verify some production processes. Verifying the scheduling scheme and programmed environment via the Plant Simulation platform is an efficient way. However, few studies investigated the verification of scheduling schemes and programmed production environment with the help of Plant Simulation.

This paper studied the verification of scheduling schemes and environments based on a discrete event simulation platform—Plant Simulation software. The distributed permutation flowshop scheduling problem is verified in Plant Simulation. The aim of this study is to provide efficient and costless verifications for the programmed scheduling environment and obtained scheduling schemes, before applying those scheduling schemes in real-world workshops. The overall system architecture of verifying scheduling schemes via Plant Simulation platform is established. The distributed permutation flowshops are established in Plant Simulation platform. The simulation results in Plant Simulation validate the correctness of the programmed scheduling environment programmed in Python and the scheduling results obtained by algorithms.

Particularly, the main contributions of this paper are as follows:

- The system architecture of scheduling verification based on scheduling optimization and Plant Simulation is established. The scheduling scheme is optimized by intelligent algorithms programmed in Python language. Then, the optimized scheduling scheme is simulated and verified in the established production model in Plant Simulation platform.
- The modelling approach for production workshops via Plant Simulation platform is proposed. The production simulation model is established by designing parametric modelling of workshops, flexible production control, and real-time data processing.
- The whole verification process is validated by a case study on the distributed permutation flowshop scheduling problem. The videos of scheduling optimization and production simulation are provided.

The rest of the paper is listed as follows. Section 2 illustrates the system architecture of the scheduling verification approach. Section 3 establishes the production workshops using Plant Simulation platform. Section 4 verifies the scheduling environment and scheme using a case study. Section 5 concludes the paper and provides suggestions for future research.

## 2. System architecture of the scheduling verification approach

The scheduling validation approach contains intelligent scheduling optimization via intelligent algorithms and production simulation via Plant Simulation. The intelligent scheduling optimization generates the scheduling scheme and results. Based on the scheduling scheme, the production model built in Plant Simulation platform executes the production process. The results obtained from Plant Simulation and those obtained from the intelligent scheduling algorithms are compared to verify whether the programmed scheduling environment and scheduling algorithms are correct. The system architecture of the scheduling verification approach is shown in Fig. 1.

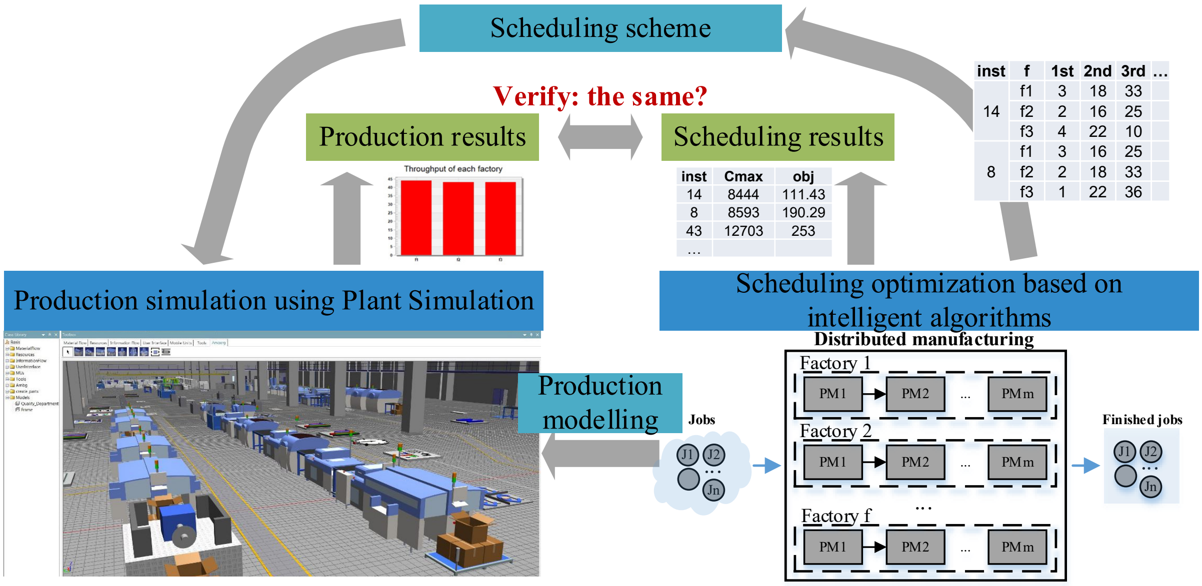


**Fig. 1** The system architecture of the proposed scheduling validation approach based on intelligent scheduling optimization and Plant Simulation

## 2.1 Scheduling optimization based on intelligent algorithms

Most production scheduling in the literature is optimized using intelligent algorithms. Before optimizing the scheduling scheme, the scheduling simulation environment should be programmed. The scheduling simulation environment can process jobs and calculate the objective of candidate schedule schemes. Some popular languages for programming the environment are C++, C#, MATLAB, Java, Python, etc. However, the real-time production interface reflecting the real-time production process is seldom programmed due to the coding complexity. Thus, it is difficult to check the correctness of the production simulation process for the programmed production environment.

The optimal scheduling scheme is obtained by performing the optimization process using intelligent algorithms. Due to extensive research, many kinds of algorithms have been proposed to solve the scheduling problems, such as heuristics, meta-heuristics [3], deep reinforcement learning algorithms [34], etc.

After the optimization process, the optimal scheduling schemes, including the job sequence for each factory, and the beginning and end processing time, are obtained. Besides, the scheduling results, including the completion time of all factories and the objective value for the scheduling scheme, are returned.

## 2.2 Production modelling and simulation execution

The production simulation model is established in Plant Simulation platform according to the production resources and processes of the studied scheduling problem. Plant Simulation software can build the production model efficiently by constructing machines, flow lines, jobs, buffers, and source jobs. The production control is programmed by SimTalk language in Plant Simulation platform. The scheduling scheme obtained by intelligent algorithms is fed to the production model in Plant Simulation to get the correct scheduling results.

## 2.3 Verification by comparing production and scheduling results

After the exact execution of the job sequences in each factory, the production results for the selected scheduling scheme are obtained from Plant Simulation platform. Then, the production results are compared with the scheduling results obtained from the intelligent algorithms. For each production scheme, the maximum completion time $C_{max}$ and objective value *obj* are compared between the production and scheduling results.

## 3. Modelling of production workshops via Plant Simulation

The production model can be established efficiently via Plant Simulation platform, which contains powerful production modelling tools. The main components of a production simulation model are the production resources, production control methods, production data, and visualization tools, as shown in Fig. 2. The production resources contain machines, buffers, production lines, etc. The production control is realized by control methods. The production data contains some necessary production and real-time data, such as processing times, arrival time, due date, etc. The visualization tools provide various charts for the real-time production status and workshop performance.

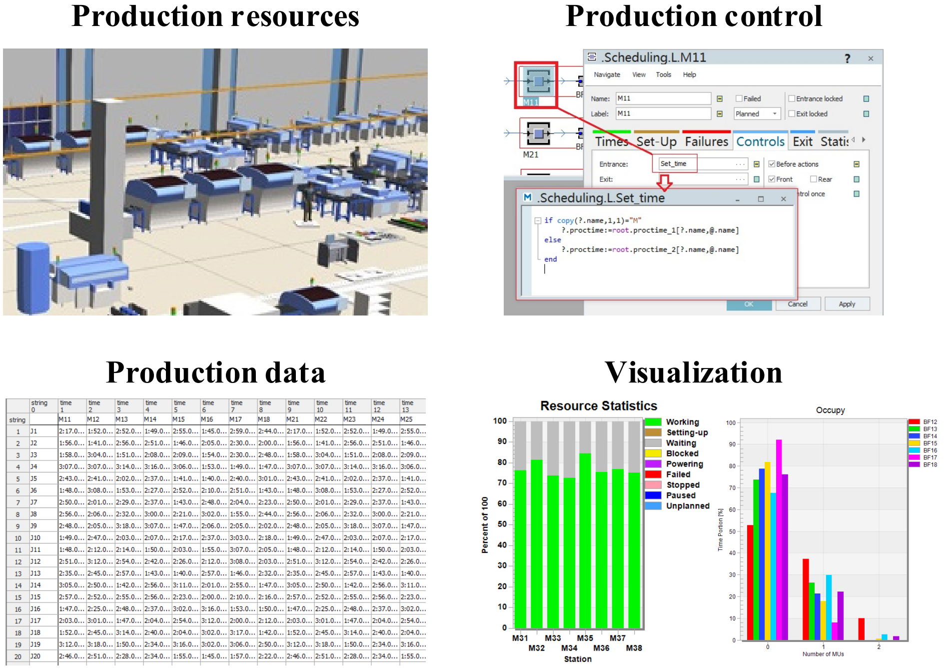


**Fig. 2** The main compensates of a production model in Plant Simulation platform

### 3.1 Parametric modelling of workshops

Workshops are established through parametric modelling. Each workshop contains job storage, buffer, machines, and transfer line between machines. To increase the efficiency of modelling, all of the above production resources are generated by the control method *Start* as shown in Fig. 3. The code for generating machines and buffers is shown in algorithm 1. The production process is modelled exactly as those used in the scheduling algorithms. Thus, the unlimited buffer size is adopted between machines, the transfer time is not considered.

Algorithm 1. Procedure of parametric modelling for generating a workshop using the SimTalk language

```
for j:=1 to n
    for i:=1 to m loop
        if i>1 then
            Name:=Sprint("BF",j,i)
            Obj2:=.Materialflow.Buffer.createObject(current, 40+i*100, 100+(26+60*n)/n*(j+1), Name)
            Obj2.ZoomX:=0.5, Obj2.ZoomY:=0.5, Obj2.Proctime:=0, Obj2.Capacity:=-1
        .Materialflow.Connector.connect(Obj, Obj2), Obj:=Obj2
        end
        Name:=Sprint("M",j,i)
        Obj2:=.Materialflow.Singleproc.createObject(current, 80+i*100,100+(26+60*n)/np*(j+1), Name)
        Obj2.Label := sprint("M",j,i), OBj2.EntranceCtrl:="Set_time"
        obj2.entrancectrlbeforeactions:=true
        if i>1 then
            .Materialflow.Connector.connect(Obj, Obj2)
        end
        Obj:=Obj2
    next
next
```

### 3.2 Modelling of production control

The production control ensures that workshops produce jobs according to the correct production processes and job sequences. Jobs are released from the source to the workshop when the arrival time is reached. The processing time is set for each machine when a new job arrived at this machine. When a job is finished in a machine, the job is transferred to the buffer of the next machine, and the next job is transferred from the previous buffer. When a job is finished in all machines of a workshop, the job is transferred to the *Drain*.

### 3.3 Modelling of production data

In addition to the production process, the production data is also fundamental to correctly simulate the production schedule. As shown in Fig. 3, the arrival time and due date of jobs are stored in the table file *Attri*. Jobs are created by the *jobs_create* method based on the arrival time of jobs. The table file *PT* stores the processing times of jobs on machines. The processing time is extracted by the method *Set_time* and set for the corresponding machines.

### 3.4 Statistical analysis and visualization

One of the advantages of the Plant Simulation platform is its powerful statistical and visualization function. As shown in Fig. 3, in the production model, the variables $C_{max}$ and *obj* denote the maximum completion time of workshops and the objective value of the current scheduling scheme, respectively. The Gantt chart shows the job sequence and processing durations on machines. The utilization chart reflects the production performance under the current scheduling scheme and production processes. In addition, the occupation of a buffer is provided to show how many jobs exist in buffers before a machine. Since buffer capability is supposed to be infinite, the exact number of existing buffer jobs can help to set buffer sizes in a real production environment.

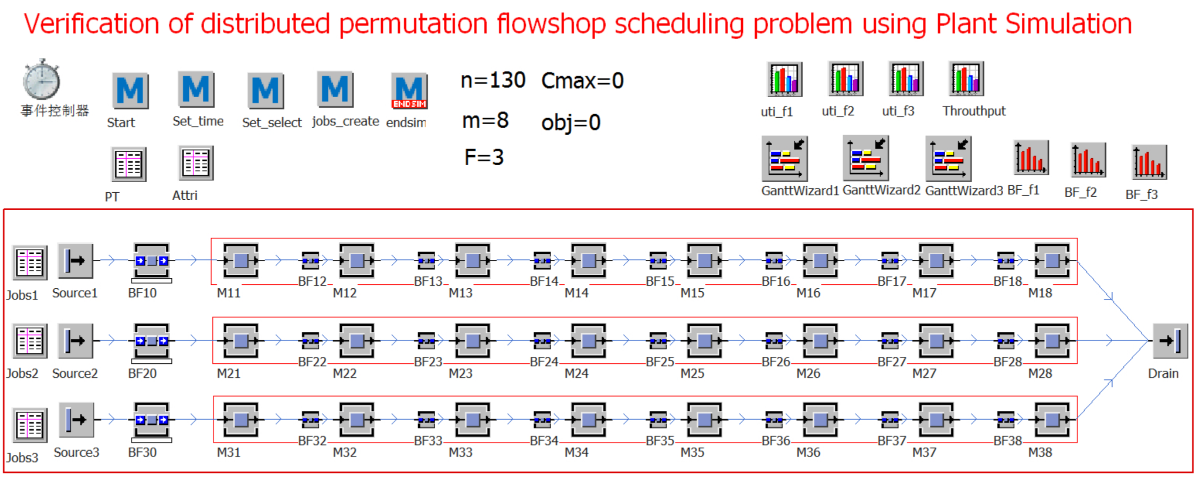


**Fig. 3** The production simulation model for the distributed permutation flowshop scheduling problem

## 4. Verification experiments: A case study

This section verifies the scheduling results obtained by the trained deep reinforcement learning (DRL) algorithm in Plant Simulation software using the modelling and validation approach proposed above. The scheduling results, including the scheduling scheme, total completion time, and objective value, are generated by a DRL algorithm—advanced actor-critic (A2C). Then, the scheduling scheme is executed exactly in the production model in Plant Simulation platform. The production simulation results verified that the scheduling results obtained by the programming environment are correct. In addition, the statistical analysis and visualization were provided via Plant Simulation platform.

### 4.1 Scheduling scheme obtained by deep reinforcement learning

The distributed permutation flowshop scheduling problem, which has attracted increasing research interest in recent several years, is selected for verification. A production case with 130 jobs, 8 machines, and 3 factories is selected as the case instance by referring to the production characteristics shown in the literature [3]. The scheduling scheme for this production instance is generated by a deep reinforcement learning algorithm A2C. After the dynamic scheduling, the scheduling results of the DRL version are obtained.

Table 1 provides the production data of the selected production instance. Since the production instance has as many as 130 jobs, Table 1 only provides the data of the first 10 jobs. As shown in Table 1, for each job $j$, the arrival time $AT_j$, due date $d_j$, unit tardiness cost $\alpha_j$, and processing times on all of the 8 machines $p_{M1,j}$-$p_{M8,j}$ are provided.

**Table 1** Production data of the studied production instance (only the data of the first 10 jobs are provided)

| $j$ | $AT_j$ | $d_j$ | $\alpha_j$ | $p_{M1,j}$ | $p_{M2,j}$ | $p_{M3,j}$ | $p_{M4,j}$ | $p_{M5,j}$ | $p_{M6,j}$ | $p_{M7,j}$ | $p_{M8,j}$ |
|---|---|---|---|---|---|---|---|---|---|---|---|
| 1 | 0.00 | 2676.00 | 0.6 | 137 | 112 | 172 | 109 | 175 | 105 | 179 | 164 |
| 2 | 0.00 | 1850.00 | 1.2 | 116 | 101 | 176 | 171 | 106 | 125 | 150 | 120 |
| 3 | 0.00 | 2711.00 | 1.3 | 118 | 184 | 111 | 128 | 129 | 114 | 150 | 168 |
| 4 | 0.00 | 2520.00 | 0.9 | 187 | 187 | 194 | 196 | 186 | 113 | 109 | 107 |
| 5 | 5.40 | 4383.40 | 1.0 | 163 | 161 | 122 | 157 | 101 | 100 | 160 | 181 |
| 6 | 18.14 | 4528.14 | 1.2 | 108 | 188 | 113 | 147 | 172 | 130 | 171 | 103 |
| 7 | 18.14 | 2593.14 | 0.6 | 170 | 121 | 149 | 157 | 103 | 168 | 124 | 143 |
| 8 | 21.74 | 1780.74 | 1.6 | 176 | 126 | 152 | 180 | 141 | 182 | 115 | 164 |
| 9 | 23.33 | 1767.33 | 0.1 | 168 | 125 | 198 | 187 | 107 | 126 | 125 | 122 |
| 10 | 24.29 | 4436.29 | 1.7 | 109 | 167 | 123 | 127 | 137 | 157 | 183 | 138 |

The scheduling scheme and results are obtained using a deep reinforcement learning algorithm by inputting the production data. The scheduling optimization interface in the Python programming environment for the studied case is shown in Fig. 4.

The video of using deep reinforcement learning to solve the studied scheduling problem is provided online. The specific solving procedures are as follows.

- Build the production environment and variable matrix in the Python environment;
- Load the production data of the studied scheduling problem;
- Load the trained model of the A2C algorithm;
- Use the loaded A2C model to make scheduling decisions at each rescheduling point;
- Record the processed jobs sequences of each factory, and calculate the objective value;
- If all jobs are finished in the system, export the total completion time of the system, the objective value of the scheduling plan, and the job sequence of each factory.

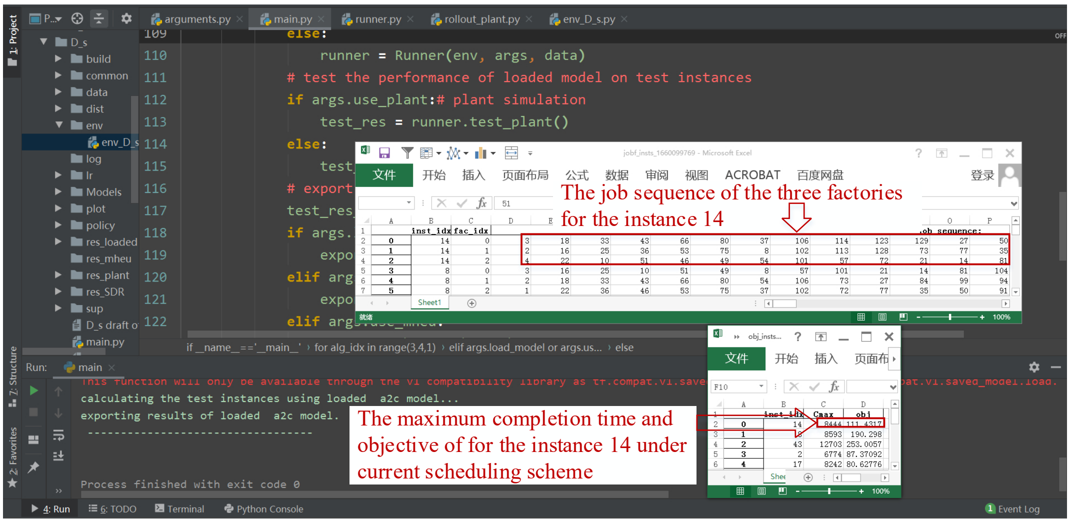


**Fig. 4** The scheduling optimization interface in the Python programming environment.
(The video of obtaining the optimal scheduling scheme by loading the DRL model is available at *https://osf.io/qxze5?view_only=e10ee0e3cec44b85ba2f569cd26071f2*)

**Table 2** The scheduling results obtained from the DRL algorithm (only the job sequence of the first 10 jobs are presented)

| Factory | Completion time | Objective value | Job sequence | | | | | | | | | |
|---|---|---|---|---|---|---|---|---|---|---|---|---|
| 1 | | | 3 | 18 | 33 | 43 | 66 | 80 | 37 | 106 | 114 | 123 |
| 2 | 8444 | 111.43 | 2 | 16 | 25 | 36 | 53 | 75 | 8 | 102 | 113 | 128 |
| 3 | | | 4 | 22 | 10 | 51 | 46 | 49 | 54 | 101 | 57 | 72 |

After the optimization, the scheduling results are provided in Table 2. As shown in Table 2, the total completion time of the system is 8444, the objective value is 111.43. Besides, the job sequence of the three factories is provided. For factory 1, job j3, j18, j33,..., is processed successively. Only the first ten processed jobs of each factory are presented in Table 2.

### 4.2 Verification using Plant Simulation

The scheduling scheme resulting from the deep reinforcement learning is executed exactly in the production simulation model built in Plant Simulation platform. After production simulation, the scheduling results obtained from Plant Simulation are compared with the results obtained from the Python environment.

Fig. 5 shows the production simulation results in Plant Simulation platform. As shown in Fig. 5, the number of jobs that enter and exit the system is 130, indicating all jobs are processed in the system successfully. The completion time of the system is 8444, and the objective of the scheduling plan is 111.43. The scheduling results obtained in the Plant Simulation platform are the same as those in the Python environment. This verifies the correctness of the simulation environment programmed in Python and the correctness of the scheduling scheme calculation. In addition, Fig. 6-8 show the Gantt chart of the three factories. From Figs. 6-8, we can see that the jobs are processed closely in each factory.

Since production validations in a real production environment cost too much, most scheduling literature did not validate the scheduling results. However, the correctness of the programmed scheduling environment should be checked before performing further scheduling optimizations, and the correctness of the scheduling scheme should be verified before applying the scheduling scheme in real workshops. Our proposed scheduling verification approach provides the necessary support for verifying the scheduling environment and plans. Besides, more statistical analysis and clear visualization can be performed via Plant Simulation platform.

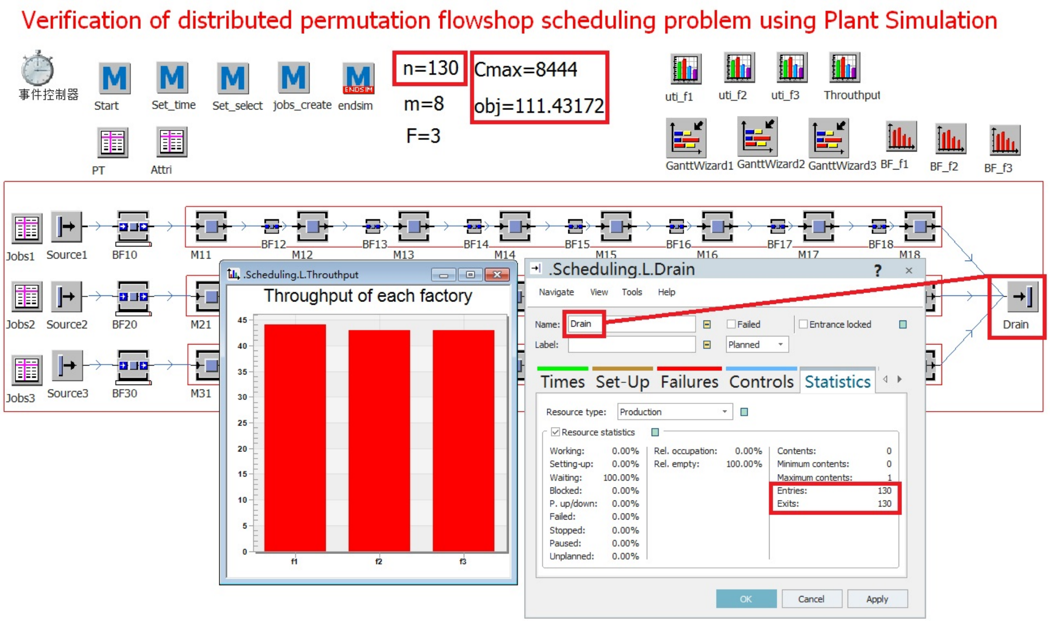


**Fig. 5** Production simulation results in Plant Simulation platform (The video of production simulation via Plant Simulation platform is available at *https://osf.io/dzc3u?view_only=e10ee0e3cec44b85ba2f569cd26071f2*)

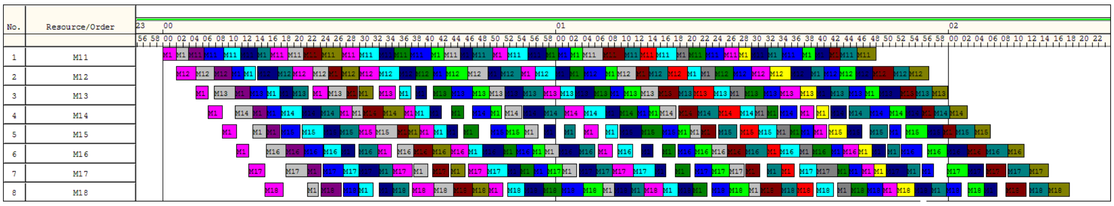

**Fig. 6** The Gantt chart of factory 1 for the studied scheduling problem

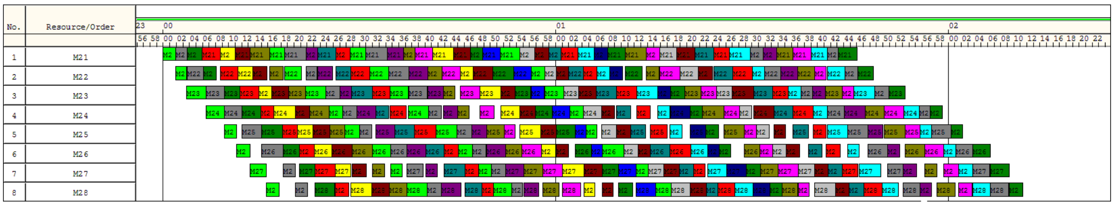

**Fig. 7** The Gantt chart of factory 2 for the studied scheduling problem

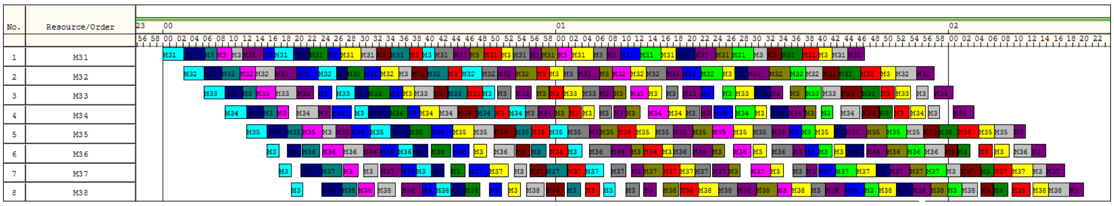

**Fig. 8** The Gantt chart of factory 3 for the studied scheduling problem

### 4.3 Statistical analysis and visualization

The Plant Simulation platform can provide powerful statistical analysis and visualization. In addition to the completion time and objective value, some production indicators are also important for assessing the efficiency and production status of the system. The utilization of machines and the occupation of buffers are analyzed.

Fig. 9 shows the real-time utilization of all machines for the three factories. As shown in Fig. 9, under the optimized scheduling plan, the utilization of machines is approximately 75 %, which is relatively high. Besides, the utilization between machines differs little, indicating that the workloads between those workshops and machines are balanced.

Fig. 10 provides the occupation of buffers in the three factories. Since infinite buffer capability is adapted as used in the scheduling literature, the number of jobs in a buffer can be 0-*inf*. As shown in Fig. 10, the most portion occurs when the number of jobs is 0. This indicates that for most cases, approximately 70-90 %, no jobs exist in the buffers. The number of jobs in all buffers can be 0,1,2,3, and 4. The second most frequent portion occurs when the number of jobs is 1. For factories 1 and 2, only a 5-10 % portion occurs when the number of jobs in buffers is 2. Factory 3 requires more buffers in BF32 and BF36. From the above analysis, we can know that for each buffer the buffer size set to 2 can fulfil most production requirements.

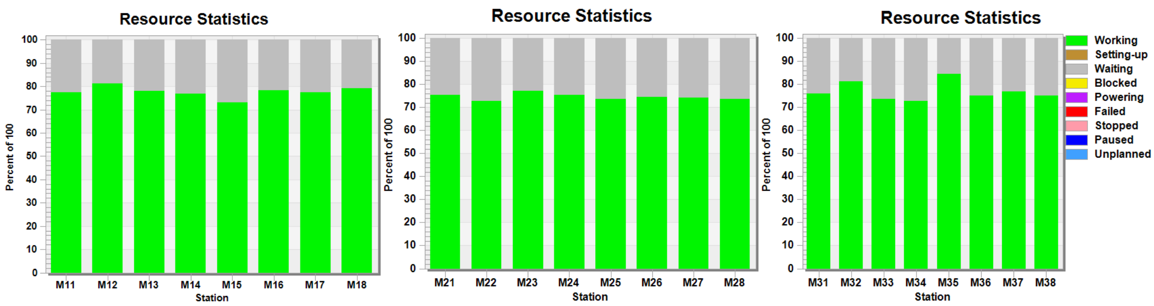


**Fig. 9** The utilization of machines in the three factories

The analysis for buffer occupation is very necessary for efficient production, since if no buffers are set the blocking will occur during production and therefore increase the completion time of the system. Most traditional scheduling literature simply assumes that infinite buffers exist between machines. However, in reality, it is impossible to set an infinite buffer size because the area between machines is limited. The buffer occupation analysis can help to determine the best buffer size to support efficient production.

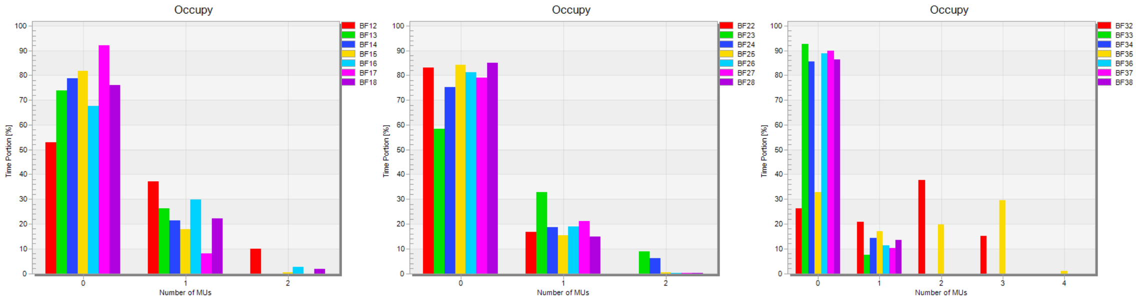


**Fig. 10** The occupation of buffers in the three factories

## 5. Conclusion

This paper studied the verification of production scheduling via discrete event simulation. Since most scheduling literature did not consider the verification of programmed scheduling environment and optimized scheduling schemes, this paper proposed a verification approach to validate the correctness of programmed scheduling environment and intelligent algorithms, by establishing the production simulation model in a Plant Simulation platform. The system architecture for validating the programmed production environment and optimized scheduling schemes are proposed. The parametric modelling method for production workshops with correct production processes is proposed. The verification experiment is carried out by taking the distributed permutation flowshop scheduling problem as a case study. Experimental results show that the scheduling results obtained by a deep reinforcement learning algorithm programmed in Python language are the same as results obtained in Plant Simulation platform. This verifies the correctness of the programmed production environment and scheduling algorithms. Besides, the utilization and Gantt charts clearly show the production efficiency under the selected scheduling scheme. The occupancy of buffers helps to determine the best buffer size before each machine. The proposed scheduling verification approach can help to verify the production environments programmed by researchers and the scheduling results obtained by intelligent algorithms.

In the future, more realistic production resources, such as automated guided vehicles, production lines, and workers, can be considered with the help of Plant Simulation platform after the verification stage to further optimize the scheduling scheme obtained by programmed scheduling algorithms. In addition, the real-time interaction between Python and Plant Simulation can be studied to check the problems of the programmed scheduling environment when the programmed environment is not correct.

## Acknowledgement

This work was supported by the National Defense Basic Scientific Research Program of China (Grant No. JCKY2021208B003), the National Key Research and Development Program of China (Grant No. 2022YFB3306000), and the National Natural Science Foundation of China (Grant No. 62073211).

## References


[1] Fernandez-Viagas, V., Ruiz, R., Framinan, J.M. (2017). A new vision of approximate methods for the permutation flowshop to minimise makespan: State-of-the-art and computational evaluation, *European Journal of Operational Research,* Vol. 257, No. 3, 707-721, doi: 10.1016/j.ejor.2016.09.055.

[2] Naderi, B., Ruiz, R. (2010). The distributed permutation flowshop scheduling problem, *Computers & Operations Research,* Vol. 37, No. 4, 754-768, doi: 10.1016/j.cor.2009.06.019.

[3] Ruiz, R., Pan, Q.-K., Naderi, B. (2019). Iterated Greedy methods for the distributed permutation flowshop scheduling problem, *Omega,* Vol. 83, No. 213-222, doi: 10.1016/j.omega.2018.03.004.

[4] Tao, X.-R., Pan, Q.-K., Gao, L. (2022). An efficient self-adaptive artificial bee colony algorithm for the distributed resource-constrained hybrid flowshop problem, *Computers & Industrial Engineering,* Vol. 169, Article No. 108200, doi: 10.1016/j.cie.2022.108200.

[5] Wang, J.-J., Wang, L. (2022). A cooperative memetic algorithm with learning-based agent for energy-aware distributed hybrid flow-shop scheduling, *IEEE Transactions on Evolutionary Computation,* Vol. 26, No. 3, 461-475, doi: 10.1109/tevc.2021.3106168.

[6] Huang, J.-P., Pan, Q.-K., Miao, Z.-H., Gao, L. (2021). Effective constructive heuristics and discrete bee colony optimization for distributed flowshop with setup times, *Engineering Applications of Artificial Intelligence,* Vol. 97, Article No. 104016, doi: 10.1016/j.engappai.2020.104016.

[7] Karabulut, K., Öztop, H., Kizilay, D., Tasgetiren, M.F., Kandiller, L. (2022). An evolution strategy approach for the distributed permutation flowshop scheduling problem with sequence-dependent setup times, *Computers & Operations Research,* Vol. 142, Article No. 105733, doi: 10.1016/j.cor.2022.105733.

[8] Shao, Z., Pi, D., Shao, W. (2020). Hybrid enhanced discrete fruit fly optimization algorithm for scheduling blocking flow-shop in distributed environment, *Expert Systems with Applications,* Vol. 145, Article No. 113147, doi: 10.1016/j.eswa.2019.113147.

[9] Chen, S., Pan, Q.-K., Gao, L. (2021). Production scheduling for blocking flowshop in distributed environment using effective heuristics and iterated greedy algorithm, *Robotics and Computer -- Integrated Manufacturing,* Vol. 71, Article No. 102155, doi: 10.1016/j.rcim.2021.102155.

[10] Li, H., Li, X., Gao, L. (2021). A discrete artificial bee colony algorithm for the distributed heterogeneous no-wait flowshop scheduling problem, *Applied Soft Computing,* Vol. 100, Article No. 106946, doi: 10.1016/j.asoc.2020.106946.

[11] Rossi, F.L., Nagano, M.S. (2021). Heuristics and iterated greedy algorithms for the distributed mixed no-idle flowshop with sequence-dependent setup times, *Computers & Industrial Engineering,* Vol. 157, Article No. 107337, doi: 10.1016/j.cie.2021.107337.

[12] Li, J.-Q., Chen, X.-L., Duan, P.-Y., Mou, J.-H. (2022). KMOEA: A knowledge-based multiobjective algorithm for distributed hybrid flow shop in a prefabricated system, *IEEE Transactions on Industrial Informatics,* Vol. 18, No. 8, 5318-5329, doi: 10.1109/tii.2021.3128405.

[13] Yang, S., Xu, Z. (2020). The distributed assembly permutation flowshop scheduling problem with flexible assembly and batch delivery, *International Journal of Production Research,* Vol. 59, No. 13, 4053-4071, doi: 10.1080/00207543.2020.1757174.

[14] Zhou, Y., Yang, J.-J., Zheng, L.-Y. (2019). Multi-agent based hyper-heuristics for multi-objective flexible job shop scheduling: A case study in an aero-engine blade manufacturing plant, *IEEE Access,* Vol. 7, 21147-21176, doi: 10.1109/access.2019.2897603.

[15] Jiang, X., Tian, Z., Liu, W., Suo, Y., Chen, K., Xu, X., Li, Z. (2022). Energy-efficient scheduling of flexible job shops with complex processes: A case study for the aerospace industry complex components in China, *Journal of Industrial Information Integration,* Vol. 27, Article No. 100293, doi: 10.1016/j.jii.2021.100293.

[16] Li, X., Xiao, S., Wang, C., Yi, J. (2019). Mathematical modeling and a discrete artificial bee colony algorithm for the welding shop scheduling problem, *Memetic Computing,* Vol. 11, No. 4, 371-389, doi: 10.1007/s12293-019-00283-4.

[17] Wang, Y., Wang, S., Li, D., Shen, C., Yang, B. (2021). An improved multi-objective whale optimization algorithm for the hybrid flow shop scheduling problem considering device dynamic reconfiguration processes, *Expert Systems with Applications,* Vol. 174, Article No. 114793, doi: 10.1016/j.eswa.2021.114793.

[18] Wang, L., Wang, J.-J., Jiang, E. (2021). Decomposition based multiobjective evolutionary algorithm with adaptive resource allocation for energy-aware welding shop scheduling problem, *Computers & Industrial Engineering,* Vol. 162, Article No. 107778, doi: 10.1016/j.cie.2021.107778.

[19] Schumacher, C., Buchholz, P. (2020). Scheduling algorithms for a hybrid flow shop under uncertainty, *Algorithms,* Vol. 13, No. 11, Article No. 277, doi: 10.3390/a13110277.

[20] Ojstersek, R., Tang, M., Buchmeister, B. (2020). Due date optimization in multi-objective scheduling of flexible job shop production, *Advances in Production Engineering & Management,* Vol. 15, No. 4, 481-492, doi: 10.14743/apem2020.4.380.

[21] Yang, S.L., Xu, Z.G., Wang, J.Y. (2019). Modelling and production configuration optimization for an assembly shop, *International Journal of Simulation Modelling,* Vol. 18, No. 2, 366-377, doi: 10.2507/ijsimm18(2)co10.

[22] Xu, N., Hou, X.Y., Jia, N. (2022). Optimization of multi-stage production scheduling of automated production, *International Journal of Simulation Modelling,* Vol. 21, No. 1, 160-171, doi: 10.2507/ijsimm21-1-co3.

[23] Wang, Y., Xu, B., Ma, T., Wang, Z. (2020). Research on the reliability allocation method for a production system based on availability, *Mathematical Problems in Engineering,* Vol. 2020, Article ID 6159462, doi: 10.1155/2020/6159462.

[24] Pekarcikova, M., Trebuna, P., Kliment, M., Mizerak, M., Kral, S. (2021). Simulation testing of the e-Kanban to increase the efficiency of logistics processes, *International Journal of Simulation Modelling,* Vol. 20, No. 1, 134-145, doi: 10.2507/ijsimm20-1-551.

[25] Yang, S.L., Xu, Z.G., Li, G.Z., Wang, J.Y. (2020). Assembly transport optimization for a reconfigurable flow shop based on a discrete event simulation, *Advances in Production Engineering & Management,* Vol. 15, No. 1, 69-80, doi: 10.14743/apem2020.1.350.

[26] Pekarcikova, M., Trebuna, P., Kliment, M., Dic, M. (2021). Solution of bottlenecks in the logistics flow by applying the Kanban module in the Tecnomatix plant simulation software, *Sustainability,* Vol. 13, No. 14, Article No. 7989, doi: 10.3390/su13147989.

[27] Li, G.Z., Xu, Z.G., Yang, S.L., Wang, H.Y., Bai, X.L., Ren, Z.H. (2020). Bottleneck identification and alleviation in a blocked serial production line with discrete event simulation: A case study, *Advances in Production Engineering & Management,* Vol. 15, No. 2, 125-136, doi: 10.14743/apem2020.2.353.

[28] Jurczyk-Bunkowska, M. (2021). Tactical manufacturing capacity planning based on discrete event simulation and throughput accounting: A case study of medium sized production enterprise, *Advances in Production Engineering & Management,* Vol. 16, No. 3, 335-347, doi: 10.14743/apem2021.3.404.

[29] Gregor, M., Hodoň, R., Grznár, P., Mozol, Š. (2022). Design of a system for verification of automatic guided vehicle routes using computer emulation, *Applied Sciences,* Vol. 12, No. 7, Article No. 3397, doi: 10.3390/app12073397.

[30] Li, G., Yang, S., Xu, Z., Wang, J., Ren, Z., Li, G. (2020). Resource allocation methodology based on object-oriented discrete event simulation: A production logistics system case study, *CIRP Journal of Manufacturing Science and Technology,* Vol. 31, 394-405, doi: 10.1016/j.cirpj.2020.07.001.

[31] Gola, A., Pastuszak, Z., Relich, M., Sobaszek, Ł., Szwarc, E. (2021). Scalability analysis of selected structures of a reconfigurable manufacturing system taking into account a reduction in machine tools reliability, *Eksploatacja i Niezawodnosc - Maintenance and Reliability,* Vol. 23, No. 2, 242-252, doi: 10.17531/ein.2021.2.4.

[32] Istokovic, D., Perinic, M., Dobovicek, S., Bazina, T. (2019). Simulation framework for determining the order and size of the product batches in the flow shop: A case study, *Advances in Production Engineering & Management,* Vol. 14, No. 2, 166-176, doi: 10.14743/apem2019.2.319.

[33] Ferro, R., Cordeiro, G.A., Ordóñez, R.E.C., Beydoun, G., Shukla, N. (2021). An optimization tool for production planning: A case study in a textile industry, *Applied Sciences,* Vol. 11, No. 18, Article No. 8312, doi: 10.3390/app11188312.

[34] Yang, S., Xu, Z. (2022). Intelligent scheduling and reconfiguration via deep reinforcement learning in smart manufacturing, *International Journal of Production Research,* Vol. 60, No. 16, 4936-4953, doi: 10.1080/00207543.2021.1943037.

APEM journal
**Advances in Production Engineering & Management** **ISSN 1854-6250**
Volume 17 | Number 4 | December 2022 | pp 413–424 Journal home: apem-journal.org
https://doi.org/10.14743/apem2022.4.445 Original scientific paper

# Demand prediction and optimization of workshop manufacturing resources allocation: A new method and a case study

**Wan, J.**[a,*]

[a]School of Economics, Wuhan Donghu University, Wuhan, P.R. China

**A B S T R A C T**

At present, great changes are taken place in the internal production management and resource allocation model of manufacturers. Under the premise of rational resource allocation, the completion period of products largely depends on the timeliness of resource allocation. The related studies mostly tackle the allocation of a single type of production resources in a single workshop, without considering much about the mutual influence between workshops. Through in-depth research on workshop manufacturing practices, this paper chooses to explore the planning, allocation, and demand prediction of manufacturing resources, which has long been a difficulty in workshop production. The research has great scientific research significance and practical value. The authors designed an algorithm based on the difference of the mean stagnation time of different production processes in the execution process, and used the algorithm to predict the number of production resources required in each period, before formulating the optimal configuration plan. This method is highly reasonable and applicable. After presenting a prediction method for the allocation demand of workshop manufacturing resources, the authors discussed whether the manufacturing resource allocation between different workshops is balanced in a fixed period. Then, a new idea was proposed for collaborative production between machines of different workshops in a specific environment, and an optimization algorithm was put forward to optimize the manufacturing resource allocation to machines facing the operation execution process. Through experiments, the authors compared the utilization rate of material, technological or human production resources in each period, and thereby verified the effectiveness of the proposed algorithm.

**A R T I C L E I N F O**

*Keywords:*
Workshop;
Manufacturing resources;
Resource demand;
Allocation;
Optimization;
Simulation;
Modelling;
Prediction

**Corresponding author:*
wanj@wdu.edu.cn
(Wan, J.)

*Article history:*
Received 6 July 2022
Revised 8 October 2022
Accepted 15 October 2022



## 1. Introduction

As consumers demand more and more personalized products, manufacturers are engaged in an increasingly fierce competition. As a result, great changes are taken place in the internal production management and resource allocation model of manufacturers [1-7]. Currently, the main challenges to manufacturers include the diversity of customized products, the small batch size, and the strict delivery period. This requires manufacturers to manage production and allocate resources scientifically and efficiently [8-11].

From the perspective of resource supply, the management department of workshop manufacturing resources must allocate resources rationally, in order to enhance machine utilization, and shorten the completion period [12-19]. Under the premise of rational resource allocation, the completion period of products largely depends on the timeliness of resource allocation.

The demand prediction for workshop manufacturing resources is to build a proper prediction model according to the workshop layout, order quantity, machine production attributes, and internal/external production conditions, and make overall forecast of the allocation demand of workshop manufacturing resources.

Clark [20] developed three models and the corresponding fast heuristics methods to identify production plans and instant setting plans for production lines with switching time. The three methods were tested statically, and then tested based on rolling period. The test results show that the methods differ in demand prediction accuracy, capacity tightness, and period length. Schneider *et al*. [21] described the Markov decision process of production scheduling, and constructed a value function specific to the current demand prediction, which can generate the optimal scheduling decision online. In addition, an industrial application and reinforcement learning approach was developed for generating the similar value function in the field. Experimental results show that value function approximation is effective in both deterministic and noisy environments.

Fiasché *et al*. [22] combined evolutionary algorithm with its quantum version into a hybrid approach. The simulation environment is ideally located inside two factories, partners and use cases of the white'R FP7 FOF MNP Project, with high manual activity to produce optoelectronics products, switching with the use of the new robotic (re)configurable island, the white'R, to highly automated production. Results show that the hybrid approach provided better answers and faster convergence than other methods. In recent years, many enterprises have shifted from single-point production to a more complex manufacturing environment, involving several multi-product facilities.

Ackermann *et al*. [23] proposed a mixed integer linear programming (MILP) model, and applied to the simultaneous material supply and scheduling of multi-site and multi-product intermittent plants with heterogenous parallel units. The applicability and performance of the model was demonstrated with numerical examples. Chernigovskiy [24] introduced ant colony optimization (ACO) to production scheduling, and compared the efficiency of the algorithm with other production scheduling algorithms on real cases. Through the comparison, they summarized the strengths of ACO, and its benefits to the manufacturing process.

The related studies mostly tackle the allocation of a single type of production resources in a single workshop, without considering much about the mutual influence between workshops. To fill the gap, this paper carries out the demand prediction and optimization simulation for workshop manufacturing resource allocation [25-31]. Based on the mean stagnation time of different production processes in the execution process, this paper designs an algorithm to predict the number of production resources required in each period, and formulate the optimal configuration plan. This method is highly reasonable and applicable. Compared with the existing algorithms, our algorithm optimizes the simulation of the allocation of workshop production and manufacturing resources under multiple working conditions, and achieves high application value for improving the workshop scheduling system. Section 2 presents a prediction method for the allocation demand of workshop manufacturing resources. After determining the prediction method, Section 3 discussed whether the manufacturing resource allocation between different workshops is balanced in a fixed period. Section 4 proposed a new idea for collaborative production between machines of different workshops in a specific environment, aiming to obtain the optimal resource allocation plan for minimizing the mean stagnation time during the execution of production operations. In addition, an optimization algorithm was put forward to optimize the manufacturing resource allocation to machines facing the operation execution process, and its flow was illustrated. Through experiments, the simulation tools based on discrete event simulation were compared with the proposed simulation optimization model. The experimental results verify the effectiveness of the proposed algorithm.

## 2. Demand prediction

In the actual situation of manufacturers, the management department of workshop manufacturing resources does not allocate resources to each workshop, but choose one workshop for resource allocation. Moreover, the resources are only allocated to a workshop when the manufacturing resources is out of balance. Therefore, this paper presents a new prediction method for workshop manufacturing resource allocation, and an index reflecting whether the resource allocation is balanced between workshops. To predict the demand for workshop manufacturing resource allocation, the key is to forecast the variation in the resource demand of each machine in the workshop. Thus, it is necessary to project the cumulative resource demand of each machine, as well as the overall resource demand of the workshop.

The XGBoost-based stacking model was adopted to predict the variation in the resource demand of each machine. On this basis, the resource demand of all machines in a workshop was predicted. Then, the demands of different workshops were added up to obtain the final prediction of resource allocation demand.

In a workshop $X$, the set of machines is denoted by $R = \{r_1, r_2, \ldots, r_m\}$. Then, the resource demand variation of each machine $r_i$ can be calculated by:

$$\hat{G}_{S_{R_i}}(o) = g_{SMVP}(r_i, o) \tag{1}$$

where, $g$ is the prediction model trained by the corresponding sample set $E$; $o$ is the time interval. Then, the resource demand variation of workshop $X$ can be calculated by:

$$\hat{G}_{S_X}(o) = \sum_{r_i \in R} \hat{G}_{S_{R_i}}(o) \tag{2}$$

Suppose the predicted resource demand variation of each machine $r_i$ has an error of $\varepsilon_i$. Then,

$$\hat{G}_{S_{R_i}}(o) = G_{S_{R_i}}(o) + \varepsilon_i \tag{3}$$

The resource demand variation of each machine in a workshop can be expressed as:

$$\hat{G}_{S_X}(o) = \textstyle\sum_{r_i \in R} G_{S_{R_i}}(o) + \sum_{i \in m} \varepsilon_i \tag{4}$$

$$\hat{G}_{S_X}(o) = G_{S_X}(o) + \textstyle\sum_{i \in m} \varepsilon_i \tag{5}$$

The resource allocation demand of a workshop can be obtained as:

$$E_X(o) = -\hat{G}_{S_X}(o) \tag{6}$$

The resource allocation demand of a workshop is the sum of the resource demand of each single-point machine. During the summation, the prediction error of each machine is also added up. It is very difficult to eliminate that error. Then, the resource demand variation of workshop $X$ can be calculated by:

The XGBoost-based stacking model was directly applied to forecast the resource demand variation of each machine in a workshop.

$$\hat{G}_{S_X}(o) = g_{SMVP}(X, o) \tag{7}$$

where, $g$ is the prediction model trained by the corresponding sample set $E$; $o$ is the time interval.

Suppose the predicted resource demand variation of each machine in workshop $X$ has an error of $\varepsilon$. Then,

$$\hat{G}_{S_X}(o) = G_{S_X}(o) + \in \tag{8}$$

The resource allocation demand of workshop $X$ can be expressed as:

$$E_X(o) = -\hat{G}_{S_X}(o) \tag{9}$$

The error of overall prediction is smaller than the cumulative error. Hence, the overall demand prediction of workshop resource allocation achieves an ideal effect.

## 3. Balance analysis

After determining the prediction method, it is necessary to discuss whether the manufacturing resource allocation between different workshops is balanced in a fixed period. Before the discussion, overall consideration should be given to the future demand variation of manufacturing resources, the maximum quantity of manufacturing resources, and the minimum quantity of manufacturing resources in each workshop.

Let $E = \{e_1, e_2, \dots, e_m\}$ be the quantity of manufacturing resources corresponding to each machine $R = \{r_1, r_2, \dots, r_m\}$ in workshop $X$. Then, the total quantity of manufacturing resources that can be accommodated by workshop $X$ can be calculated by:

$$Y_{Max_X} = \sum_{e_i \in E} e_i \tag{10}$$

The maximum $\varphi_{up}$ and minimum $\varphi_{down}$ of the quantity of manufacturing resources can be respectively defined as:

$$\varphi_{up_X} = Y_{Max_X} * \xi_{up} \tag{11}$$

$$\varphi_{down_X} = Y_{Max_X} * \xi_{down} \tag{12}$$

where, $\xi_{up}$ and $\xi_{down}$ are two parameters that control $\varphi_{up}$ and $\varphi_{down}$, respectively.

Let $Y_{Max_X}$ denote the highest resource demand of each machine in workshop $X$. Then, the maximum and minimum quantities of manufacturing resources can be respectively described by $\varphi_{up_X}$ and $\varphi_{down_X}$, respectively:

$$\phi_{up_X} = Y_{Max_X} * \xi_{up} \tag{13}$$

$$\phi_{down_X} = Y_{Max_X} * \xi_{down} \tag{14}$$

The balance of resource allocation between workshops can be detailed as follows:

(1) If $E_X(o)$ is greater than zero, then workshop manufacturing resources diminish. In this case, when $E_X(o) \leq \varphi_{down_X}$, the manufacturing resource allocation of a workshop is balanced, eliminating the need for replenishing manufacturing resources. When $\varphi_{down_X} < E_X(o) \leq \varphi_{up_X}$, the allocation is out of balance, i.e., the machines are not fully utilized, and manufacturing resources should be replenished immediately to meet the demand $E_X(o)$. When $E_X(o)$, the allocation is still out of balance, but simple addition of manufacturing resources will bring another problem, i.e., the manufacturing resource quantity may far exceed the capacity of machines. Thus, it is necessary to set $E_X(o) = \varphi_{up_X}$.

(2) If $E_X(o)$ is smaller than zero, then workshop manufacturing resources increase. In this case, when $|E_X(o)| \leq \varphi_{down_X}$, the manufacturing resource allocation of a workshop is balanced, eliminating the need for transferring manufacturing resources. When $\varphi_{down_X} < |E_X(o)| \leq \varphi_{up_X}$, the allocation is out of balance, i.e., the machines are unable to handle so many manufacturing resources, and the excessive quantity $|E_X(o)|$ of manufacturing resources should be transferred away immediately. When $|E_X(o)| > \varphi_{up}$, the allocation is still out of balance, but simple reduction of manufacturing resources will bring another problem, i.e., the manufacturing resource quantity may fall far short of the capacity of machines. Thus, it is necessary to set $|E_X(o)| = -\varphi_{up_X}$.

## 4. Proposed allocation optimization approach

The production tasks of machines are planned by the workshop, and each machine has a fixed production efficiency. When the order quantity increases, the shortage of manufacturing resources may occur easily. This will definitely affect the mean stagnation time during the execution of some operations.

To solve the problem, we proposed a new idea for collaborative production between machines of different workshops in a specific environment, aiming to obtain the optimal resource allocation plan for minimizing the mean stagnation time during the execution of production operations, and avoid the unfavorable state that some machines are busy while some machines are idle. This section details the optimization algorithm was put forward to optimize the manufacturing resource allocation to machines facing the operation execution process.

Fig. 1 lists six functions of the optimization algorithm, including reading and storage of production state data, calculation of machine delay function, visual simulation of machines, calculation of mean stagnation time of each operation, resource allocation optimization for collaborative production, and update of manufacturing resource allocation schedule. The six functions are intercorrelated, and work together to ensure the realization of the optimization objective of manufacturing resource allocation.

Fig. 2 shows the three-layer architecture of the optimization algorithm. The functional display layer mainly realizes the man-machine interaction during the simulation. The main functions on this layer include generation of new allocation plan, display of mean stagnation time of each operation, selection of machines for collaboration request, display of production task planning, and real-time visual simulation of production state. The logical processing layer is responsible for all computations and data processing. It mainly has five functions: processing of production state data, update of unoptimized number of machines, calculation of delay function, calculation of mean stagnation time of each operation, and sorting of delay functions. The data access layer stores the important information collected and calculated by the algorithm, mainly including production state data file, production task database, and resource allocation database. The above architecture connects all functional modules of the algorithm, realizes the target functions, and meets the actual production needs of workshops.

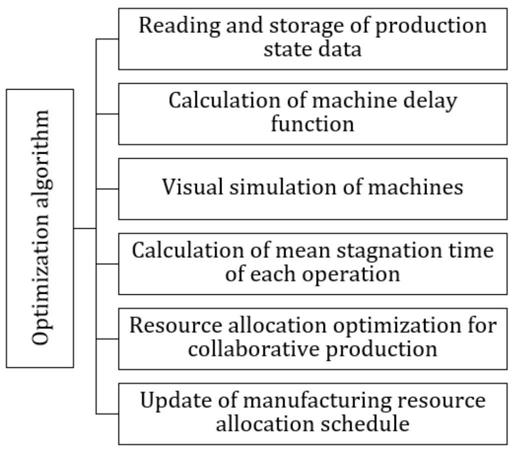


**Fig. 1** Some functions of the optimization algorithm

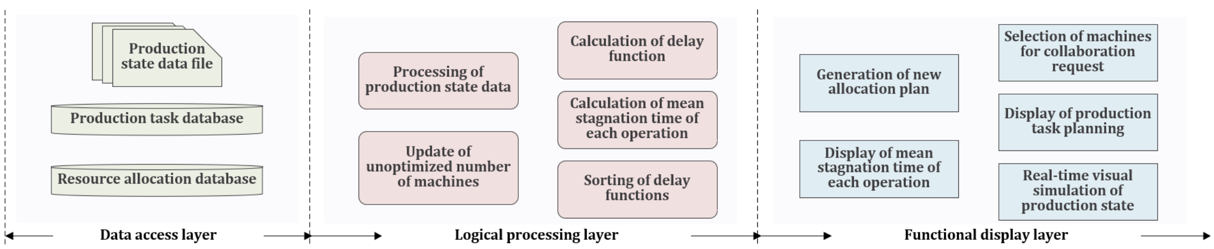


**Fig. 2** Architecture of optimization algorithm

The logical processing layer is the core of the algorithm. The structure of this layer is detailed in Fig. 3.

If the initial schedule of manufacturing resources allocation is known, then the manufacturing resources pending allocation optimization will be selected based on the delay function. Next, an optimization model would be constructed for manufacturing resources for simulation and optimization. Then, the allocation of all resources would be optimized iteratively, thereby minimizing the mean stagnation time of each operation in execution.

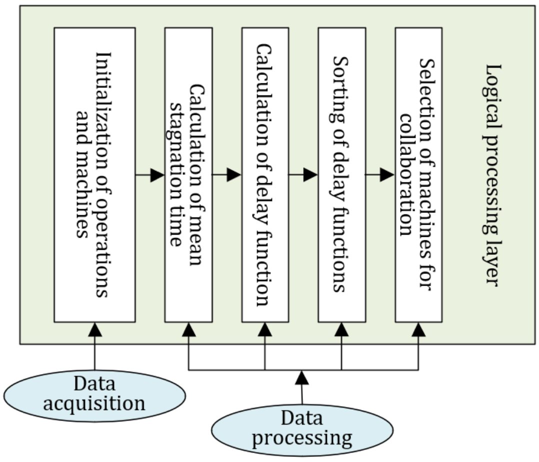


**Fig. 3** Structure of logical processing layer

This paper introduces the idea of collaborative production to the optimization algorithm for the manufacturing resource allocation to machines facing the operation execution process: Under certain production conditions, machines with similar production efficiencies can borrow manufacturing resources from each other to execute the same operation, such as to improve the allocation effect of resources throughout the execution process.

After incorporating the above idea, our optimization algorithm breaks the limit of the original schedule of resource allocation: For each operation, only one machine receives manufacturing resources, making it impossible to optimize the resource allocation. Our algorithm can also reasonably reallocate resources to solve the problem that the machines, which are assigned insufficient production tasks, cannot easily respond to the real-time changes of order quantity. In other words, the traditional algorithms are unable to effectively reduce the mean stagnation time of operations, while our algorithm overcomes this limitation.

The collaborative production involves a requestor and a responder. Before optimization simulation, it is important to determine which machines need to request collaboration from others. Two types of machines may become requestors. The first type refers to the machines that cannot timely execute operations, because they are assigned insufficient production tasks. Even if the allocation of a certain type of resources is optimized, these machines have the maximum delay. Then, such machine would request collaboration from others. The second type of machines are selected based on the limitation of the optimization algorithm. If only one machine receives manufacturing resources, and if it has a large delay, then it needs to request collaboration from others.

The responding machine should have the same operations with the requestor, and the minimum delay. The manufacturing resources of the responder needs to be transferred to the requestor. Then, the manufacturing resource allocation is optimized for both parties engaging in collaboration. The above process is implemented iteratively until the algorithm meets the termination condition.

Let $m$ be the current operation; $E_m$ be the set of delay functions of all machines in operation $m$; $E_m^*$ be the set of delay functions of all machines facing the same operations in operation $m$; $w_m^*$ be the machine selected from operation $m$ for optimizing the allocation of manufacturing resources; $z_m^*$ be the machine facing the same operations selected from operation $m$ for responding to collaboration requests; $ST$ be the set of all machines; $DE(m)$ be the mean stagnation time of operation $m$ after the optimization of manufacturing resource allocation; $v$ be the unoptimized number of machines during operation $m$.

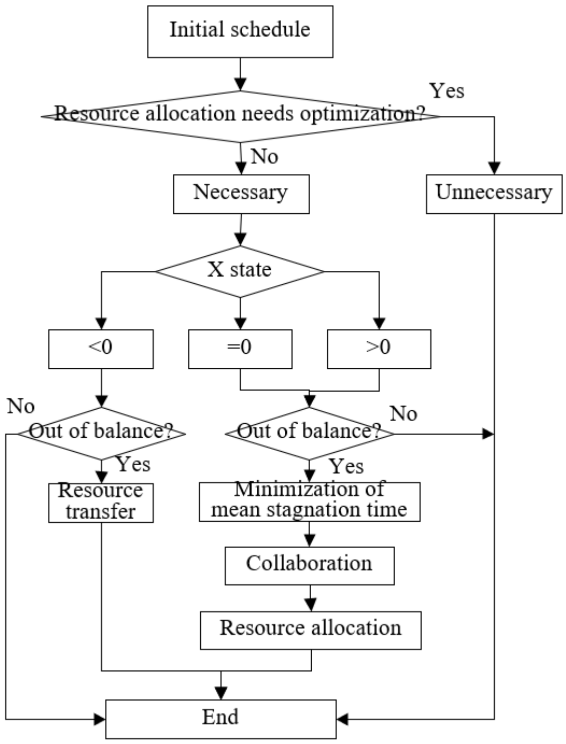


**Fig. 4** Steps of our optimization algorithm

As shown in Fig. 4, the specific steps of our optimization algorithm are as follows:

Step 1. In the initial allocation schedule of manufacturing resources, all $\forall w$ satisfy $w \in ST$, i.e., all machines belong to the optimization range of manufacturing resource allocation.
Step 2. The manufacturing resources of all machines are initially allocated as per the original schedule, with $m = 0$, and $w_0^* = \emptyset$.
Step 3. The initial schedule is simulated to solve the current $DE(m)$.
Step 4. For all $w \in ST$, the delay function of each machine is obtained for the current moment.
Step 5. All $E_m$ values are sorted in descending order, with $v = 1$ and $m = m + 1$.
Step 6. If $|v \leq |ST|$, go to Step 7; otherwise, terminate the iteration.
Step 7. The $u$-th $w$ of $E_{m-1}[v]$ is selected as $w_m^*$.
Step 8. If $w_m^* = w_{m-1}^*$, all $E_m$ values are sorted in descending order. Then, the machine with the minimum delay $z_m^*$ is selected, and its resources are transferred to $w_m^*$.
Step 9. The resource allocation is optimized for the requestor $w_m^*$ and the responder $z_m^*$ separately, according to the allocation optimization model.
Step 10. If $w_m^*$ does not receive resources after optimization, $v = v + 1$, and go to Step 6; otherwise, go to Step 11.
Step 11. The new allocation schedule is simulated to obtain the corresponding $DE(m)$.
Step 12. If $DE(m) < DE(m - 1)$, go to Step 4; otherwise, $v = v + k$, and go to Step 6.

## 5. Simulation results analysis and discussion

Our optimization algorithm for the manufacturing resource allocation to machines facing the operation execution process was verified through multiple simulations. The performance of our algorithm was compared with the traditional manufacturing resource allocation algorithm under the same case, using our independently developed software solution. Table 1 displays the delay functions of all machines in each operation, and the machines needing collaboration in each operation. It can be inferred that the case involves eight operations from the initial allocation schedule of manufacturing resources to the optimal schedule. Some machines requested collaboration in two consecutive operations. These machines lack manufacturing resources severely, failing to meet the real-time demand. Then, out of the machines with the same operations, the machine with the minimum delay should be selected to respond to the collaboration request: their resources should be transferred to the requestor. The calculation results show that the delays of the requestors dropped significantly in a few operations, but the delays of other machines remained largely the same. This verifies the feasibility of collaborative production.

Table 2 shows the stagnation and waiting of each machine in each operation, after the optimization of manufacturing resource allocation. The data in the table further verifies the feasibility of our optimization algorithm. Our simulation optimization model is more effective than the simulation tools of discrete event simulation. It can be seen that the resource allocation to each machine in each operation was improved, and the optimal solution of the allocation schedule was about 50 % lower than the initial solution in terms of stagnation, and 3/4 lower in terms of waiting time. Both stagnation and waiting times were declined from the levels of the traditional resource allocation algorithm.

Figs. 5 and 6 present the quantities of material type and technology/manpower type manufacturing resources pending allocation in each period, respectively. The red and purple lines indicate the resource quantities in the initial situation, and those under the optimal allocation schedule. It can be observed that both types of resources declined significantly, indicating that the new allocation schedule can effectively weaken the obstacles to the flow of manufacturing resources between machines. In addition, different types of manufacturing resources varied in the quantity being processed by machines, owing to the interplay between production efficiencies of different machines in the same workshop.

Figs. 7 and 8 present the machine utilizations of material type and technology/manpower type manufacturing resources in each period, respectively. The red and purple lines indicate the machine utilizations in the initial situation, and those under the optimal allocation schedule. It can be inferred that the machine utilizations improved obviously for both types of resources. In the initial allocation of resources, some machines may be busy, while others may be idle, and some machines were continuously engaged in high-intensity production, owing to the imbalance between resources. These problems were basically eliminated after the allocation optimization.

**Table 1** Delay function of each machine in each operation

| Machine number | 1 | 2 | 3 | 4 | 5 | 6 | 7 | 8 |
|---|---|---|---|---|---|---|---|---|
| Operation 0 | 0.251 | 0.562 | 93.154 | 61.592 | 0.374 | 132.651 | 114.518 | 0.025 |
| Operation 1 | 0.284 | 0.469 | 152.43 | 52.618 | 0.218 | 41.629 | 132.542 | 0.021 |
| Operation 2 | 0.359 | 0.526 | 21.417 | 62.352 | 0.348 | 13.607 | 152.041 | 0.029 |
| Operation 3 | 0.152 | 0.564 | 25.168 | 53.627 | 0.241 | 13.521 | 56.128 | 0.027 |
| Operation 4 | 0.137 | 0.462 | 24.847 | 52.195 | 0.418 | 11.415 | 28.419 | 0.024 |
| Operation 5 | 0.168 | 0.641 | 28.415 | 14.219 | 0.482 | 16.294 | 25.318 | 0.023 |
| Operation 6 | 0.159 | 0.451 | 27.462 | 13.258 | 0.374 | 18.492 | 15.625 | 0.025 |
| Operation 7 | 0.156 | 0.537 | 18.526 | 11.416 | 0.351 | 15.415 | 18.207 | 0.028 |
| Operation 8 | 0.193 | 0.412 | 7.652 | 8.439 | 0.318 | 5.627 | 18.439 | 0.051 |

**Table 2** Stagnation and waiting of resources in each operation

| | Operation 0 | Operation 1 | Operation 2 | Operation 3 | Operation 4 |
|---|---|---|---|---|---|
| Mean stagnation time | 1.251 | 1.748 | 1.625 | 1.205 | 0..947 |
| Mean waiting time | 1.326 | 1.485 | 0.718 | 0.625 | 0.495 |
| | Operation 5 | Operation 6 | Operation 7 | Percentage of reduction | |
| Mean stagnation time | 0.961 | 0.815 | 0.853 | 52.64 | |
| Mean waiting time | 0.357 | 0.495 | 0.285 | 74.51 | |

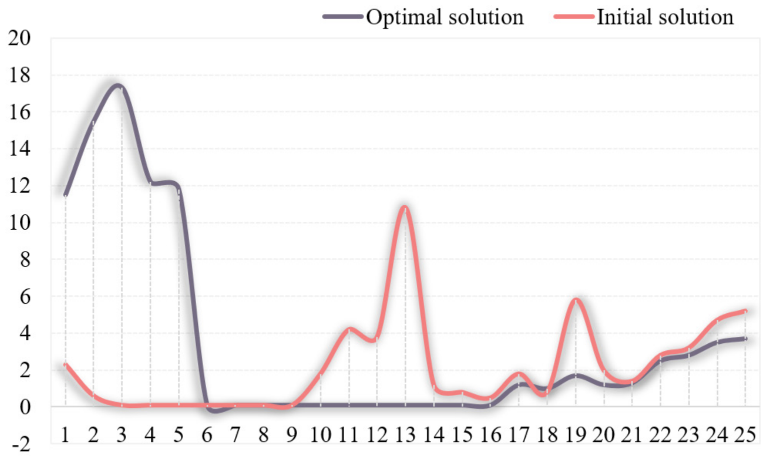


**Fig. 5** Quantities of material type manufacturing resources pending allocation

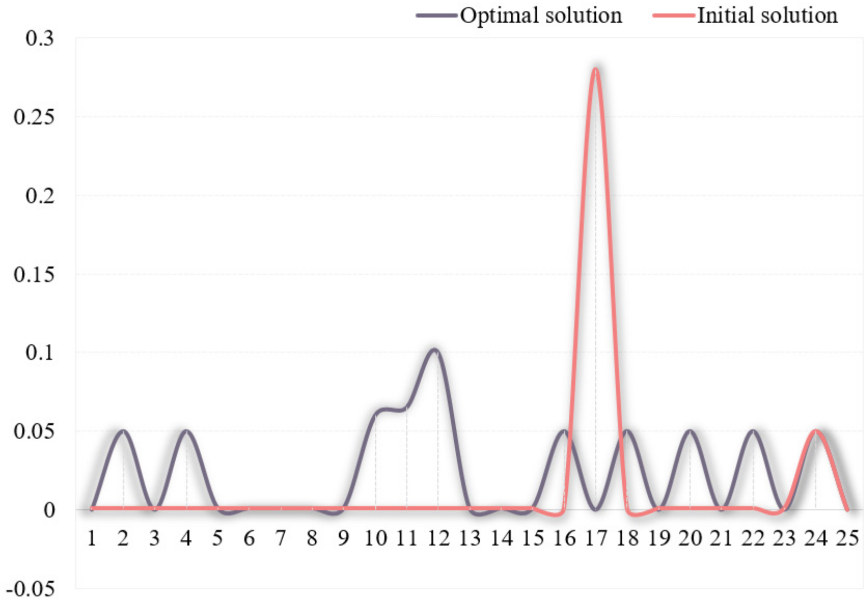


**Fig. 6** Quantities of technology/manpower type manufacturing resources pending allocation

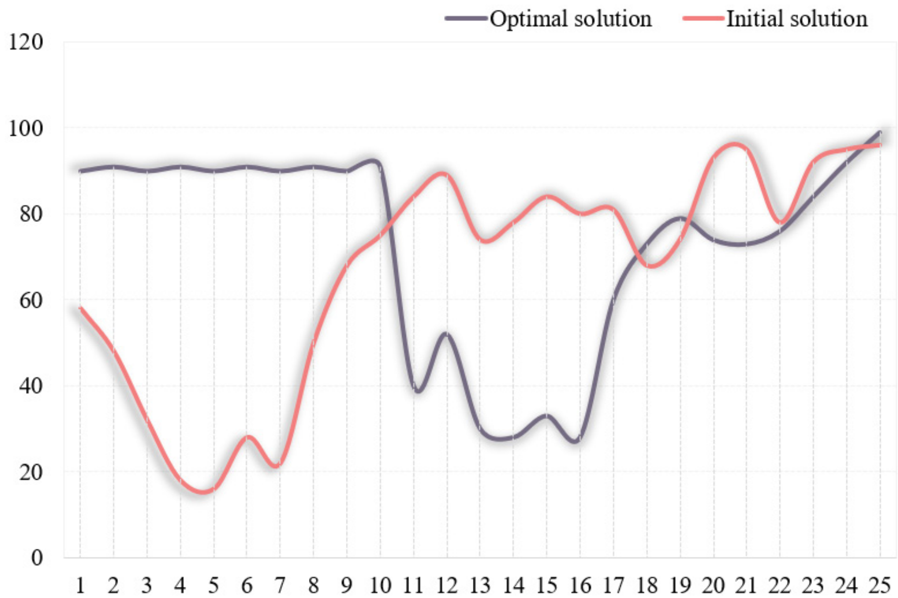


**Fig. 7** Machine utilizations of material type manufacturing resources

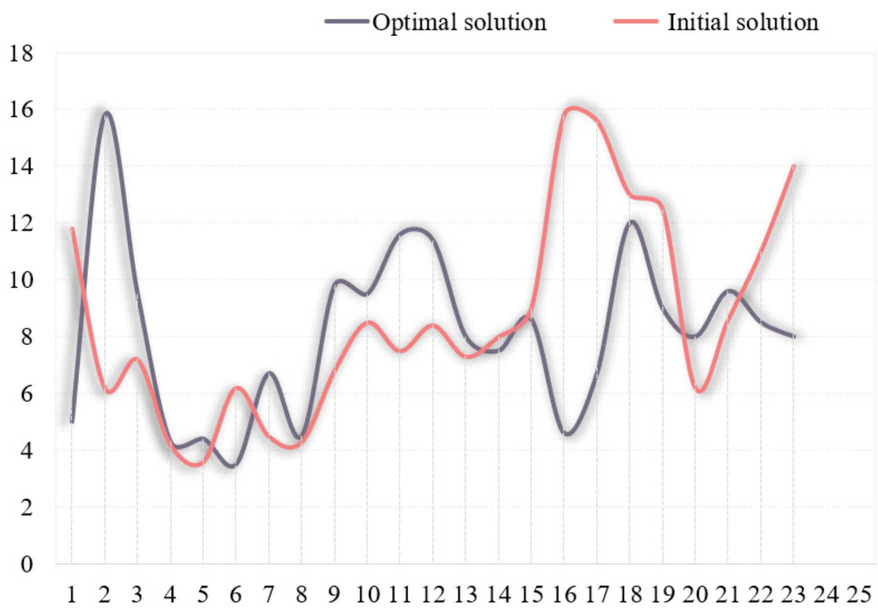


**Fig. 8** Machine utilizations of technology/manpower type manufacturing resources

## 6. Conclusions

This paper carries out the demand prediction and optimization simulation for workshop manufacturing resource allocation. After presenting a prediction method for the allocation demand of workshop manufacturing resources, the authors discussed whether the manufacturing resource allocation between different workshops is balanced in a fixed period. Then, a new idea was proposed for collaborative production between machines of different workshops in a specific environment, and an optimization algorithm was put forward to optimize the manufacturing resource allocation to machines facing the operation execution process. The algorithm flow was detailed.

Through experiments, we displayed the delay functions of each machine in each operation, identified the machines needing collaborative production in each operation, and verified the feasibility of the idea of collaborative production. The effectiveness of our algorithm was further confirmed by obtaining the stagnation and waiting situation of each machine in each operation, after the resource allocation is optimized. Finally, we compared the quantities of material type and technology/manpower type manufacturing resources pending allocation in each period, and contrasted the machine utilizations of material type and technology/manpower type manufacturing resources in each period.

This paper mines the historical dataset of workshop production and manufacturing, researched and established a model and an analysis method, and achieved certain research results. However, the allocation of workshop production and manufacturing resources is affected by various factors, which have intricated correlations. For reasons of dataset and data quality, it is impossible to fully consider and thoroughly explore all the influencing factors and their correlations. In the future, these issues will be considered for further improvement.

## Acknowledgement

This paper was supported by Wuhan Donghu University (Grant No.: 2021dhsk005).

## References

[1] Bagheri Rad, N., Behnamian, J. (2022). Recent trends in distributed production network scheduling problem, *Artificial Intelligence Review*, Vol. 55, No. 4, 2945-2995, doi: 10.1007/s10462-021-10081-5.

[2] Rezvani, M.Q., Chaudhary, N., Huseynov, R., Li, M.H., Sharma, A., Jafarova, R., Huseynova, C. (2021). Impact of organisational commitment on employee productivity during Covid-19: Evidence from Afghanistan and India, *Journal of Corporate Governance, Insurance and Risk Management*, Vol. 8, No. 2, 59-74.

[3] Aghighi, S., Niaki, S.T.A., Mehdizadeh, E., Najafi, A.A. (2021). Open-shop production scheduling with reverse flows, *Computers & Industrial Engineering*, Vol. 153, Article No. 107077, doi: 10.1016/j.cie.2020.107077.

[4] Li, Y., Goga, K., Tadei, R., Terzo, O. (2020). Production scheduling in Industry 4.0, In: Barolli, L., Poniszewska-Maranda, A., Enokido, T. (eds.), *Complex, intelligent and software intensive systems, CISIS 2020, Advances in intelligent systems and computing,* Vol. 1194, Springer, Cham, Switzerland, 355-364, doi: 10.1007/978-3-030-50454-0_34.

[5] Febriana, T.H., Hasbullah, H. (2021). Analysis and defect improvement using FTA, FMEA, and MLR through DMAIC phase: Case study in mixing process tire manufacturing industry, *Journal Européen des Systèmes Automatisés*, Vol. 54, No. 5, 721-731, doi: 10.18280/jesa.540507.

[6] Huang, J., Chang, Q., Arinez, J. (2020). Distributed production scheduling for multi-product flexible production lines, In: *Proceedings of 2020 IEEE 16th International Conference on Automation Science and Engineering (CASE)*, Hong Kong, China, 1473-1478, doi: 10.1109/CASE48305.2020.9216944.

[7] Arena, M., Di Pasquale, V., Iannone, R., Miranda, S., Riemma, S. (2022). A maintenance driven scheduling cockpit for integrated production and maintenance operation schedule, *Advances in Manufacturing*, Vol. 10, No. 2, 205-219, doi: 10.1007/s40436-021-00380-z.

[8] Yang, L., Jiang, G., Chen, X., Li, G., Li, T., Chen, X. (2019). Design of integrated steel production scheduling knowledge network system, *Cluster Computing*, Vol. 22, 10197-10206, doi: 10.1007/s10586-017-1215-7.

[9] Choi, B.-C., Min, Y., Park, M.-J., Kim, K.M. (2020). Production scheduling considering outsourcing options and carrier costs, *Journal of Advanced Transportation*, Vol. 2020, Article ID 7069291, doi: 10.1155/2020/7069291.

[10] Abedini, A., Li, W., Badurdeen, F., Jawahir, I.S. (2020). A metric-based framework for sustainable production scheduling, *Journal of Manufacturing Systems*, Vol. 54, 174-185, doi: 10.1016/j.jmsy.2019.12.003.

[11] Hu, F., Xi, X., Zhang, Y. (2021). Influencing mechanism of reverse knowledge spillover on investment enterprises' technological progress: An empirical examination of Chinese firms, *Technological Forecasting and Social Change*, Vol. 169, Article No. 120797, doi: 10.1016/j.techfore.2021.120797.

[12] Yue, Q., Chen, Z.-L., Wan, G. (2019). Integrated pricing and production scheduling of multiple customized products with a common base product, *IISE Transactions*, Vol. 51, No. 12, 1383-1401, doi: 10.1080/24725854.2019.1589659.doi: 10.1016/j.techfore.2021.120797

[13] Liu, M., Chu, F., He, J., Yang, D., Chu, C. (2019). Coke production scheduling problem: A parallel machine scheduling with batch preprocessings and location-dependent processing times, *Computers & Operations Research*, Vol. 104, 37-48, doi: 10.1016/j.cor.2018.12.002.

[14] Varelmann, T., Erwes, N., Schäfer, P., Mitsos, A. (2022). Simultaneously optimizing bidding strategy in pay-as-bid-markets and production scheduling, *Computers & Chemical Engineering*, Vol. 157, Article No. 107610, doi: 10.1016/j.compchemeng.2021.107610.

[15] Yang, Y., De La Torre, B., Stewart, K., Stewart, K., Lair, L., Phan, N.L., Das, R., Gonzalez, D., Lo, R.C. (2022). The scheduling of alkaline water electrolysis for hydrogen production using hybrid energy sources, *Energy Conversion and Management*, Vol. 257, Article No. 115408, doi: 10.1016/j.enconman.2022.115408.

[16] Maryani, E., Purba, H.H., Sunadi (2021). Analysis of aluminium alloy wheels product quality improvement through DMAIC method in casting process: A case study of the wheel manufacturing industry in Indonesia, *Journal Européen des Systèmes Automatisés*, Vol. 54, No. 1, 55-62, doi: 10.18280/jesa.540107.

[17] Villa, A., Taurino, T. (2018). Event-driven production scheduling in SME, *Production Planning & Control*, Vol. 29, No. 4, 271-279, doi: 10.1080/09537287.2017.1401143.

[18] Aghelinejad, M., Ouazene, Y., Yalaoui, A. (2018). Production scheduling optimisation with machine state and time-dependent energy costs, *International Journal of Production Research*, Vol. 56, No. 16, 5558-5575, doi: 10.1080/00207543.2017.1414969.

[19] Waschneck, B., Reichstaller, A., Belzner, L., Altenmüller, T., Bauernhansl, T., Knapp, A., Kyek, A. (2018). Deep reinforcement learning for semiconductor production scheduling, In: *Proceedings of 2018 29th Annual SEMI Advanced Semiconductor Manufacturing Conference (ASMC),* Saratoga Springs, New York, USA, 301-306, doi: 10.1109/ASMC.2018.8373191.

[20] Clark, A.R. (2005). Rolling horizon heuristics for production planning and set-up scheduling with backlogs and error-prone demand forecasts, *Production Planning & Control*, Vol. 16, No. 1, 81-97, doi: 10.1080/09537280412331286565.

[21] Schneider, J.G., Boyan, J.A., Moore, A.W. (1998). Stochastic production scheduling to meet demand forecasts, In: *Proceedings of the 37th IEEE Conference on Decision and Control (Cat. No. 98CH36171)*, Tampa, Florida, USA, 2722-2727, doi: 10.1109/CDC.1998.757865.

[22] Fiasché, M., Liberati, D.E., Gualandi, S., Taisch, M. (2018). Quantum-inspired evolutionary multiobjective optimization for a dynamic production scheduling approach, In: Esposito, A., Faudez-Zanuy, M., Morabito, F., Pasero, E. (eds.), *Multidisciplinary Approaches to Neural Computing, Multidisciplinary approaches to neural computing, Smart innovation, systems and technologies,* Vol. 69, Springer, Cham, Switzerland, 191-201, doi: 10.1007/978-3-319-56904-8_19.

[23] Ackermann, S., Fumero, Y., Montagna, J.M. (2018). Optimization framework for the simultaneous batching and scheduling of multisite production environments, *Industrial & Engineering Chemistry Research*, Vol. 57, No. 48, 16395-16406, doi: 10.1021/acs.iecr.8b03140.

[24] Chernigovskiy, A.S., Kapulin, D.V., Noskova, E.E., Yamskikh, T.N., Tsarev, R.Y. (2017). Production scheduling with ant colony optimization, *IOP Conference Series: Earth and Environmental Science*, Vol. 87, Article No. 062002, doi: 10.1088/1755-1315/87/6/062002.

[25] Wang, Y.J., Wang, N.D., Cheng, S.M., Zhang, X.C., Liu, H.Y., Shi, J.L., Ma, Q.Y., Zhou, M.J. (2021). Optimization of

disassembly line balancing using an improved multi-objective Genetic Algorithm, *Advances in Production Engineering & Management*, Vol. 16, No. 2, 240-252, doi: 10.14743/apem2021.2.397.

[26] Duan, W., Ma, H., Xu, D.S. (2021). Analysis of the impact of COVID-19 on the coupling of the material flow and capital flow in a closed-loop supply chain, *Advances in Production Engineering & Management*, Vol. 16, No. 1, 5-22, doi: 10.14743/apem2021.1.381.

[27] Tian, W., Zhang, H.P. (2021). A dynamic job-shop scheduling model based on deep learning, *Advances in Production Engineering & Management*, Vol. 16, No. 1, 23-36, doi: 10.14743/apem2021.1.382.

[28] Jiang, H., Liu, C.Y. (2019). Scheduling optimization of cloud resource supply chain through multi-objective particle swarm optimization, *International Journal of Simulation Modelling*, Vol. 18, No. 1, 163-174, doi: 10.2507/IJSIMM18(1)CO3.

[29] Janes, G., Perinic, M., Jurkovic, Z. (2017). An efficient genetic algorithm for job shop scheduling problems, *Tehnički Vjesnik–Technical Gazette,* Vol. 24, No. 4, 1243-1247, doi: 10.17559/TV-20150527133957.

[30] Meng, J.L. (2021). Demand prediction and allocation optimization of manufacturing resources, *International Journal of Simulation Modelling*, Vol. 20, No. 4, 790-801, doi: 10.2507/IJSIMM20-4-CO20.

[31] Ojstersek, R., Buchmeister, B. (2021). Simulation based resource capacity planning with constraints, *International Journal of Simulation Modelling*, Vol. 20, No. 4, 672-683, doi: 10.2507/IJSIMM20-4-578.

APEM journal

**Advances in Production Engineering & Management**
Volume 17 | Number 4 | December 2022 | pp 425–438
https://doi.org/10.14743/apem2022.4.446

**ISSN 1854-6250**
Journal home: apem-journal.org
Original scientific paper

# Monte Carlo Tree Search improved Genetic Algorithm for unmanned vehicle routing problem with path flexibility

**Wang, Y.D.**[a], **Lu, X.C.**[b,*], **Song, Y.M.**[c], **Feng, Y.**[d], **Shen, J.R.**[e]

[a]Beijing Jiaotong University, Shangyuan Village, Haidian District, Beijing, P.R. China
[b]Beijing Jiaotong University, Shangyuan Village, Haidian District, Beijing, P.R. China
[c]Beijing Jiaotong University, Shangyuan Village, Haidian District, Beijing, P.R. China
[d]Beijing Jiaotong University, Shangyuan Village, Haidian District, Beijing, P.R. China
[e]Beijing Capital Agribusiness & Food Group Co. Ltd., Xicheng District, Beijing, P.R. China

**ABSTRACT**

With the gradual normalization of the COVID-19, unmanned delivery has gradually become an important contactless distribution method around China. In this paper, we study the routing problem of unmanned vehicles considering path flexibility and the number of traffic lights in the road network to reduce the complexity of road conditions faced by unmanned vehicles as much as possible. We use Monte Carlo Tree Search algorithm to improve the Genetic Algorithm to solve this problem, first use Monte Carlo Tree Search Algorithm to compute the time-saving path between two nodes among multiple feasible paths and then transfer the paths results to Genetic Algorithm to obtain the final sequence of the unmanned vehicles fleet. And the hybrid algorithm was tested on the actual road network data around four hospitals in Beijing. The results showed that compared with normal vehicle routing problem, considering path flexibility can save the delivery time, the more complex the road network composition, the better results could be obtained by the algorithm.

**ARTICLE INFO**

*Keywords:*
Unmanned vehicle;
Path flexibility;
Vehicle routing problem;
Genetic Algorithm (GA);
Monte Carlo Tree Search algorithm (MCTS);
COVID-19;
Pandemics

**Corresponding author:*
xclu@bjtu.edu.cn
(Lu, X.C.)

*Article history:*
Received 15 August 2022
Revised 9 October 2022
Accepted 15 October 2022



## 1. Introduction

The Novel Coronavirus Disease (COVID-19) broke out globally in 2020, and in November 2021, the mutant virus Omicron was discovered and spread rapidly around the world. According to WHO, the strain spreads faster and is more transmissible. By February 2022, the Omicron strain has become a major epidemic strain worldwide. Due to the wide range and high contagiousness of the epidemic, especially the significant characteristics of human-to-human transmission, the Chinese government has always taken strict precautions and implemented closed-off management in high-risk areas to minimize the spread of the epidemic. Thus, unmanned and contactless techniques have become important force in the fight against the epidemic. With the spread of the epidemic, more and more cities, such as Changsha and Shanghai have begun to use unmanned vehicles to distribute medical suppliers to the epidemic areas.

Compared to conventional manned vehicles, unmanned delivery vehicles are far more reliant on road conditions. For technical reasons, unmanned vehicles are less able to adapt to complex road conditions than normal vehicles. Hence the major research on unmanned vehicles usually focus on the design of algorithms based on uncertain traffic situations or obstacle avoidance for unmanned vehicles. However, under circumstance of the epidemic, considering of all technological aspects to plan thorough routes for unmanned vehicles can better meet the requirements of contactless delivery. The traditional vehicle routing problems consider the distribution sequences between demand points solely and ignore the fact that there are frequently multiple alternate paths between demand points in the actual distribution processes. The traffic situations and journey times of various routes are different and have substantial impact on the safety and efficiency of unmanned vehicles.

In reality, usually the more traffic lights need to go through, the more complex information needs to be processed, so this paper incorporates the number of traffic lights in the road network into the vehicle routing problem, considers to select a safer and faster path for unmanned vehicles. Establishing a vehicle routing problem model with paths flexibility (VRP-PF) with the goal of minimizing distribution time for unmanned vehicles.

## 2. Literature review

Since the unmanned vehicles relies heavily on road conditions and traffic situations, for unmanned delivery vehicles, most researchers take into account the unmanned vehicles' ability of avoiding obstacles and adapting to the traffic conditions.

Hu [1] *et al*. designed a genetic simulated annealing algorithm to solve the unmanned vehicles routing problem with road conditions updates, and adjusted the delivery plan in real time based on the local update strategy for the pre-optimize paths based on the road condition information, and the results showed that the algorithm has more advantages than traditional genetic algorithms under complex road conditions. Guan [2] proposed an unmanned vehicles routing problem model based on traffic situations. To improve the adaptability of unmanned vehicles to road conditions, a DQN local optimization model with heuristic reward and adaptive exploration strategy was proposed. This model could reduce delivery time and increase delivery efficiency, but it did not involve the obstacle avoidance problem of unmanned vehicles and was not tested on real traffic data. Zhu [3] and Han [4] both studied the unmanned vehicle routing problem using deep reinforcement learning, with the difference that Zhu's research targeted the obstacle avoidance problem of unmanned vehicles in dynamic environments, while Han's research considered the objective of minimizing distance and the number of vehicles from the perspective of unmanned fleets. Tavoosi [5] *et al*. designed an improved particle swarm algorithm to process certain and uncertain obstacles to obtain the optimal paths. Based on total driving distance and waiting time, Shi W. *et al*. proposed a multi-objective scheduling model to solve the path conflict problem of automated guided vehicles (AGVs) and used the A* path planning algorithm to search the shortest path of AGV [6]. Erenoglu used the Unmanned Aerial Vehicles (UAV) based 3D city modelling approach to be manage and plan urban areas [7]. In view of many scholars consider the real-time traffic conditions in unmanned vehicles routing problem, Wang [8] *et al*. proposed a routing model for unmanned vehicles in the case of GPS system failure. Additionally, Levy [9] *et al*. considered the unmanned vehicles routing problem under fuel-limited conditions and designed multiple neighbourhood shakes to improve the variable neighbourhood search algorithm, which was able to obtain better results compared with the traditional variable neighbourhood search algorithm but the result was not an optimal solution. Zhao [10] designed a genetic algorithm to solve the unmanned vehicles routing problem considering the charging and switching requirements of unmanned vehicles. It can be seen that the research on unmanned vehicles routing problem mainly focus on obstacle avoidance considering traffic conditions and energy supply of unmanned vehicles. Besides, heuristic algorithms are the main solution approaches used.

There are many different variants of the VRP, like Split-Delivery VRP [11], Heterogeneous VRP with Time Windows [12], stochastic VRP [13], VRP with Pickup and Delivery [14], ConVRP (Consistent Vehicle Routing Problem) [15] and EVRP (electric vehicle routing problem) [16] etc. But few research focus on the vehicle routing problem with path flexibility (VRP-PF). This problem was first defined by Huang [17] *et al*. in 2017, and they developed model considering time windows under deterministic and uncertain traffic conditions. The model was solved by CPLEX and obtained the approximate optimal solutions. Liu [18] *et al*. proposed a green vehicles routing model considering the fuel consumption of vehicle acceleration and waiting at traffic lights and established the model with path flexibility to minimizing fuel and other costs. Due to the high complexity of the model, it could only solve instances with 10 demand points. But their research proves that routes planning considering path flexibility can save costs. Wang [19] *et al*. proposed a vehicle routing problem model with path flexibility for electric vehicles, considering the selection of charging stations. Then they designed a variable neighbourhood search algorithm to solve this problem, but they only considered multiple choices of charging stations, multiple paths between the stations are not involved. Guo [20] *et al*. developed a time-dependent bus routing problem model considering traffic congestions with path flexibility, and designed a tabu search algorithm to solve it. Given that the safety of unmanned vehicles is highly dependent on road conditions and the distribution of epidemic supplies are time-efficient, we incorporate the waiting time during traffic lights to measure road conditions and establish a vehicle routing problem model with path flexibility. Then we design a hybrid heuristic algorithm, using Monte Carlo tree search algorithm to improve the Genetic Algorithm to solve the routing problem with path flexibility.

## 3. Model and algorithm of vehicle routing problem with path flexibility

### 3.1 Problem description and mathematic model

The vehicle routing problem with path flexibility is defined on a directed graph $G = (V, P)$, where $V = \{0,1,2,\ldots,n\}$ is the set of vertices, $P = \{(i, j, p): i, j \in V, i \neq j, p \in P_{ij}\}$ is the set of paths, and $P_{ij}$ is the optional path from vertex $i$ to vertex $j$. In the set $V$, vertex 0 denotes the starting point and the rest vertices denote the demand points. In the set $P$, the length of the path $p_{ij}$ is $d_{ijp}$, the number of traffic lights is $l_{ijp}$. $N$ denotes the set of unmanned vehicles, where all vehicles are homogeneous, and the capacity of the vehicle is $C$. The vehicle meets a red light with a certain probability $S$ and the waiting time is w. The speed of unmanned vehicle is $v_{ijp}$, which is related to time and the road area where the unmanned vehicle is located. The objective is to minimise the time cost and find a solution that satisfies the following constraints: (1) the demand at each demand point is satisfied and the demand cannot be split; (2) all vehicles depart from and return to the starting point; (3) minimise the number of traffic lights in the optimal paths. An example diagram of this problem is shown in Fig. 1.

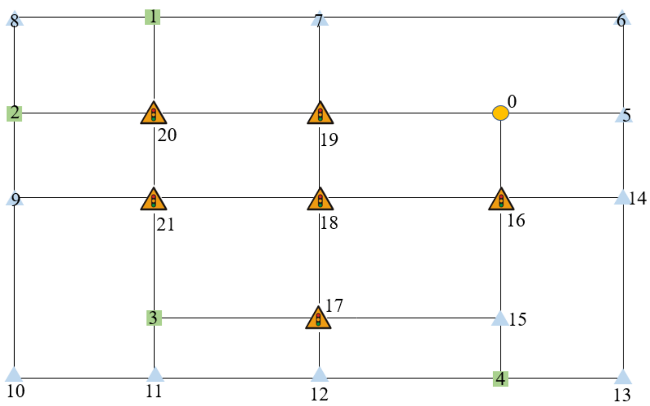


**Fig. 1** Schematic diagram of VRP-PF

Assuming the fleet of unmanned vehicles are homogeneous, the yellow dot 0 in Fig. 1 indicates the departure point of all vehicles in the fleet, the green square dots 1,2,3,4 are demand points, the traffic light marker indicates that there is a traffic light at this junction and vehicles may need to wait for a while when the light is red. The blue triangular dots are non-demand nodes in the road network. Suppose that all nodes in the diagram are disconnected, and the unmanned vehicle needs to travel from point 0 to demand point 1, there are multiple paths to choose, such as 0-5-6-7-1, 0-19-7-1 or 0-19-20-1. For the road network with only 22 nodes shown in Fig. 1, there are more than dozens of feasible paths between each two demand points, which greatly increases the complexity of the problem than traditional routing problem.

Unmanned delivery vehicles are low-speed vehicles, and the Implementation Rules for the Management of Unmanned Delivery Vehicles promulgated by the Beijing Economic and Technological Development Area in May 2021 requires that the speed of unmanned delivery vehicles should not exceed 15 km/h. Besides, the speed of unmanned vehicles varies with the traffic conditions in real life. Therefore, we map the traffic indexes crawled from Baidu map to the speeds of unmanned vehicles, and the corresponding table of traffic indexes and speeds is shown in Table 1. The expression of speed is a piecewise function which is shown in Fig. 2.

**Table 1** Correspondence between traffic index and travel speed

| Real-time vehicle speed | Traffic index | Unmanned vehicle's speed |
|---|---|---|
| >30 | 1 | 15 |
| 10-30 | 2 | 10 |
| <10 | 3 | 5 |

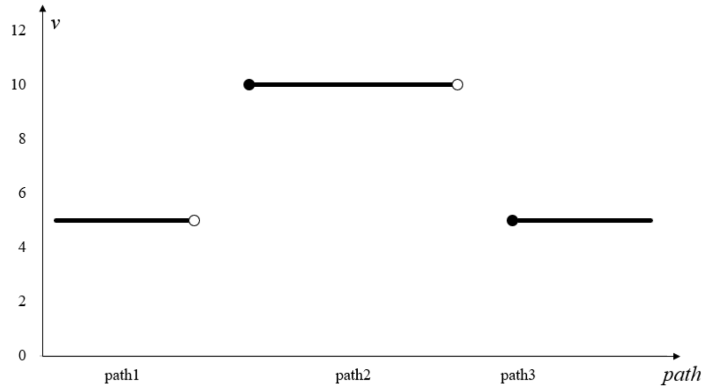


**Fig. 2** Speeds of unmanned vehicles on different roads

The optimization objective in this paper is delivery time of unmanned vehicles, as shown in Eq. 1.

$$\min T = \sum_{(i,j)\in V} \sum_{p\in P} \frac{d_{ijp}}{v_{ijp}} x_{ijp}^k + Sw_{ijp} l_{ijp} x_{ijp}^k, \forall k \in N \tag{1}$$

Define the decision variables and associated parameters as follows.

$$x_{ij}^k = \begin{cases} 1, & \text{if arc } (i,j) \text{ } is \text{ on the optimal route} \\ 0, & \text{otherwise} \end{cases}$$

$$x_{ijp}^k = \begin{cases} 1, & \text{if the vehicle travels path } P_{ijp} \text{ on the arc } (i,j) \\ 0, & \text{otherwise} \end{cases}$$

$C_{ijp}^k$ is actual capacity when vehicle $k$ is on arc $(i,j,p)$, and $q_i$ is demand of customer $i$. Therefore, the question can be formulated as follows.

*s.t.*

$$\sum_{i\in V, i\neq j} x_{ij} - \sum_{i\in V, i\neq j} x_{ji} = 0, \qquad \forall j \in V \tag{2}$$

$$q_j x_{ij} \leq C_{ij}^k \leq (C - q_i) x_{ij}, \forall (i,j) \in V \tag{3}$$

$$\sum_{p\in P} x_{ijp}^k = x_{ij}, \qquad \forall (i,j) \in V \tag{4}$$

$$\sum_{p\in P} C_{ijp} = C_{ij}, \qquad \forall(i,j) \in V \tag{5}$$

$$q_j x_{ijp} \le C_{ijp}^k \le (C - q_i)x_{ijp}, \forall(i,j) \in V, p \in P \tag{6}$$

$$x_{ij} \in \{0,1\}, \forall(i,j) \in V \tag{7}$$

$$C_{ij} \ge 0, \forall(i,j) \in V \tag{8}$$

$$x_{ijp} \in \{0,1\}, \forall(i,j) \in V, p \in P \tag{9}$$

$$C_{ijp} \ge 0, \forall(i,j) \in V, p \in P \tag{10}$$

$$q_i > 0, \forall i \in V\backslash\{0\} \tag{11}$$

$$q_0 = 0 \tag{12}$$

Eq. 2 is the vehicle flow conservation constraint. Constraint Eq. 3 ensures that the volume of unmanned vehicles at each node does not exceed the maximum vehicle capacity. Eq. 4 ensures that each unmanned vehicle selects only one feasible path from node $i$ to node $j$. Constraints Eqs. 5-6 ensure that supplies are transported on only one feasible path and do not exceed the maximum vehicle capacity. The rest are specific constraints of the variables.

### 3.2 Monte Carlo Tree Search algorithm (MCTS)

The vehicle routing problem belongs to NP-hard problem, and the vehicle routing problem with path flexibility is more difficult because the decisions to make are not only the routing decision but also the path selection decision depending on the departure time and the congestions in the relevant road network. The problem can be regarded as a two-stage problem with finding the optimal sequence of demand points and the optimal path selection between demand points. Moreover, the sequence of demand points affects path selection between points, and different paths affect the sequence of demand points in reverse. Since in the real road network, roads are crisscrossed and there are often numerous feasible paths between two points, Huang [17] *et al.* used Dijkstra's algorithm to find the shortest path between two points when considering path flexibility. However, the contrasting traffic conditions of different roads and the variational speed on different roads increase the difficulties of using exact algorithms. Hence, we apply the Monte Carlo tree search algorithm (MCTS) to solve the path flexibility of the problem and adopt MCTS to improve the genetic algorithm to solve the whole problem.

MCTS is a method for determining the optimal policy in a given domain. It is a simulation-based search algorithm with a tree structure that combines depth-first search and breadth-first search. Furthermore, it maintains superior results when the search space is huge and is widely used in fields such as games [21-24]. Therefore, MCTS is able to find the acceptable path rapidly for the large datasets. The process of MCTS can be divided into four steps: selection, expansion, simulation, and backpropagation, repeated these four steps until convergence [25].

The selection process is commonly implemented using the Upper Confidence Bound for Tree (UCT) algorithm, which searches and selects the next node to be visited among all the nodes, the formula of UCT is shown as Eq. 13.

$$UCT = \overline{X_j} + 2C_p\sqrt{\frac{2\ln n}{n_j}} \tag{13}$$

where $n$ is the number of times the current parent node has been visited, $n_j$ is the number of times the child node has been visited, $C_p$ is a constant greater than zero, and the value of $\overline{X_j}$ usually between [0,1], [24].

Even though the UCT strategy can provide acceptable outcomes, the rate of convergence is modest. To improve the efficiency, the weight of the node depends on the travel time, and the shorter the travel time is, the higher the weight is and the node is more likely to be selected. Therefore, the pseudo for the algorithm can be written as Algorithm1.

**Algorithm1**：path search for MCTS

**Input**：origin node $n_o$, destination node $n_d$
**Output**: optimal path $p$ between $n_o$ and $n_d$

function PathSearch($Array$, $n_o$, $n_d$)
Disconnect $n_o$ from other nodes and initialize trial nodes list $L$
**if** $Array[d_{oj}]$ != 0 **then**
  $L \leftarrow$ add $n_j$ to $L$
**end if**
**while** $n_i$ != $n_d$ **do**
  $n_i \leftarrow$ Select a node $n_i$ from $L$ according to the weight
  $p \leftarrow$ add $n_i$ to $p$
**end while**
**return** $p$
**end function**

Unlike complex games such as Go (Weiqi), game theory is not involved during the routing search process and therefore there is no need to switch decisions, so we omit the backpropagation process. The routing search is able to find a solution inevitably (if the path is not feasible can be named as a non-feasible solution), so by setting a certain number of iterations we can implement the simulation process in MCTS. By simulating $k_{max}$ times, the final output of the path with the highest weight can be fed back to the genetic algorithm, the flow chart of MCTS algorithm is shown in Fig. 3.

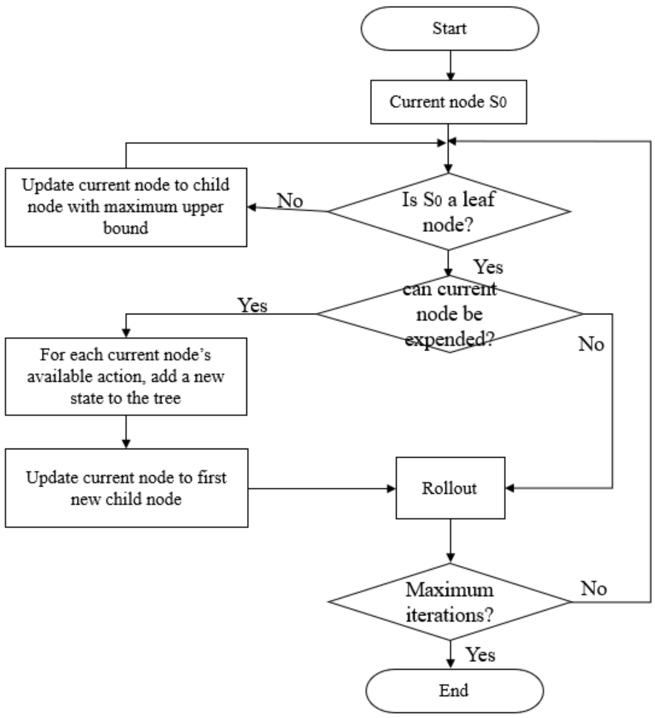


**Fig. 3** Flow Chart of MCTS Algorithm

### 3.3 Monte Carlo Tree Search Improved Genetic Algorithm (MCTS-GA)

The Monte Carlo tree search algorithm can find the optimal path between two nodes effectively, but it cannot solve the vehicle routing problem. In contrast, the genetic algorithm has better search capability and scalability, so we use the framework of the genetic algorithm and combined with the Monte Carlo tree search algorithm to solve the entire problem.

*Coding design*

Chromosomes are encoded using decimal coding that is frequently used in genetic algorithms in this paper, but each node includes an attribute label. The nodes in the road network are divided into four categories, starting nodes (point 0 in Fig. 1), customer demand nodes (green square nodes in Fig. 1), road nodes without demand (blue triangular nodes in Fig. 1) and traffic lights nodes (nodes with traffic light signs in Fig. 1), which together form a complete road network. In the actual distribution work, the customer demand nodes are the nodes that required to make decisions about the order of distribution for the vehicle routing problem, while the road nodes and traffic lights nodes are the nodes that required to make decisions about whether or not to pass for path flexibility.

Therefore, the attribute labels of the different nodes need to be assigned to the nodes in order for the algorithm to identify the nodes to be processed at different stages when coding. A schematic of the coding scheme is shown in Fig. 4 (using a feasible path in the road network of Fig. 1 as an example).

Fig. 4 shows a complete feasible route for an unmanned vehicle, which includes both the demand nodes to be delivered and all road nodes in the road network to be passed through during delivery. But when computing the vehicle routing problem with genetic algorithm, the code of chromosome can be streamlined to retain only the starting nodes and customer demand nodes, which means the code shown in Fig. 4 only needs to be processed as (0,2,1,0). This route is the delivery route for an unmanned vehicle without path flexibility (assuming that the sum of the demand does not exceed the vehicle capacity). In contrast, in the process of MCTS, the entire road network needs to be processed, that means the path with minimized travel time and traffic lights between each two nodes in the route needs to be found in turn. For example, a feasible path from the starting point to customer demand node 2 can be expressed as (0,19,20,2).

| 0 | 19 | 20 | 2 | 8 | 1 | 7 | 6 | 5 | 0 |
|---|---|---|---|---|---|---|---|---|---|
| Origin | Traffic light | Traffic light | Customer node | Road node | Customer node | Rode node | Rode node | Rode node | Origin |

**Fig. 4** Schematic of complete route coding scheme

*Crossover, mutation and heredity*

Both the crossover and mutation operations are directed at the vehicle routing problem, without considering path flexibility. The crossover process uses a two-opt crossover. To avoid duplicate fragments or missing fragments in the offspring generated after the crossover, we first randomly select sample fragments from parent 2 and inserts them into the corresponding positions of the offspring, and then traverses parent 1 and inserts the genes that are not duplicated with the sample fragments therein in turn to form new offspring. The crossover process is shown in Fig. 5 (the crossover process does not consider road nodes and traffic lights nodes, assuming that all nodes except node 0 in Fig. 5 are customer demand nodes).

The mutation process is a two-point mutation, which means that two genes on a chromosome that do not contain the first and last gene are randomly selected to swap positions. To improve the efficiency of the search, an elitist selection strategy is used, whereby the top 2 % of the offspring in each generation are retained and placed directly into the next generation. Besides, the idea of an invasive weed algorithm is involved so that the more adapted individuals produce relatively more offspring.

| | | | | | | | | | | |
|---|---|---|---|---|---|---|---|---|---|---|
| P1 | 0 | 19 | 20 | 2 | 8 | 1 | 7 | 6 | 5 | 0 |
| P2 | 0 | 6 | 20 | 1 | 7 | 5 | 8 | 2 | 19 | 0 |
| Child | 0 | 19 | 20 | 1 | 7 | 5 | 8 | 2 | 6 | 0 |

**Fig. 5** Schematic diagram of the crossover process

*Adaptability function*

After the allocation sequence of customer demand nodes has been generated by the genetic algorithm, the MCTS can be used to obtain the optimal path between the customer demand nodes then the travel time and total length of the path as well as the times of traffic lights passed can be calculated. The individual with the greater the fitness is more retainable, so according to Eq. 1 the fitness function can be expressed as Eq. 14.

$$fitness = {}^{1}/_{T} \tag{14}$$

*MCTS-GA algorithm flow*

The above describes the process of selecting feasible paths between nodes using the MCTS algorithm and the solution of the vehicle routing problem using genetic algorithm respectively, but the two processes need to be carried out in unison to obtain a complete solution for the problem. The flowchart of the Monte Carlo Tree Search Improved Genetic Algorithm (MCTS-GA) is shown in Fig. 6.

After generating the sequence of customer demand nodes by the genetic algorithm, we use the MCTS to find the optimal path between each two nodes and the search result is transferred to the genetic algorithm for population fitness calculation. Then cross and mutation operations are carried out to generate the new population, and the complete path is finally output after repeated iterations until reach the maximum number of iterations.

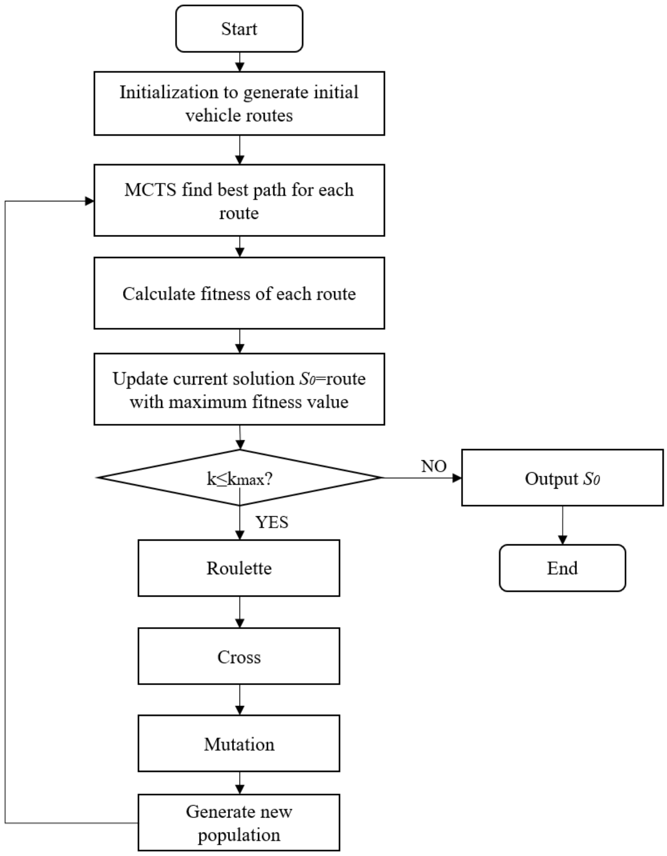


**Fig. 6** Flow chart of MCTS-GA algorithm

## 4. Numerical experiments: Results and discussion

In this section, the algorithm performance is tested by numerical experiments using real road network in Beijing. As adopting unmanned vehicles to delivery epidemic medicine is considered, we choose some of the hospitals in Beijing as the starting points for medicine distribution. The unmanned vehicles start from the hospital to the community, and the road networks around the target hospitals are established as examples for testing.

The algorithm is implemented using Python code in an Intel(R) Core (TM) i5-8250U CPU @ 1.60 GHz and 8GB of RAM. The parameters of algorithm and unmanned vehicles are shown in Table 2, the example information is shown in Table 3.

**Table 2** Algorithm parameters and unmanned vehicle performance parameter settings

| Parameters | Value |
|---|---|
| Crossover probability | 0.8 |
| mutation probability | 0.2 |
| Iterations of GA | 100 |
| Iterations of MCTS | 500 |
| Probability of encountering a red light | 0.5 |
| Red light waiting time | 90 seconds |
| capacity of unmanned vehicle | 20 pieces |

**Table 3** Instance information table

| Instance name | Number of customer nodes | Number of road nodes | Number of traffic lights | Total amount of nodes |
|---|---|---|---|---|
| Hospital23 | 6 | 11 | 5 | 23 |
| Hospital29 | 8 | 17 | 3 | 29 |
| Hospital39 | 11 | 21 | 7 | 39 |
| Hospital58 | 15 | 28 | 14 | 58 |

In this paper, three Beijing hospitals are selected as target hospitals, and two small-scale road networks and one medium-scale road network were established as examples. Example Hospital23 is the Sixth Hospital of Peking University, with a road network consisting of 23 nodes; Example Hospital29 is Hospital 466, with a total of 29 nodes in the road network. Example Hospital39 is the Chinese Armed Police General Hospital, with a total of 39 nodes in the road network. Example Hospital58 is the Bayi Children's Hospital, with a total of 58 nodes in the road network. The results of examples are shown in Figs. 7-10 respectively, where the road network is shown in Figs. (a) and the distribution results are shown in Figs. (b), and the green square nodes in Figs. (b) are customer demand nodes. Tables 4-7 show the specific distribution paths of each example.


(a) (b)

**Fig. 7** Results of Hospital23

**Table 4** Detailed distribution paths of Hospital23

| Unmanned vehicle | Customer nodes | Load pieces | Load Factor (%) | Distribution path | Times of passing through traffic lights |
|---|---|---|---|---|---|
| 1 | 21,13,1 | 16 | 80 | 0,2,21,13,12,1,0 | 0 |
| 2 | 8,5 | 20 | 100 | 0,2,3,8,9,10,11,6,5,4,3,2,0 | 3 |
| 3 | 19 | 15 | 75 | 0,2,21,13,14,15,19,15,14,13,21,2,0 | 2 |

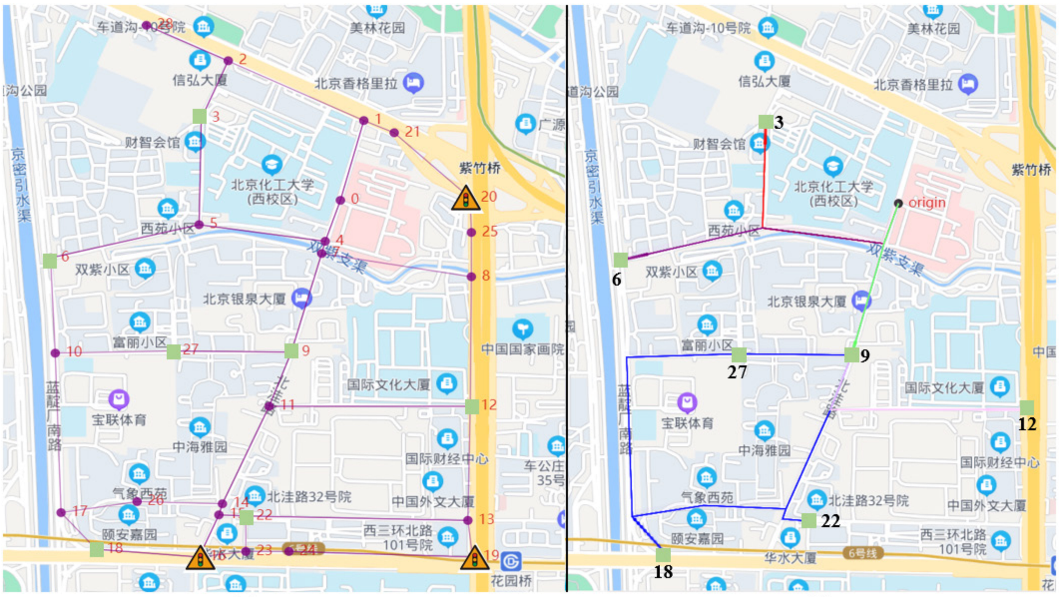


**Fig. 8** Results of Hospital29

**Table 5** Detailed distribution paths of Hospital29

| Unmanned vehicle | Customer nodes | Load pieces | Load factor | Distribution path | Times of passing through traffic lights |
|---|---|---|---|---|---|
| 1 | 18,22,27 | 20 | 100 | 0,4,7,9,11,14,15,22,15,14,26 ,17,18,17,10,27,9,7,4,0 | 0 |
| 2 | 3 | 20 | 100 | 0, 4, 5, 3, 5, 4,0 | 0 |
| 3 | 6 | 18 | 90 | 0, 4, 5, 6, 5, 4,0 | 0 |
| 4 | 9,12 | 19 | 95 | 0, 4, 7, 9, 11, 12, 11, 9, 7, 4,0 | 0 |
| 5 | 20 | 20 | 100 | 0, 1, 21, 20, 25, 8, 7, 4,0 | 0 |
| 6 | 28 | 18 | 90 | 0,4,5,3,2,28,2,3,5,4,0 | 0 |

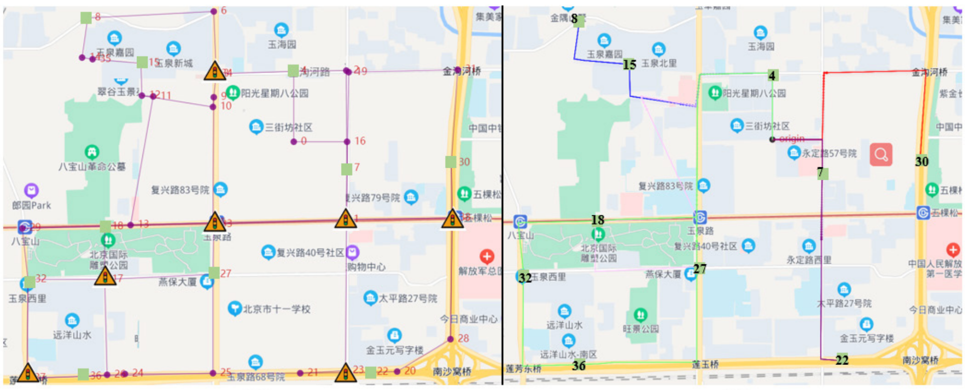


**Fig. 9** Results of Hospital39

**Table 6** Detailed distribution paths of Hospital39

| Unmanned vehicle | Customer nodes | Load pieces | Load factor (%) | Distribution path | Times of passing through traffic lights |
|---|---|---|---|---|---|
| 1 | 8,15 | 20 | 100 | 0,4,3,9,10,12,15,35,14,8,1 4,35,15,12,10,9,3,4,0 | 0 |
| 2 | 7,30 | 17 | 85 | 0,16,7,16,19,31,30,31,19,1 6,0 | 0 |
| 3 | 22 | 18 | 90 | 0,16,7,1,23,22,23,1,7,16,0 | 4 |
| 4 | 4,18,27 | 19 | 95 | 0,4,3,9,10,11,5,18,17,27,5, 9,3,4,0 | 2 |
| 5 | 24,32,36 | 16 | 80 | 0,4,3,9,5,27,25,24,26,36,3 7,32,29,18,13,5,9,3,4,0 | 3 |

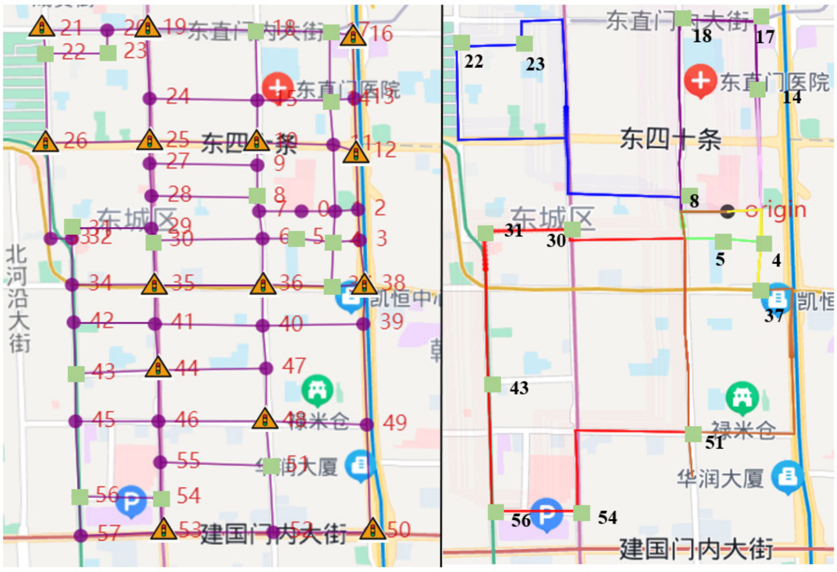


(a) (b)

**Fig. 10** Results of Hospital58

**Table 7** Detailed distribution paths of Hospital58

| Unmanned vehicle | Customer nodes | Load pieces | Load factor (%) | Distribution path | Times of passing through traffic lights |
|---|---|---|---|---|---|
| 1 | 22,23 | 19 | 95 | 0, 7, 8, 28, 27, 25, 24, 19, 20, 23, 22, 26, 25, 27, 28, 8,7,0 | 4 |
| 2 | 30,31,43,56,54 | 20 | 100 | 0, 7,6,30,29, 31, 32, 34, 42, 43, 45, 56, 54, 55, 46, 48, 47, 40, 36, 6,7,0 | 2 |
| 3 | 17,18,8 | 17 | 85 | 0,1,11,14,17,18,15,10,9, 8,7,0 | 1 |
| 4 | 14 | 15 | 75 | 0, 1, 11,14, 11, 1,0 | 0 |
| 5 | 5 | 12 | 60 | 0, 7, 6, 5, 4, 1,0 | 0 |
| 6 | 4,51 | 17 | 85 | 0, 1, 4, 37, 38, 39, 49, 48, 51, 48, 47, 40, 36, 6, 7,0 | 4 |
| 7 | 37 | 20 | 100 | 0, 1, 4, 37, 4, 1,0 | 0 |

**Table 8** Comparison of VRP-PF and VRP-SP

| Indicator | Instance | VRP-PF | VRP-SP | *D* |
|---|---|---|---|---|
| Total time (min) | Hospital23 | 20 | 23 | -3 |
| | Hospital29 | 44 | 50 | -6 |
| | Hospital39 | 59 | 69 | -10 |
| | Hospital58 | 64 | 79 | -15 |
| Total distance (m) | Hospital23 | 5742 | 5532 | 210 |
| | Hospital29 | 11380 | 9680 | 1700 |
| | Hospital39 | 15188 | 12352 | 2836 |
| | Hospital58 | 16322 | 15243 | 1079 |
| Times of passing through traffic lights | Hospital23 | 5 | 7 | -2 |
| | Hospital29 | 0 | 2 | -2 |
| | Hospital39 | 9 | 21 | -12 |
| | Hospital58 | 11 | 16 | -5 |

The results illustrate that 3 unmanned vehicles are required for delivery in Example Hospital23, with an average load factor of 85 %. 6 unmanned vehicles are required for delivery in Example Hospital29, with an average load factor of 96 %. 5 unmanned vehicles are required for delivery in Example Hospital39, with an average load factor of 90 % and 7 unmanned vehicles are required for delivery in Example Hospital58, with an average load factor of 86 %. As Hospital23, Hospital39 and Hospital58 contains many traffic lights in the road networks, it is difficult to avoid going through the traffic lights during path selection. In the result of Example Hospital39, the times of passing through traffic lights is obviously reduced. Table 8 shows the results of considering path flexibility compared with considering the shortest path between two points, where VRP-PF is the results considering path flexibility using the algorithm proposed in this paper, VRP-SP is the results without considering path flexibility using Dijkstra algorithm to find the shortest path between two points. Meanwhile, *D* is the optimization difference, where the negative value means our algorithm got better results than Dijkstra algorithm.

From the results, it can be seen that considering path flexibility can reduce the times of passing through traffic lights and improve the delivery efficiency at the expense of increasing the total path length. For the sake of presentation, the reduction in total distance is divided by a thousand to uniform the order of magnitude with other indicators in Fig. 11. It can be seen that in Example Hospital58, total time decreases 15 minutes compared with Dijkstra algorithm while total time only decreases 3 minutes in Example Hospital23. The times of passing through traffic lights reduces 5 and 12 times in Example Hospital58 and Hospital39 respectively while this indicator only reduce 2 times in Hospital29 and Hospital23. The optimization is more obvious in the case of complex road network with more traffic lights.

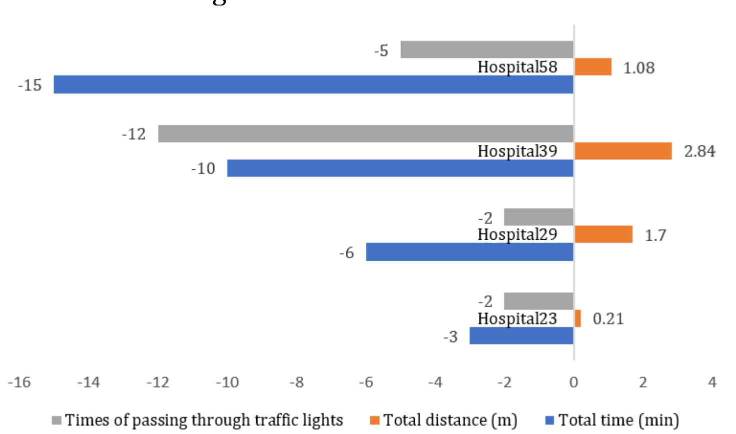


**Fig. 11** Comparison of numerical examples

## 5. Conclusion

The normalization of epidemics has prompted the development of contactless distribution. In this paper, the path flexibility between demand points is considered when dealing with vehicle routing problem for unmanned vehicles. In the case where there are multiple feasible paths between two demand points, the number of traffic lights in the road network is considered from the perspective of driving safety of unmanned vehicles. We build the mathematic model of path flexibility vehicle routing problem with the objective to minimize the distribution time. The MCTS algorithm is used to select the feasible paths between two nodes, and the results are fed back to the genetic algorithm for further optimization to finally determine the complete driving scheme. Finally, we adopt actual road networks in Beijing as examples, obtain solutions under different sizes of road networks, and the results show that the algorithm can select better paths with less driving time for different sizes of instances, and can maintain a high vehicle full load rate. Compared with routing problem that does not consider path flexibility, the results show that considering path flexibility can not only reduce the delivery time but also reduce the times of passing through traffic lights for unmanned vehicles. For more complex road conditions, the better results the algorithm can get.

The algorithm considering path flexibility can not only be used for the routing planning of unmanned vehicles in the distribution of emergency supplies, but also for the path planning of AGV picking and distribution in the warehouse. In the process of vehicle navigation, the algorithm based on Monte Carlo tree search can also flexibly take into account the driver's experience and other factors, and get better results in the congested road sections. Hence the algorithm proposed in this paper can also enrich the navigation algorithms. However, the method requires complete road network information in the process of preliminary data preparation, including node coordinates, connectivity between nodes as well as distances and driving speed of segmented roads, which is the weakness of the algorithm. In addition, for unmanned vehicles, real-time road condition can also be considered to be passed into the algorithm to improve distribution efficiency while improving the ability of unmanned vehicles to cope with complex road conditions and driving safety.

## Acknowledgement

We thank the Editor and anonymous referees for their many helpful comments on an earlier version of our paper. This work was supported in part by the National Natural Science Foundation of China under grant numbers 72171016; and the Beijing Logistics Informatics Research Base.

## References

[1] Hu, H., Tang, Z.Q., Liu, F.X., Wang, Y.Q., He, X.F., Zhao, J. (2022). Optimization of contactless distribution of medical protective materials under the epidemic, *Chinese Journal of Management Science*, 1-11, doi: 10.16381/j.cnki.issn1003-207x.2020.1925.
[2] Guan, M. (2021). *Research on route planning of unmanned vehicle logistics distribution,* Master's thesis, Beijing University of Posts and Telecommunications, Beijing, China, doi: 10.26969/d.cnki.gbydu.2021.002076.
[3] Zhu, J. (2021). *Research on path planning of unmanned vehicles based on deep reinforcement learning*, Master's thesis, Xi'an University of Technology, Xi'an, China, doi: 10.27391/d.cnki.gxagu.2021.000661.
[4] Han, Y.F. (2021). *Research on distribution path planning of unmanned logistics fleet based on deep reinforcement learning*, Master's thesis, Dalian University of Technology, Dalian, China, doi: 10.26991/d.cnki.gdllu.2021.002725.
[5] Tavoosi, V., Marzbanrad, J., Golnavaz, M. (2020). Optimised path planning of an unmanned vehicle in an unknown environment using the PSO algorithm, *IOP Conference Series: Materials Science and Engineering,* Vol. 671, Article No. 012009, doi: 10.1088/1757-899x/671/1/012009.
[6] Shi, W., Tang, D.B., Zou, P. (2021). Multi-objective automated guided vehicle scheduling based on MapReduce framework, *Advances in Production Engineering & Management,* Vol. 16, No. 1, 37-46, doi: 10.14743/apem2021.1.383.
[7] Erenoglu, R.C., Erenoglu, O., Arslan, N. (2018). Accuracy assessment of low cost UAV based city modelling for urban planning, *Tehnički Vjesnik – Technical Gazette*, Vol. 25, No. 6, 1708-1714, doi: 10.17559/TV-20170904202055.
[8] Wang, B., Misra, S., Sundar, K., Rathinam, S., Sharma, R. (2018). Routing multiple unmanned vehicles in GPS denied environments, In: *AIAA Information Systems-AIAA Infotech @ Aerospace, AIAA SciTech Forum*, 1-10, doi: 10.2514/6.2018-0897.
[9] Levy, D., Sundar, K., Rathinam, S. (2014). Heuristics for routing heterogeneous unmanned vehicles with fuel constraints, *Mathematical Problems in Engineering*. Vol. 2014, Article ID 131450, doi: 10.1155/2014/131450.
[10] Zhao, S.Y. (2021). *Research on path optimization of unmanned ground delivery vehicles in charging and power swapping model,* Master's thesis, Beijing Jiaotong University, Beijing, China, doi: 10.26944/d.cnki.gbfju.2021.003341.
[11] Min, J.N., Jin, C., Lu, L.J. (2019). Split-delivery vehicle routing problems based on a multi-restart improved sweep approach, *International Journal of Simulation Modelling*, Vol. 18, No. 4, 708-719, doi: 10.2507/IJSIMM8(4)CO19.
[12] Liu, M.L., Zhang, C., Wu, Q.L., Meng, B.R. (2021). Vehicle routing problem with soft time windows of cargo transport O2O platforms, *International Journal of Simulation Modelling*, Vol. 20, No. 2, 351-362, doi: 10.2507/IJSIMM20-2-564.
[13] Anuar, W.K., Lee, L.S., Seow, H.-V., Pickl, S.A. (2021). A multi-depot vehicle routing problem with stochastic road capacity and reduced two-stage stochastic integer linear programming models for rollout algorithm, *Mathematics*, Vol. 9, No. 13, Article No. 1572, doi: 10.3390/math9131572.
[14] Amalia, I.S., Bakhtiar, T., Jaharuddin. (2021). Minimizing the handling time in VRP with pickup-and-delivery and time windows, *Journal Conference Series, of Physics,* Vol. 1863, Article No. 012002, doi: 10.1088/1742-6596/1863/1/012002.
[15] Barros, L., Linfati, R., Escobar, J.W. (2020). An exact approach for the consistent vehicle routing problem (ConVRP), *Advances in Production Engineering & Management*, Vol. 15, No. 3, 255-266, doi: 10.14743/apem2020.3.363.
[16] Huang, A.Q., Zhang, Y.Q., He, Z.F., Hua, G.W., Shi, X.L. (2021). Recharging and transportation scheduling for electric vehicle battery under the swapping mode, *Advances in Production Engineering & Management*, Vol. 16, No. 3, 359-371, doi: 10.14743/apem2021.3.406.
[17] Huang, Y., Zhao, L., Van Woensel, T., Gross, J.-P. (2017). Time-dependent vehicle routing problem with path flexibility, *Transportation Research Part B: Methodological*, Vol. 95, 169-195, doi: 10.1016/j.trb.2016.10.013.
[18] Liu, X., Qi, M., Cheng, C. (2017). Green vehicle routing problem with path flexibility: In: *Proceedings of 2017 IEEE International Conference on Industrial Engineering and Engineering Management (IEEM)*, Singapore, 1037-1041, doi: 10.1109/IEEM.2017.8290050.
[19] Wang, L., Gao, S., Wang, K., Li, T., Li, L., Chen, Z. (2020). Time-dependent electric vehicle routing problem with time windows and path flexibility, *Journal of Advanced Transportation*, Vol. 2020, Article ID 3030197 doi: 10.1155/2020/3030197.

[20] Guo, R., Zhang, W., Guan, W., Ran, B. (2021). Time-dependent urban customized bus routing with path flexibility, *IEEE Transactions on Intelligent Transportation Systems*, Vol. 22, No. 4, 2381-2390, doi: 10.1109/TITS.2020.3019373.

[21] Sironi, C.F., Liu, J., Winands, M.H.M. (2020). Self-adaptive Monte Carlo tree search in general game playing, *IEEE Transactions on Games*, Vol. 12, No. 2, 132-144, doi: 10.1109/TG.2018.2884768.

[22] Sironi, C.F., Winands, M.H.M. (2018). Analysis of self-adaptive Monte Carlo tree search in general video game playing, In: *Proceedings of 2018 IEEE Conference on Computational Intelligence and Games (CIG)*, Maastricht, Netherlands, 1-4, doi: 10.1109/CIG.2018.8490402.

[23] Kimura, K., Tu, Y., Tanji, R., Mozgovoy, M. (2021). Creating adjustable human-like AI behavior in a 3D tennis game with Monte-Carlo tree search, In: *Proceedings of 2021 IEEE Symposium Series on Computational Intelligence (SSCI)*, Orlando, USA, 1-6, doi: 10.1109/SSCI50451.2021.9659551.

[24] Browne, C.B., Powley, E., Whitehouse, D., Lucas, S.M., Cowling, P.I., Rohlfshagen, P., Tavener, S., Perez, D., Samothrakis, S., Colton, S. (2012). A survey of Monte Carlo tree search methods, *IEEE Transactions on Computational Intelligence and AI in Games*, Vol. 4, No. 1, 1-43, doi: 10.1109/TCIAIG.2012.2186810.

[25] Zhou, K., Hong, Z., Hu, L. (2019). Cable diameter control based on Monte Carlo tree search, *Computer Engineering and Design*. Vol. 40, No. 8, 2389-2395, doi: 10.16208/j.issn1000-7024.2019.08.048.

APEM journal

**Advances in Production Engineering & Management**
Volume 17 | Number 4 | December 2022 | pp 439–454
https://doi.org/10.14743/apem2022.4.447

**ISSN 1854-6250**
Journal home: apem-journal.org
Original scientific paper

# End-of-line delivery vehicle routing optimization based on large-scale neighbourhood search algorithms considering customer-consumer delivery location preferences

**Niu, X.Y.**[a], **Liu, S.F.**[a,*], **Huang, Q.L.**[a]

[a]School of Economics and Management, Beijing Jiaotong University, Beijing, P.R. China

**A B S T R A C T**

Logistics is an important guarantee for economic and social development. Among the various aspects of logistics, the urban logistics end distribution link, which involves the direct connection between distribution personnel and customers, has a direct impact on customers' sense of experience and satisfaction with logistics services. At present, there are unscientific and unreasonable selection methods for logistics end distribution paths, often based on the subjective experience of distribution personnel, which often results in a mismatch between distribution paths and distribution needs, affecting market demand while further increasing the distribution costs of enterprises. Therefore, based on the characteristics of customer-consumers, this paper considers that consumers can select multiple receiving addresses, and each address has a corresponding time window limit. This paper finds that it needs to spend a lot of costs for the enterprise to improve the service level of distribution, and the enterprise can save the cost from time window, as well as obtain the better distribution time by using alternative addresses through the verification and analysis of an example. Based on the above analysis, this paper proposes the urban logistics terminal distribution path optimization path based on large-scale neighbourhood search algorithm, which can promote the further matching between logistics distribution enterprises and customer needs, so as to improve the probability of consumers receiving goods in time as well as reduce the cost of enterprises.

**A R T I C L E  I N F O**

*Keywords:*
Distribution;
Vehicle routing;
Optimization;
Path optimization;
End-of-line;
Large-scale neighbourhood search algorithm

**Corresponding author:*
(Liu, S.F.)
shfliu@bjtu.edu.cn

*Article history:*
Received 29 January 2022
Revised 23 August 2022
Accepted 3 September 2022



## 1. Introduction

With the development of e-commerce and the residents' travel behaviour always change, consumers often encounter the problem of receiving express delivery effectively at the end of the delivery. For customers, each day's life trajectory is distributed in different areas, there are living areas, work areas, entertainment areas, etc. Each area is often distributed in different places, and the life trajectory and time have a close relationship. For office workers, during the working day, the 9 to 5 hours are at the company, while the time spent at home is usually in the evening. The mismatch between courier services and customers' usage needs and living habits can result in lower service satisfaction. If the delivery address is filled in as the place of residence, there may be a situation where the customer is at work and signs for the delivery in person, which may end up being collected by the doorman or placed at an inconvenient pick-up point, easily resulting in lost items. If the delivery address is the workplace, there may be a meeting or business trip where the courier cannot be signed for in person. This puts the flexibility of the "last mile" delivery location to the test. The current courier delivery model can only choose one address for a customer's delivery, which can easily cause a mismatch between the delivery location and the customer's location of activity, which can also cause the consumer to not receive the goods in a timely manner, and the courier company's delivery failure will also increase the cost of delivery.

The changing nature of consumers' activity locations over time has led to new consumer expectations for services with diverse delivery locations. If consumers can provide multiple delivery locations in a single delivery service, the delivery company can flexibly deliver according to the consumer's delivery location, which not only increases the probability of timely receipt of goods by the consumer, but also avoids the cost of secondary delivery.

This paper considers the vehicle path problem with alternative addresses, which is an extension of the vehicle path problem with time windows. In this case, each customer may provide more than one delivery address in a delivery, each delivery address has priority, and each delivery address has its own time window. A large-scale neighbourhood search algorithm is also designed to solve the problem. The analysis of consumers who do not follow the first address for delivery reveals the following characteristics of these consumers: the time window does not match other consumers in that neighbourhood of the path; the preferred address is far from the delivery area of the path, while the alternative address is closer to the delivery area; and consumers who choose the alternative address tend to be at the beginning or the end of the path. The relationship between a company's distribution costs and service level was also analysed and it was found that the service level required the highest costs when the service level was in the medium to high range.

## 2. Literature review

The vehicle path problem was originally proposed by Dantzig and Ramser [1] equal to 1959 and applied to logistics and distribution activities. The vehicle path problem refers to the method of seeking the goods from the distribution centre to the customer under the constraints of multiple factors, such as the number of goods, the number of distribution vehicles, the address of the distribution centre and the address of the passenger and cargo receipt, etc. Through analysis and planning of reasonable distribution routes, the whole distribution process can achieve the least distribution time, the shortest distance and the lowest distribution cost. With the continuous expansion and deepening of theories in the field of logistics, the optimization of vehicle paths for end-of-line distribution has gradually become a key and hot issue of concern in the logistics industry in recent years, causing scholars to explore and research continuously. The article summarizes and analyses the vehicle path problem of end-delivery from three perspectives: path optimization considering self-pickup service, path optimization considering consumer preference, and path optimization considering differentiated service.

### 2.1 Vehicle route optimisation considering self-pick-up services

Self-pick-up service is an important part of terminal distribution, and with the diversification of consumer demand for self-pick-up, it has become increasingly important to improve the level of service, so it is imperative to continuously optimise the vehicle path of self-pick-up service. In the process of optimising the delivery route, the main considerations are the radiation range of the pick-up site, the service capacity of the site, the layout of the site, consumer satisfaction, the operating cost of the site and the price of the pick-up service.

In recent years, scholars at home and abroad have carried out diverse and extensive in-depth studies on the optimization of self-pickup services. Current and Schilling [2] pointed out that the pickup site must be within the service area of the delivery vehicle, and used the travel merchant problem to analyse and interpret the self-pickup behaviour of consumers. Li and Mao [3, 4] pointed out that no matter what form of self-pickup points such as Jingdong self-pickup cabinets, Feng Chao express cabinets, CaiBird post stations, etc., they all face the problem of optimizing the path for reasonable self-pickup services, and then the authors used indicators such as construction cost, customer satisfaction, and service capability to evaluate the service capability of self-pickup points, and also established a combined integer planning model with the lowest logistics service cost as the goal. Zhou *et al.* [5, 6] proposed the current path optimization problem faced by self-pickup services, i.e., consumers are widely and densely distributed, and it is impossible to accurately calculate the distribution path of goods, and took the customer points within the streets of Yudong in Banan District of Chongqing as the research object, argued the relationship between the location of self-pickup points and path optimization, and built a path optimization model for self-pickup distribution. Koç *et al.* [7] and Hua *et al.* [8] pointed out that the location of logistics distribution centres is an important task in the overall network optimisation of logistics systems, and a scientific centre location can assist in improving the relevant effects of path optimisation. To solve the location problem of distribution centres, Hua *et al.* [8] proposed an adaptive particle swarm optimisation algorithm with non-linear inertia weights and time-varying acceleration coefficients. Sankaran *et al.* [9] sorted out the problem of siting two groups of high-capacity facility locations and proposed a method for optimizing the siting of self-pickup sites by aggregating consumer pickup point information. Wang *et al.* [10] pointed out that there is a certain correlation between the price of self-service and brand image, and constructed a correlation function between the reachable distance of self-pickup path, the price of self-pickup service and the brand of self-pickup service. Guo *et al.* [11] conducted a study on vehicle route optimization and service strategies based on consumers' pickup radius, and pointed out that self-pickup considering consumers' pickup radius can effectively reduce the number of delivery vehicles and personnel, which can achieve the purpose of reducing the operation cost of end-distribution.

### 2.2 Vehicle path optimisation considering consumer preferences and behavior

In end-of-line delivery, consumers will consider various factors such as delivery method, delivery time and delivery price, and their preferences and behaviour towards different choices will also have an impact on vehicle route optimisation. In terms of delivery methods, 2.1 summarises the vehicle path optimisation considering self-pick-up services; meanwhile, domestic and international scholars have conducted in-depth and extensive research on vehicle path optimisation for home delivery, which is summarised in this summary. In terms of path optimisation for end-delivery home delivery services, Khouadjia [12] *et al.*, and Okulewicz and Mańdziuk [13] argue that in the end-delivery process, once a delivery person has accepted the instruction to deliver to a consumer, he or she cannot change the new delivery target until the current delivery task is completed before the next task can be carried out; based on this premise, Okulewicz and Mańdziuk [13] used a meta-heuristic to optimise the paths associated with the receipt of delivery instructions to vehicle assignment. Abdallah *et al.* [14] considered the end-of-pipe delivery problem as dynamic vehicle path optimisation and suggested that, for more efficient delivery of continuous goods, delivery personnel should go to a nearby planning delivery node at the completion of the delivery task and wait at the node for new delivery instructions and vehicle scheduling solutions. Keçeci *et al.* [15] pointed out the path optimisation for home delivery as variational path optimisation with pickup and delivery functions, and proposed a hybrid meta-heuristic based on simulated annealing algorithm and local search algorithm of SA-LS with minimum delivery cost as the objective. Silvestrin and Ritt [16] analysed the scenario of multi-carriage vehicles, where several different qualities or types of products that must be kept or handled separately and use a forbidden search algorithm to solve the problem. Soto *et al.* [17] solve the multi-warehouse open vehicle routing problem, which is a generalised case of capacity vehicle path optimisation; in this scenario, vehicles perform delivery services from different warehouses, visit consumers and complete the delivery of goods, without the goods deliverer then having to return to the end of the route at the warehouse.

Consumers' preferences for delivery time and delivery price also affect the path optimisation of delivery vehicles. Most of the current research on delivery time focuses on time window theory, while most of the research on delivery price focuses on delivery pricing theory. In terms of end distribution time, Taş *et al.* [18] studied the vehicle path problem with time window and random travel time, combined the relationship between transportation cost and service cost, i.e., the total vehicle travel distance and cargo arrival time, and proposed a path optimisation model based on this. Zhu *et al*. [19] considered the constrained situation of time window and built a path optimisation model for multi-vehicle logistics distribution under different environments with the objective of lowest total delivery cost and shortest delivery time. Gutierrez *et al*. [20] set the vehicle travel time and service time as random variables and solved the vehicle path optimisation problem under the premise that each consumer is served. Guedes and Borenstein [21] borrowed the processing method of space-time grid for distribution path optimisation and analysed the multi-warehouse vehicle type scheduling problem. Veenstra *et al*. [22] studied the problem of goods distribution and delivery based on the time window. Kim *et al*. [23] combined the uncertainties of delivery time, delivery demand, and real-time traffic conditions to build a logistics and delivery model for path optimisation. In terms of end-delivery prices, Tounsi *et al*. [24] develop a new heuristic algorithm for the delivery service pricing problem, where the delivery service and path optimization are carried out by the delivery side according to the price of the service chosen by the consumer. Hayel *et al*. [25] point out that consumer behaviour, especially the choice of a reasonable price, affects the path optimisation of end-delivery, and the authors later use a game theoretical. The topic was studied from a game theoretical perspective; Yang *et al*. [26] considered the different delivery costs of consumers for different delivery time slots, thus building a route optimization model with real-time pricing.

End-delivery is the last link in the transportation of goods, and the consumer as the participant in the final link can have a profound impact on route optimisation, regardless of the behaviour, in addition to the factors summarised above. For example, Ren *et al*. [27] argue that consumer preference behaviour can have an impact on end delivery and that customers may hold different attitudes towards different types of goods, while the authors later build a 4PL path optimisation model to conduct relevant research, proving the scientific validity of their view. Therefore, paying attention to consumer preferences and their behaviours has a positive significance and important role in the route optimisation of end-delivery, and can effectively improve the service efficiency of end-delivery.

### 2.3 Vehicle route optimization considering differentiated service provision

In the process of end-delivery, in addition to the service demand for ordinary delivery, increasingly diverse and differentiated services have emerged [28, 29], with the existence of cold chain logistics end-delivery, takeaway delivery, same-city delivery and end-delivery services in emergency scenarios (such as the delivery of emergency materials after a disaster). In addition, some end-delivery services are subject to certain additional top-up fees to ensure efficient delivery of goods.

The delivery target of cold chain logistics is usually frozen food, so the delivery service has to be completed within the period of food refrigeration to avoid food spoilage. As cold chain logistics plays an indispensable role in people's lives, research on cold chain logistics has been a hot topic for experts and scholars at home and abroad. Among them, in the end distribution of cold chain logistics, Deng *et al*. [30] and others believe that the end distribution process of cold chain logistics needs to increase the consideration of factors such as the degree of goods loss and goods refrigeration market, and through the introduction of the concepts of penalty cost, goods loss cost, refrigeration cost, out-of-stock cost, transportation cost and fixed cost, the path optimization of the end distribution of cold chain logistics is carried out. Zhang *et al*. [31] and others constructed a path optimisation model for cold chain logistics vehicles using a soft time window model and solved the optimal solution using an improved genetic algorithm. Ren *et al*. [32] studied a distribution scenario with multiple distribution centres sharing resources under the premise of ensuring on-time food delivery and established a vehicle path optimisation model for delivery at the lowest delivery cost of fresh food.

Food delivery service is a special kind of end delivery driving, the start and end point of food delivery are in the same city, and the delivery distance is significantly shortened compared to other methods. In addition, as consumers have the actual demand for fast meals, there are higher requirements for their takeaway delivery speed. Wang *et al*. [33] argued that merchants would have certain time requirements for delivery services to improve consumers' satisfaction with takeaway delivery, while the authors later used the relevant random travel time based on the purpose of improving consumer satisfaction Chen and Shi [34] considered factors such as consumer time satisfaction and optimised the traditional pick-up and delivery vehicle path model. Liu [35] introduced the k-means concept to build a dynamic demand-based path optimisation model for the complexity of the takeaway model. Similar to takeaway delivery, same-city delivery also belongs to same-city proximity delivery, and now also belongs to the category of end-of-line delivery, and the route optimization approach is also very similar to that of takeaway delivery. Tounsi *et al*. [24] developed a new heuristic algorithm for the delivery service pricing problem, in which the delivery service is developed by the delivery provider according to the price level of the service chosen by the consumer Hayel *et al*. [25] show that consumers' behaviour, especially their choice of reasonable price, affects the route optimisation of end-delivery, and then use a game-theoretic perspective to study this topic. Yang *et al*. [26] build a route optimisation model with real-time pricing by considering the different delivery costs of consumers at different delivery timeslots.

Scholars have widely applied large-scale neighbourhood search algorithm in the research of terminal distribution vehicle routing to solve the vehicle routing problem, such as the routing problem with delivery options, the terminal distribution routing problem using UAVs, the routing optimization of multiple warehouses and vehicles, and the vehicle routing optimization problem with time windows [7, 36-38]. The studies summarised above are all about the distribution of goods in safe and stable scenarios, but there are also demands for the distribution of goods in various unexpected scenarios caused by accidents, and emergency scenarios, such as the emergency distribution of materials after a disaster, play an even more vital and irreplaceable role. The scenarios analysed above do not cover all the differentiated logistics distribution [39]. Different distribution modes of different nature are applicable to different consumer needs or distribution occasions, all of which play a unique role in people's production life and are indispensable in the logistics service industry.

## 3. Model building and algorithm design

### 3.1 Model building

A distribution station in the city is responsible for supply, and goods are transported from the distribution station to each consumer point by multiple vehicles within the time required by the consumer, and then the delivery vehicles return to the distribution station. Each customer-consumer may provide more than one delivery address in a single delivery, and each delivery address has priority, and each delivery address has its own time window. The vehicle can select any one of these locations for delivery. As shown in Fig. 1, the blue triangle in the diagram represents the distribution center from which the vehicle departs from the delivery station and delivers to each consumer point. The same-coloured dots represent the delivery locations set by the consumer. The vehicle simply serves one of these and eventually returns to the distribution station.

The precise algorithm is still more suitable for small-scale distribution scenarios. Although the algorithm can calculate the optimal route of vehicles, it considers fewer constraints and has a slow speed in large-scale and complex scenarios Genetic algorithm (GA) is an algorithm for searching the optimal solution, which is proposed by simulating the genetic principle and evolutionary process of biology. It has certain advantages in solving complex combinatorial problems and has been widely studied and applied by many industries. Therefore, the application scope of the precise algorithm in the end distribution route optimization is less than that of the meta heuristic algorithm and the adaptive large-scale neighbourhood search algorithm. The neighbourhood search algorithm searches for the "neighbourhood" solution of the current solution through countless iterations and obtains a better solution through comparative analysis. The larger the neighbourhood, the better the solution. At present, the application of neighbourhood search algorithm has been extended to the field of vehicle routing optimization in terminal distribution. Each customer $i$ has a demand $q_i$ and each customer has a preferred delivery location. As a result, customers have different satisfaction levels for each address and the overall delivery of the vehicle needs to meet the overall satisfaction level constraint.

The earliest and latest time windows $[e_{i^a}, l_{i^b}]$ are different for different delivery locations $i^a$ for each customer i. The vehicle may arrive earlier than the earliest time window of the customer, but needs to wait until the earliest time window to be served, being subject to a waiting cost, and is subject to a delayed service penalty if it arrives later than the latest time window. The vehicle arrives at customer point $i^a$ with a service time of $s_{i^a}$ and leaves immediately after servicing that point. There is no limit to the number of vehicles $k$ available for use at the depot, but each vehicle incurs an operating cost $\theta_k$. The vehicles are homogeneous. The model notation is illustrated as follows:

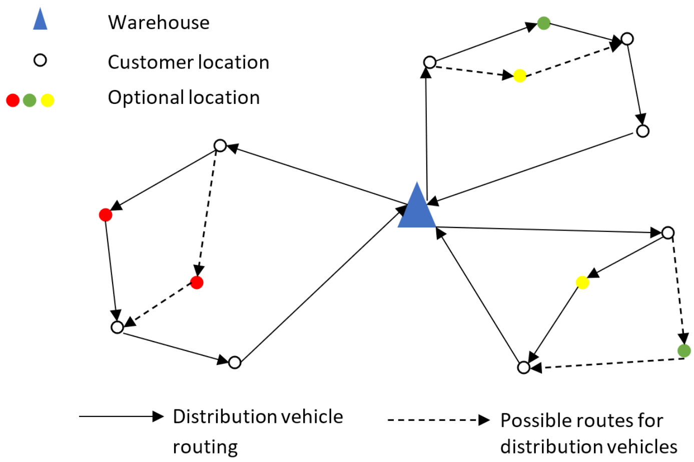


**Fig. 1** Distribution vehicle route planning diagram

| | |
|---|---|
| 0 | Warehouse |
| $C$ | Collection of customers, $C = \{1,2,\dots,m\}$ |
| $N$ | Collection of customers and warehouses, $N = \{0,1,2,\dots,m\}$ |
| $K$ | Vehicle collection, $K = \{1,2,\dots,k\}$ |
| $L_i$ | Collection of optional distribution locations for $L_i$ customer $i$ |
| $d_{i^a j^b}$ | Arc the distance between $(i^a, j^b)$, i.e. the distance from ath optional distribution location of customer $i$ to $b$-th optional distribution location of customer $j$ |
| $c_{i^a j^b}$ | Arc running cost between $(i^a, j^b)$ |
| $q_j$ | Customer $j$ demand |
| $e_{i^a}, l_{i^a}$ | Time window for customer $i$'s $a$-th optional delivery location |
| $\varepsilon_{j^b}$ | Customer satisfaction when vehicle delivers customer $j$'s $b$-th delivery location |
| $r_{i^a}$ | The time to start serving customer $i$'s $a$-th optional delivery location |
| $s_{i^a}$ | Service time of customer $i$'s $a$-th optional delivery location |
| $t_{j^b}$ | Minimum waiting time or minimum delayed service time for customer $i$'s $a$-th optional delivery location |
| $P$ | Unit waiting costs or delayed service penalty costs for $P$ vehicles |
| $\theta_k$ | Operating costs of $\theta_k$ vehicles |
| $Q_k$ | Capacity limits for $\theta_k$vehicles |
| $D_k$ | Distance limit for vehicles |
| $v_k$ | Average speed of the vehicle |
| $S$ | Overall customer satisfaction required by warehouse $S$ |
| $M$ | A sufficiently large positive number |
| $u_{il}$ | Auxiliary decision variables |
| $x^k_{i^a j^b}$ | Is 1 if vehicle $k$ passes through arc$(i^a, j^b)$; otherwise it is 0 |
| $y^k_{j^b}$ | Is 1 if customer $j$'s bth optional delivery location is served by vehicle $k$; 0 otherwise $z_k$ |
| $z_k$ | Vehicle $k$ is used or not |

Based on the above scenario description and assumptions, the model for this path planning problem is shown below.

Objective function:

$$min\ c \sum_{k\in K}\sum_{i\in N}\sum_{a\in L_i}\sum_{j\in N}\sum_{b\in L_j} x^k_{i^a j^b} d_{i^a j^b} + \sum_{k\in K} z_k\theta_k + \sum_{j\in N}\sum_{b\in L_j} Pt_{j^b} \tag{1}$$

Binding conditions：

$$\sum_{i\in N}\sum_{a\in L_i} x^k_{i^a j^b} = y^k_{j^b},\ \ \forall k\in K, j\in N_c, b\in L_j \tag{2}$$

$$\sum_{k\in K}\sum_{b\in L_j} y^k_{j^b} = 1,\ \ \forall j\in C \tag{3}$$

$$\sum_{k\in K}\sum_{j\in N}\sum_{a\in L_i}\sum_{b\in L_j} x^k_{i^a j^b} = 1, \qquad \forall i\in C \tag{4}$$

$$\sum_{i\in C}\sum_{a\in L_i} x^k_{0 i^a} = \sum_{i\in C}\sum_{a\in L_i} x^k_{i^a 0},\ \ \ \forall k\in K \tag{5}$$

$$u_{i^a} - u_{j^b} + |N| x^k_{i^a j^b} \le |N| - 1,\ \ \ \forall i,j\in C, i\ne j, a\in L_i, b\in L_j, k\in K \tag{6}$$

$$r_{i^a} + s_{i^a} + \frac{d_{i^a j^b}}{v} \le M\left(1 - x^k_{i^a j^b}\right) + r_{j^b}\ \ \ \forall\ i,j\in N, k\in K \tag{7}$$

$$y^k_{i^a} e_{i^a} \le r_{i^a}\ \ \ \ \forall i\in C, k\in K, a\in L_i \tag{8}$$

$$t_{j^b} \ge max\left[ y^k_{j^b} e_{j^b} - \left( r_{i^a} + s_{i^a} + \frac{d_{i^a j^b}}{v}\right), 0, y^k_{j^b}\left(r_{j^b} + s_{j^b}\right) - l_{j^b}\right], \tag{9}$$
$$\forall i,j\in C, i\ne j, a\in L_i, b\in L_j, k\in K$$

$$\sum_{k\in K}\sum_{b\in L_j} y^k_{j^b} q_j \le Q_k, \qquad \forall\ k\in K \tag{10}$$

$$\sum_{i\in N}\sum_{a\in L_i}\sum_{j\in N}\sum_{b\in L_j} x^k_{i^a j^b} d_{i^a j^b} \le D_k, \forall\ k\in K \tag{11}$$

$$\sum_{k\in K}\sum_{j\in C}\sum_{b\in L_j} y^k_{j^b}\ \varepsilon_{j^b} \ge S(|N| - 1) \tag{12}$$

$$z_k \ge y^k_{j^b},\ \ \ \forall i\in C, b\in L_j, k\in K \tag{13}$$

$$x^k_{i^a j^b} \in \{0,1\},\ \ \ \ \forall i,j\in N, a\in L_i, b\in L_j, k\in K \tag{14}$$

$$y^k_{j^b} \in \{0,1\},\ \ \forall j\in C, b\in L_j, k\in K \tag{15}$$

$$u_{i^a}, u_{j^b} > 0,\ \ \forall i,j\in N, a\in L_i, b\in L_j \tag{16}$$

Eq. (1) is the objective function with two components: distribution cost and vehicle operating cost. Constraints Eqs. 2 to 4 indicate that all of each customer can only be delivered by one vehicle. Constraint Eq. 5 indicates that the vehicle departs from and returns to the warehouse. Constraint Eq. 6 is a Miller-Tucker-Zemlin constraint that prevents the creation of subloops so that each vehicle's delivery route forms a loop, where $u_{i^l}, u_{j^e}$ are auxiliary variables. Constraint Eq. 7 represents the relationship between the starting service moments of two adjacent customer points visited by the vehicle. Constraint Eq. 8 represents the service time of the delivery vehicle cannot be earlier than the time requested by the customer. Constraint Eq. 9 represents the minimum waiting time or delayed service time for each customer point. Constraint Eq. 10 represents the vehicle capacity constraint, each vehicle cannot exceed its maximum load capacity.

Constraint Eq. 11 represents the vehicle travel distance constraint, the constraint Eq. 11 represents the vehicle distance constraint that each vehicle cannot travel more than its maximum distance. Constraint Eq. 12 represents the overall satisfaction rate of the delivery to be higher than the required satisfaction rate. Constraint Eq. 13 determines whether the vehicle is used or not. Constraints Eqs. 14 to 16 are the decision variables definition fields.

### 3.2 Algorithm design

*Initial setting*

Since the objective function is profit maximisation, we need to start with the objective function. Eq.17 is the corresponding function expression.

$$T = O(S^0) \times P_{init} \tag{17}$$

*Neighbourhood structure*

Since the delivery method of customers who have ticked the value-added service will no longer change, we add new removal and insertion policies to the original removal and insertion policies to improve the feasibility of the path. For ease of description, we will refer to consumers who have ticked the value-added service as value consumers. The basic idea behind these two strategies is that the higher the proportion of value consumers included in a path, the lower the number of solutions generated by adjusting the customer delivery method for that path, and the less favourable it is to generate feasible solutions in the early stages of the algorithm. Therefore, our two strategies operate mainly on such paths to ensure the convergence speed of the algorithm.

*Path removal strategy*

Step1: Count the proportion of each path in a solution S that contains consumers of value, and then arrange them in descending order.
Step2: Remove the paths until the number of removed is $n_r$.

*Distribution location factor insertion strategy*

The distribution location factor insertion strategy is based on the distribution location to determine whether consumer points are allowed to be inserted.
Step1: Calculate the distribution location association of the arc with the consumer point to be inserted.

Since the arc $(i, j)$ is assumed to be an arc on the $P$ path, $K$ is the target insertion point and $E_i \leq E_k \leq E_j$. The association between the arc $(i, j)$ and the consumer point $K$ distribution location is calculated as

$$\sigma_{ik} = \begin{cases} max\{L_i - E_k, 0\} & E_i \leq E_k \\ min\{L_i, L_k\} - E_i & E_k < E_i \leq L_k \\ max\{L_k - E_i, 0\} & E_i > L_k \end{cases} \tag{18}$$

$$\sigma_{kj} = \begin{cases} max\{L_k - E_j, 0\} & E_k \leq E_j \\ min\{L_k, L_j\} - E_k & E_j < E_k \leq L_j \\ max\{L_j - E_k, 0\} & E_k > L_j \end{cases} \tag{19}$$

$$\sigma_{ij} = \sigma_{ik} + \sigma_{kj} \tag{20}$$

Step2: Insert the consumer point $K$ into the arc $(i, j)$ with the highest correlation to the distribution location.

The delivery location correlation here is different from the previous chapter, mainly because later in the algorithm, due to the presence of value consumers, basic constraints such as vehicle capacity are easy to satisfy, but satisfying the delivery location constraint is more difficult and incurs a larger penalty cost that needs to be specifically addressed for the delivery location. In contrast, the increased cost of considering arcs $(i, j)$ to insert consumer points $K$ does not require much consideration. Therefore, we need to recalculate the correlation.

# 4. Example analysis: Results and discussion

## 4.1 Calculation example using

In this paper, five neighbourhoods near Beixiaoguan Street in Haidian District, Beijing are used as the basis for the calculation of the example analysis. Steel Research Community, Jiaoda Jiayuan, Mingguang Village neighbourhood, Tianzhao Home and Changhewan neighbourhood are selected as the community delivery area, and the number of delivery customers in each neighbourhood is 89, 87, 99, 85 and 75 respectively. To simplify the analysis and to better present the results, the delivery points of consumers in each neighbourhood are simplified to 5 (see Fig. 2). Based on the research of the actual courier company, the distribution centre was selected in this paper at the ground floor of the Yihai Business Hotel, No. 33 College South Road, Haidian District.


**Fig. 2** Community distribution district selection

## 4.2 Optimal route and delivery method

*First path analysis*

The primary delivery area for Path 1 is in the Mingguang Village neighbourhood. The numbering of those consumers who are not at their preferred delivery address is as follows in Table 1.

The time windows for these consumers' preferred addresses are in the afternoon, and if delivery is made to the preferred address, there is a long wait time. To save time window waiting time costs, the delivery person should deliver to these consumers' second or third addresses (Table 2). In addition, this consumer's alternative address is also closer to the Mingguang Village neighbourhood, and delivering these consumers together with the Mingguang Village neighbourhood could reduce costs (see Fig. 3).

**Table 1** Table of path results

| Serial No. | Path |
|---|---|
| 1 | [0,200,367,399,293,403,424,427,309,142,246,304,225,349,82,402,385,8,129,44,141,283,429,325,338,71,87,114,120,149,289,131,324,308,110,166,102,162,206,207,209,247,279,316,331,397,400,421,428,431,328,9,255,124,136,178,321,226,21,83,224,152,30,0] |
| 2 | [0,258,274,359,391,194,327,416,299,377,99,395,145,157,244,61,89,37,176,184,195,48,20,201,222,251,317,330,271,323,128,96,430,273,352,197,307,411,92,150,305,27,42,74,57,298,75,93,112,155,223,172,272,280,379,387,393,396,10,77,239,84,58,122,0] |
| 3 | [0,132,35,50,115,436,337,390,264,350,346,168,270,230,2,426,62,368,404,40,189,343,205,334,383,250,101,358,23,39,290,372,432,281,417,98,180,183,243,186,314,144,1,277,109,116,103,164,284,419,153,364,67,49,407,127,4,143,192,126,287,0] |
| 4 | [0,265,326,237,345,348,433,41,175,312,319,306,167,181,216,435,214,282,382,68,80,117,208,66,295,365,212,3,170,320,14,229,165,146,19,63,130,335,344,418,204,18,218,11,28,160,177,187,231,275,398,107,233,422,356,106,234,81,51,0] |
| 5 | [0,73,333,156,260,388,232,256,384,140,125,238,423,235,353,425,378,413,303,286,374,373,242,7,249,31,252,104,147,16,105,78,43,64,297,69,95,301,190,60,196,203,245,254,217,360,278,336,339,340,351,406,357,434,76,354,161,253,262,0] |
| 6 | [0,313,137,219,148,113,261,292,266,25,276,329,53,72,210,386,401,26,90,311,392,310,332,36,47,52,355,97,65,86,94,179,408,322,376,100,185,34,410,227,381,108,22,6,236,118,220,409,79,135,241,291,13,55,29,294,375,173,0] |
| 7 | [0,17,268,347,199,341,369,202,415,88,134,5,56,121,380,389,45,139,318,366,257,123,420,414,302,159,191,394,12,54,151,171,174,32,405,363,24,211,163,91,138,296,111,361,248,371,267,38,300,33,133,198,85,269,59,70,188,193,221,240,263,412,362,119,342,315,0] |
| 8 | [0,15,35,132,213,169,50,115,436,259,288,370,154,182,215,285,46,158,228,0] |

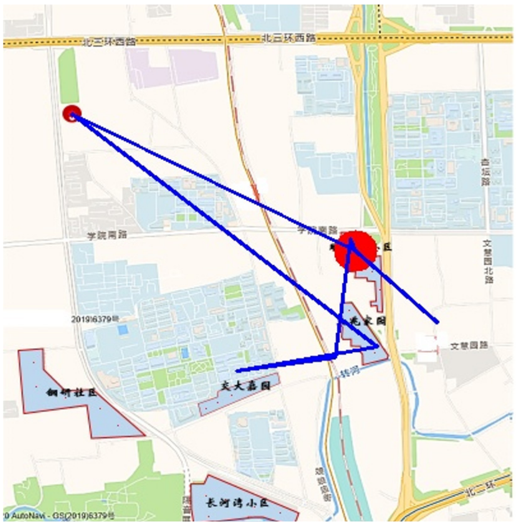

**Fig. 3** Distribution of consumers for path 1 and the optimal path

**Table 2** Consumers in path 1 who were not delivered to their preferred address

| No. | Address serial number |
|---|---|
| 200 | 2 |
| 367 | 3 |
| 399 | 2 |
| 225 | 2 |

**Fig. 4** Distribution of consumers for path 2 and the optimal path

The main delivery areas for Path 2 are in the Mingguang Village neighbourhood and the Tianzhao Home (see Fig. 4). The consumers who are not preferred delivery addresses are numbered 416 and 239, both of which are second addresses. By analysing the characteristics of the consumers, it can be found that the preferred address of consumer 416 is in Mingguang Village Sub-district, but the time window of the preferred address is after 3pm, while the consumers in Mingguang Village Sub-district all made their deliveries before 1pm, so to deliver consumer 416, they need to drive from Tianzhao Home to Mingguang Village Sub-district and back to Tianzhao Home after 3pm. However, the time window for the second address of consumer 416 is in the morning and is between Mingguangcun Subdistrict and Tianzhao Home, so it is a better choice to deliver according to the second address.239 The time window for the preferred address of consumer 239 is in the afternoon, but the preferred address is in Steel Research Community, which is farther away from Tianzhao Home and Mingguangcun Subdistrict, and the second address is closer to Tianzhao Home, and the time window of the second address also better match, so delivery at the second address is more appropriate.

The main delivery area for Path 3 is also in the Mingguang Village neighbourhood and Tianzhao Home, but there are also a small number of consumers in the Jiaoda Jiayuan and Steel Research neighbourhoods (see Fig. 5). The consumers who are not the preferred delivery address are numbered 132 and 35, both of which are second addresses. By analysing the characteristics of the consumers, we can find that the preferred address of consumer 132 is in Jiaoda Jiayuan, but the time window of the preferred address is 8:00-12:00, while the consumers in Jiaoda Jiayuan in route 3 all deliver after 8:00 pm, so it is not suitable for delivery with other consumers in Jiaoda Jiayuan. In this case, it is more appropriate to choose the second address of consumer 132 and deliver in the morning.35 The preferred address of consumer 35 is in Changhewan district, but there are no other consumers in Changhewan district in route 3, and the second address of this consumer is closer to Tianzhao Home and Mingguang Village district, so delivery can be made through the second address.

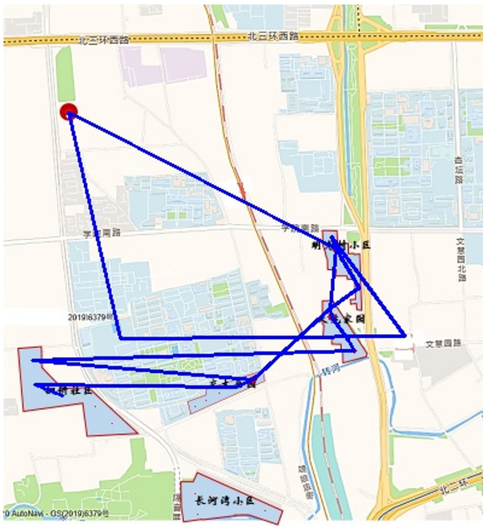


**Fig. 5** Distribution of consumers for path 3 and the optimal path

The main delivery areas for Path 4 are in Jiaoda Jia Yuan and the Steel Research community. The consumers who are not preferred delivery addresses are numbered 265 and 41, both of which are second addresses (see Fig. 6). By analysing the characteristics of the consumers, it can be found that the preferred addresses of both 265 and 41 consumers are in Jiaoda Garden. However, the time window for consumer 265's preferred address was after 1pm, which did not lend itself to delivery in the morning with other consumers in Jiaoda Jiaoyuan, so delivery to the second address was chosen. In fact, Consumer 265's second address was closer to the Tianzhao Home and Mingguang Village neighbourhoods, so why was it not delivered in a path where the main delivery area was these two neighbourhoods? The reason is that although the distance is close, the time window for 265's second address is after 10am, whereas the initial delivery time in the other paths is often before 10am, so the time windows do not match. Consumer 41, although both the time window and address match those in the Long River Bay subdivision in path 4, is preferable to its second address for delivery due to the high number of consumers in the Long River Bay subdivision and the fact that they are mainly concentrated in the afternoon and do not have the spare time to make additional deliveries to 41.

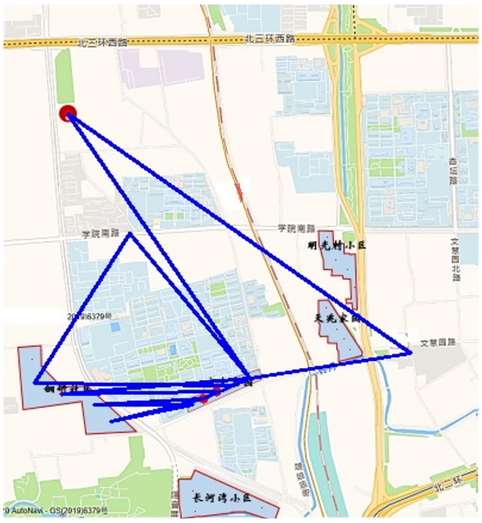


**Fig. 6** Distribution of consumers for path 4 and the optimal path

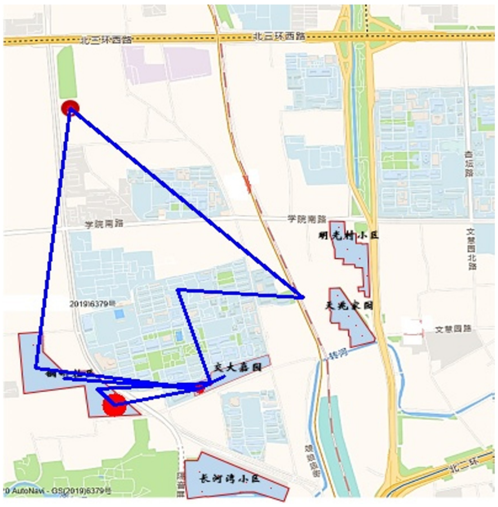


**Fig. 7** Distribution of consumers for path 5 and the optimal path

The primary delivery area for Path 5 is in Jiaoda Jia Yuan and the Steel Research community. The consumers who are not preferred delivery addresses are numbered 333 and 353, both of which are second addresses (see Fig. 7). 333 and 353 consumers' preferred addresses are both in the main delivery area of Path 5, but why are they not delivered at their preferred addresses? Analysis of the consumers' characteristics reveals that the time window for consumer 333's preferred address is after 12pm, while other consumers in the Steel Research community where consumer 333 is located concentrate their deliveries in the morning, so they can be delivered at the second address in the morning through the time window. The main reason for Consumer 353 to deliver with a second address is also due to the more suitable time window for 353 and the proximity of the second addresses of 333 and 353 to the Steel Research Community and Jiaoda Jiayuan.

The main delivery areas for path 6 are in Jiaoda Jiayuan, the Steel Research community and the Changhewan neighbourhood (see Fig. 8). The number of the consumer who is not the preferred delivery address is 137, the second address. 137 The preferred address is Jiaoda Jiayuan and the time window is after 4pm, but the time window for all other consumers in Path 6 is before 4pm, so in order not to have to make additional deliveries separately, the closer second address can be chosen for delivery.

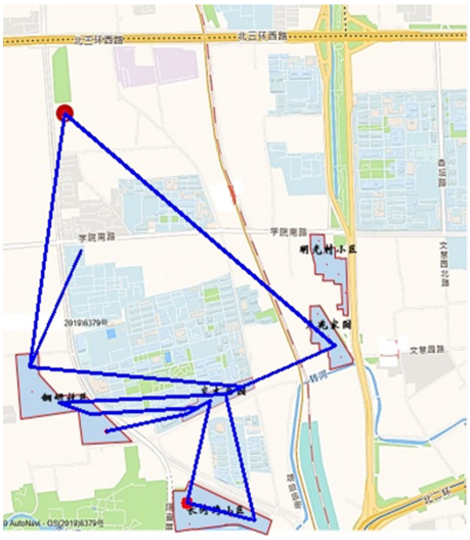

**Fig. 8** Distribution of consumers for path 6 and the optimal path

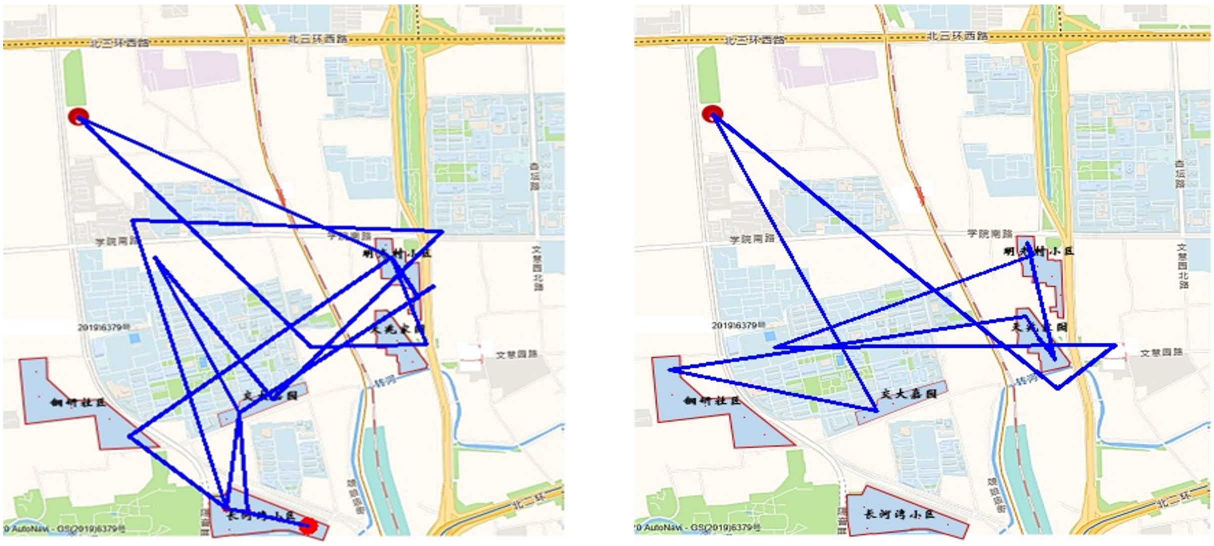

**Fig. 9** Distribution of consumers for path 7 and path 8 and optimal path

Path 7 and Path 8 have a wider delivery area coverage, both with more than 4 heel cells (see Fig. 9). There were more of these consumers who were not preferred delivery addresses, with consumer numbers 17, 268, 88, 151, 296, 111, 248, 362, 342, 15, 35, and 132.

An analysis of consumers who are not preferred addresses for delivery reveals the following characteristics of these consumers:

- Time windows that do not match other consumers in that neighbourhood on that path.
- The preferred address is further away from the delivery area of the path, while the alternative address is closer to the delivery area.
- Consumers who choose the alternative address tend to be at the beginning or the end of the path to reduce detours.

### 4.3 Cost analysis

This paper compares the total cost of the model without alternative addresses with the total cost of the model with alternative addresses. The comparison shows that the total cost of the model with alternative addresses is 283.43 compared to the total cost of the model without alternative addresses of 307.89, a total cost saving of 24.46. By consumers providing alternative addresses, the distribution company saves 24.46. For consumers, total satisfaction decreased as there were some consumers who did not receive goods from the preferred address. In terms of time window penalty cost, the model saved mainly in terms of time window, which was reduced through alternative addresses and thus better delivery times. Although consumer satisfaction is reduced, consumers are also willing to provide alternative addresses as alternative addresses may allow consumers to get their goods earlier.

### 4.4 Sensitivity analysis

During the calculations, it was observed that the presence of a service level constraint tends to make the VRPBA algorithm more difficult to solve, so a sensitivity analysis is performed in this section to explore more precisely the effect of different service levels on the total cost, computation time and number of optimal solution instances.

Due to the service level constraint, we make the service level required for the first priority vary between 60 % and 100 % in 4 % steps, i.e. note that a 4 % increase means that 10 additional consumers out of 250 are required whose delivery method must be the first delivery method chosen by the consumer.

The relationship between average path cost and service level is depicted in Fig. 10. As expected, increasing the level of service leads to an increase in total costs. $\beta_1$ = 1.0 is approximately 22 % higher than $\beta_1$ = 0.6. The impact on total cost and calculation time is analysed according to the VRPBA example. Fig. 9 also shows the average running time and confirms that the problem difficulty decreases when the service level is increased. Furthermore, the service level requires the highest costs, i.e. the absolute slope of the curve, when the service level is at the upper end of the medium range, i.e. when the value of $\beta_1$ is between 0.7 and 0.85.

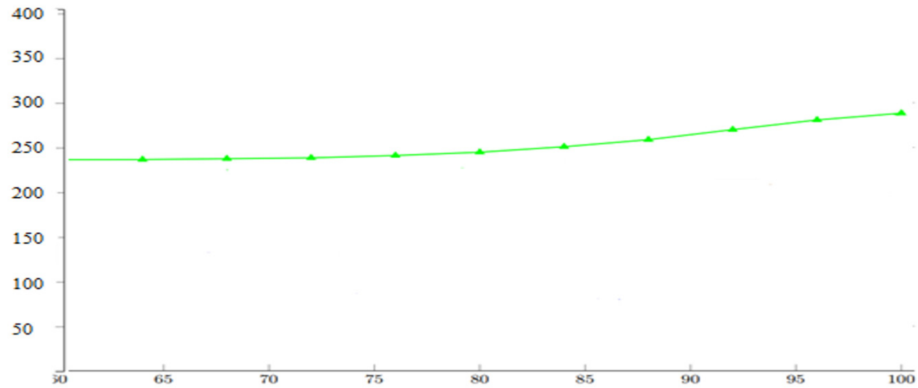


**Fig.** 10 Relationship between service levels and costs

## 5. Research conclusions

In this paper, a vehicle path optimisation model based on consumer delivery locations was established to optimise the driving paths and delivery methods of end-of-line delivery vehicles, and the same solution algorithm was designed. Based on the improved algorithm and the construction method of consumer portraits, this paper establishes a solution algorithm based on the data of five real communities and plans the delivery routes and delivery methods. This paper considers the vehicle path problem with alternative addresses, which is an extension of the vehicle path problem with time windows. In this case, each consumer may provide more than one delivery address in a delivery, each delivery address has a priority, and each delivery address has its own time window. The analysis of the arithmetic solution shows that the model saves mainly in terms of time window penalty costs, which are reduced by alternative addresses and thus better delivery times, and therefore time window violation costs. Although consumer satisfaction is reduced, consumers are also willing to provide alternative addresses, as alternative addresses may allow consumers to get their goods earlier.

In addition, this paper considers the vehicle routing problem with multiple delivery addresses, and use large-scale neighbourhood search algorithm to analyse the characteristics of users who do not deliver according to the first address, and analyse the relationship between the distribution cost and service level of enterprises. The user preference related data in this paper mainly comes from the questionnaire and belongs to static data, which limits the application of the algorithm to a certain extent. Further research can use the machine learning and big data based on historical data is also meaningful. The research focus of this paper only focuses on the logistics terminal distribution path, that is, the link of the urban logistics distribution terminal, and analyses the corresponding path optimization methods. This study does not extend the research to the level of the whole industry chain, especially the logistics distribution within the production system which is an important research point.

## References


[1] Dantzig, G.B., Ramser, J.H. (1959). The truck dispatehing problem, *Management Science,* Vol. 6, No. 1, 80-91, doi: 10.1287/mnsc.6.1.80.

[2] Current, J.R., Schilling, D.A. (1989). The covering salesman problem, *Transportation Science*, Vol. 23, No. 3, 208-213, doi: 10.1287/trsc.23.3.208.

[3] Li, Z.P., Mao, S.C. (2018). Location and assignment problem of pickup points under multiple types of demands, *Computer Integrated Manufacturing Systems*, Vol. 24, No. 11, 2889-2897, doi: 10.13196/j.cims.2018.11.023.

[4] Li, Z.P., Yang, M.Y. (2018). Research on partitioning regions serviced by logistic, *Mathematics in Practice and Theory*, Vol. 48, No. 5, 298-303.

[5] Zhou, X., Xu, M.Z., Lu, Q.G., Li, D. (2019). Self-*pickup* point location-path optimization based on customer point administrative address, *Computer Integrated Manufacturing Systems,* Vol. 25, No. 8, 2069-2078, doi: 10.13196/j.cims.2019.08.021.

[6] Zhou, X., Xu, M.Z., Lu, Q.G. (2018). A gradual coverage site selection model for self-pickup points based on customer point distribution, *Computer Integrated Manufacturing Systems,* Vol. 24, No. 11, 2879-2888, doi: 10.13196/j.cims.2018.11.022.

[7] Koç, C., Bektaş, T., Jabali, O., Laporte, G. (2016). The fleet size and mix location-routing problem with time windows: Formulations and a heuristic algorithm, *European Journal of Operational Research*, Vol. 248, No. 1, 33-51, doi: 10.1016/j.ejor.2015.06.082.

[8] Hua, X., Hu, X., Yuan, W. (2016). Research optimization on logistics distribution center location based on adaptive particle swarm algorithm, *Optik*, Vol. 127, No. 20, 8443-8450, doi: 10.1016/j.ijleo.2016.06.032.

[9] Sankaran, J.K. (2007). On solving large instances of the capacitated facility location problem, *European Journal of Operational Research,* Vol. 178, No. 3, 663-676, doi: 10.1016/j.ejor.2006.01.035.

[10] Wang, Y., Ma, X., Lao, Y., Wang, S. (2014). A fuzzy-based customer clustering approach with hierarchical structure for logistics network optimization, *Expert Systems with Applications,* Vol. 41, No. 2, 521-534, doi: 10.1016/j.eswa.2013.07.078.

[11] Guo, F., Huang, H.J., Yang, J. (2020). Study on the electric vehicle routing optimization and service strategy with the consideration of customer self-pickup radius, Journal of Industrial Engineering/Engineering Management, Vol. 34, No. 1, 154-163, doi: 10.13587/j.cnki.jieem.2020.01.017.

[12] Khouadjia, M.R., Sarasola, B., Alba, E., Jourdan, L., Talbi, E.-G. (2012). A comparative study between dynamic adapted PSO and VNS for the vehicle routing problem with dynamic requests, *Applied Soft Computing,* Vol. 12, No. 4, 1426-1439, doi: 10.1016/j.asoc.2011.10.023.

[13] Okulewicz, M., Mańdziuk, J. (2017). The impact of particular components of the PSO-based algorithm solving the dynamic vehicle routing problem, *Applied Soft Computing,* Vol. 58, 586-604, doi: 10.1016/j.asoc.2017.04.070.

[14] Abdallah, A.M.F.M., Essam, D.L., Sarker, R.A. (2017). On solving periodic re-optimization dynamic vehicle routing problems, *Applied Soft Computing,* Vol. 55, 1-12, doi: 10.1016/j.asoc.2017.01.047.

[15] Keçeci, B., Altıparmak, F., Kara, I. (2021). A mathematical formulation and heuristic approach for the heterogeneous fixed fleet vehicle routing problem with simultaneous pickup and delivery, *Journal of Industrial and Management Optimization,* Vol. 17, No. 3, 1069-1100, doi: 10.3934/jimo.2020012.

[16] Silvestrin, P.V., Ritt, M. (2017). An iterated tabu search for the multi-compartment vehicle routing problem, *Computers & Operations Research,* Vol. 81, 192-202, doi: 10.1016/j.cor.2016.12.023.

[17] Soto, M., Sevaux, M., Rossi, A., Reinholz, A. (2017). Multiple neighborhood search, tabu search and ejection chains for the multi-depot open vehicle routing problem, *Computers & Industrial Engineering,* Vol. 107, 211-222, doi: 10.1016/j.cie.2017.03.022.

[18] Taş, D., Dellaert, N., van Woensel, T., de Kok, T. (2017). Vehicle routing problem with stochastic travel times including soft time windows and service costs, *Computers & Operations Research,* Vol. 40, No. 1, 214-224, doi: 10.1016/j.cor.2012.06.008.

[19] Zhu, Z.G., Guang, X.P., Guo, M. (2021). Multi vehicle logistics distribution path optimization under uncertain environment, *Transportation Technology and Economy,* Vol. 23, No. 2, 6-12.

[20] Gutierrez, A., Dieulle, L., Labadie, N., Velasco, N. (2018). A multi-population algorithm to solve the VRP with stochastic service and travel times, *Computers &. Industrial Engineering,* Vol. 125, 144-156, doi: 10.1016/j.cie.2018.07.042.

[21] Guedes, P.C., Borenstein, D. (2018). Real-time multi-depot vehicle type rescheduling problem, *Transportation Research Part B: Methodological,* Vol. 108, 217-234, doi: 10.1016/j.trb.2017.12.012.
[22] Veenstra, M., Cherkesly, M., Desaulniers, G., Laporte, G. (2017). The pickup and delivery problem with time windows and handling operations, *Computers & Operations Research,* Vol. 77, 127-140, doi: 10.1016/j.cor.2016.07.014.
[23] Kim, J., Chung, B.D., Kang, Y., Jeong, B. (2018). Robust optimization model for closed-loop supply chain planning under reverse logistics flow and demand uncertainty, *Journal of Cleaner Production,* Vol. 196, 1314-1328, doi: 10.1016/j.jclepro.2018.06.157.
[24] Tounsi, B., Hayel, Y., Quadri, D., Brotcorne, L. (2016). Mathematical programming with stochastic equilibrium constraints applied to optimal last-mile delivery services, *Electronic Notes in Discrete Mathematics,* Vol. 52, 5-12, doi: 10.1016/j.endm.2016.03.002.
[25] Hayel, Y., Quadri, D., Jiménez, T., Brotcorne, L. (2016). Decentralized optimization of last-mile delivery services with non-cooperative bounded rational customers, *Annals of Operations Research,* Vol. 239, 451-469, doi: 10.1007/s10479-014-1647-x.
[26] Yang, X., Strauss, A.K., Currie, C.S.M., Eglese, R. (2016). Choice-based demand management and vehicle routing in e-fulfillment, *Transportation Science,* Vol. 50, No. 2, 473-488, doi: 10.1287/trsc.2014.0549.
[27] Ren, L., Huang, M., Wang, X.W. (2016). A 4PL path optimization problem considering customer delay aversion behavior, *Computer Integrated Manufacturing Systems,* Vol. 22, No. 4, 1148-1154, doi: 10.13196/j.cims.2016.04.029.
[28] Ge, X.L., Xu, J.P., Wang, W.X. (2017). Research on intermodal urban logistics based on vehicle collaboration under traffic restriction conditions, *China Management Science,* Vol. 25, No. 10, 130-139, doi: 10.16381/j.cnki.issn1003-207x.2017.10.014.
[29] Zhao, Q.W., Zhao, J.P., Lin Y. (2017). Research on the optimization of urban distribution network of large retail enterprises based on O2O, *China Management Science,* Vol. 25, No. 9, 159-167, doi: 10.16381/j.cnki.issn1003-207x.2017.09.018.
[30] Deng, H.X., Liu, M., Wang, M. (2020). Research on cold chain logistics path optimization based on stochastic demand, *Transportation Technology and Economy,* Vol. 22, No. 1, 1-6.
[31] Zhang, L., Gao, Y., Sun, Y., Fei, T., Wang, Y. (2019). Application on cold chain logistics routing optimization based on improved genetic algorithm, *Automatic Control and Computer Sciences.* Vol. 53, 169-180, doi: 10.3103/S0146411619020032.
[32] Ren, X.Y., Chen, C.F., Xiao, Y.L., Du, S.C. (2019). Path optimization of cold chain distribution with multiple distribution centers considering carbon emissions, *Applied Ecology and Environmental Research,* Vol. 17, No. 4, 9437-9453, doi: 10.15666/aeer/1704_94379453.
[33] Wang, S., Zhao, L.J., Hu, Q.M. (2017). Random travel time for take-out O2O delivery vehicle path problem, *Logistics Technology,* Vol. 40, No. 1, 93-101, doi: 10.13714/j.cnki.1002-3100.2017.01.024.
[34] Chen, J., Shi, J. (2019). A multi-compartment vehicle routing problem with time windows for urban distribution – A comparison study on particle swarm optimization algorithms, *Computers & Industrial Engineering,* Vol. 133, 95-106, doi: 10.1016/j.cie.2019.05.008.
[35] Liu, W. (2020). Route optimization for last-mile distribution of rural e-commerce logistics based on ant colony optimization, *IEEE Access,* Vol. 8, 12179-12187, doi: 10.1109/ACCESS.2020.2964328.
[36] Barros, L., Linfati, R., Escobar, J.W. (2020). An exact approach for the consistent vehicle routing problem (ConVRP), *Advances in Production Engineering & Management,* Vol. 15, No. 3, 255-266, doi: 10.14743/apem2020.3.363.
[37] Min, J.N., Jin, C., Lu, L.J. (2019). Maximum-minimum distance clustering method for split-delivery vehicle-routing problem: Case studies and performance comparisons, *Advances in Production Engineering & Management,* Vol. 14, No. 1, 125-135, doi: 10.14743/apem2019.1.316.
[38] Min, J.N., Jin, C., Lu, L.J. (2019). Split-delivery vehicle routing problems based on a multirestart improved sweep approach, *International Journal of Simulation Modelling,* Vol. 18, No. 4, 708-719, doi: 10.2507/IJSIMM8(4)CO19.
[39] Zhao, P.X., Luo, W.H., Han, X. (2019). Time-dependent and bi-objective vehicle routing problem with time windows, *Advances in Production Engineering & Management*, Vol. 14, No. 2, 201-212, doi: 10.14743/apem2019.2.322.

APEM journal

**Advances in Production Engineering & Management** | **ISSN 1854-6250**
Volume 17 | Number 4 | December 2022 | pp 455–468 | Journal home: apem-journal.org
https://doi.org/10.14743/apem2022.4.448 | Original scientific paper

# An approach to maintenance sustainability level assessment integrated with Industry 4.0 technologies using Fuzzy-TOPSIS: A real case study

**Patalas-Maliszewska, J.**[a,*], **Łosyk, H.**[a]

[a]Institute of Mechanical Engineering, University of Zielona Góra, Poland

**A B S T R A C T**

Sustainable development (SD) activities within a manufacturing should be integrated with the Industry 4.0 (I4.0) technologies implementation due to ensure the continuous evaluation and even prediction the SD level. Such integration should be provided cross all company areas but must be strictly defined for each core process realised within a company. Therefore, the main purpose of the study is to build the new approach to assess the maintenance sustainability (MS) level in a manufacturing company, as a good example of integrating I4.0 technologies and SD activities within a company, using Fuzzy Technique for Order of Preference by Similarity to Ideal Solution (F-TOPSIS). The major contributions of the work are as follows: 1) to the existing literature by identification the key objectives of MS, in the context of Industry 4.0 2) using the F-TOPSIS method and based on the empirical data received from 125 Polish manufacturing enterprises, 3) the establishment of the integrated approach, which allow continuous monitor the level of the MS within a manufacturing, 4) demonstrating the usefulness of the fresh framework in managerial practice through its verification in the five Polish manufacturing companies. Managers of manufacturing enterprises, thanks to the use of the proposed approach, may assess and constant monitor the MS level, while application of the I4.0 technologies.

**A R T I C L E   I N F O**

*Keywords:*
Maintenance sustainability (MS);
Assessment;
Manufacturing;
Industry 4.0;
Multi-criteria decision making (MCDM);
Fuzzy Technique for Order of Preference by Similarity to Ideal Solution (Fuzzy TOPSIS);
Empirical research;
Real case studies

**Corresponding author:*
j.patalas-maliszewska@iim.uz.zgora.pl
(Patalas-Maliszewska, J.)

*Article history:*
Received 8 February 2022
Revised 19 December 2022
Accepted 21 December 2022



## 1. Introduction

Production and industrial systems consume a huge amount of resources and energy, constituting a sector with a large percentage of emissions to the environment. That is why the modern industry is directed in its activities to support the three pillars of Sustainable Development (SD): social, economic and environmental. In that way, industrial enterprises and more precisely manufacturing ones seek to integrate the environment into their strategy by conducting an innovative rationalization of production as promoted by industrial ecology and circular economy paradigms [1]. Maintenance plays a key role in this regard, as a possibility for the prolong the life of manufacturing [2]. Standard maintenance is an integration of technical, administrative and managerial aspects of production [3]. Usually, the view of maintenance activities is narrowed down to the economic dimension. However, the increasing complexity of production systems indicates the need to broaden the horizons related to the effects of maintenance activities with an environmental and social dimension. It seems necessary to the implementation of the process approach to the design and operations of a company, an integrated management system based on the application of certain standards (quality, environment, safety at work, etc.) and elements of business excellence of a company [4].

The growing interest in the field of maintenance management is indicated by numerous publications in this area [5-8] indicating the possibility of including SD objectives in the maintenance management strategy. The literature on the subject indicates attempts to imply the assumptions of Sustainable Development (SD) in the assessment of maintenance results [9-12]. The Global Reporting Initiative - GRI [13] provides guidance on SD reporting for organizations where "the G4 Guidelines provide global guidance for a standardized approach to reporting, promoting clarity and consistency of information that is necessary to acquire useful and reliable content for the market and the public" [13]. SD reporting in accordance with the standards set by GRI is used by, among others, such companies as Orlen, Allegro, and PGNiG. SD, within manufacturing, should also be seen in the three areas: (1) production processes, (2) production durability and (3) product development. In the article, based on the literature (e.g., 14-16) the objectives of maintenance sustainability (MS) were defined.

The contemporary challenge of society is, therefore, the implementation of SD goals in the era of Industry 4.0. Zhou *et al*. [17] indicate that it is a futuristic and multifaceted process with many opportunities and challenges. Industry 4.0 can be started as the industrial transformation that provides new technological solutions by integrating information technologies and automation that communicate among themselves to achieve better results [18]. However, the growing importance of industry requires extensive measures to protect the well-being of m.in stocks, the environment, and dignified life. There is growing interest in sustainability practices for organisations [19]. Industry 4.0 can be used to increase SD's ability to achieve its goals by enabling organizations to diagnose in real-time and to optimize and improve the system's ability to adapt to a dynamically changing environment [20]. Thus, the organization is able to capture data from the actual implementation of production and quickly analyse the state of individual process parameters. Active data collection helps managers track, monitor, and then make sustainable decisions about their processes. Another important aspect is the use of the latest technologies in production systems to increase efficiency. This solution, in turn, provides a competitive advantage to the organization by producing high-quality products at a lower cost [21].

Therefore, the main idea of this paper is to evaluate the maintenance sustainability level in manufacturing companies integrated with Industry 4.0 technologies using one of the Decision Making (MCDM) methods. In the research process, two methods of multi-criteria analysis were considered to evaluate the maintenance sustainability level in manufacturing companies integrated with Industry 4.0 technologies: Analytic Hierarchy Process (AHP) and Fuzzy Technique for Order of Preference by Similarity to Ideal Solution (F-TOPSIS). The choice of the AHP method was considered due to the ability to capture quantitative and qualitative attributes in a simple way, as well as the ability to handle rare or low-quality data. The use of the AHP method also allows for simple verification of the quality of expert judgments by performing a consistency test. The next step in the research process was the use of the F-TOPSIS method due to the complete autonomy of individual experts in making assessments. The IFWA operator was used to aggregate expert assessments. In the process of verification of selected MCDM methods, the F-TOPSIS method was used in the further part of the work due to the uncertainty and imprecision of the assessment of decision options in relation to the adopted criteria in the context of multifacetedness: evaluate the maintenance sustainability level in manufacturing companies.

MCDM methods are designed to solve such manufacturing problems [22]. It is indicated that the MCDM constitutes an excellent decision-making tool for evaluating and ranking/prioritizing the alternatives even when the criteria involved are complex [23]. The literature indicates the effective application of MCDM in the field of manufacturing enterprises, including flow control in a manufacturing system with three production lines is described [24], selection of the lean six sigma project [25], identifying key performance factors for sustainability development [26], materials selection [27]. To build the new approach to assess the maintenance sustainability level in manufacturing companies, using F-TOPSIS and IFWA operator the Decision Makers (DMs) opinions are needed. Therefore 125 Polish manufacturing companies from western Poland in the automotive industries were researched to assess the activities of the organization for the benefit of MS. Next, the research results obtained using the F-TOPSIS method represent the key objectives of MS in production enterprises. The values of the key MS objectives set should be determined based on the data included in applied I4.0 technologies within manufacturing. Finally, the universality of the proposed approach and its adaptability to the specificity of a given company was demonstrated and employed in five different types of Polish manufacturing enterprises.

## 2. Materials and methods

In the industrial scope, one of the key areas that directly influence the manufacturing sustainability of each company is maintenance [15].

The Decision Making (MCDM) methods refer to the methods of utilizing different data sources comprehensively to select optimization alternatives [28]. The MCDM methods focus on decision problems in which the set of all permissible decisions is a discrete set containing a finite, predetermined number of possible solution variants. MCDM tool can handle concurrently the various criteria which may be dimensional or non-dimensional in nature [23]. It is indicated that the MCDM constitutes an excellent decision-making tool for evaluating and ranking/prioritizing the alternatives even when the criteria involved are complex [23]. The literature indicates the effective application of MCDM methods in the field of a manufacturing company, including flow control in a manufacturing system with three production lines is described [24], selection of the lean six sigma project [25], identifying key performance factors for sustainability development [26], materials selection [27].

For the purpose of the assessment of the MS level, the F-TOPSIS and IFWA methods seem to be appropriate for this research. The F-TOPSIS method was presented by [29].

Fuzzy TOPSIS method and IFWA operator to rank the adopted alternatives and criteria. Along with the TOPSIS method, Intuitionistic Fuzzy Sets (IFS) were used. IFS A in the finite set X can be defined as follows [30]:

$$A = \{< x, \mu_A(x), v_A(x) > | x \in X\}, \text{where:} \tag{1}$$

$$\mu_A: x \to [0,1], v_A: x \to [0,1] \text{ and } 0 \le \mu_A(x) + v_A(x) \le 1 \; \forall \; x \in X \tag{2}$$

$\mu_A(x)$ and $v_A(x)$ determine the degree of membership and non-membership of $x$ to $A$. For each IFS $A$ of $X$ there is also a third parameter called the degree of fluctuation, defined as:

$$\pi_A(x) = 1 - \mu_A(x) - v_A(x) \tag{3}$$

therefore, it is obvious that:

$$0 \le \pi_A(x) \le 1 \tag{4}$$

When the value of $\pi_A(x)$ is small, then the information about $x$ is more certain, whereas when the value of $\pi_A(x)$ has a larger range, the information becomes uncertain.

The multiplication operator for intuitionistic fuzzy numbers (IFNs), where $A$ and $B$ belong to the set $F$ is as follows:

$$A \otimes B = \{\mu_A(x).\mu_B(x), v_A(x) + v_B(x) - v_A(x).v_B(x) | \, x \in X \tag{5}$$

Multiplication of matrix components is calculated by the formula:

$$A \circ B = [< min\{\mu_A(x), \mu_B(x)\}, max\{\mu_A(x), \mu_B(x)\} >] \tag{6}$$

In order to establish the integrated approach, which allows continuous monitor the level of the MS within manufacturing the F-TOPSIS and IFWA methods were employed according to the following steps:

*Step I. Calculation of weights for selected DMs*

The group was assumed to include $l$ decision-makers. The importance of individual decision-makers is represented by intuitionistic fuzzy numbers. Assuming that $D_k = [\mu_A, v_A, \pi_A]$, then IFN is showing the overall importance of Decision Maker $k$-th in the ranking. The $k$-th DM weight is calculated using the following formula:

$$\lambda_k = \frac{(\mu k + \pi_k(\frac{\mu k}{(\mu k + \ vk\ )})}{\Sigma_{k=1}^{l}(\mu k + \pi_k(\frac{\mu k}{\mu k + v_k})}, \tag{7}$$

where assuming that:

$$\sum_{k=1}^{l} \lambda k = 1$$

*Step II. Create the aggregated intuitionistic fuzzy decision matrix according to the DMs opinions*

It was assumed that intuitionistic fuzzy decision matrix for each DM takes the form of $R^k = \left(r_{ij}^{(k)}\right)_{mnx} = \{1,2,\ldots,l\}$, then weights of individual $DM\ \sum_{k=1}^{l} k = 1 \in [0,1]$. Opinions of all members should be combined into a group decision. For this purpose, the operator Intuitionistic Fuzzy Weighted Averaging (IFWA) proposed by [19] was used, assuming that:

$$r_{ij} = IFWA_\lambda\ \left(r_{ij}^{(1)}, r_{ij}^{(2)}, \ldots, r_{ij}^{(l)}\right) = \lambda_1 r_{ij}^{(1)} \oplus \lambda_2 r_{ij}^{(2)} \oplus \ldots \oplus \lambda_l r_{ij}^{(l)} = \tag{8}$$
$$= \left[1 - \prod_{k=1}^{l}\left(1 - \mu_{ij}^{(k)}\right)\lambda_k, \prod_{k=1}^{l}\left(\nu_{ij}^{(k)}\right)\lambda_k, \prod_{k=1}^{l}\left(1 - \mu_{ij}^{(k)}\right)\lambda \mathrm{k}\ - \prod_{k=1}^{l}\left(\nu_{ij}^{(k)}\right)\lambda_k\right]$$

and

$$r_{ij}\ = (\mu_{Ai}(xj), \nu_{Ai}\ (x_j), \pi_{Ai}(x_j))\ \ (\ i\ =\ (1,2,\ldots,m;\ \ j\ = 1,2,\ldots,n)$$

Then, the aggregated IF decision matrix can be presented as:

$$\mathrm{R} = \begin{bmatrix} \mu_{A1}(x1), \nu_{A1}(x1), \pi_{A1}(x1) & \mu_{A1}(x2), \nu_{A1}(x2), \pi_{A1}(x2) & \cdots & \mu_{A1}(x3), \nu_{A1}(x3), \pi_{A1}(x3) \\ \mu_{A2}(x1), \nu_{A2}(x1), \pi_{A2}(x1) & \mu_{A2}(x2), \nu_{A2}(x2), \pi_{A2}(x2) & \cdots & \mu_{A2}(x3), \nu_{A2}(x3), \pi_{A2}(x3) \\ \vdots & \vdots & \ddots & \vdots \\ \mu_{Am}(x1), \nu_{Am}(x1), \pi_{Am}(x1) & \mu_{Am}(x2), \nu_{Am}(x2), \pi_{Am}(x2) & \cdots & \mu_{Am}(xn), \nu_{Am}(xn), \pi_{Am}(xn) \end{bmatrix} \tag{9}$$

$$\mathrm{R} = \begin{bmatrix} \mu_{A1}(x1), \nu_{A1}(x1), \pi_{A1}(x1) & \mu_{A1}(x2), \nu_{A1}(x2), \pi_{A1}(x2) & \cdots & \mu_{A1}(x3), \nu_{A1}(x3), \pi_{A1}(x3) \\ \mu_{A2}(x1), \nu_{A2}(x1), \pi_{A2}(x1) & \mu_{A2}(x2), \nu_{A2}(x2), \pi_{A2}(x2) & \cdots & \mu_{A2}(x3), \nu_{A2}(x3), \pi_{A2}(x3) \\ \vdots & \vdots & \ddots & \vdots \\ \mu_{Am}(x1), \nu_{Am}(x1), \pi_{Am}(x1) & \mu_{Am}(x2), \nu_{Am}(x2), \pi_{Am}(x2) & \cdots & \mu_{Am}(xn), \nu_{Am}(xn), \pi_{Am}(xn) \end{bmatrix} \tag{10}$$

$$\mathrm{R} = \begin{bmatrix} r_{11} & r_{12} \cdots & r_{1m} \\ r_{21} & r_{22} \cdots & r_{2m} \\ \vdots & \vdots & \vdots \\ r_{n1} & r_{n2} & r_{nm} \end{bmatrix} \tag{11}$$

To create the aggregated intuitionistic fuzzy decision matrix, a set of alternatives and also the Decision Makers (DMs) opinions are needed. Therefore, at the end of 2020, we researched 125 Polish manufacturing companies from western Poland (from the Lubuskie Voivodeship, Lower Silesia, Opole, Greater Poland and West Pomeranian Voivodeship) in the automotive industries to assess the activities of the organization for the benefit of SM. The tests were carried out using the survey method. The survey questionnaire included multi-choice, closed questions. The research group represents 1 % of manufacturing companies from the automotive industry, in western Poland [31] based on data from the Central Statistical Office of Poland, Warsaw. 61 % of the companies surveyed carry out an analysis in the area of energy consumption, although it is an essential tool for energy efficiency measures in the plant. Improving energy efficiency can have measurable effects in the form of energy savings, thereby reducing costs and reducing negative environmental impacts. It should be emphasised that energy efficiency protects land resources and is an important element of sustainable development. The survey data shows that 67 % of the companies surveyed carry out an analysis. So, based on the research results the set of decision-makers were defined:

DMs = {DM1, DM2}.

DM1 (an Owner) and DM2 (a Maintenance Manager) were selected based on the survey results, where the responses received in the positions of an owner and a maintenance manager accounted for the largest number of responses. The percentage for each position that was responsible for completing the survey is as follows: an owner 34 %, a co-owner 6.7 %, a board chairman 3.5 %, a board member 1.6 %, an administrative director 2.4 %, a sales director 0.8 %, a managing director 0.8 %, a director 0.8 %, a manager 3.2 %, a production manager 7.1 %, a maintenance manager 20 %, an assistance maintenance manager 0.8 %, a workshop manager 1.6 %, a service manager 0.8 %, a process engineer 4%, an engineer 0.8 %, a superintendent/caretaker 2.4 %, a chief accountant 0.8 %, an accountant 0.8 %, a technical specialist 0.8%, a maintenance specialist 1.7 %, a financial controller 0.8 %, a specialist 3.2 %.

*Step III. Determine the weights of criteria and sub-criteria*

Since it cannot be assumed that all criteria and sub-criteria are equally important, a $W$ degree of importance should be set for them. To obtain the $W$ parameter, opinions of individual DMs on the validity of criteria and sub-criteria must be combined into one assessment.

Suppose that $w_j^{(k)} = \left[\mu_j^{(k)}, v_j^{(k)}, \pi_j^{(k)}\right]$, then IFN is assigned to criterion $Xj$ by $k$-th decision maker. Next, the weight for a particular criterion and sub-criterion is determined using the IFWA operator:

$$w_{ij} = IFWA_\lambda \left(w_j^{(1)}, w_j^{(2)}, \dots, w_j^{(l)}\right) = \lambda_1 w_j^{(1)} \oplus \lambda_2 w_j^{(2)} \oplus \dots \oplus \lambda_l w_j^{(l)} =$$

$$= \left[1 - \prod_{k=1}^{l}\left(1-\mu_{ij}^{(k)}\right)\lambda_k, \prod_{k=1}^{l}\left(v_{ij}^{(k)}\right)\lambda_k, \prod_{k=1}^{l}\left(1-\mu_{ij}^{(k)}\right)\lambda_k - \prod_{k=1}^{l}\left(v_{ij}^{(k)}\right)\lambda_k\right] \quad (12)$$

$$W = \left[w_1, w_2, \dots, w_j\right],$$

where

$$w_j = (\mu_j, v_j, \pi_j) \quad (j = 1,2,\dots,n) \quad (13)$$

Then a multiplication of the matrix components is used to combine the weights of each criterion with the corresponding sub-criteria (Eq. 6).

*Step IV. Create the aggregated weighted intuitionistic fuzzy decision matrix*

Calculation of criteria and sub-criteria weights ($W$) allows to create the aggregated weighted IF decision matrix. The aggregated weighted IF decision matrix based on [32]:

$$R \otimes W = \{x, \mu_{Ai}(x) \bullet \mu_W(x), \nu_{Ai}(x) + \nu_W(x) - \nu_{Ai}(x) + \nu_W(x) | \, x \in X \quad (14)$$

and

$$\pi_{Ai \bullet W} = 1 - \nu_{Ai}(x) - \nu_W(x) - \mu_{Ai}(\mathrm{x}) \bullet \mu_W(x) + \nu_{Ai}(x) + \nu_W(x) \quad (15)$$

*Step V. Appoint the intuitionistic fuzzy positive-ideal solution and intuitionistic fuzzy negative-ideal solution*

Suppose that $J1$ is a benefit criterion, while $J2$ is a cost criterion. $A^+$ is intuitionistic fuzzy positive ideal solution and $A^-$ is intuitionistic fuzzy negative ideal solution. Eqs. 16 and 17 determine $A^+$ and $A^-$:

$$A^+ = (\mu_{A^+W}(x_j), \nu_{A^+W}(x_j) \text{ and } A^- = (\mu_{A^-W}(x_j), \nu_{A^-W}(x_j) \quad (16)$$

where:

$$\mu_{A^+W}(x_j) = ((max_i \ \mu_{AiW}(x_j) | \, j \in J1), (min_i \ \mu_{AiW}(x_j) | \, j \in J2) \quad (17)$$

$$\nu_{A^+W}(x_j) = ((min_i \ \nu_{AiW}(x_j) | \, j \in J1), (max_i \ \nu_{AiW}(x_j) | \, j \in J2) \quad (18)$$

$$\mu_{A^+W}(x_j) = ((min_i \ \mu_{AiW}(x_j) | \, j \in J1), (max_i \ \mu_{AiW}(x_j) | \, j \in J2) \quad (19)$$

$$\nu_{A^-W}(x_j) = ((max_i \ \nu_{AiW}(x_j) | \, j \in J1), (min_i \ \nu_{AiW}(x_j) | \, j \in J2) \quad (20)$$

*Step VI. Calculate the separation measures and closeness coefficient*

Measuring the separations between alternatives in Intuitionistic fuzzy set can be done by using a number of distance measures proposed by [33] or [32] including Hamming distance, Euclidean distance and their normalized distance measures [1]. After selecting the distance measure, the separation measures ($S_{i^+}$ and $S_{i^-}$) for each alternative from intuitionistic fuzzy positive ideal and negative ideal solutions the selection is made. The article uses normalized Euclidean distance:

$$S^+ = \sqrt{\frac{1}{2n}\sum_{j=1}^{n}[(\mu_{AiW}(x_j) - \mu_{A^+W}(x_j))^2 + (\nu_{AiW}(x_j)^2 - \nu_{A^+W}(x_j))^2 + (\pi_{AiW}(x_j)^2 - \pi_{A^+W}(x_j))^2]} \quad (21)$$

$$S^- = \sqrt{\frac{1}{2n}\sum_{j=1}^{n}[(\mu_{AiW}(x_j) - \mu_{A^-W}(x_j))^2 + (\nu_{AiW}(x_j)^2 - \nu_{A^-W}(x_j))^2 + (\pi_{AiW}(x_j)^2 - \pi_{A^-W}(x_j))^2]} \quad (22)$$

Then the relative closeness coefficient to the ideal solution is:

$$C_i = \frac{S_{i-}}{S_{i-} + S_{i+}}, \text{where } 0 \le C_i \le 1 \quad (23)$$

*Step VII. Rank the alternatives*

After calculating the relative closeness coefficients of each alternatives, a ranking of the alternative has been made, based on $C_i$'s decreasing value.

## 3. Research results

In order to create a framework for assessing the maintenance sustainability level in manufacturing companies, integrated with I4.0 technologies, the following elements should be defined: Element 1: a set of criteria: C = {C1, C2,…., C12}, Element 2: a set of sub-criteria: I = {I1, I2,…, I14}, Element 3: a set of alternatives: Av = {Av1, Av2, Av3}.

Based on the analysis of our previous works and based on the literature, e.g. [14-16, 34], the set of criteria: C = {C1, C2,…, C7} and a set of sub-criteria: I = {I1, I2,…, I14} were determined. It should be noted that the selected criteria and sub-criteria for maintenance sustainability are related to the industry concerned (manufacturing) to meet the unique needs of the manufacturing sector. A set of alternatives: Av = {Av1, Av2, Av3} was determined as the management levels within an enterprise: the operational (Av1), as well as tactical (Av2) and strategic level (Av3). The adopted criteria (Table 1) were also divided into a benefit (criteria for which the higher value then better) and cost (criteria for which the lower value then better). Benefit and cost criteria are presented in Table 2.

**Table 1** Selected criteria and sub-criteria

| Criteria | | Sub-criteria | |
|---|---|---|---|
| Staff education | C1 | Cost of training for maintenance<br>Preventive maintenance time causing downtime | I1<br>I2 |
| Timeliness | C2 | Timeliness of order | I2 |
| Reduction of downtime costs | C3 | Total number of downtime related to maintenance | I4 |
| Environmental protection | C4 | Number of failures causing potential damage to the environment | I5 |
| Reduction of production costs | C5 | Reduction costs of losses related to production stoppages resulting from breakdowns | I6 |
| Safety | C6 | Reduction costs connected with potentially accidental events and accidents of maintenance workers, operators and third parties during maintenance works | I7 |
| Investment profitability | C7 | Return on eco-friendly maintenance investment and innovation | I8 |
| Resources saving | C8 | Total of spare parts used/ Original spare parts used<br>Recycled spare parts used/ Re-purposed spare parts used | I9<br>I10 |
| Good practices | C9 | Skill improvement related to sustainable maintenance practices | I11 |
| Innovation and modernization | C10 | Modernization carried out in the last six months related to sustainable maintenance | I12 |
| Use of renewable energy | C11 | Renewable energy consumption | I13 |
| Reduction of non-renewable energy consumption | C12 | Non-renewable energy consumption | I14 |

**Table 2** Benefit and cost criteria

| Action | Criteria | Benefit | Cost |
|---|---|---|---|
| MS (maintenance sustainability) | C1 | x | |
| | C2 | x | |
| | C3 | | x |
| | C4 | | x |
| | C5 | | x |
| | C6 | x | |
| | C7 | x | |
| | C8 | x | |
| | C9 | x | |
| | C10 | x | |
| | C11 | x | |
| | C12 | | x |

Selected DMs (section 2) was assigned the importance of weights based on their involvement in the adopted action (maintenance sustainability). To determine the importance of weights for DM, the following formula was used Eq. 7.

The results of the studies allowed to assess the involvement of the selected DMs in the activities of the organization for the benefit of SD. The assessment of involvement in the implementation of particular DMs criteria was carried out on the basis of the adopted linguistic terms and Intuitionistic Fuzzy Numbers. Linguistic terms for ranking the importance of the DMs, criteria and sub-criteria: little consequence (LC) – IFN ∈ (0.10, 0.90); medium consequence (MC) – IFN ∈ (0.25, 0.70); important (I) – IFN ∈ (0.45, 0.50; very important (VI) – IFN ∈ (0.75, 0.20); crucial (C) –IFN ∈ (0.90, 0.10). The importance of DMs and their weights: DM1 – Crucial; Weight 0.539, and DM2 – Very Important; Weight 0.461**.**

**Table 3** The ratings of the alternatives

| Action | SD objective | Level of management in company | DMs | | | |
|---|---|---|---|---|---|---|
| | | | DM1 | DM2 | DM1 | DM2 |
| MS | C1 | ST | VHL | VHL | (1.00, 0.00) | (1.00, 0.00) |
| | | TA | SL | HL | (0.55, 0.35) | (0.75, 0.25) |
| | | OP | IL | ML | (0.20, 0.65) | (0.40, 0.50) |
| | C2 | ST | SL | HL | (0.55, 0.35) | (0.75, 0.25) |
| | | TA | HL | VHL | (0.75, 0.25) | (1.00, 0.00) |
| | | OP | ML | ML | (0.40, 0.50) | (0.40, 0.50) |
| | C3 | ST | HL | HL | (0.75, 0.25) | (0.75, 0.25) |
| | | TA | VHL | VHL | (1.00, 0.00) | (1.00 , 0.00) |
| | | OP | IL | ML | (0.20, 0.65) | (0.40, 0.50) |
| | C4 | ST | VHL | VHL | (1.00, 0.00) | (1.00, 0.00) |
| | | TA | HL | SL | (0.75, 0.25) | (0.55, 0.35) |
| | | OP | IL | NL | (0.20, 0.65) | (0.00, 1.00) |
| | C5 | ST | VHL | HL | (1.00, 0.00) | (0.75, 0.25) |
| | | TA | HL | ML | (0.75, 0.25) | (0.40, 0.50) |
| | | OP | IL | IL | (0.20, 0.65) | (0.20, 0.65) |
| | C6 | ST | HL | HL | (0.75, 0.25) | (0.75, 0.25) |
| | | TA | VHL | VHL | (1.00, 0.00) | (1.00 , 0.00) |
| | | OP | IL | IL | (0.20, 0.65) | (0.20, 0.65) |
| | C7 | ST | SL | HL | (0.55, 0.35) | (0.75, 0.25) |
| | | TA | HL | VHL | (0.75, 0.25) | (1.00, 0.00) |
| | | OP | ML | SL | (0.40, 0.50) | (0.55, 0.35) |
| | C8 | ST | VHL | VHL | (1.00, 0.00) | (1.00, 0.00) |
| | | TA | HL | HL | (0.75, 0.25) | (0.75, 0.25) |
| | | OP | IL | NL | (0.20, 0.65) | (0.00, 1.00) |
| | C9 | ST | HL | HL | (0.75, 0.25) | (0.75, 0.25) |
| | | TA | SL | SL | (0.55, 0.35) | (0.55, 0.35) |
| | | OP | NL | NL | (0.00, 1.00) | (0.00, 1.00) |
| | C10 | ST | VHL | VHL | (1.00, 0.00) | (1.00, 0.00) |
| | | TA | VHL | VHL | (1.00, 0.00) | (1.00, 0.00) |
| | | OP | IL | ML | (0.20, 0.65) | (0.40, 0.50) |
| | C11 | ST | VHL | VHL | (1.00, 0.00) | (1.00, 0.00) |
| | | TA | HL | HL | (0.75, 0.25) | (0.75, 0.25) |
| | | OP | ML | SL | (0.40, 0.50) | (0.55, 0.35) |
| | C12 | ST | VHL | VHL | (1.00, 0.00) | (1.00, 0.00) |
| | | TA | VHL | HL | (1.00, 0.00) | (0.75, 0.25) |
| | | OP | IL | NL | (0.20, 0.65) | (0.00, 1.00) |

The linguistic terms (LT) and IFNs for the adopted alternatives were then determined:

- LT: Very high level (VHL) – IFN ∈ [1.00;0.00]
- LT: High level (HL) – IFN ∈ [0.75;0.25]
- LT: Significant level (SL) – IFN ∈ [0.55;0.35]
- LT: Medium level (ML) – IFN ∈ [0.40;0.50]
- LT: Insignificant level(IL) – IFN ∈ [0.20;0.65]
- LT: Nonsignificant level (NL) – IFN ∈ [0.00;1.00]

Based on Table 1, the experts assessed the criteria in terms of the alternatives adopted (Table 3).

The aggregated Intuitionistic Fuzzy Decision Matrix according to the DMs opinions presented on Table 4 (Eq. 8).

**Table 4** Aggregated Intuitionistic Fuzzy Decision Matrix

| | | ST | TA | OP |
|---|---|---|---|---|
| R = | C1 | (1.000, 0.000, 0.000) | (0.656, 0.210, 0.043) | (0.299, 0.576, 0.124) |
| | C2 | (0.657, 0.299, 0.043) | (1.000, 0.000, 0.000) | (0.400, 0.500, 0.100) |
| | C3 | (0,750. 0.250, 0.000) | (1.000, 0.000, 0.000) | (0.299, 0.576, 0.125) |
| | C4 | (1.000, 0.000, 0.000) | (0.672, 0.291, 0.036) | (0.113, 0.792, 0.093) |
| | C5 | (1.000, 0.000, 0.000) | (0.625, 0.344, 0.030) | (0.200, 0.650, 0.150) |
| | C6 | (0,750. 0.250, 0.000) | (1.000, 0.000, 0.000) | (0.200, 0.650, 0.150) |
| | C7 | (0.656, 0.210, 0.043) | (1.000, 0.000, 0.000) | (0.475, 0.424, 0.101) |
| | C8 | (1.000, 0.000, 0.000) | (0,750, 0.250, 0.000) | (0.113, 0.792, 0.093) |
| | C9 | (0,750. 0.250, 0.000) | (0.550, 0.350, 0.150) | (0.000, 1.000, 0.000) |
| | C10 | (1.000, 0.000, 0.000) | (1.000, 0.000, 0.000) | (0.299, 0.576, 0.125) |
| | C11 | (1.000, 0.000, 0.000) | (0,750. 0.250, 0.000) | (0.475, 0.424, 0.101) |
| | C12 | (1.000, 0.000, 0.000) | (1.000, 0.000, 0.000) | (0.133, 0.793, 0.094) |

DMs evaluated selected criteria and sub-criteria using linguistic terms (Table 5, Table 6). The opinions received in form of linguistic terms were then translated into intuitionistic fuzzy numbers (Table 7, Table 8).

**Table 5** The criteria importance weight

| Action | Criteria | DMs | |
|---|---|---|---|
| | | DM1 | DM2 |
| MS | C1 | C | VI |
| | C2 | VI | C |
| | C3 | VI | VI |
| | C4 | I | VI |
| | C5 | C | VI |
| | C6 | I | MC |
| | C7 | MC | I |
| | C8 | VI | VI |
| | C9 | I | I |
| | C10 | VI | VI |
| | C11 | C | C |
| | C13 | C | C |

**Table 6** The sub-criteria importance weight

| Action | Sub-criteria | DMs | |
|---|---|---|---|
| | | DM1 | DM2 |
| MS | I1 | C | VI |
| | I2 | VI | C |
| | I3 | I | VI |
| | I4 | VI | I |
| | I5 | C | VI |
| | I6 | MC | LC |
| | I7 | I | I |
| | I8 | I | VI |
| | I9 | VI | VI |
| | I10 | MC | I |
| | I11 | C | VI |
| | I12 | VI | VI |
| | I13 | VI | I |
| | I14 | C | C |

**Table 7** The rating of criteria based on intuitionistic fuzzy numbers

| Action | Criteria | DMs | |
|---|---|---|---|
| | | DM1 | DM2 |
| MS | I1 | (0.90, 0.10) | (0.75, 0.25) |
| | I2 | (0.75, 0.25) | (0.90, 0.10) |
| | I3 | (0.75, 0.25) | (0.75, 0.25) |
| | I4 | (0.45, 0.55) | (0.75, 0.25) |
| | I5 | (0.90, 0.10) | (0.75, 0.25) |
| | I6 | (0.45, 0.55) | (0.25, 0.75) |
| | I7 | (0.25, 0.75) | (0.45, 0.55) |
| | I8 | (0.75, 0.25) | (0.75, 0.25) |
| | I9 | (0.45, 0.55) | (0.45, 0.55) |
| | I10 | (0.75, 0.25) | (0.75, 0.25) |
| | I11 | (0.90, 0.10) | (0.90, 0.10) |
| | I12 | (0.90, 0.10) | (0.90, 0.10) |

**Table 8** The rating of sub-criteria based on intuitionistic fuzzy numbers

| Action | Sub-criteria | DMs | |
|---|---|---|---|
| | | DM1 | DM2 |
| MS | I1 | (0.90, 0.10) | (0.75, 0.25) |
| | I2 | (0.75, 0.25) | (0.90, 0.10) |
| | I3 | (0.45, 0.55) | (0.75, 0.25) |
| | I4 | (0.75, 0.25) | (0.45, 0.55) |
| | I5 | (0.90, 0.10) | (0.75, 0.25) |
| | I6 | (0.25, 0.75) | (0.10, 0.90) |
| | I7 | (0.45, 0.55) | (0.45, 0.55) |
| | I8 | (0.45, 0.55) | (0.75, 0.25) |
| | I9 | (0.75, 0.25) | (0.75, 0.25) |
| | I10 | (0.25, 0.75) | (0.45, 0.55) |
| | I11 | (0.90, 0.10) | (0.75, 0.25) |
| | I12 | (0.75, 0.25) | (0.75, 0.25) |
| | I13 | (0.75, 0.25) | (0.45, 0.55) |
| | I14 | (0.90, 0.10) | (0.90, 0.10) |

Aggregation of criteria and sub-criteria importance according to DMs opinions is presented in Table 9 (Eq. 6). The final weights for aggregated criteria and sub-criteria (ACI) are presented in Table 10 (Eq. 11).

**Table 9** The aggregated importance of criteria and sub-criteria

| Action | Combination | DMs | |
|---|---|---|---|
| | | DM1 | DM2 |
| MS | I1 | (0.90, 0.10) | (0.75, 0.20) |
| | I2 | (0.75, 0.20) | (0.90, 0.10) |
| | I3 | (0.45, 0.50) | (0.75, 0.20) |
| | I4 | (0.45, 0.50) | (0.45, 0.50) |
| | I5 | (0.90, 0.10) | (0.75, 0.20) |
| | I6 | (0.25, 0.70) | (0.10, 0.90) |
| | I7 | (0.25, 0.70) | (0.45, 0.55) |
| | I8 | (0.75, 0.20) | (0.75, 0.20) |
| | I9 | (0.25, 0.70) | (0.45, 0.50) |
| | I10 | (0.75, 0.20) | (0.75, 0.20) |
| | I11 | (0.75, 0.20) | (0.45, 0.50) |
| | I12 | (0.90, 0.10) | (0.90, 0.10) |

**Table 10** The final weight of Aggregated Criteria and Sub-criteria (ACI)

| | | |
|---|---|---|
| W = | ACI1 | (0.8474, 0.1525, 0.0001) |
| | ACI2 | (0.8361, 0.1638, 0.0001) |
| | ACI3 | (0.6176, 0.3823, 0.0391) |
| | ACI4 | (0.6176, 0.3823, 0.0001) |
| | ACI5 | (0.8474, 0.1525, 0.0001) |
| | ACI6 | (0.1842, 0.8157, 0.0001) |
| | ACI7 | (0.3499, 0.6501, 0.0000) |
| | ACI8 | (0.7500, 0.2500, 0.0000) |
| | ACI9 | (0.3499, 0.6501, 0.0000) |
| | ACI10 | (0.7500, 0.2500, 0.0000) |
| | ACI11 | (0.6404, 0.3596, 0.0000) |
| | ACI12 | (0.9000, 0.1000, 0.0000) |

Based on Aggregated Intuitionistic Fuzzy Decsion Matrix (Table 4) and the weightings of criteria and sub-criteria ($W$) the aggregated weighted intuitionistic fuzzy decision matrix was created, where Eq. 14 and Eq. 15 were used.

**Table 11** The aggregated weighted intuitionistic fuzzy decision matrix

| | | ST | TA | OP |
|---|---|---|---|---|
| | C1 | (0.874,0.153,0.001) | (0.556, 0.330,0.114) | (0.253, 0.641,0.106) |
| | C2 | (0.549,0.414,0.037) | (0.836,0.164,0.000) | (0.334,0.582,0.084) |
| | C3 | (0.493,0.519,0.042) | (0.618,0.382,0.000) | (0.131,0.728,0.141) |
| | C4 | (0.617,0.382,0.001) | (0.415,0.562,0.023) | (0.082,0.871,0.047) |
| | C5 | (0.847,0.153,0.000) | (0.529,0.444,0.027) | (0.169,0.703,0.128) |
| R' = | C6 | (0.138,0.862,0.000) | (0.184,0.816,0.002) | (0.037,0.935,0.028) |
| | C7 | (0.229,0.724,0.047) | (0.349,0.650,0.001) | (0.166,0.798,0.036) |
| | C8 | (0.750,0.250,0.000) | (0.563,0.437,0.000) | (0.085,0.844,0.071) |
| | C9 | (0.262,0.737,0.001) | (0.192,0.773,0.035) | (0.000,1.000,0.000) |
| | C10 | (0.750,0.250,0.000) | (0.750,0.250,0.000) | (0.224,0.682,0.094) |
| | C11 | (0.640,0.359,0.001) | (0.480,0.519,0.001) | (0.304,0.631,0.065) |
| | C12 | (0.900,0.100,0.000) | (0.900,0.100,0.000) | (0.119,0.814,0.067) |

In accordance with the division presented in Table 2 the selected criteria belong respectively to the following: J1 = { C1,C2,C6,C7,C8,C9,C10,C11} and J2 = {C3,C5,C12}.

T he intuitionistic fuzzy positive-ideal solution and intuitionistic fuzzy negative-ideal solution made by using Eqs. 16 to 20.

$$A^{+}=\begin{pmatrix} (0.253,0.641,0.106) & (0.836,0.164,0.000) & (0.131,0,780,0.089\,) & (0.617,0.382,0.001) \\ (0.847,0.153,0.000) & (0.184,0.816,0.000) & (0.166,0.650,0.184\,) & (0.750,0.000,0.250) \\ (0.480,0.250,0.270) & 0.847,0.153,0.000 & 0.640,0.359,0.001) & 0.900,0.100,0.000 \end{pmatrix}$$

$$A^{-}=\begin{pmatrix} (0.847,0.153,0.000) & (0.334,0.582,0.084) & (0.618,0.382,0.000) & (0.082,0.872,0.046) \\ (0.169,0.703,0.128\,) & (0.037,0.935,0.028) & (0.349,0.650,0.001) & (0.085,0.844,0.071) \\ (0.311,0.623,0.066) & (0.253,0.641,0.106) & (0.024,0.962,0.014) & (0.403,0.512,0.085) \end{pmatrix}$$

Measurement of separation between alternatives in the Intuitionistic fuzzy set was made by using normalized Euclidean distance (Eqs. 21 and 22). Then, the relative closeness coefficient to the ideal solution (Eq. 23) was set. The results are presented in Table 12.

**Table 12** The relative closeness coefficient and separation measures of each level

| Level of management in company | $S^{+}$ | $S^{-}$ | $Ci^{*}$ | Rank |
|---|---|---|---|---|
| ST | 0.219 | 0.238 | 0.520 | 2nd |
| TA | 0.206 | 0.227 | 0.523 | 1st |
| OP | 0.305 | 0.251 | 0.451 | 3rd |

In order to rank the alternatives, the Ci* factor was first calculated and then the alternatives were ranked in decreasing order of Ci*. In the adopted case study, three levels were adopted, which were arranged as follows TA < ST < OP. As a result of calculations, the ST level was accepted as crucial for the examined company. Then, based on the results of the aggregated weighted intuitionistic fuzzy decision matrix (Table 11) key indicators were selected for the SD level by descending order of the $\mu$ parameter (Table 13).

**Table 13** Key SD objectives for the defined MS level in the context I4.0

| Rank | Criteria | Sub-criteria |
|---|---|---|
| 1 | C12 | I14 |
| 2 | C2 | I3 |
| 3 | C10 | I12 |
| 4 | C3 | I4 |
| 5 | C8 | I9 |
| | | I10 |
| 6 | C1 | I1 |
| 7 | C5 | I6 |
| 8 | C11 | I13 |
| 9 | C7 | I8 |
| 10 | C4 | I5 |
| 11 | C9 | I11 |
| 12 | C6 | I7 |

The results obtained using the F-TOPSIS method represent the key objectives of MS in production enterprises. These objectives should be pursued first, as they form the basis for further activities carried out in the organisation for the benefit of the MS in the context of I4.0. Therefore the values of the key SD objectives set should be determined based on the data included in IT in the I4.0 context (Table 14).

**Table 14** Data source in IT in I4.0 context for the values of the key SD objectives set

| Rank | Criteria | Data source |
|---|---|---|
| 1 | C12 | ERP |
| 2 | C2 | ERP |
| 3 | C10 | MANUALLY |
| 4 | C3 | ERP |
| 5 | C8 | ERP |
| 6 | C1 | ERP |
| 7 | C5 | ERP |
| 8 | C11 | ERP |
| 9 | C7 | MANUALLY |
| 10 | C4 | MANUALLY |
| 11 | C9 | MANUALLY |
| 12 | C6 | MANUALLY |

## 4. Verification and discussion

The proposed approach was verified and implemented in five Polish metal companies from the SME sector, in order to verify the usability of applying our model to select SD objectives and to define the needed corrective actions to increase the level of SD in the company.

The following company's activities that are supported by an IT in I4.0 (an ERP system) and its functionality were indicated, namely: Production planning (F1), Cost accounting (F2), Manufacturing execution system (F3), Production technology management (F4), Customer relationship management (F5), Service and repair planning (F6), Personnel management (F7), Warehouse Management (F8), Transport improvement (F9).

The following SD indicator values in the analysed company were obtained (Table 15).

**Table 15** The base of SD indicator values in the analysed companies

| C | S-C | Data source | Functionality of the ERP system | Value | | | | |
|---|---|---|---|---|---|---|---|---|
| | | | | I | II | III | IV | V |
| C12 | I14 | ERP | F2 | 640000 kWh | 38128 kWh | 25000 kWh | 26141 kWh | 41344 kWh |
| C2 | I3 | ERP | F1 | over 90 % | over 90 % | less than 80 % | between 80-90 % | less than 80 % |
| C10 | I12 | MANUALLY | - | YES | YES | NO | YES | YES |
| C3 | I4 | EPP | F6 | 10 | 20 | 0 | 0 | 16 |

To determine the reference SD indicators values for a given class of enterprises in a given area the statistical data on a given country, which should be averaged out for a given industry of enterprises should be adopted. Therefore the reference MS indicators values for a given class of enterprises were obtained based on the statistical data in Poland [35] and REACH; ISO 14001; ISO50001; OHSAS 18001 were obtained (Table 16).

**Table 16** The reference values

| SD objective | SD Indicators | Reference values I |
|---|---|---|
| C12 | I14 | -5 % |
| C2 | I3 | over 90 % |
| C10 | I12 | YES |
| C3 | I4 | 0 |

However, to apply our approach to enterprises in other countries, the reference MS indicators values for a given class of enterprises based on the statistical data in the country of the surveyed enterprise should be adopted.

Finally, the setting of SD recommendations for the analysed company is possible based on the comparison of the obtained key SD indicator values with the reference values for the SD indicators (Table 17, Table 18).

**Table 17** Range of values for determining the level of SD

| MS level | Compartment |
|---|---|
| Good | < 90-100 % references values |
| Medium | < 85-60 % references values |
| Low | > 60 % references values |

**Table 18** The base of the obtained SD indicators values in the company compared with the reference values

| Enterprise | Criteria | Sub-Criteria | Reference values | Obtained values | SD level |
|---|---|---|---|---|---|
| I | C12 | I14 | -5 % | 640000 | Check after implementing changes |
| | C2 | I3 | over 90 % | over 90 % | Good |
| | C10 | I12 | YES | YES | Good |
| | C3 | I4 | 0 | 10 | Low |
| II | C12 | I14 | -5 % | 38128 | Check after implementing changes |
| | C2 | I3 | over 90 % | over 90 % | Good |
| | C10 | I12 | YES | YES | Good |
| | C3 | I4 | 0 | 20 | Low |
| III | C12 | I14 | -5 % | 25000 | Check after implementing changes |
| | C2 | I3 | over 90 % | less than 80 % | Low |
| | C10 | I12 | YES | NO | Low |
| | C3 | I4 | 0 | 0 | Good |
| IV | C12 | I14 | -5 % | 26141 | Check after implementing changes |
| | C2 | I3 | over 90 % | between 80-90 % | Medium |
| | C10 | I12 | YES | YES | Good |
| | C3 | I4 | 0 | 0 | Good |
| V | C12 | I14 | -5 % | 41344 | Check after implementing changes |
| | C2 | I3 | over 90 % | less than 80 % | Low |
| | C10 | I12 | YES | YES | Good |
| | C3 | I4 | 0 | 16 | Low |

Thanks to the implementation of our model in the analysed company, it is possible to define the key SD objectives:

- C12: non-renewable energy consumption
- C2: cost of training for maintenance, preventive maintenance time causing downtime
- C10: number of innovations carried out related to sustainable maintenance.

Moreover, based on Table 18, it is possible to define the needed corrective actions that the company must take to increase its SD level. In the considered case:

- reduction of non-renewable energy consumption: e.g., control energy consumption, systematic maintenance and service of machines, use of renewable energy,
- staff education: conservation according to the schedule, regular training of maintenance staff,
- innovation: intelligent solutions, modern warning systems, automated lubrication, operational diagnostics.

The universality of the proposed approach and its adaptability to the specificity of a given company allows it to be employed in different types of enterprises.

## 5. Conclusion

Industry 4.0 technologies and sustainability are popular organizational trends that are vital to increasing sustainable production [36]. However, despite numerous considerations regarding the positive aspects of the implementation of Industry 4.0 technology in the SD concept, further negative effects on the environment are also indicated by throwing outdated equipment [37], and therefore increased greenhouse gas emissions or the production of a large amount of waste [38].

As with all studies, this study owns up to certain limitations that further research should be able to overcome. Firstly, the use of normalized Euclidean distance, which does not take into account the correlation between attributes, and the lack of correlation between criteria and sub-criteria are considered limitations of the proposed approach. Secondly, the verification of a model was shown in the example of the Polish companies investigated and all the indicators were measured at the same moment in time; it would, therefore, be useful to provide such research over a longer time period. These conclusions and limitations suggest proposals for the direction of future research.

## Acknowledgement

This work is supported by the programme of the Polish Minister of Education and Science under the name "Regional Initiative of Excellence" 2019 - 2023, project no. 003/RID/2018/19, funding amount 11 936 596.10 PLN..

## References

[1] Iung, B., Levart, E. (2014). Advanced maintenance services for promoting sustainability, *Procedia CIRP*, Vol. 22, 15-22, doi: 10.1016/j.procir.2014.07.018.

[2] Nezami, F.G., Yildirim, M.B. (2013). A sustainability approach for selecting maintenance strategy, *International Journal of Sustainable Engineering,* Vol. 6, No. 4, 332-343, doi: 10.1080/19397038.2013.765928.

[3] EN 13306:2017 Maintenance – Maintenance terminology, *https://www.en-standard.eu/bs-en-13306-2017-maintenance-maintenance-terminology/*.

[4] Djurović, D., Bulatović, M., Soković, M., Stoić, A. (2015). Measurement of maintenance excellence, *Tehnički Vjesnik – Technical Gazette,* Vol. 22, No. 5, 1263-1268, doi: 10.17559/TV-20140922094945.

[5] Singh, R.K., Gupta, A. (2020). Framework for sustainable maintenance system: ISM–fuzzy MICMAC and TOPSIS approach, *Annals of Operations Research*, Vol. 290, 643-676, doi: 10.1007/s10479-019-03162-w.

[6] Boral, S., Chaturvedi, S.K., Naikan, V.N., Howard, I.M. (2019). Hybrid AI based conceptual decision making model for sustainable maintenance strategy selection, In: Chatterjee, P., Yazdani, M., Chakraborty, S., Panchal, D, Bhattacharyya, S. (eds.), *Advanced multi-criteria decision making for addressing complex sustainability issues,* IGI Global, Hershey, Pennsylvania, USA, 63-93, doi: 10.4018/978-1-5225-8579-4.ch004.

[7] Franciosi, C., Di Pasquale, V., Iannone, R., Miranda, S. (2021). Multi-stakeholder perspectives on indicators for sustainable maintenance performance in production contexts: An exploratory study, *Journal of Quality in Maintenance Engineering*, Vol. 27, No. 2, 308-330, doi: 10.1108/JQME-03-2019-0033.

[8] Franciosi, C., Voisin, A., Miranda, S., Riemma, S., Iung, B. (2020). Measuring maintenance impacts on sustainability of manufacturing industries: From a systematic literature review to a framework proposal, *Journal of Cleaner Production*, Vol. 260, Article No. 121065, doi: 10.1016/j.jclepro.2020.121065.

[9] Costantino, F., Di Gravio, G., Tronci, M. (2013). Integrating environmental assessment of failure modes in maintenance planning of production systems, *Applied Mechanics and Materials*, Vol. 295-298, 651-660, doi: 10.4028/www.scientific.net/AMM.295-298.651.

[10] Sénéchal, O., Trentesaux, D. (2019). A framework to help decision makers to be environmentally aware during the maintenance of cyber physical systems, *Environmental Impact Assessment Review,* Vol. 77, 11-22, doi: 10.1016/j.eiar.2019.02.007.

[11] Pires, S.P., Sénéchal, O., Loures, E.F.R., Jimenez, J.F. (2016). An approach to the prioritization of sustainable maintenance drivers in the TBL framework, *IFAC-PapersOnLine*, Vol. 49, No. 28, 150-155, doi: 10.1016/j.ifacol.2016.11.026.

[12] Amrina, E., Yulianto, A. (2018). Interpretive structural model of key performance indicators for sustainable maintenance evaluatian in rubber industry, *IOP Conference Series: Materials Science and Engineering*, Vol. 319, Article No. 012055, doi: 10.1088/1757-899X/319/1/012055.

[13] GRI, GRI, 2016. G4 Reporting Guidelines, *https://www.globalreporting.org/standards/*.

[14] Sénéchal, O. (2018). Performance indicators nomenclatures for decision making in sustainable conditions based maintenance, *IFAC-PapersOnLine*, Vol. 51, No. 11, 1137-1142, doi: 10.1016/j.ifacol.2018.08.438.

[15] Jasiulewicz-Kaczmarek, M., Żywica, P., Gola, A. (2021). Fuzzy set theory driven maintenance sustainability performance model: A multiple criteria approach, *Journal of Intelligent Manufacturing*, Vol. 32, 1497-1515, doi: 10.1007/s10845-020-01734-3.

[16] Sari, E., Shaharou, A.M., Ma'aram, A., Yazid, A.M. (2015). Sustainable maintenance performance measures: A pilot survey in Malaysian automotive companies, *Procedia CIRP*, Vol. 26, 443-448, doi: 10.1016/j.procir.2014.07.163.

[17] Zhou, K., Liu, T., Zhou, L. (2016). Industry 4.0: Towards future industrial opportunities and challenges, In: *Proceedings of 2015 12th International Conference on Fuzzy Systems and Knowledge Discovery (FSKD),* Zhangjiajie, China, 2147-2152, doi: 10.1109/FSKD.2015.7382284.

[18] Jayashree, S., Reza, M.N.H., Malarvizhi, C.A.N., Mohiuddin, M. (2021). Industry 4.0 implementation and triple bottom line sustainability: An empirical study on small and medium manufacturing firms, *Heliyon*, Vol. 7, No. 8, Article No. e07753, doi: 10.1016/j.heliyon.2021.e07753.

[19] Braccini, A.M., Margherita, E.G. (2019). Exploring organizational sustainability of Industry 4.0 under the triple bottom line: The case of a manufacturing company, *Sustainability*, Vol. 11, No. 1, Article No. 36, doi: 10.3390/su11010036.

[20] Büchi, G., Cugno, M., Castagnoli, R. (2020). Smart factory performance and Industry 4.0, *Technological Forecasting and Social Change*, Vol. 150, Article No. 119790, doi: 10.1016/j.techfore.2019.119790.

[21] Makris, D., Hansen, Z.N.L., Khan, O. (2019). Adapting to supply chain 4.0: An explorative study of multinational companies, *Supply Chain Forum: An International Journal,* Vol. 20, No. 2, 116-131, doi: 10.1080/16258312.2019.1577114.

[22] Fattoruso, G. (2022). Multi-criteria decision making in production fields: A structured content analysis and implications for practice, *Journal of Risk and Financial Management,* Vol. 15, Article No. 431, doi: 10.3390/jrfm15100431.

[23] Devatha, C.P., Thalla, A.K. (2019). Prioritizing cropping alternatives based on attribute specification and comparison using MADM models, *Journal of the Saudi Society of Agricultural Sciences,* Vol. 18, No. 3, 337-343, doi: 10.1016/j.jssas.2017.09.007.

[24] Rudnik, K., Kacprzak, D. (2017). Fuzzy TOPSIS method with ordered fuzzy numbers for flow control in a manufacturing system, *Applied Soft Computing,* Vol. 52, 1020-1041, doi: 10.1016/j.asoc.2016.09.027.

[25] Shukla, V., Swarnakar, V., Singh, A.R. (2021). Prioritization of lean six sigma project selection criteria using best worst method, *Materials Today: Proceedings,* Vol. 47, Part 17, 5749-5754, doi: 10.1016/j.matpr.2021.04.038.

[26] Hsu, C.-H., Chang, A.-Y., Luo, W. (2017). Identifying key performance factors for sustainability development of SMEs – integrating QFD and fuzzy MADM methods, *Journal of Cleaner Production,* Vol. 161, 629-645, doi: 10.1016/j.jclepro.2017.05.063.

[27] Yang, W.-C., Chon, S.-H., Choe, C.-M., Kim, U.-H. (2019). Materials selection method combined with different MADM methods, *Journal on Artificial Intelligence,* Vol. 1, No. 2, 89-99, doi: 10.32604/jai.2019.07885.

[28] Zhang, H., Peng, Y., Tian, G., Wang, D., Xie, P. (2017). Green material selection for sustainability: A hybrid MCDM approach, *Plos One,* Vol. 12, No. 5, Article No. e0177578, doi: 10.1371/journal.pone.0177578.

[29] Chang, A.-Y., Cheng, Y.-T. (2019). Analysis model of the sustainability development of manufacturing small and medium - sized enterprises in Taiwan, *Journal of Cleaner Production,* Vol. 207, 458-473, doi: 10.1016/j.jclepro.2018.10.025.

[30] Atanassov, K.T. (1986). Intuitionistic fuzzy sets, *Fuzzy Sets and Systems,* Vol. 20, No. 1, 87-96, doi: 10.1016/S0165-0114(86)80034-3.

[31] Rajak, S., Vinodh, S. (2015). Application of fuzzy logic for social sustainability performance evaluation: A case study of an Indian automotive component manufacturing organization, *Journal of Cleaner Production,* Vol. 108, Part A, 1184-1192, doi: 10.1016/j.jclepro.2015.05.070.

[32] Abedini, A., Li, W., Badurdeen, F., Jawahir, I.S. (2020). A metric-based framework for sustainable production scheduling, *Journal of Manufacturing Systems*, Vol. 54, 174-185, doi: 10.1016/j.jmsy.2019.12.003.

[33] Anggraeni, W., Kusumawardani, R.P., Ardianto, R. (2014). Penerapan fuzzy analytical hierarchy process pada sistem penilaian pegawai di rumah sakit onkologi Surabaya, In: *Seminar Nasional Sistem Informasi Indonesia (SESINDO).*

[34] Patalas-Maliszewska, J., Łosyk, H. (2020). An approach to assessing sustainability in the development of a manufacturing company, *Sustainability*, Vol. 12, No. 21, Article No. 8787, doi: 10.3390/su12218787.

[35] Statistical Yearbook of Industry – Poland, 2018, *https://stat.gov.pl/en/topics/statistical-yearbooks/statistical-yearbooks/statistical-yearbook-of-industry-poland-2021,5,15.html*.

[36] Bai, C., Dallasega, P., Orzes, G., Sarkis, J. (2020). Industry 4.0 technologies assessment: A sustainability perspective, *International Journal of Production Economics,* Vol. 229, Article No. 107776, doi: 10.1016/j.ijpe.2020.107776.

[37] Bonilla, S.H., Silva, H.R.O., da Silva, M.T., Gonçalves, R.F., Sacomano, J.B. (2018). Industry 4.0 and sustainability implications: A scenario-based analysis of the impacts and challenges, *Sustainability*, Vol. 10, No. 10, Article No. 3740, doi: 10.3390/su10103740.

[38] Birkel, H.S., Veile, J.W., Müller, J.M., Hartmann, E., Voigt, K.-I. (2019). Development of a risk framework for Industry 4.0 in the context of sustainability for established manufacturers, *Sustainability*, Vol. 11, No. 2, Article No. 384, doi: 10.3390/su11020384.

APEM journal
**Advances in Production Engineering & Management**
Volume 17 | Number 4 | December 2022 | pp 469–478
https://doi.org/10.14743/apem2022.4.449
**ISSN 1854-6250**
Journal home: apem-journal.org
Original scientific paper

# Optimization of the rhomboidity of continuously cast billets using linear regression and genetic programming: A real industrial study

**Kovacic, M.**[a,b,c,*], **Zuperl, U.**[b], **Brezocnik, M.**[d]

[a]ŠTORE STEEL, d.o.o., Research and Development, Štore, Slovenia
[b]University of Ljubljana, Faculty of Mechanical Engineering, Laboratory for Fluid Dynamics and Thermodynamics, Ljubljana, Slovenia
[c]College of Industrial Engineering, Celje, Slovenia
[d]University of Maribor, Faculty of mechanical engineering, Maribor, Slovenia

**A B S T R A C T**

During the continuous casting of steel billets, several geometrical, inner and surface defects can occur due to the thermomechanical behavior during solidification. One of them is rhombic distortion (i.e. rhomboidity), which can lead to the occurrence of off-corner cracks and twisting of cast billets during further plastic deformation (i.e. rolling). Based on data of 2088 cast batches (64 different hypoeutectoid steel grades), 109,514 billets, produced from January 2022 to September 2022 in Štore Steel Ltd. (Slovenia), chemical composition (content of C, Si, Mn, S, Cr, Mo, Ni and V), casting parameters (average casting temperature, average difference between input and output cooling water, melt level, average cooling water flow and pressure in the first and second zone of secondary cooling) the linear regression and genetic programming were used in order to predict rhomboidity of continuously cast billets. The rhomboidity, in our case defined as relative diagonal difference, was determined using in-house developed computer vision system for measuring of rhomboidity. Based on the modelling results 9 batches (419 billets) of 42CrMos4 were cast in September 2022 with a 10 % higher water pressure in the first zone of secondary cooling (from 2.41 bar to 2.67 bar). The rhomboidity of continuously cast billets improved by 18.18 % (from 1.43 % to 1.21).

**A R T I C L E   I N F O**

*Keywords:*
Continuous casting of steel;
Casting defects;
Rhombic distortion;
Rhomboidity;
Machine learning;
Modelling;
Optimization;
Prediction;
Linear regression;
Genetic programming

**Corresponding author:*
miha.kovacic@store-steel.si
(Kovacic, M.)

*Article history:*
Received 15 June 2022
Revised 19 December 2022
Accepted 22 December 2022



## 1. Introduction

Continuous casting, as one of the most important processes in the modern steel industry, takes place when the melt cools rapidly while passing through a copper mould in a horizontal or vertical direction. During primary cooling, the heat from continuously withdrawn strand is taken away by the water-cooled jacket surrounding the mould, and the metal solidifies. Then solidification continues with secondary cooling, where the cast structure is additionally cooled in the air with help of water sprays. During solidification, the solidified shell is exposed to thermomechanical stresses, which can cause many casting defects. In the case of square billets, due to nonuniform shell solidification (i.e. nonuniform heat removal in the mould), it can be rhombic distortion (i.e. rhomboidity), which can lead to occurrence of off-corner cracks [1, 2] and twisting of the billets during plastic deformation (i.e. rolling) [3]. Generally, relative diagonal difference is used as a measure of rhomboidity of billets [1]:

$$R = 2\frac{|d_1 - d_2|}{d_1 + d_2} \tag{1}$$

where $d_1$and $d_2$ are the lengths of the opposite diagonals of the rhombus.

The rhomboidity of the billets is affected by the following parameters [1, 2, 4, 5]:

- steel chemical composition [6],
- casting temperature,
- casting speed,
- mould (i.e. primary cooling):
  - chemical composition,
  - mould thickness [7, 8],
  - mould tapper [7, 8],
  - mould support,
  - water jacket geometry and its alignment [9],
  - operation (e.g. oscillation, water flow, water quality) [9],
- secondary cooling:
  - water quality,
  - nozzles geometry,
  - nozzles assembly,
  - water pressure.

Researches can be divided into measurements and model calculations of the temperature field based on the melt velocity field (e.g. [1, 2]). During the measurements, the rhomboidity and/or temperature of the solidified shell are measured [1, 4, 7, 8, 10].

In this paper the improvement of rhomboidity of continuously cast billets in an industrial environment is presented. A wide range of influencing parameters, not only chemical composition but also casting parameters, have been used to predict of rhomboidity of continuously cast billets for several hypoeutectoid steel grades. Linear regression and genetic programming were used for modelling. At the beginning of the paper, the results of rhomboidity measurements and the influencing parameters are presented. Next, the prediction of rhomboidity of continuously cast billets using linear regression and genetic programming is presented. The results of the optimization of the continuous casting process are also presented and implemented into practice. The casting parameters for 42CrMoS4 steel grade, which is one of the most problematic steel grades in Štore Steel Ltd. in terms of surface defects occurrence, were optimized. Finally, conclusions and future work are highlighted.

## 2. Materials, methods, and experimental results

Štore Steel Ltd. is one of the major flat spring steel producers in Europe. More than 1000 steel grades with different chemical composition are produced. The main steps of the production include the following steps: melting of the scrap using electric arc furnace, tapping, ladle treatment, and continuous casting of the billets. The cooled billets are reheated and rolled in the rolling plant. The rolled bars can be subjected to additionally production operations.

Since March 2016, a new two strand continuous casting machine with a radius of 9 m has been in use (Fig. 1). Solidification of the melt takes place during primary cooling in water cooled copper mould, secondary cooling with water sprays, and tertiary radiation in air cooling.

Secondary cooling consists of 3 zones. The spray ring in zone 1 is connected directly below the mould support. It consists of 3 rows with spray nozzles which allow a uniform cooling of the billet when it leaves the mould. The upper row is equipped with 8 nozzles, the lower two rows with 4 nozzles.

The spray ring system in zone 2 is mounted on the structure in the cooling chamber. It consists of 2 parts – zone 2a and zone 2b. Zone 2a and 2b consist of 8 and 6 rows with spray nozzles, respectively. 5 rows are installed in zone 3. All rows are equipped with 4 nozzles.

The continuous casting machine and its cooling zones are schematically presented in Fig. 1.

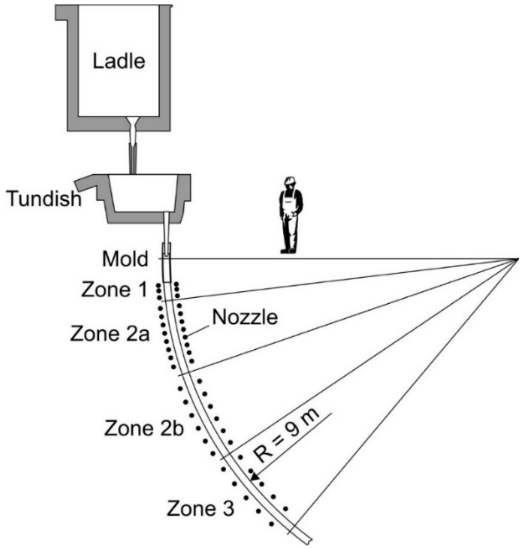


**Fig. 1** The continuous casting machine and its cooling zones

The company uses in-house developed computer vision system for measurements of rhomboidity. Before entering the cooling bad, each billet is photographed, analyzed, selected features automatically recognized (e.g. billet corners) using computer vision algorithms and finally calculated relative diagonal-difference is stored in the informational system. The in-house developed computer vision system for measurement of rhomboidity of billets is presented in Fig. 2.

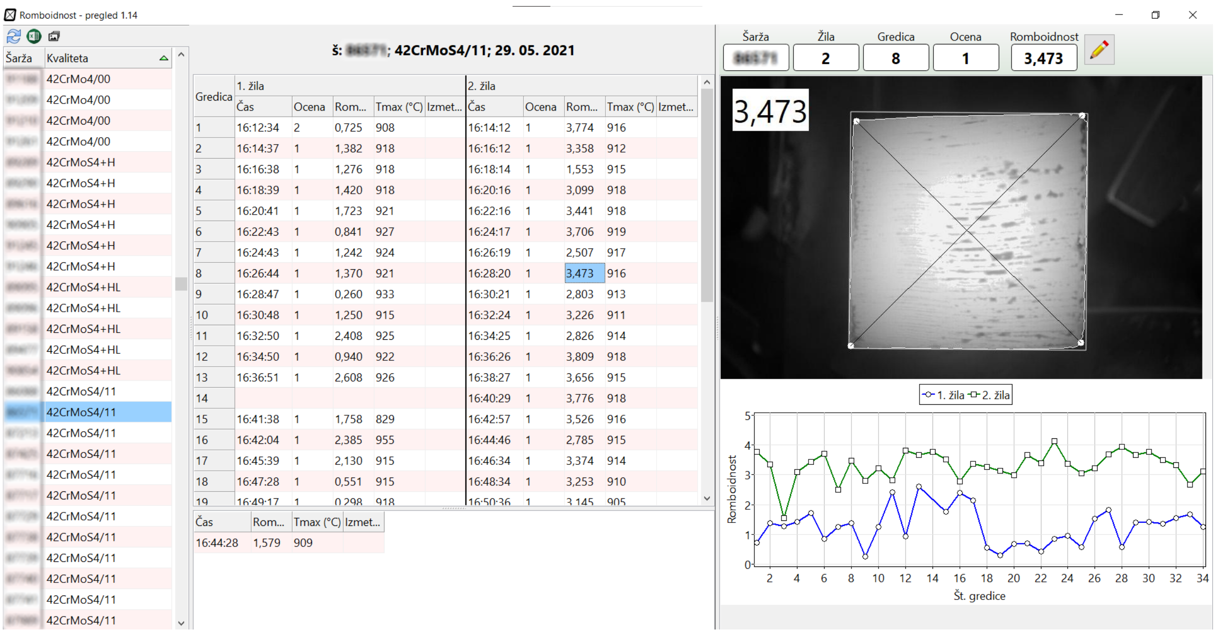


**Fig. 2** In-house developed computer vision system for measurement of rhomoboidity of billets in Štore Steel Ltd.

From January 2022 to September 2022, 2088 batches was produced (64 different hypoeutectoid steel grades), and as a result, 109514 billets were cast in Štore Steel Ltd. To reduce the rhomboidity of continuously cast billets following parameters were gathered:

- Chemical composition. The content of carbon, silicon, manganese, sulfur, chromium, molybdenum, nickel and vanadium were taking into account. Chemical composition influence on material properties also during solidification (e.g. shrinkage, tensile strength).
- Casting parameters were:
  - Average casting temperature (°C). Casting temperature influences the thermal field in the mould, which influence the heat removal and solidification.
  - Mould water flow (l/min]. The highest heat removal occurs in the mould, where thermomechanical behavior influences on shell solidification.
  - Average difference between input and output mould cooling water temperature (°C). This temperature difference is a measure of efficiency of heat removal from the mould (i.e. primary cooling). The mould is cooled with the water. The heating up of the cooling water flowing through the mould indicates the efficiency of heat removal, which influences the thermomechanical behavior during solidification.
  - Mould metal level (%) expressed as a ratio between operational height of the melt level in the mould and length of the moud (mould is 1 m long copper tube). Delicate melt level movement influences on uniform shell solidification. Nonuniform shell formation leads to rhombic distortion.
  - The average cooling water pressure (bar) and flow (l/min) in the first (directly below the mould) and the second zone of secondary cooling. The melt primarily solidifies in the mould. After exiting the mould, the strand is cooled by water sprays, where water flux can be automatically set, varying water pressure/flow. Secondary cooling also influences on thermomechanical behavior during solidification.
- The rhomboidity of continuously cast billets (%) was determined using in-house developed computer vision system.

The average values and standard deviations of gathered influential parameters are presented in Table 1.

**Table 1** Minimal and maximal values of gathered parameters

| Parameter | Label | Average | Standard deviation |
|---|---|---|---|
| Carbon content (%) | C | 0.40 | 0.152 |
| Silicon content (%) | SI | 0.38 | 0.330 |
| Manganese content (%) | MN | 0.98 | 0.270 |
| Sulfur content (%) | S | 0.02 | 0.019 |
| Chromium content (%) | CR | 0.66 | 0.444 |
| Molybdenum content (%) | MO | 0.06 | 0.067 |
| Nickel content (%) | NI | 0.21 | 0.300 |
| Vanadium content (%) | V | 0.06 | 0.051 |
| Average casting temperature (°C) | CASTING_TEMPERATURE | 1528.71 | 16.978 |
| Mould water flow (l/min) | MOULD_WATER_FLOW | 1835.71 | 77.142 |
| Average difference between input and output mould cooling water temperature (°C) | MOULD_WATER_DELTA_TEMPERATURE | 7.36 | 0.757 |
| Mould metal level (%) | STEEL_LEVEL | 78.09 | 0.932 |
| The average cooling water flow in the first zone of secondary cooling (l/min) | ZONE1_WATER_FLOW | 32.80 | 3.432 |
| The average cooling water pressure in the first zone of secondary cooling (bar) | ZONE1_WATER_PRESSURE | 2.21 | 0.504 |
| The average cooling water flow in the second zone of secondary cooling (l/min) | ZONE2_WATER_FLOW | 50.72 | 3.981 |
| The average cooling water pressure in the second zone of secondary cooling (bar) | ZONE2_WATER_PRESSURE | 2.20 | 0.482 |
| Rhomboidity (%) | RHOMB | 1.36 | 1.012 |

**Table 2** Analyzed hypoeutectoid steel grades and number of continuously cast billets

| Steel grade | Number of continuously cast billets |
|---|---|
| 51CrV4 | 26684 |
| C45S | 7387 |
| 16MnCrS5 | 6694 |
| 20MnV6 | 5805 |
| 46MnVS5 | 5442 |
| C45 | 4363 |
| C50 | 3880 |
| 30MnVS6 | 3542 |
| 52CrMoV4 | 3454 |
| 38B3 | 3045 |
| S355J2 | 2496 |
| 28MnCrB7 | 2205 |
| 20MnCrS5 | 1798 |
| 16MnCr5 | 1729 |
| 25CrMo4 | 1346 |
| 34CrNiMo6 | 1190 |
| 28MnCrNiB | 1115 |
| 42CrMoS4 | 1113 |
| 42CrMo4 | 1112 |
| 18CrNiMo7-6 | 1001 |
| 23MnNiCrMo5-2 | 985 |
| 61SiCr7 | 977 |
| 38MnVS6 | 861 |
| 20CrMoS5 | 742 |
| 16NiCrS4 | 640 |
| 31CrV3 | 588 |
| P460NH | 516 |
| C22 | 516 |
| 20MnCr5 | 505 |
| 18CrMo4 | 476 |
| 100Cr6+S | 461 |
| C60 | 455 |
| 60MnSiCr4 | 454 |
| 30MnB5 | 441 |
| 30CrNiMo8 | 437 |
| 15CrNi6 | 338 |
| 52SiCrNi5 | 315 |
| 55Si7 | 265 |
| 30NiCrMoV | 252 |
| 20NiCrMo2 | 234 |
| 37CrV3 | 230 |
| 100Cr6 | 166 |
| 30CrMnV | 153 |
| 65Si7 | 153 |
| 50CrMo4 | 144 |
| 45Mn5S | 117 |
| C35 | 116 |
| 31CrMoV9 | 110 |
| 15NiCr13 | 106 |
| C75 | 102 |
| 38MnVS5 | 98 |
| 50Mn7 | 97 |
| 20NiMoCr6-5 | 96 |
| 36MnVS4 | 93 |
| 70MnVS4 | 87 |
| 54SiCr6 | 78 |
| 20MoCrS4 | 68 |
| C15 | 62 |
| S235JR | 51 |
| 41CrS4 | 50 |
| 55Cr3 | 49 |
| 60SiMnMoV | 47 |
| 25CrMoS4 | 46 |
| S235J2 | 43 |

Table 2 shows 64 analyzed hypoeutectoid steel grades and number of continuously cast billets.

Fig. 3 shows the average rhomboidity and its standard deviation of continuously cast billets of 20 most problematic hypoeutectoid steel grades.

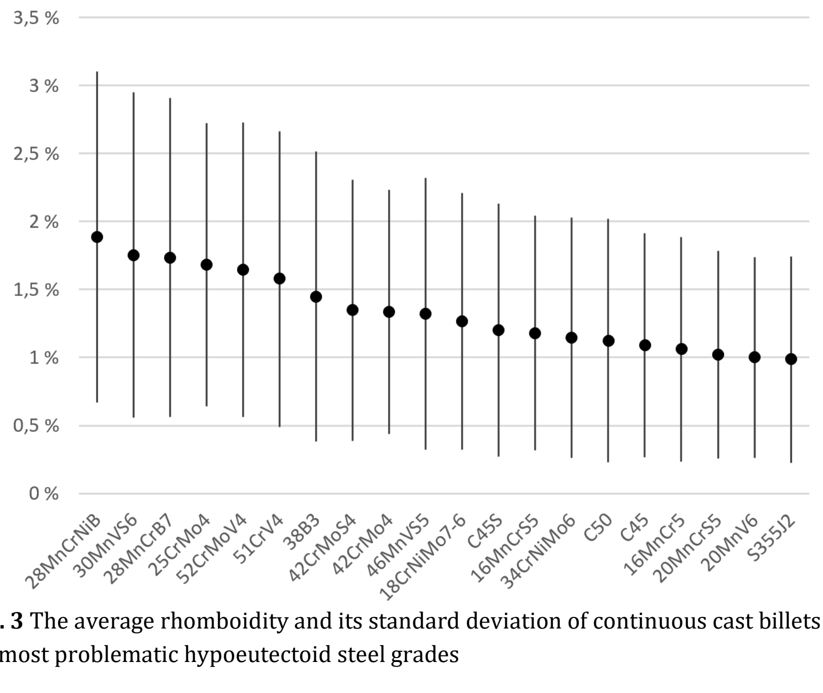


**Fig. 3** The average rhomboidity and its standard deviation of continuous cast billets of 20 most problematic hypoeutectoid steel grades

## 3. Results and discussion

Based on the collected data (Table 1), the prediction of rhomboidity of continuously cast billets was conducted. In this paper, two methods are used to support the final decisions more reliably: linear regression approach and the genetic programming evolutionary computational method. The average deviation between predicted and experimental data was selected as the fitness function expressed as:

$$\Delta = \frac{\sum_{i=1}^{n} \left| RHOMB_i - RHOMB'_i \right|}{n}, \tag{2}$$

In Eq. 1, $n$ is the size of the monitored data, where $RHOMB'_i$ and $RHOMB_i$ are the actual and the predicted actual rhomboidity of continuously cast billets, respectively.

### 3.1 Modelling of rhomboidity of continuously cast billets using linear regression

Based on the linear regression results, we realized that the model significantly predicts the rhomboidity of continuously cast billets ($p < 0.05$, ANOVA). Additionally, only 0.048 % of total variances can be explained by independent variables variances (R-square). All parameters are significantly influential except the mould metal level (STEEL_LEVEL), and the average cooling water flow in the first zone of secondary cooling (ZONE1_WATER_FLOW) ($p > 0.05$).

The obtained linear regression model is:

$$\begin{gathered} \mathrm{RHOMB} = -0.426 \cdot \mathrm{C} + 0.112 \cdot \mathrm{SI} + 0.189 \cdot \mathrm{MN} - 1.365 \cdot \mathrm{S} + 0.035 \cdot \mathrm{CR} + 0.461 \cdot \mathrm{MO} - 0.111 \cdot \mathrm{NI} - \\ 0.271 \cdot \mathrm{V} - 0.002 \cdot \mathrm{CASTING\_TEMPERATURE} + 0.002 \cdot \mathrm{MOULD\_WATER\_FLOW} - 0.0004 \cdot \\ \mathrm{MOULD\_WATER\_DELTA\_TEMPERATURE} + 0.201 \cdot \mathrm{STEEL\_LEVEL} + 0.010 \cdot \mathrm{ZONE1\_WATER\_FLOW} + \\ 0.168 \cdot \mathrm{ZONE1\_WATER\_PRESSURE} - 0.062 \cdot \mathrm{ZONE2\_WATER\_FLOW} - 0.086 \cdot \\ \mathrm{ZONE2\_WATER\_PRESSURE} + 6.156, \end{gathered} \tag{3}$$

The average deviation from experimental data is 6.23 %. The calculated influences of individual parameters on the rhomboidity of continuously cast billets while separately changing individual parameter within the individual parameter range are shown in Fig. 4. While overlooking significant influences, it seems that the mould metal level (STEEL_LEVEL) and the average cooling water flow in the second zone of secondary cooling (ZONE2_WATER_FLOW) are most influential.

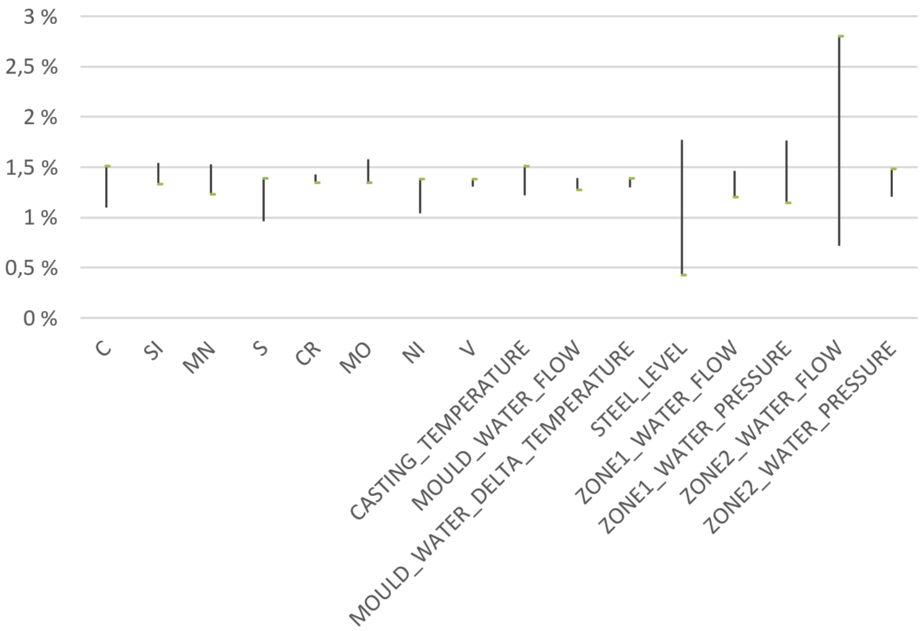


**Fig. 4** The calculated influences of individual parameters on the rhomboidity of continuously cast billets based on linear regression model

### 3.2 Modelling of rhomboidity of continuously cast billets using genetic programming

Genetic programming is a machine learning approach that mimics the natural biological evolution of natural systems. Genetic programming is a general evolutionary optimization method similar to genetic algorithms. Both methods are successfully using to solve very different problems in engineering fields and in many other areas (11-14). In genetic programming, the organisms that undergo adaptation are in fact mathematical expressions (models) of various sizes and contents [15-17]. The content depends on the nature of the problem we are solving. These models consist of the selected and/or defined functions (e.g. mathematical operations of addition, subtraction, multiplication, division) and terminals (e.g. independent input parameters, and random floating-point constants). In the initial generation, random models (i.e. computer programs) of various forms and lengths are generated. In subsequent generations, models are modified by the genetic operations, such as crossover and mutation. After the completion of the variation of the computer programs, a new generation is obtained. During the simulated evolution, each model is evaluated. In most cases, we use experimental data and fitness function for evaluation of models. The iterative process continues until a model that meets the set criteria is obtained.

For the purpose of this research, an in-house genetic programming system [18] developed in AutoLISP was used. The following evolutionary parameters were used. The genetic operations of reproduction and crossover were used in the population size of 1000, maximum number of generations was set to 200, probability of reproduction was 0.4, probability of crossover 0.6, and minimum and maximum permissible depth of models in the initial population and after execution of crossover operation was 2 and 6, respectively. For selection of organisms, the tournament method with tournament size 7 was used. One hundred independent runs were caried out. The best mathematical model for prediction of the rhomboidity of continuously cast billets obtained from 100 runs of genetic programming system is:

$$\mathrm{RHOMB} = \frac{1}{\mathrm{ZONE1\_WATER\_FLOW}}\left(MN - S - 0.014\left(\frac{C}{S} + S + \frac{C^2}{S \cdot SI}\right)\left(\frac{C}{MN} + \frac{\mathrm{ZONE1\_WATER\_PRESSURE}}{\mathrm{ZONE1\_WATER\_FLOW}}\right) + \frac{\left(CASTING\_TEMPERATURE - C - \frac{C}{SI}\right)(C + MN + ZONE1\_WATER\_FLOW)}{C - \frac{C^2}{MN \cdot S} + CASTING\_TEMPERATURE - ZONE1\_WATER\_FLOW + \frac{ZONE1\_WATER\_FLOW}{SI}}\right). \tag{4}$$

The average deviation from experimental data produced by the model in Eq. 4 was 5.79 %. The model obtained by genetic programming was 7.52 % better than the one obtained using linear regression. The calculated influences of individual parameters on the rhomboidity of continuously cast billets while separately changing individual parameter within the individual parameter range are shown in Fig. 5. Based on calculated influences it seems that beside chemical composition the average cooling water flow in the first zone of secondary cooling (ZONE1_WATER_FLOW) is most influential. Please mind that content of Cr (CR), Mo (MO), Ni (NI), V (V), average casting temperature (CASTING_TEMPERATURE), mould water flow (MOULD_WATER_FLOW), average difference between input and output mould cooling water temperature (MOULD_WATER_DELTA_TEMPERATURE), mould metal level (STEEL_LEVEL), the average cooling water flow (ZONE2_WATER_FLOW) and pressure (ZONE2_WATER_PRESSURE) in the second zone of secondary cooling are missing in the Eq. 4. Based on this fact, we can conclude that natural selection and crossover operations select the components (i.e. functions or terminals) of mathematical expressions which best describe the collected data.

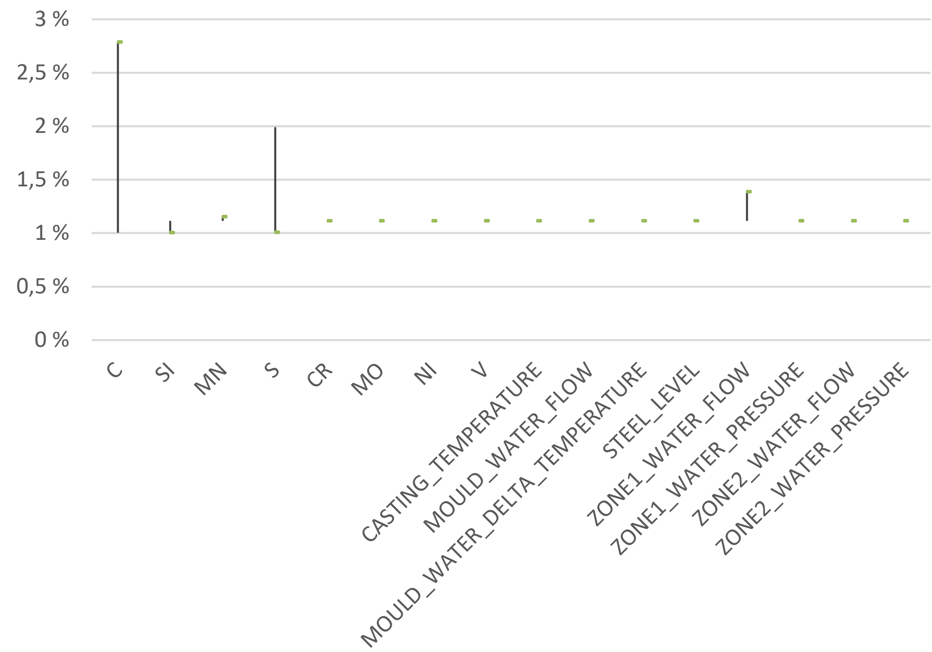


**Fig. 5** The calculated influences of individual parameters on the rhomboidity of continuously cast billets based on genetic programming model

### 3.3 Modelling results and validation

42CrMoS4 steel grade as special structural steel used for highly stressed components for the automotive industry and mechanical engineering (e.g. shafts, connecting rods, crankshafts, screws) is one of the most problematic steel grades in Štore Steel Ltd. in terms of surface defects occurrence. The scrap rate after automatic control line examination of rolled material reaches up to 25 %. As a result, the optimization of the casting parameters was conducted to improve rhomboidity of continuously cast billets. The off-corner cracks and rhomboidity of continuously cast billet of 42CrMoS4 steel grade are presented in Fig. 6. Off-corner cracks at obtuse corners are indicated by arrows.

Based on modelling results 9 batches (419 billets) of 42CrMos4 were cast in September 2022 with 10 % higher water pressure in the first zone of secondary cooling (from 2.41 bar to 2.67 bar). The rhomboidity of continuously cast billets improved for 18.54 % (from 1.43 % to 1.21 %).

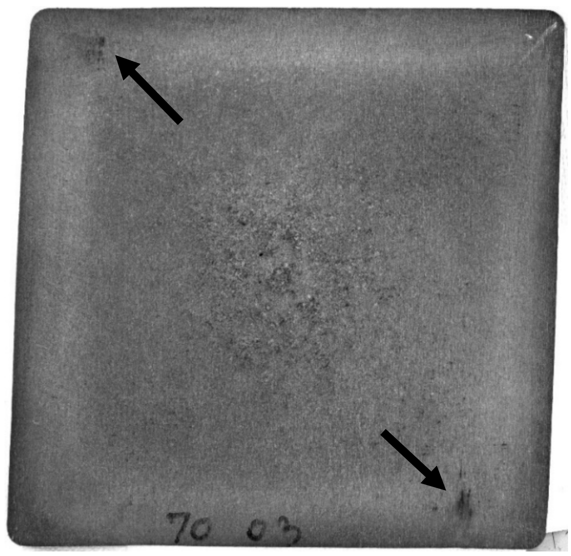


**Fig. 6** The off-corner cracks and rhomboidity of continuous cast billet of 42CrMoS4 steel grade

The average deviation from experimental data (9 batches, 419 billets of 42CrMoS4 steel grade) of linear regression and genetic programming model for rhomboidity of continuously cast billets are practically the same 0.60 % and 0.59 %, respectively.

## 4. Conclusions

In this paper, the improvement of rhomboidity of continuously cast billets in industrial environment is presented. The wide range of influencing parameters, not only chemical composition but also casting parameters, were used for prediction of rhomboidity of continuously cast billets for several hypoeutectoid steel grades. These are: content of carbon, silicon, manganese, sulfur, chromium, molybdenum, nickel and vanadium, average casting temperature, average difference between input and output cooling water, melt level, average cooling water flow and pressure in the first and second zone of secondary cooling. The in-house developed computer vision system for measurement of rhomboidity of continuously cast billets was used which is installed in the steel plant before cast billets enter the cooling bad. The relative diagonal difference was used as a measure of rhomboidity of billets.

To predict the rhomboidity of continuously cast billets, a data of 2088 cast batches (64 different hypoeutectoid steel grades), 109,514 billets, produced from January 2022 to September 2022 in were used.

Based on linear regression results all parameters except mould metal level and the average cooling water flow in the first zone of secondary cooling ($p > 0.05$) are significantly influential. Based on genetic programming results beside chemical composition only the average cooling water flow in the first zone of secondary cooling is influential.

42CrMoS4 steel grade is one of the most problematic steel grades in Štore Steel Ltd. in terms of surface defects occurrence. The scrap rate after automatic control line examination of rolled material reaches up to 25 %.

Based on modelling results 9 batches (419 billets) of 42CrMos4 were cast in September 2022 with 10 % higher water pressure in the first zone of secondary cooling (from 2.41 bar to 2.67 bar). The rhomboidity of continuous cast billets improved for 18.54 % (from 1.43 % to 1.21 %). The average deviation from experimental data (9 batches, 419 billets of 42CrMos4 steel grade) of linear regression and genetic programming model for rhomboidity of continuously cast billets are practically the same 0.60 % and 0.59 %, respectively.

In the future, secondary metallurgy (i.e. ladle treatment) parameters, refractory material and mould wear-out, strand temperature and other geometrical features of continuously cast billets (e.g. depressions, concavity) will be also taken into account in order to improve the modelling performance.

## References


[1] Patra, P., Tiwari, A., Rathore, P. (2020). In-situ online measurement of rhombic distortion in billets, *Engineering Science*, Vol. 5, No. 2, 10-16, doi: 10.11648/j.es.20200502.11.

[2] Sotnikov, A.L., Strichenko, S.M., Kireev, V.N., Fomenko, Y.V. (2020). State and prospects of upgrading equipment for billet CC machines, *Steel in Translation*, Vol. 50, 696-706, doi: 10.3103/S0967091220100113.

[3] Smirnov, E.N., Smirnov, A.N., Sklyar, V.A., Marchuk, M.V., Orlov, G.A., Belevitin, V.A., Verzilov, A.P. (2021). Investigation of contact conditions in box pass at sectional rolling of CCB possessing rhomboidity defect, *Steel in Translation*, Vol. 51, No. 11, 814-821, doi: 10.3103/S0967091221110115.

[4] Kumar, S., Meech, J.A., Samarasekera, I.V., Brimacombe, J.K., Rakocevic, V. (1999). Development of intelligent mould for online detection of defects in steel billets, *Ironmaking & Steelmaking*, Vol. 26, No. 4, 269-284. doi: 10.1179/030192399677130.

[5] Wu, H., Chen, J., Peng, Z. (2020). Simulation of the flow-heat transfer process in billet mold and analysis of the billet rhomboidity phenomenon, *Applied Thermal Engineering*, Vol. 173, Article No. 115235, doi: 10.1016/j.applthermaleng.2020.115235.

[6] Chakraborty, S., Ganguly, S., Talukdar, P. (2020). Determination of thermal resistance at mould-strand interface due to shrinkage in billet continuous casting – Development and application of a novel integrated numerical model, *International Journal of Thermal Sciences*, Vol. 152, Article No. 106305, doi: 10.1016/j.ijthermalsci.2020.106305.

[7] Chakraborty, S., Ganguly, S., Talukdar, P. (2019). Determination of optimal taper in continuous casting billet

mould using thermo-mechanical models of mould and billet, *Journal of Materials Processing Technology*, Vol. 270, 132-141, doi: 10.1016/j.jmatprotec.2019.02.032.

[8] Ray, K., Basak, I. (2020). A comprehensive approach to design the copper mold tubes for steel continuous casting, *Transactions of the Indian Institute of Metals*, Vol. 73, No. 6, 1629-1636, doi: 10.1007/s12666-020-01953-5.

[9] Kovacic, M., Brezocnik, M. (2018). Reduction of surface defects and optimization of continuous casting of 70MnVS4 steel, *International Journal of Simulation Modelling*, Vol. 17, No. 4, 667-676, doi: 10.2507/IJSIMM17(4)457.

[10] Swain, A.N.S.S., Ganguly, S., Sengupta, A., Chacko, E.Z., Dhakate, S., Pandey, P.K. (2022). Investigation of corner cracks in continuous casting billet using thermomechanical model and plant measurements, *Metals and Materials International*, Vol. 28, No. 10, 2434-2447, doi: 10.1007/s12540-021-01135-y.

[11] Gusel, L., Boskovic, V., Domitner, J., Ficko, M., Brezocnik, M. (2018). Genetic programming method for modelling of cup height in deep drawing process, *Advances in Production Engineering & Management*, Vol. 13, No. 3, 358-365, doi: 10.14743/apem2018.3.296.

[12] Nguyen, T., Pham, Q., Dang, X., Doan, T., Le, X. (2019). Optimization parameters of milling process of mould material for decreasing machining power and surface roughness criteria, *Tehnički vjesnik – Technical Gazette,* Vol. 26, No. 5, 1297-1304, doi: 10.17559/TV-20180715085107.

[13] Istokovic, D., Perinic, M., Dobovicek, S., Bazina, T. (2019). Simulation framework for determining the order and size of the product batches in the flow shop: A case study, *Advances in Production Engineering & Management*, Vol. 14, No. 2, 166-176, doi: 10.14743/apem2019.2.319.

[14] Qian, Y., Zeng, J., Zhang, S., Xu, D., Wei, X. (2020). Short-term traffic prediction based on genetic algorithm improved neural network, *Tehnički Vjesnik – Technical Gazette,* Vol. 27, No. 4, 1270-1276, doi: 10.17559/TV-20180402112949.

[15] Koza, J.R. (1990). Genetically breeding populations of computer programs to solve problems in artificial intelligence, In: *Proceedings of the 2nd International IEEE Conference on Tools for Artificial Intelligence,* Herndon, USA, 819-827, doi: 10.1109/TAI.1990.130444.

[16] Koza, J.R. (1994). *Genetic programming II: Automatic discovery of reusable programs*, MIT Press, Cambridge, USA.

[17] Koza, J.R., Andre, D., Bennett, F.H., Keane, M.A. (1999). *Genetic programming III: Darwinian invention & problem solving,* Morgan Kaufmann, San Francisco, USA.

[18] Kovačič, M., Župerl, U. (2020). Genetic programming in the steelmaking industry, *Genetic Programming and Evolvable Machines*, Vol. 21, 99-128, doi: 10.1007/s10710-020-09382-5.

APEM journal

**Advances in Production Engineering & Management** | **ISSN 1854-6250**
Volume 17 | Number 4 | December 2022 | pp 479–493 | Journal home: apem-journal.org
https://doi.org/10.14743/apem2022.4.450 | Original scientific paper

# Cause-related marketing strategy in a supply chain: A theoretical analysis and a case study

**Xu, G.Y.[a], Liu, H.[a], Duan, H.W.[b,*]**

[a]School of Management, Nanjing University of Posts and Telecommunications, Nanjing, P.R. China
[b]School of Management, Xihua University, Chengdu, P.R. China

**A B S T R A C T**

With the development of commodity market, corporate social responsibility (CSR) has become a topic of widespread concern for both enterprises and society. Cause-related marketing (CRM), as an effective marketing tool for enterprises to fulfill their social responsibility, is rapidly being applied to all stages of the supply chain. However, there is no conclusive evidence on the implementation strategy of CRM for supply chain members. In this paper, we study the decision and pricing strategies of CRM for the manufacturer and the retailer by constructing models for two scenarios: the manufacturer implements CRM, and the retailer implements CRM. We conclude that the donation percentage and the pro-sociality of consumers have a significant impact on the strategic and pricing decisions for supply chain members. The wholesale and selling prices will be higher when the manufacturer implements CRM. Our result also shows that the manufacturer and retailer are profitable in CRM only when the donation amount exceeds a certain percentage. In addition, to maximize profits, the manufacturer is more likely to allow a retailer to implement CRM, and the retailer is only optimally positioned to implement CRM when the pro-sociality of consumers is high or when the donation percentage is high.

**A R T I C L E I N F O**

*Keywords:*
Supply chain management;
Cause-related marketing;
Corporate social responsibility;
Optimal decision;
Stackelberg game

**Corresponding author:*
vividyhua@mail.xhu.edu.cn
(Duan, H.W.)

*Article history:*
Received 22 March 2022
Revised 8 October 2022
Accepted 15 October 2022



## 1. Introduction

In a market environment where the price and quality of goods are becoming more and more similar, the single provision of quality products or services can no longer meet the long-term stable development of enterprises [1, 2]. At the same time, with the pursuit of a higher quality experience, consumers are increasingly concerned about the ethical and sustainable conduct of companies [3-5]. Some scholars believe that the social, economic, and environmental behavior of a company is positively related to the profitability of the organization [6-7]. Therefore, the fulfilment of CSR has become one of the key factors indispensable for companies to gain greater competitiveness [8, 9]. As early as 1953, Bowen pointed out that companies should be socially responsible in their business activities and should make corporate decisions based on the goals and values of society. Smith *et al.* [10] considered corporate responsibility as something that goes beyond economics and law; enterprises also need to focus on politics, education, and welfare. In order to seek better survival and development, it has become a goal for companies to strive to find a marketing method that can balance the acquisition of profit and fulfill social responsibility [11, 12]. Cause-related marketing (CRM), as a combination of CSR and marketing, which can not only help firms fulfil their social responsibility and enhance brand image, but also have a positive impact on consumers' willingness to purchase, gradually becomes an effective tool in the marketing area [13].

CSR was introduced in the 1980s and has become one of the major concerns of the business community [14], and CRM is one of the ways in which companies can fulfill their social responsibility. In 1981, American Express partnered with a non-profit organization to link consumers with donations by donating two pennies to the charity for every purchase made with an Express card. The campaign not only generated additional revenue for Express, but also supported the daily operations of the charity. Another example of CRM is the Chinese brand Nongfu Spring, which launched a campaign in 2001, stating that for every mineral water sold, one cent of the proceeds would be donated to support the Olympic bid matters. When a company chooses to engage in CSR, consumers' purchasing decisions may depend not only on the intrinsic value of the product, but also on its social impact. CRM not only builds brand dependence among consumers, and creates higher revenue for the company, but also contributes to society and the environment, creating a win-win situation [15]. It is because of the multiple positive impacts of CRM for businesses that it has become a successful initiative for all types of organizations [16-17]. CRM is also widely used in all stages of the supply chain, with upstream suppliers and downstream retailers participating [18]. Supply chain members practice CRM by partnering with non-profit organizations to donate a portion of the proceeds from the sales to the community. At the same time, they will advertise for charity events. A survey shows that most consumers learn about and participate in causes through advertising [19].

In this paper, we analyze the manufacturer's and retailer's decisions and pricing strategies for implementing CRM by constructing a model in the context of the supply chain and discuss the impact of donation percentage and pro-sociality of consumers on the manufacturer's and retailer's decisions. We pose and address the following questions:

- How should the price of the manufacturer and retailer price when they implement CRM and how does the donation percentage affect pricing?
- How does the donation percentage and the pro-sociality of consumers in the target market to CRM affect the manufacturer's and retailer's decisions?
- What kind of marketing strategy should the manufacturer and the retailer develop for the benefit of the supply chain as a whole?

We consider a supply chain system consisting of a manufacturer and a retailer who play a Stackelberg game with the goal of maximizing their respective profits. We solve and analyze the optimal and equilibrium solutions of the model by constructing two scenarios, one for the manufacturer and one for the retailer. Our work will provide a suggestion for the implementation of CRM and supply chain management.

The remainder of this paper is organized as follows: Section 2 summarizes the previous literature. Section 3 illustrates the notation in this paper and models for the manufacturer and the retailer. In Section 4, we analyze the pricing and CRM decisions, and discuss the effects of donation percentage and consumer's pro-sociality. Section 5 uses arithmetic examples to validate the analysis in the previous sections. Finally, we draw conclusions in Section 6. All proofs of the paper are in the Appendix.

## 2. Literature review

This paper examines the CRM strategies of supply chain members who fulfill their CSR. Therefore, we build our study on supply chain CSR and CRM.

Many scholars have quantitatively analyzed supply chain CSR using empirical methods. Mani *et al.* [20] found that corporate engagement in CSR promotes mutual benefits among supply chain partners, increases trust to foster long-term trusting relationships. Maloni *et al.* [21] have studied CSR in the food industry and developed a comprehensive framework for supply chain CSR in this industry. Valdez-Juárez *et al.* [22] showed that CSR and SCM have a strong interdependence. Many scholars have analyzed the issue of supply chain CSR performance and influencing factors by building models. Arya *et al.* [23] analyzed the situation where the social benefits of a company's CSR strategy have nothing to do with product sales. Raza [24] demonstrated that it is feasible for manufacturers to undertake CSR investments to improve the profitability of their supply chain. Hsueh [8] analyzed the supply chain CSR and concluded that a new revenue-sharing contract with corporate social responsibility (RS-CSR) can achieve the goal of improving both performance and total supply chain profitability. Panda *et al.* [25] explored channel coordination and profit-sharing in socially responsible supply chains, concluding that CSR and its share are key determinants of channel members' net profits, and that supply chain members should pay attention to the CSR practices of other members. Liu *et al.* [26] concluded that a certain range of government subsidies can promote CSR among supply chain members and improve the overall performance and social welfare. Yan *et al.* [27] have shown that the retailer with CSR investment practices earns more profits than those without CSR investments. Most of the existing literature has studied CSR in terms of its performance and influencing factors, while little research has been done on the decision-making aspects of supply chain members. In contrast, we combine CRM and supply chain to study the pricing and strategic decisions of supply chain members in fulfilling social responsibility by building a model.

In terms of the effectiveness of CRM, Cheng *et al.* [28] found that consumers are more likely to buy brands that implement CRM. However, Furman *et al.* [29] argued that not all CRM campaigns are effective in influencing consumer decisions. Arya *et al.* [23] found by constructing a model that implementing CRM leads to an increase in the price of cause-related products. In contrast, Gao [18] argued that the implementation of CRM results in lower product pricing. There are also some scholars who have given conclusions on the relationship between CRM and consumers. Kraft *et al.* [30] thought that consumers in the segment have different pro-sociality. Silva *et al.* [31] concluded that consumers' cause-related identification has a positive impact on their perceived value. Vyravene *et al.* [32] demonstrated that the product-cause fit affects consumer attitudes toward the brand.

A subset of scholars has examined the role of the donation amount. Moosmayer *et al.* [33] believed that the higher the amount of giving, the better the consumer perception of the CRM campaign. Tsiros *et al.* [34] considered that both the total amount donated and the method of communication influence consumer response to CRM. Kerr *et al.* [35] concluded that for individuals with a high perceived need, purchase intentions for the exact donation form are greater when the product-cause fit is low, regardless of the donation form. Grolleau *et al.* [36] believed the crowding-out effect may be particularly strong if the cause-linked products are targeted at consumers who have provided direct donations.

In terms of CRM in the supply chain, Barone *et al.* [37] thought that consumer perceptions of retailers' motivation to engage in CRM, the affinity of CRM, and the interaction effects associated with the two moderators can have a significant impact on retailer-cause fit. Choi *et al.* [38] indicated that for the label to be able to convey information to consumers about the fulfillment of CSR, manufacturers should therefore make special designs for the packaging. Heydari *et al.* [39] proposed a cost-sharing contract and collaboration model when the manufacturer implements CRM and concluded that the collaboration model can increase the profits of channel members. Although Gao [18] explored that decentralized supply chains can generate more social value through CRM, he did not consider the promotional costs of CRM in his study.

In summary, previous research has been extremely fruitful, whether from the perspective of consumers or effects for supply chain, but little literature has considered the decision to implement CRM for supply chain members. In addition, while we examine the implementation strategy of CRM, we also consider the cost of promotion during CRM, which has not been addressed in the previous literature.

## 3. Model formulation and notation

In this paper, we consider a supply chain consisting of a manufacturer and a retailer, where both of them are risk-neutral and perfectly rational, making decisions to maximize their profits. The manufacturer is the leader, and the retailer is the follower in the Stackelberg game. The manufacturer has to decide whether to implement CRM himself or to delegate CRM to the retailer, as well as price strategies. The retailer reacts according to the manufacturer's strategy. The manufacturer produces the product at a production cost of $c$ and distributes it to the retailer at a wholesale price of $w$. The retailer sells the product to the consumer at a selling price of $p$.

It is assumed that both the manufacturer and the retailer will advertise for their CRM campaign, and therefore incur promotional costs $A$. The cost of promotion will affect consumer utility. Since the utility does not increase indefinitely with the cost, we assume that the additional utility of CRM by the manufacturer or retailer is $\sqrt{A}$. Additionally, we denote $v$ by the consumer's perceived value of the product, $v$ serving a uniform distribution between 0 and 1, i.e., $v \sim U[0,1]$. Show that in a market of size 1, the price that consumers are willing to pay for this product is uniformly distributed between 0 and 1. At the same time, we use $\delta$ to denote consumer's prosociality, i.e., the degree of consumer sensitivity to CRM, and the degree to which the level of CRM donations stimulates consumer buying behavior. We use $\eta$ to indicate the donation percentage of sales per unit of product, and in other words, it is the donation amount as a percentage of the sales price or wholesale price. Thus, the utility function is $U = v - p + \delta\eta\sqrt{A}$. And we assume that a consumer will buy the product only if the utility function is greater than zero, i.e., $v \geq p + \delta\eta\sqrt{A}$. The number of consumers in a market of size 1 is $1 - p + \delta\eta\sqrt{A}$, and the demand function can be obtained as $d = 1 - p + \delta\eta\sqrt{A}$.

The parameters and variables mentioned in the model and their meanings are listed in the table below:

**Table 1** Model parameters and decision variables

| Notation | Description |
|---|---|
| $c$ | The unit production cost of the product |
| $p$ | The unit sales price of the product |
| $w$ | The unit wholesale price of the product |
| $\delta$ | Consumer sensitivity to cause-related marketing （$\delta \geq 0$） |
| $\eta$ | The proportion of wholesale price or sales price per unit donation amount |
| $A$ | Promotional costs arising from the implementation of CRM |
| $\pi_m$ | The profit of the manufacturer |
| $\pi_r$ | The profit of the manufacturer |
| $\pi_s$ | Total social welfare |
| $\cdot^M$ | The scenario of the manufacturer implementing CRM |
| $\cdot^R$ | The scenario of the retailer implementing CRM |

To avoid a meaningless discussion, we propose the following assumptions:

(1) We assume that $\eta < \frac{(2-\sqrt{1+3c})}{3}$ and $1 - c - \eta > 0$, the profit is guaranteed to be greater than zero when the supply chain members implement CRM and the amount donated is limited by the production cost, which is in line with the real meaning.

(2) We assume that $\delta < \frac{\sqrt{2(1-\eta)}}{\eta(1-\eta)}$, it suggests that consumers' sensitivity to CRM is influenced by the percentage of the donation, and that this sensitivity is bounded and does not increase indefinitely as the donation amount increases.

(3) Assuming that both the manufacturer and the retailer are equipped to implement CRM and are skilled in CRM techniques.

### 3.1 The manufacturer implements cause-related marketing

In this scenario, the manufacturer implements CRM by donating a percentage of the wholesale price to the charity for each unit of product sold incurring promotional costs for CRM. When the manufacturer implements CRM, the profit functions for the manufacturer and the retailer, as well as the social welfare, are as follows:

$$\pi_m^M = (w - \eta w - c)d - A \tag{1}$$

$$\pi_r^M = (p - w)d \tag{2}$$

$$\pi_s^M = \pi_m^M + \pi_r^M = (p - \eta w - c)d - A \tag{3}$$

Proposition 1: We obtain the optimal solutions when the manufacturer implements CRM as follows:

$$A^{M*} = \frac{(1-c-\eta)^2\delta^2\eta^2}{8+\delta^2\eta^3-\delta^2\eta^2} \tag{4}$$

$$w^{M*} = \frac{4(1-c-\eta)-c\delta^2(1-\eta)}{(1-\eta)(8+\delta^2\eta^3-\delta^2\eta^2)} \tag{5}$$

$$p^{M*} = \frac{2(3+c-3\eta)-c\delta^2(1-\eta)}{(1-\eta)(8+\delta^2\eta^3-\delta^2\eta^2)} \tag{6}$$

From Proposition 1 we can obtain Eqs. 7-9：

$$\pi_m^{M*} = \frac{(1-c-\eta)^2}{(1-\eta)(8+\delta^2\eta^3-\delta^2\eta^2)} \tag{7}$$

$$\pi_r^{M*} = \frac{4(1-c-\eta)^2}{(1-\eta)^2(8+\delta^2\eta^3-\delta^2\eta^2)^2} \tag{8}$$

$$\pi_s^{M*} = \frac{(1-c-\eta)^2(12-8\eta-\delta^2\eta^2(1-2\eta-\eta^2))}{(1-\eta)^2(8+\delta^2\eta^3-\delta^2\eta^2)^2} \tag{9}$$

We obtain Corollary 1 and Corollary 2 by finding the first-order derivatives of Eqs. 4-9 with respect to $\eta$.

Corollary 1: $\frac{dA^{M*}}{d\eta} > 0, \frac{dw^{M*}}{d\eta} > 0, \frac{dp^{M*}}{d\eta} > 0.$

Corollary 1 shows that when the manufacturer implements CRM, the pricing strategies are influenced by the donation percentage. Within the constraint, the cost of promotion, the manufacturer's wholesale price, and the retailer's selling price increase with the donation amount. This is because when the manufacturer makes a charitable donation, if the amount of donation is relatively higher, then the wholesale price will also increase, and therefore the retailer will also increase the sales price. At the same time, as the number of donations increases, the manufacturer will also spend more to publicize the behavior.

Corollary 2:

(i) If $0 < \delta < \delta_r^M$, then $\frac{d\pi_m^{M*}}{d\eta} < 0$ and $\frac{d\pi_r^{M*}}{d\eta} < 0$;

(ii) If $\delta_r^M < \delta < \delta_m^M$, then $\frac{d\pi_m^{M*}}{d\eta} < 0$ and $\frac{d\pi_r^{M*}}{d\eta} > 0$;

(iii) If $\delta_m^M < \delta < \frac{\sqrt{2(1-\eta)}}{\eta(1-\eta)}$, then $\frac{d\pi_m^{M*}}{d\eta} > 0$ and $\frac{d\pi_r^{M*}}{d\eta} > 0$.

Where $\delta_r^M = 2\sqrt{\frac{2c}{\eta(1-\eta)((3\eta+4c-5)\eta+2(1-c))}}$, $\delta_m^M = 2\sqrt{\frac{1-c-\eta}{\eta(1-\eta)((\eta+2c-2)\eta+1-c)}}$.

It is known from Corollary 2 that the profits of the manufacturer and the retailer are jointly affected by the proportion of donation and the pro-sociality of the consumer to CRM. From Corollary 2(i) we are able to obtain that when the pro-sociality of consumer to CRM is less than the threshold value $\delta_r^M$ , the profits of the manufacturer and the retailer decrease simultaneously with the donation amount; while when the pro-sociality of consumers to CRM is greater than $\delta_r^M$ and less than $\delta_m^M$ , the profits of the manufacturer still decrease, while the profits of the retailer increase with the donation ratio; finally, when the pro-sociality of consumer to CRM is greater than $\delta_m^M$ , the profits of the manufacturer and the retailer increase simultaneously.

The Corollary 1 and Corollary 2 show that the profits of the manufacturer and retailer decrease and then increase with the percentage of donations. However, both the manufacturer and the retailer are motivated to implement CRM only if their profits both increase under the influence of the donation amount. At the same time, the manufacturer and retailer's profits are governed by consumer sensitivity to CRM in the segment. When the manufacturer implements CRM, if the segment consumers are relatively low pro-sociality, the donation will have a negative impact on the profits of the manufacturer and retailer, or even reduce the profits; while the target market consumer's pro-sociality is middle, the donation activities are beneficial for the retailer at this time, but not for the manufacturer; and when the consumer in the target market is more sensitive to public welfare behaviour, the implementation of CRM for the manufacturer can not only increase his own profits, the retailer can also be profitable.

### 3.2 The retailer implements cause-related marketing

In this case, the retailer implements CRM, donating a percentage of the selling price to the charity for each unit of product sold, as well as spending the advertising costs of the CRM. Then, when the retailer implements CRM, the profit functions of the manufacturer and the retailer as well as social welfare are as follows.

$$\pi_m^R = (w - c)d \tag{10}$$

$$\pi_r^R = (p - \eta p - w)d - A \tag{11}$$

$$\pi_s^R = \pi_m^R + \pi_r^R = (p - \eta p - c)d - A \tag{12}$$

Proposition 2: We obtain the optimal solutions when the retailer implements CRM as follows.

$$A^{R*} = \frac{(1 + c - \eta)^2 \delta^2 \eta^2}{4(4 + \delta^2 \eta^3 - \delta^2 \eta^2)^2} \tag{13}$$

$$w^{R*} = \frac{1 - c - \eta}{2} \tag{14}$$

$$p^{R*} = \frac{2(1 + 3c - 3\eta) - c\delta^2\eta^2(1 - \eta) - \delta^2\eta^2(1 + \eta^2 - 2\eta)}{2(1 - \eta)(4 + \delta^2\eta^3 - \delta^2\eta^2)} \tag{15}$$

From Proposition 2 we can obtain Eqs. 16-18：

$$\pi_m^{R*} = \frac{(1 - c - \eta)^2}{2(1 - \eta)(4 + \delta^2\eta^3 - \delta^2\eta^2)} \tag{16}$$

$$\pi_r^{R*} = \frac{(1 - c - \eta)^2}{4(1 - \eta)(4 + \delta^2\eta^3 - \delta^2\eta^2)} \tag{17}$$

$$\pi_s^{M*} = \frac{3(1 - c - \eta)^2}{4(1 - \eta)(4 + \delta^2\eta^3 - \delta^2\eta^2)} \tag{18}$$

We obtain Corollary 3 and Corollary 4 by finding the first order derivatives of Eqs. 13-18 with respect to $\eta$.

Corollary 3: $\frac{dA^{R*}}{d\eta} > 0, \frac{dw^{R*}}{d\eta} < 0, \frac{dp^{R*}}{d\eta} > 0.$

Through Corollary 3, the promotional costs, sales prices, and the manufacturers' wholesale prices are influenced by the proportion of donations in the retailer's donation behaviour. Within the constraint, the advertising cost required for CRM and the retailer's selling price increase with the percentage of donation. That is, when the retailer implements CRM, if he donates a higher amount, it should be equipped with more publicity. Also, to ensure profitability, the retailer's selling price will increase. In contrast, the manufacturer's wholesale price differs from the previous analysis in that it tends to decrease as the proportion of donations increases. In another words, as long as the retailer implements CRM, the cost he has to spend to obtain the product at the manufacturer will decrease.

Corollary 4:

(i) If $0 < \delta < \delta^R$, then $\frac{d\pi_m^{R*}}{d\eta} < 0$ and $\frac{d\pi_r^{R*}}{d\eta} < 0$;

(ii) If $\delta^R < \delta < \frac{\sqrt{2(1-\eta)}}{\eta(1-\eta)}$, then $\frac{d\pi_m^{R*}}{d\eta} > 0$ and $\frac{d\pi_r^{R*}}{d\eta} > 0$.

Where $\delta^R = 2\sqrt{\frac{2(1-c-\eta)}{\eta(1-\eta)((\eta+2c-2)\eta+1-c)}}$.

Corollary 4 suggests that when retailer practices CRM, profits are equally influenced by consumers' pro-sociality and the percentage of his donations. When consumer's pro-sociality is below than the threshold $\delta^R$, the profits of both the manufacturer and the retailer decrease as the donation percentage increases; conversely, when consumer's pro-sociality is above the $\delta^R$, the profits of both the manufacturer and the retailer increase as the donation ratio increases. In the case of a retailer implementing CRM, the benefits to both the manufacturer and the retailer are synchronized, with both tending to decrease and then increase as the percentage of donations increases. This means that when consumers in the target market are relatively less pro-social, the implementation of CRM by the retailer does not help to improve the profitability of both, and it is only when the social awareness of the consumer base is relatively higher that the retailer comes to implement CRM to the benefit of the supply chain.

## 4. Analysis

From the Corollary 1 and 3, pricing strategies as well as promotional cost is not influenced by the pro-sociality of consumers in the segment, but only by the percentage of donations made when they implement CRM.

Corollary 5: $A^{M*} < A^{R*}, w^{M*} > w^{R*}, p^{M*} > p^{R*}$.

Corollary 5 suggests that when the manufacturer implements CRM, the wholesale prices and sales prices will be relatively high but promotional costs will be less. That is the higher wholesale price will result in a corresponding increase in selling price. In terms of pricing alone, it makes sense for the manufacturer to implement CRM for supply chain members. This is because it costs less and generates more income.

Corollary 6:

(i) $\pi_m^{M*} < \pi_m^{R*}$;

(ii) When $0 < \eta < \frac{1}{9}$, if $0 < \delta < \delta'$, then $\pi_r^{M*} > \pi_r^{R*}$; if $\delta' < \delta < \frac{\sqrt{2(1-\eta)}}{\eta(1-\eta)}$, then $\pi_r^{M*} < \pi_r^{R*}$;

(iii) When $\eta > \frac{1}{9}$, then $\pi_r^{M*} > \pi_r^{R*}$.

Where $\delta' = \frac{\sqrt{8(\sqrt{\eta}-\eta)}}{\eta(1-\eta)}$.

Corollary 6(i) indicates that the manufacturer can make higher profits when the retailer implements CRM. Even at a lower cost and a higher price, the manufacturer is not more profitable. From Corollary 6(ii) and (iii), for the retailer, the percentage of donations affects the outcome of the decisions. For the retailer, Corollary 6(ii) suggests that it is more advantageous for the manufacturer to implement CRM when both the amount of donation and the pro-sociality of the consumer are lower. However, if the percentage of donations is small but the consumers are more aware of charity, it is more beneficial for the retailer to implement CRM. Conversely, CRM by the manufacturer is more beneficial to the retailer if a larger percentage of donations are made.

Since our discussion is focused on the manufacturer as the leader, the manufacturer will choose to maximize its profits by delegating the implementation of CRM to the retailer. It is not that the retailer does not profit from CRM at this point, but it is less profitable than when the manufacturer implements CRM.

Corollary 7:

If $0 < \delta < \delta_s$, then $\pi_s^{M*} > \pi_s^{R*}$; if $\delta_s < \delta < \frac{\sqrt{2(1-\eta)}}{\eta(1-\eta)}$, then $\pi_s^{M*} < \pi_s^{R*}$.

Where $\delta_s = \frac{2\sqrt{2(1-\sqrt{1-\eta+\eta^2})}}{\eta(1-\eta)}$.

Corollary 7 illustrates the effect of the pro-sociality of the segment on social welfare. When the pro-sociality of consumers is lower than the threshold $\delta_s$, the social welfare of the manufacturer's implementation is higher, but when the sensitivity of the target market to CRM exceeds the threshold $\delta_s$, the social welfare of the retailer's implementation of CRM is higher.

## 5. Numerical examples

In this section, we present numerical examples to illustrate the theoretical results. We let the manufacturing cost $c = 0.2$ and show the effect of the donation percentage on the decision variables, optimal profit, and the pro-sociality of the segment on social welfare in the form of figures.

### 5.1 Effect of donation percentage on decision variables

We plot the effect on the advertising costs, the optimal wholesale price and the optimal sales price of donation percentage $\eta$ .

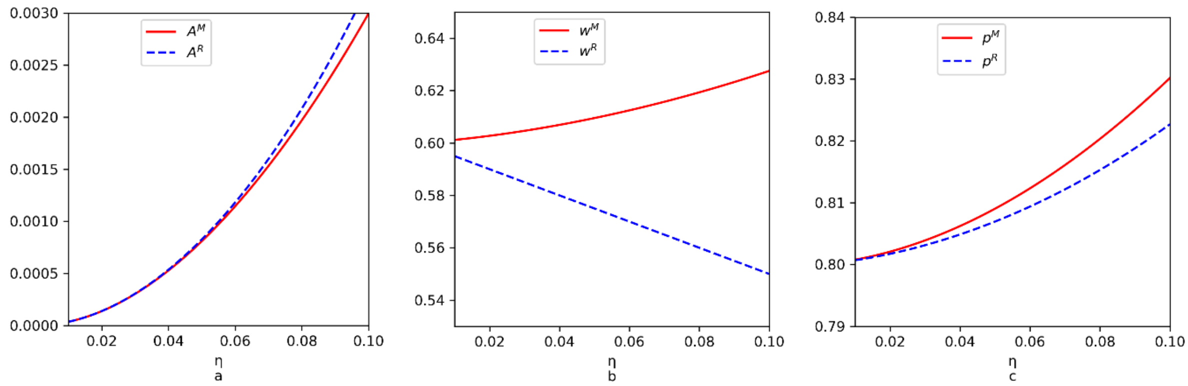


**Fig. 1** Effect of donation percentage on decision variables ($\delta = 6$)

Fig. 1 reflects the effect of the proportion of CRM donations on the decision variables in Corollary 1 and Corollary 3. Fig 1(a) shows that as the donation percentage increases for both the manufacturer and the retailer, the promotional costs and selling price become larger. Further, the retailer's promotional costs are higher when CRM is implemented. As shown in fig. 1(b), for the wholesale price, it decreases with the increase of the donation percentage when the retailer implements the CRM, while the opposite is true when the manufacturer implements the CRM. And when the manufacturer implements CRM, the wholesale price is higher. From Fig. 1(c), we can conclude that the product price increases after the implementation of CRM, and the price increases faster when the manufacturer implements donations.

### 5.2 Effect of donation percentage on optimal profits

We show the effect of the donation percentage on the implementation of CRM strategies by the manufacturer and the retailer at different levels of consumer pro-sociality in the form of arithmetic examples. Through the previous analysis of optimal profit, when the manufacturer implements CRM, we can classify the degree of pro-sociality of the market segment into low, medium and high levels.

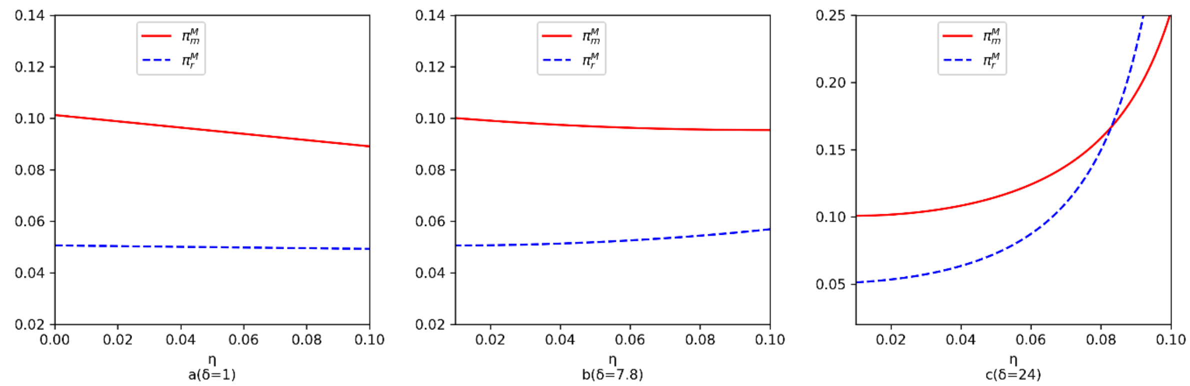


**Fig. 2** Effect of donation parentage on profit when the manufacturer implements CRM

The three images in Fig. 2 represent how the percentage of donations affects the profits of the manufacturer and the retailer when the manufacturer implements CRM for three different magnitudes of consumer's pro-sociality. As shown in the previous analysis, when the pro-social awareness of consumers is weak, as in Fig. 2(a), these consumers do not care about the public welfare behavior of companies, therefore, they will not be motivated to make purchases by the welfare activities of companies. In this case, the manufacturer only invests the donation amount and the promotion cost but does not obtain the desired effect of revenue. While the wholesale price increases due to the increase of the donation amount, so the profit of the manufacturer and the retailer is in a simultaneous decline in this case.

Fig. 2(b) shows the profitability when the manufacturer implements CRM when the consumer's sensitivity to CRM is at a medium level. As shown in the figure, the manufacturer's profit is still decreasing, but the decreasing trend is slowing down, which means that as the amount of donation increases, the impact of its change on the company's maximum profit is gradually becoming weaker; at the same time, the optimal profit of the retailer increases with the donation percentage, because of higher pro-sociality, the benefits of CRM can already offset the costs and bring additional benefits for the retailer.

Fig. 2(c) shows a situation where the consumer base has a high awareness of public goods, and consumers are influenced by CRM to make purchases. At this point, if the manufacturer carries out donation activities, it will benefit both itself and the retailer, and the benefits of both will increase as the donation amount increases.

We have used the images above to verify the effect of consumer pro-sociality and donation percentage on the optimal profits when the manufacturer implements CRM, and we will now look at the scenario when the retailer implements CRM. When the retailer implements CRM, we classify the pro-sociality of consumers into two levels.

Fig. 3 represents the trend of profitability when the retailer implements CRM. Like the manufacturer's implementation, the optimal profit of the retailer and the manufacturer is affected by the strength of the pro-sociality of the consumers. When this sensitivity is weak, the donation of the retailer will result in losses for both manufacturer and retailer. Conversely, in more pro-social consumer markets, a cause campaign can generate higher returns for both the manufacturer and the retailer, and the higher the amount donated, the greater the return.

Below we validate the strategic decisions of the manufacturer and retailer to CRM. In the figure, we show the impact of consumer's pro-sociality on the CRM decisions of the manufacturer and the retailer in terms of low and high donation percentages. We use $\Delta\pi_m$ to denote $\pi_m^R$-$\pi_m^M$ and $\Delta\pi_m$ to denote $\pi_r^R$-$\pi_r^M$ . From Fig. 4, we can conclude that the donation strategies are not the same for different donation percentages.

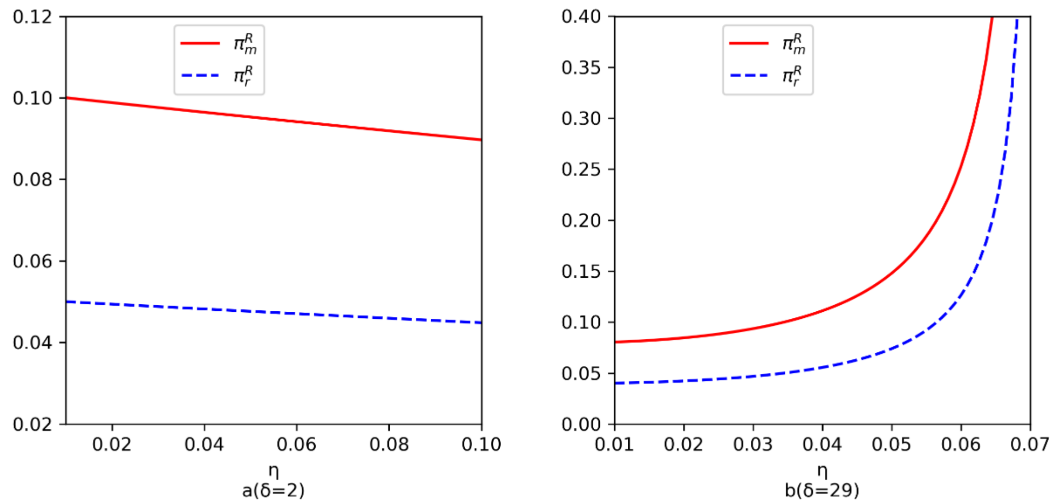


**Fig. 3** Effect of donation parentage on profit when the retailer implements CRM

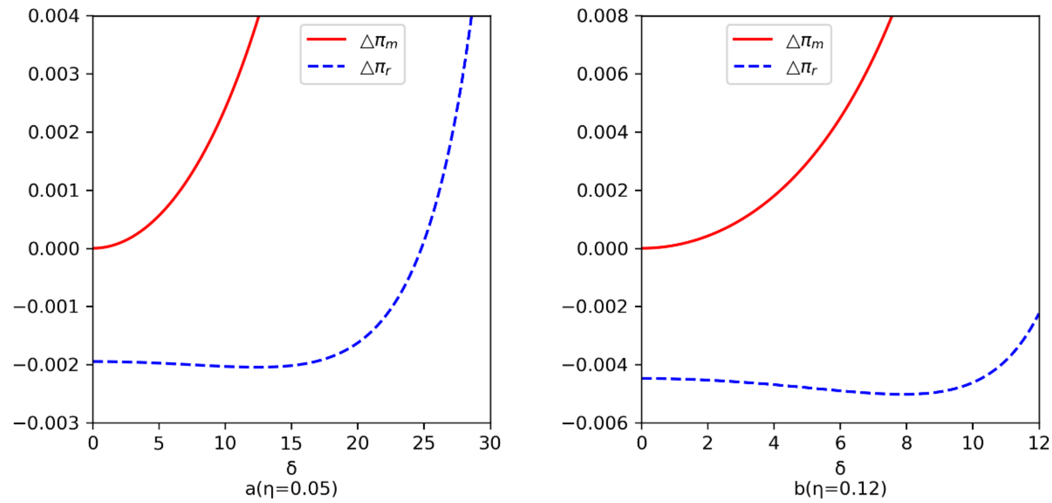


**Fig. 4** Effect of consumer's pro-sociality on optimal profit with different donation percentage

As can be seen from the two graphs in Fig. 4, the manufacturer's decision is not influenced by the donation percentage and consumer sensitivity to CRM. Further, the manufacturer receives higher profits whenever the retailer implements CRM, so the manufacturer with the retailer should implement CRM. Differently, the retailer's decision is influenced by both the donation percentage and the consumer's sensitivity. Fig. 4(a) shows that if the donation percentage chosen by the donor is small and the consumer's pro-social awareness is weak, the retailer will not choose to implement CRM; if the consumer's sensitivity is high relatively, it is profitable for the retailer to implement CRM. Fig. 4(b) illustrates that it is more beneficial for the retailer when the manufacturer to implements CRM with a higher donation amount.

### 5.3 Impact of consumer's pro-sociality on social welfare

In the previous analysis, we obtained that the pro-sociality of consumers in the segment affects the retailer's decision, while the manufacturer's decision is independent of it. In this section, we use images to represent the impact of consumer pro-sociality on the overall profitability of the supply chain, also known as social welfare. We let $\eta = 0.05$ .

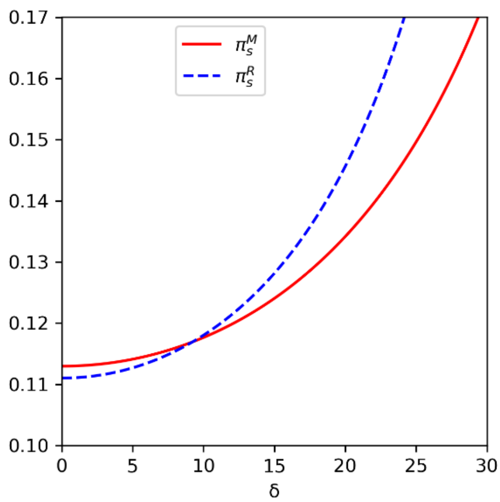


**Fig. 5** Impact of consumer's pro-sociality on social welfare

Fig. 5 analyses the social welfare of the whole supply chain from the point of view of consumer's pro-sociality. As can be seen from the figure, the sensitivity of consumers to CRM affects the subject of implementing CRM. If the overall pro-social awareness of the consumer group in the market is low, the manufacturer's implementation of CRM is more beneficial to the supply chain as a whole; if the pro-social awareness of the consumer in the target market is high, then the retailer's implementation of CRM is beneficial to the whole supply chain.

## 6. Conclusion

In this paper, we examine the pricing and decision-making issues of implementing CRM by socially responsible supply chain members. We analyze two scenarios of the manufacturer and the retailer's implementation of CRM and conclude that donation amount and the pro-sociality of consumer groups in the segment are important. We make recommendations for the decisions of the manufacturer and the retailer in CRM and analyze the impact of donation amount and consumer's pro-sociality on pricing and strategy decisions.

In product pricing, we conclude that the retailer incurs higher advertising costs when implementing CRM, while the manufacturer has higher wholesale and selling prices when implementing CRM. In addition, if the retailer implements CRM, the higher the donation amount, the lower the wholesale price required; in other cases, regardless of who implements CRM, an increase in the donation amount will result in higher wholesale and product prices. However, it is not always advantageous for the manufacturer and the retailer to implement CRM. CRM decisions are influenced by a combination of donation amount and consumer's pro-sociality. Only when the pro-sociality of the segment market exceeds a critical threshold is the implementation of CRM profitable. From the manufacturer's point of view, it is always optimal to entrust the retailer to implement CRM; for the retailer, if the donation amount is small, it is also necessary to consider the pro-sociality of the consumer group: the retailer is willing to implement CRM only when the pro-sociality of the consumer is strong. If the donation percentage is larger, the retailer is the best choice to implement CRM.

We also analyzed the problem of the manufacturer and retailer's decision from social welfare perspective. The implementation of CRM is beneficial for maximizing social welfare for both the manufacturer and the retailer. Again, the pro-sociality of consumers remains an influential factor; if the pro-sociality of the consumer group is low, the manufacturer's implementation of CRM maximizes social welfare; if the pro-sociality of the consumer group is high, the retailer's implementation of public good marketing is optimal.

## Acknowledgement

This article was financially supported by the Nanjing University of Posts and Telecommunications research Fund project for Introducing Talents (high-level teachers) (No. NYY219002).


## References


[1] Smith, S.M., Alcorn, D.S. (1991). Cause marketing: A new direction in the marketing of corporate responsibility, *Journal of Consumer Marketing*, Vol. 8, No. 3, 19-35, doi: 10.1108/07363769110035054.

[2] Hu, H., Zhang, Z., Wu, Q., Han, S. (2020). Manufacturer's customer satisfaction incentive plan for duopoly retailers with Cournot or collusion games, *Advances in Production Engineering & Management*, Vol. 15, No. 3, 345-357, doi: 10.14743/apem2020.3.370.

[3] Choi, J., Chang, Y.K., Li, Y.J., Jang, M.G. (2016). Doing good in another neighborhood: Attributions of CSR motives depend on corporate nationality and cultural orientation, *Journal of International Marketing*, Vol. 24, No. 4, 82-102, doi: 10.1509/jim.15.0098.

[4] Nazzaro, C., Lerro, M., Marotta, G. (2018). Assessing parental traits affecting children's food habits: An analysis of the determinants of responsible consumption, *Agricultural and Food Economics*, Vol. 6, Article No. 23, doi: 10.1186/s40100-018-0119-z.

[5] Awaga, A.L., Xu, W., Liu, L., Zhang, Y. (2020). Evolutionary game of green manufacturing mode of enterprises under the influence of government reward and punishment, *Advances in Production Engineering & Management,* Vol. 15, No. 4, 416-430, doi: 10.14743/apem2020.4.375.

[6] Engert, S., Rauter, R., Baumgartner, R.J. (2016). Exploring the integration of corporate sustainability into strategic management: A literature review, *Journal of Cleaner Production*, Vol. 112, Part 4, 2833-2850, doi: 10.1016/j.jclepro.2015.08.031.

[7] Wu, Y., Li, H., Gou, Q., Gu, J. (2017). Supply chain models with corporate social responsibility, *International Journal of Production Research*, Vol. 55, No. 22, 6732-6759, doi: 10.1080/00207543.2017.1346833.

[8] Hsueh, C.-F. (2014). Improving corporate social responsibility in a supply chain through a new revenue sharing contract, *International Journal of Production Economics*, Vol. 151, 214-222, doi: 10.1016/j.ijpe.2013.10.017.

[9] Leksic, I., Stefanic, N., Veza, I. (2020). The impact of using different lean manufacturing tools on waste reduction, *Advances in Production Engineering & Management*, Vol. 15, No. 1, 81-92, doi: 10.14743/apem2020.1.351.

[10] McGuire, J.W. (1964). Business and society, *Southern Economic Journal*, Vol. 30, No. 3, 289-290, doi: 10.2307/1055948.

[11] Franco, S., Caroli, M.G., Cappa, F., Del Chiappa, G. (2020). Are you good enough? CSR, quality management and corporate financial performance in the hospitality industry, *International Journal of Hospitality Management*, Vol. 88, Article No. 102395, doi: 10.1016/j.ijhm.2019.102395.

[12] Hussain, S., Jahanzaib, M. (2018). Sustainable manufacturing – An overview and a conceptual framework for continuous transformation and competitiveness, *Advances in Production Engineering & Management*, Vol. 13, No. 3, 237-253, doi: 10.14743/apem2018.3.287.

[13] Andrews, M., Luo, X., Fang, Z., Aspara, J. (2014). Cause marketing effectiveness and the moderating role of price discounts, *Journal of Marketing*, Vol. 78, No. 6, 120-142, doi: 10.1509/jm.14.0003.

[14] Sen, S., Bhattacharya, C.B., Korschun, D. (2006). The role of corporate social responsibility in strengthening multiple stakeholder relationships: A field experiment, *Journal of the Academy of Marketing Science*, Vol. 34, 158-166, doi: 10.1177/0092070305284978.

[15] Heidarzadeh Hanzaee, K., Sadeghian, M., Jalalian, S. (2019). Which can affect more? Cause marketing or cause-related marketing, *Journal of Islamic Marketing*, Vol. 10, No. 1, 304-322, doi: 10.1108/jima-04-2016-0028.

[16] Melero, I., Montaner, T. (2016). Cause-related marketing: An experimental study about how the product type and the perceived fit may influence the consumer response, *European Journal of Management and Business Economics*, Vol. 25, No. 3, 161-167, doi: 10.1016/j.redeen.2016.07.001.

[17] Adomaviciute, K., Bzikadze, G., Cherian, J., Urbonavicius, S. (2016). Cause-related marketing as a commercially and socially oriented activity: What factors influence and moderate the purchasing?, *Engineering Economics*, Vol. 27, No. 5, 578-585, doi: 10.5755/j01.ee.27.5.15166.

[18] Gao, F. (2020). Cause marketing: Product pricing, design, and distribution, *Manufacturing & Service Operations Management*, Vol. 22, No. 4, 775-791, doi: 10.1287/msom.2019.0772.

[19] Mohr, L.A., Webb, D.J., Harris, K.E. (2010). Do consumers expect companies to be socially responsible? The impact of corporate social responsibility on buying behaviour, *Journal of Consumer Affairs*, Vol. 35, No. 1, 45-72, doi: 10.1111/j.1745-6606.2001.tb00102.x.

[20] Mani, V., Gunasekaran, A., Delgado, C. (2018). Enhancing supply chain performance through supplier social sustainability: An emerging economy perspective, *International Journal of Production Economics*, Vol. 195, 259-272, doi: 10.1016/j.ijpe.2017.10.025.

[21] Maloni, M.J., Brown, M.E. (2006). Corporate social responsibility in the supply chain: An application in the food industry, *Journal of Business Ethics*, Vol. 68, 35-52, doi: 10.1007/s10551-006-9038-0.

[22] Valdez-Juárez, L.E., Gallardo-Vázquez, D., Ramos-Escobar, E. (2018). CSR and the supply chain: Effects on the results of SMEs, *Sustainability*, Vol. 10, No. 7, Article No. 2356, doi: 10.3390/su10072356.

[23] Arya, A., Mittendorf, B. (2015). Supply chain consequences of subsidies for corporate social responsibility, *Production and Operations Management*, Vol. 24, No. 8, 1346-1357, doi: 10.1111/poms.12326.

[24] Raza, S.A. (2018). Supply chain coordination under a revenue-sharing contract with corporate social responsibility and partial demand information, *International Journal of Production Economics*, Vol. 205, 1-14, doi: 10.1016/j.ijpe.2018.08.023.

[25] Panda, S., Modak, N.M. (2016). Exploring the effects of social responsibility on coordination and profit division in a supply chain, *Journal of Cleaner Production*, Vol. 139, 25-40, doi: 10.1016/j.jclepro.2016.07.118.

[26] Liu, Y., Quan, B.-T., Xu, Q., Forrest, J.Y.-L. (2019). Corporate social responsibility and decision analysis in a supply chain through government subsidy, *Journal of Cleaner Production*, Vol. 208, 436-447, doi: 10.1016/j.jclepro.2018.10.121.

[27] Yan, Y., Yao, F. (2021). Pricing strategy of closed loop supply chain considering different CSR investment modes, *MATEC Web of Conferences*, Vol. 336, Article No. 09005, doi: 10.1051/matecconf/202133609005.

[28] Cheng, H.-W., Chen, H.-L. (2013). Analysis of cause-related marketing effects: The case of duopoly retailing store, *Chiao Da Management Review,* Vol. 33, 105-138.

[29] Furman, A., Maison, D. (2020). Influence of different cause-related marketing (CRM) strategies on consumer decision making, *Procedia Computer Science*, Vol. 176, 2979-2988, doi: 10.1016/j.procs.2020.09.205.

[30] Kraft, T., Valdés, L., Zheng, Y. (2018). Supply chain visibility and social responsibility: Investigating consumers' behaviors and motives, *Manufacturing & Service Operations Management*, Vol. 20, No. 4, 617-636, doi: 10.1287/msom.2017.0685.

[31] Silva, S.C., Duarte, P., Machado, J.C., Martins, C. (2020). Cause-related marketing in online environment: The role of brand-cause fit, perceived value, and trust, *International Review on Public and Nonprofit Marketing,* Vol. 17, 135-157, doi: 10.1007/s12208-019-00237-z.

[32] Vyravene, R., Rabbanee, F.K. (2021). Corporate negative publicity – The role of cause related marketing, *Australasian Marketing Journal*, Vol. 24, No. 4, 322-330, doi: 10.1016/j.ausmj.2016.11.006.

[33] Moosmayer, D.C., Fuljahn, R. (2010). Consumer perceptions of cause related marketing campaigns, *Journal of Consumer Marketing*, Vol. 27, No. 6, 543-549, doi: 10.1108/07363761011078280.

[34] Tsiros, M., Irmak, C. (2020). Lowering the minimum donation amount increases consumer purchase likelihood of products associated with cause-related marketing campaigns, *Journal of Marketing Research*, Vol. 57, No. 4, 755-770, doi: 10.1177/0022243720916463.

[35] Kerr, A.H., Das, N. (2014). Thinking about fit and donation format in cause marketing: The effects of need for cognition, *Journal of Marketing Theory and Practice*, Vol. 21, No. 1, 103-112, doi: 10.2753/mtp1069-6679210107.

[36] Grolleau, G., Ibanez, L., Lavoie, N. (2016). Cause-related marketing of products with a negative externality, *Journal of Business Research*, Vol. 69, No. 10, 4321-4330, doi: 10.1016/j.jbusres.2016.04.006.

[37] Barone, M.J., Norman, A.T., Miyazaki, A.D. (2007). Consumer response to retailer use of cause-related marketing: Is more fit better?, *Journal of Retailing*, Vol. 83, No. 4, 437-445, doi: 10.1016/j.jretai.2007.03.006.

[38] Choi, S., Lee, S., Friske, W. (2018). The effects of featured advertising and package labeling on sustainability of cause-related marketing (CRM) products, *Sustainability*, Vol. 10, No. 9, Article No. 3011, doi: 10.3390/su10093011.

[39] Heydari, J., Mosanna, Z. (2018). Coordination of a sustainable supply chain contributing in a cause-related marketing campaign, *Journal of Cleaner Production*, Vol. 200, 524-532, doi: 10.1016/j.jclepro.2018.07.055.


## Appendix A

Proof of proposition 1: It is easy to obtain Eq. 2 as a concave function with respect to $p$. Making the first order derivative of Eq. 2 with respect to equal to zero yields the reaction function of the selling price as $p=\frac{(\delta\eta\sqrt{A}+w+1)}{2}$. Substituting it into Eq. 1, the Hesse matrix of Eq. 1 is obtained as:

$$\begin{pmatrix} -(1-\eta) & \dfrac{(1-\eta)\delta\eta}{4\sqrt{A}} \\ \dfrac{(1-\eta)\delta\eta}{4\sqrt{A}} & -\dfrac{(w-\eta w-c)\delta\eta}{A^{3/2}} \end{pmatrix} \tag{A1}$$

The principal sub formulas of the Hesse matrix are $-(1-\eta)<0$, $\frac{\delta\eta(1-\eta)(\delta\eta\sqrt{A}(\eta-1)-2(\eta w+c-w))}{16A^{3/2}}>0$ , it can be obtained that (A1) is a negative definite matrix. Since Eq. 1 is a concave function with respect to $w$ and $A$ , respectively.

Find the first-order derivatives of Eq. 1 to $w$ and $A$, respectively, and make them equal to zero. Then we give Eqs. 4, 5 and 6. Substituting them into Eqs. 1-3 and simplifying them gives Eqs. 7-9.

Proof of Corollary 1: Taking the first order derivative of $A^{M*}$ to $\eta$ . We have

$$\frac{dA^{M*}}{d\eta}=\frac{2\delta^2\eta(1-c-\eta)(\delta^2\eta^2(\eta^2-2\eta+2c\eta-c+1)+8(1-2\eta-c))}{(8+\delta^2\eta^3-\delta^2\eta^2)^3} \tag{A2}$$

Similarly, we can obtain (A2) and (A3) as follows:

$$\frac{dw^{M*}}{d\eta}=\frac{c\delta^4\eta^4(1-\eta)^2+4\eta\delta^2(1-\eta)(-3\eta^2+5\eta+2c-2)+32c}{(1-\eta)^2(8+\delta^2\eta^3-\delta^2\eta^2)^2} \tag{A3}$$

$$\frac{dp^{M*}}{d\eta}=\frac{c\delta^4\eta^4(1-\eta)^2+2\eta\delta^2(1-\eta)(9\eta^2-15\eta+2c\eta-6c+6)+16c}{(1-\eta)^2(8+\delta^2\eta^3-\delta^2\eta^2)^2} \tag{A4}$$

It is easy to determine (A1), (A2) and (A3) > 0.

Proof of Corollary 2: Taking the first order derivative of $\pi_m^{M*}$ with respect to $\eta$ . We obtain (A5):

$$\frac{d\pi_m^{M*}}{d\eta}=\frac{2(1-c-\eta)(\eta(1-\eta)(\eta^2-2\eta+2c\eta-c+1)\delta^2-4(1-\eta+c))}{(1-\eta)^2(8+\delta^2\eta^3-\delta^2\eta^2)^2} \tag{A5}$$

because of $\frac{2(1-c-\eta)}{(1-\eta)^2(8+\delta^2\eta^3-\delta^2\eta^2)^2}>0$ , we only need to determine the positive and negative of $\eta(1-\eta)(\eta^2-2\eta+2c\eta-c+1)\delta^2-4(1-\eta+c)$ . We obtain that if $0<\delta<\delta_m^M$ , then $\frac{d\pi_m^{M*}}{d\eta}<0$; if $\delta_m^M<\delta<\frac{\sqrt{2(1-\eta)}}{\eta(1-\eta)}$ , then $\frac{d\pi_m^{M*}}{d\eta}>0$ .

Taking the first order derivative of $\pi_r^{M*}$ to $\eta$ . We obtain (A6)

$$\frac{d\pi_m^{M*}}{d\eta}=\frac{8(1-c-\eta)(\eta(1-\eta)(3\eta^2-5\eta+4c\eta-2c+2)\delta^2-8c)}{(1-\eta)^3(8+\delta^2\eta^3-\delta^2\eta^2)^3} \tag{A6}$$

Similarly, we can obtain that if $0<\delta<\delta_r^M$ , then $\frac{d\pi_m^{M*}}{d\eta}<0$ ; if $\delta_r^M<\delta<\frac{\sqrt{2(1-\eta)}}{\eta(1-\eta)}$ , then $\frac{d\pi_r^{M*}}{d\eta}>0$ . Since $\delta_r^M<\delta_m^M$ , we can proof Corollary 2.

Proof of proposition 2 The Hesse matrix of Eq. 10 is given by

$$\begin{pmatrix} -2(1-\eta) & \frac{(1-\eta)\delta\eta}{2\sqrt{A}} \\ \frac{(1-\eta)\delta\eta}{2\sqrt{A}} & -\frac{(p-\eta p+w)\delta\eta}{4A^{3/2}} \end{pmatrix} \tag{A7}$$

Its principal sub formulas are $-2(1-\eta)<0$ , $\frac{\delta\eta(1-\eta)(\delta\eta\sqrt{A}(\eta-1)-2(\eta p+p-w))}{4A^{3/2}}>0$ respectively. From this we can obtain Eq. 10 as a concave function of $A$ and $w$ . We let the first-order derivative of Eq. 10 with respect to $p$ and $A$ be equal to zero to obtain the reaction function $p=\frac{w\delta^2\eta^2(\eta-1)-2(\eta-w-1)}{(1-\eta)(4+\delta^2\eta^3-\delta^2\eta^2)}$, $A=\frac{(\eta+w-1)^2\delta^2\eta^2}{(4+\delta^2\eta^3-\delta^2\eta^2)^2}$. Then we have Eqs. 13-15. Substituting them into Eqs. 10-12 and simplifying them gives Eqs. 16-18.

Proof of Corollary 3: Taking the first order derivative of $A^{R*}$ to $\eta$ . We have (A8):

$$\frac{dA^{R*}}{d\eta}=\frac{\delta^2\eta(1-\eta)(\delta^2\eta^2(\eta^2-2\eta+2c\eta-c+1)+4(1-2\eta-c))}{4(4+\delta^2\eta^3-\delta^2\eta^2)^3} \tag{A8}$$

Similarly, we can obtain (A9) and (A10) as follows:

$$\frac{dw^{R*}}{d\eta}=\frac{1}{2} \tag{A9}$$

$$\frac{dp^{R*}}{d\eta}=\frac{\delta^4\eta(1-\eta)(\delta^2\eta^3c(1-\eta)+6\eta^2+4c+10\eta-4)+8c}{2(1-\eta)^2(4+\delta^2\eta^3-\delta^2\eta^2)^2} \tag{A10}$$

It is easy to obtain (A8), (A9) > 0 and (A10) < 0.

Proof of Corollary 4: Taking the first order derivative of $\pi_m^{R*}$ to $\eta$ . We obtain (A11):

$$\frac{d\pi_m^{R*}}{d\eta} = \frac{(1-c-\eta)(\delta^2\eta(1-\eta)(\eta^2+2c\eta-c-2\eta+1)\delta^2-2(1-\eta+c))}{(1-\eta)^3(8+\delta^2\eta^3-\delta^2\eta^2)^3} \tag{A11}$$

We obtain that if $0<\delta<\delta^R$, then $\frac{d\pi_m^{R*}}{d\eta}<0$ and $\frac{d\pi_r^{R*}}{d\eta}<0$ ; if $\delta^R<\delta<\frac{\sqrt{2(1-\eta)}}{\eta(1-\eta)}$, then $\frac{d\pi_m^{R*}}{d\eta}>0$ and $\frac{d\pi_r^{R*}}{d\eta}>0$. We can proof Corollary 4.

<u>Proof of Corollary 5</u>: we can obtain

$$A^{M*}-A^{R*} = \frac{\delta^4\eta^4(1-\eta)(16+3\delta^2\eta^3-3\delta^2\eta^2)}{4(4+\delta^2\eta^3-\delta^2\eta^2)^2(8+\delta^2\eta^3-\delta^2\eta^2)^2} \tag{A12}$$

$$w^{M*}-w^{R*} = \frac{\eta(\eta(1-\eta)(\eta^2+2c\eta-c-2\eta+1)\delta^2+8(1-\eta+c))}{(1-\eta)(8+\delta^2\eta^3-\delta^2\eta^2)} \tag{A13}$$

$$p^{M*}-p^{R*} = \frac{\delta^2\eta^2(1-c-\eta)(2+\delta^2\eta^3-\delta^2\eta^2)}{2(4+\delta^2\eta^3-\delta^2\eta^2)(8+\delta^2\eta^3-\delta^2\eta^2)} \tag{A14}$$

It can be judged that (A12) < 0, (A13) > 0 and (A14) > 0.

<u>Proof of Corollary 6</u>: Since

$$\pi_m^{M*}-\pi_m^{R*} = \frac{\delta^2\eta^2(1-c-\eta)^2}{2(4+\delta^2\eta^3-\delta^2\eta^2)(8+\delta^2\eta^3-\delta^2\eta^2)} \tag{A15}$$

It is easy to get (A15)> 0.

$$\pi_r^{M*}-\pi_r^{R*} = -\frac{\eta(1-c-\eta)^2((1-\eta)^3\delta^4\eta^3+16(1-\eta)^3\delta^2\eta^3+64)}{4(1-\eta)^2(4+\delta^2\eta^3-\delta^2\eta^2)^2(8+\delta^2\eta^3-\delta^2\eta^2)} \tag{A16}$$

To determine the positive and negative of (A16). We need to determine the positive and negative of $(1-\eta)^3\delta^4\eta^3+16(1-\eta)\delta^2\eta^3+64$, we can solve when $0<\eta<\frac{1}{9}$, if $\delta'<\frac{\sqrt{2(1-\eta)}}{\eta(1-\eta)}$, then $\pi_r^{M*}<\pi_r^{R*}$ ; if $\delta'<\delta<\frac{\sqrt{2(1-\eta)}}{\eta(1-\eta)}$, there is $\pi_r^{M*}>\pi_r^{R*}$ . When $\eta>\frac{1}{9}$, there is $\delta'>\frac{\sqrt{2(1-\eta)}}{\eta(1-\eta)}$, then $\pi_r^{M*}>\pi_r^{R*}$ .

<u>Proof of Corollary 7</u>: There is

$$\pi_s^{M*}-\pi_s^{R*} = \frac{\eta(1-c-\eta)^2(\delta^4\eta^3(1-\eta)^3-\delta^2\eta(1-\eta)+64)}{4(1-\eta)^2(4+\delta^2\eta^3-\delta^2\eta^2)(8+\delta^2\eta^3-\delta^2\eta^2)} \tag{A17}$$

since that when $\pi_s^{M*}>\pi_s^{R*}$, there is $\delta^4\eta^3(1-\eta)^3-\delta^2\eta(1-\eta)+64>0$, then $\pi_s^{M*}>\pi_s^{R*}$; when $\delta_s<\delta<\frac{\sqrt{2(1-\eta)}}{\eta(1-\eta)}$, there $\delta^4\eta^3(1-\eta)^3-\delta^2\eta(1-\eta)+64<0$, then $\pi_s^{M*}<\pi_s^{R*}$ .

APEM journal

**Advances in Production Engineering & Management**
Volume 17 | Number 4 | December 2022 | pp 494–504
https://doi.org/10.14743/apem2022.4.451

**ISSN 1854-6250**
Journal home: apem-journal.org
Original scientific paper

# Impact of Cobot parameters on the worker productivity: Optimization challenge

**Javernik, A.**[a]**, Buchmeister, B.**[a]**, Ojstersek, R.**[a,*]

[a]University of Maribor, Faculty of Mechanical Engineering, Maribor, Slovenia

**A B S T R A C T**

In the era of Industry 4.0 and the introduction of new technologies, collaborative workplaces represent the potential to increase the efficiency of manufacturing systems. The presented research focuses on studying the impact of changing the speed and acceleration of a Cobot to the number of finished products at a collaborative workstation, the average assembly time, and the utilization of the Cobot and worker. In a laboratory experiment, it was demonstrated that changing the parameters of the Cobot significantly affects the optimization parameters of the collaborative workstation productivity. The results indicate an increase in production capacity with an increase in the speed and acceleration of the Cobot, while at the same time highlighting the importance of uniform utilization and occupancy of the Cobot and worker. The findings are particularly interesting from the influence of the Cobot's audio and video effects on worker, when reducing the average assembly time while increasing the Cobot's capabilities. The results and findings presented open up important new areas of research in the field of social, time and financial justification of collaborative workplaces.

**A R T I C L E   I N F O**

*Keywords:*
Collaborative robot;
Cobot;
Collaborative operation;
Robot parameters;
Worker productivity;
Working scenarios;
Manufacturing efficiency;
Optimization

**Corresponding author:*
robert.ojstersek@um.si
(Ojstersek, R.)

*Article history:*
Received 10 September 2022
Revised 19 December 2022
Accepted 22 December 2022



## 1. Introduction

In the era of Industry 4.0 [1], where the role of making the right decisions in optimizing existing or newly proposed manufacturing system is key to achieving global competitiveness of the company. The optimization of manufacturing systems and its efficiency refers to both machines (technology) and workers (their knowledge and social paradigms) [2, 3]. The correct and equal distribution of occupancy between workers and machines plays a key role in sustainable production systems in terms of social, environmental and financial aspects. Implementing an effective model to acquire new knowledge about technologies that can increase efficiency is crucial [4]. According to the literature [5], classical single-objective approaches do not provide satisfactory solutions, especially when dealing with problems with high market dynamics and continuous optimization trends. Given the global shortage of workers (especially in developed countries), collaborative robots (Cobots) represent a new opportunity for companies willing to invest into new financially feasible technologies. In this case the research question appears: how efficient we can place them into the existing or newly proposed manufacturing system [6]. Proper design of collaborative workplaces (cooperation between worker and Cobot) is the main challenge for researchers and engineers who want to increase manufacturing efficiency [7]. In doing so, we encounter the issues of collaboration safety, time and economic justification, and their impact on the entire manufacturing system under consideration [8]. The researchers point out the importance of using simulation modelling methods [9] that allow us to effectively evaluate the time efficiency of collaborative workplaces from the individual optimization parameters of the system [10] in a real-world industrial environment [11]. Different applications of collaborative workplaces [12] require the use of different optimization approaches [13], where we need to ensure safe and efficient parameters of the collaborative machines (Cobot) due to the specificity of the considered cases [14]. In this case, data-driven predictive models [15] prove to be the most reliable methods, where we use numerical and graphical simulation results to investigate the appropriateness of introducing and correctly determining collaborative machines [16]. Collaborative workplaces and their design in manufacturing systems present new challenges also from the ergonomic design point of view [17, 18], where the classical methods of ergonomic studies do not satisfy the criteria of a collected big data at high production dynamics. The impact of collaborative workplaces on the efficiency of the manufacturing systems [19] and the link with adaptive models [20] to monitor the importance of effective implementations are based on the performance of preliminary studies in which researchers compare simulation and real-world data of manufacturing systems [21]. The major limitation of the existing research is in the area of describing how the parameters of the Cobot affect the efficiency of the co-worker, not only from the worker's point of view, but also with respect to the efficiency of the Cobot and the manufacturing system as a combined unit.

In this research, we address the research question of whether changing the operating parameters of a Cobot affects the efficiency of the manufacturing system and the occupancy of the worker itself. Based on the results, limitations, and issues of previous research works [19, 21], in this paper, we aim to present an experimental method to study the change of speed and acceleration of a Cobot on the effectiveness of a collaborative workplace. We focus on the multi-objective evaluation of the collaborative workplace optimization parameters with the detailed study of the assembly times, production quantities, and occupancy of the collaborative workplace from the Cobot and worker perspective.

## 2. Problem description

Cobot's properly set parameters can have a big impact on the efficiency and capacities of the manufacturing system. To set up a proper parameter of robots/machines can be a real challenge, especially when it comes to Cobot's. It is not necessary that highest working parameters brings the highest number of finished orders, shortest operating times and highest machine utilization. The optimum working parameters depends on the structure of collaborative workplace, application type and defined sequence of tasks [22].

Most integrators/production engineers define Cobot's working parameters their preference and existing knowledge or based on suggestions from Cobot's producers. In many cases, parameters are not set up properly or are even set up to the maximum limit of the machine. With higher defined parameters, integrators want to achieve more finished products in less time. In most cases, such a decision leads to positive results as the machine's operating time is reduced, but is it really only about the machine operating time, or there are also other variables we have overlooked inside the collaborative workplace?

At observing of collaborative workplaces and their operations, we noticed that worker movements change or adapt according to parameters of the collaborative device [19, 22]. Such a finding, immediately raised a question of whether the speed and acceleration of the Cobot could have an impact on workers performance indicators (average worker assembly time, number of finished products and worker occupancy)? To determine the correctness or incorrectness of our predictions in the best possible way, we had proposed the design of the collaborative workplace and determine the most suitable type of collaborative application, presented in section three.

### 2.1 Collaborative workplaces

To find out if there is a relation between the parameters of the collaborative robot and the assembly time of the workers, we had to design the structure of the experiment, a collaborative workplace layout and a collaborative operation. In the initial research phase, we had to think about what type of application and type of collaboration between the Cobot and the worker to design.

In Fig. 1 four types of collaboration between the Cobot and the worker are presented. The first type is a caged cell. At caged cell type, a collaboration level is zero, the robots are in cages and there is no possible interaction between the worker and the robot. At this type mainly industrial robots are installed. At second type, so called coexistence, the Cobot and the worker work in the same space without fence between them, but they do not share the same workspace. Next type of collaboration is sequential or synchronized. The worker and the Cobot share their workspace but not at the same time, movements needs to be sequential. The last type of collaboration according to literature [23] is cooperation. At this type of work, the level of collaboration is the highest, the worker and the Cobot share the same workspace at the same time. In cooperation type the use of Cobot instead of industrial robot is necessary, because of integrated safety features that allow to work in direct contact. Even that in Cobot safety features are installed, the integrator still needs to perform risk assessment and design the operation as save as possible [24].

To mention, definition of collaboration types differs between the individuals, because the community is still split about their opinions and definitions. But there is not a lot of differences between the sources, mainly in names and small details.

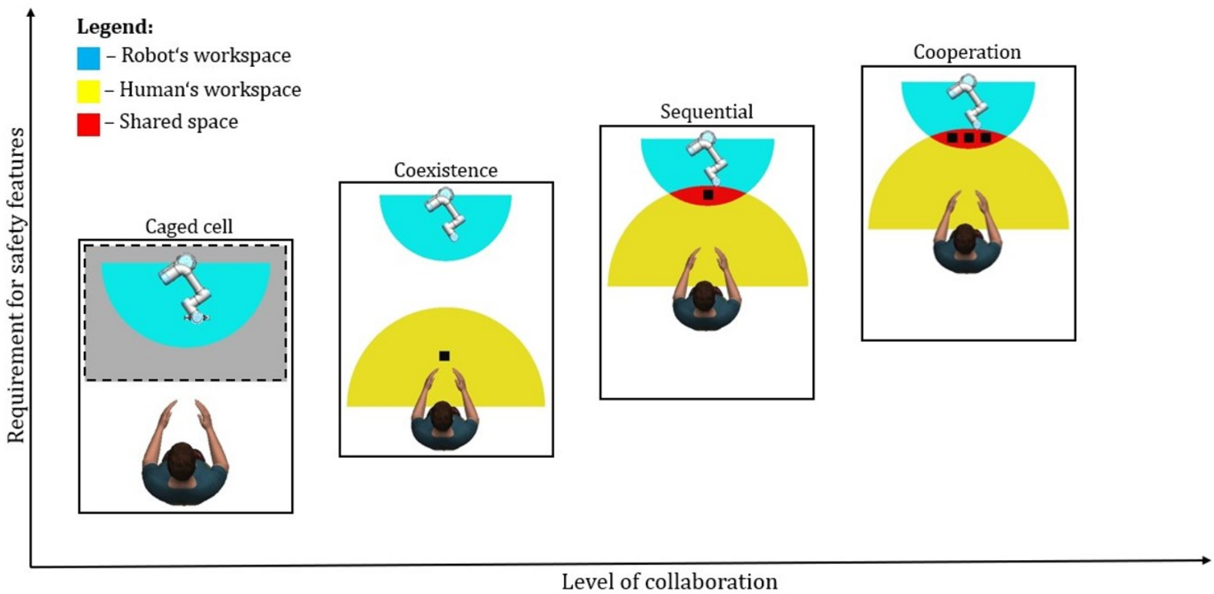


**Fig. 1** Types of Cobot and worker collaboration

### 2.2 Manufacturing efficiency

Initially, the definition of manufacturing productivity in terms of production is the ratio of output to input in production and is a measure of efficiency. If something is produced, we want to know how long it takes to produce it. While productivity focuses more on increasing the quantity produced, efficiency refers to the quality and effectiveness of the manufacturing system. In our research work we are focused on the collaborative workplace's efficiency in correlation to its performance parameters. We are focusing on evaluating the ability to do or produce products without wasting material, time, cost, or energy. The efficiency is often expressed as a percentage, with 100 % being the ideal goal so that the product is produced at the lowest average total cost per item at the highest possible workplace occupancy. In presented research work we are measuring efficiency with the parameter of the number of hours of productive quality assembly work divided by the number of minutes available in the experiment run. The optimization methods and workers training can lead to improved manufacturing efficiency. For this purpose, the key performance indicators (KPI) were used to help evaluate Cobot and worker efficiency when the parameters of Cobot speeds and accelerations are changing. In general: if you want to increase manufacturing efficiency, you essentially want to produce more output in the same amount of time. Finding a constant balance between productivity and manufacturing efficiency is critical to keeping your manufacturing running optimally. In Fig. 2 we can see optimization perspectives with which company can achieve high manufacturing system KPI's.

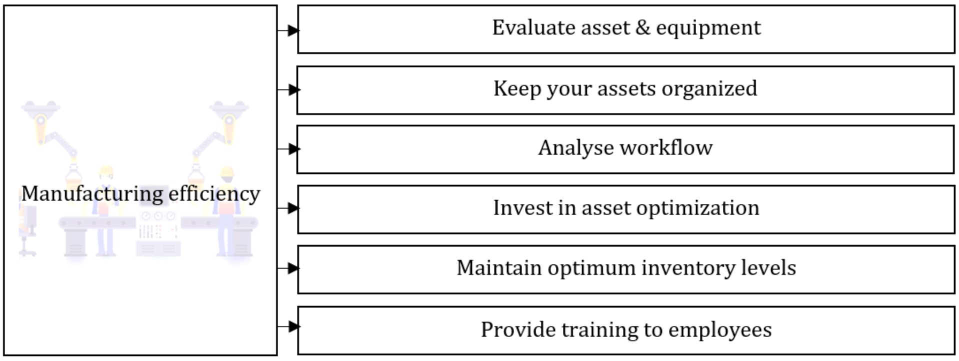


**Fig. 2** Manufacturing efficiency, optimization perspectives

## 3. Experiment description

The presented experiment was prepared according to the collaborative workplace standards listed in the literature [7], the research focuses on the reproducibility of the experiment in a laboratory environment, initial simulation model in Siemens software is shown in Fig. 3, where the selected building blocks are standard elements, as presented in subsection 3.1. The experimental environment is presented in detail in the subsections of the collaborative workspace description and the experimental design, where the experiment design is prepared in correlation with different experts from the field of social, medicine and technical sciences.

**Fig. 3** Collaborative workplace simulation model for laboratory experiments

### 3.1 Collaborative workplace description

The experiment was conducted with the laboratory environment, so the collaborative workplace was adapted to laboratory conditions in terms of size and application type. Collaborative workplace consisted of a worktable ③, a collaborative robot UR3e ⑦, a collaborative gripper Robotiq 2F-85 ⑥, a switch with indicators light in green and red colour ④ and button ⑤, and two types of semi-finished products ① ②. A Lego brick size of 4×2 represented the semi-finished product 1 ① while a brick size of 2×2 represented the semi-finished product 2 ②. The finish product consisted of one semi-finished product ① and two semi-finished products ② assembled together, as shown in Fig. 4.

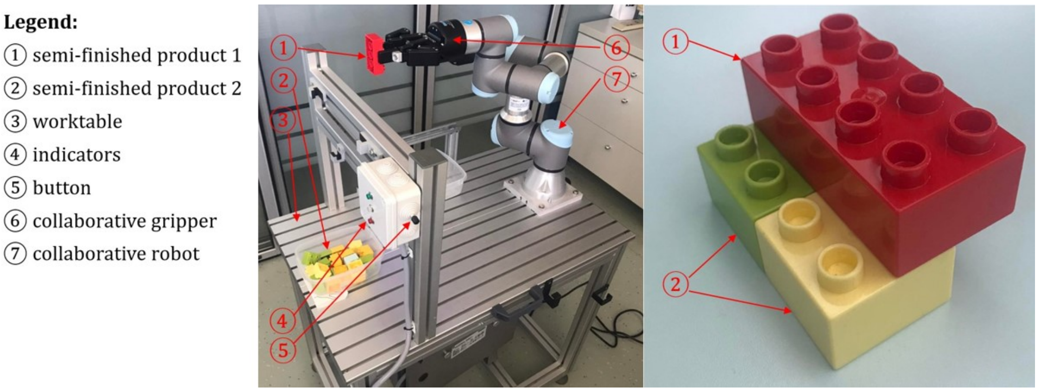


**Fig. 4** Layout of the collaborative workplace (left) and the finished product (right)

The assembly operation consisted of assembling three semi-finished products into one finished product. The sequence of assembling was predefined to get the most objective results. At the beginning of the collaborative operation, the indicator light glowed red. The red light signalled that the Cobot is working and the worker is not approved to enter the robot area, but the worker can prepare himself. At the beginning, the collaborative robot picked up the semi-finished product and brought it to the collaboration/assembly area. When the robot reached the assembly area, it stopped, the indicator light changed from red to green and the worker was allowed to assemble. After the worker attached two semi-finished products ② to the semi-finished product ①, he or she pressed the button to send the signal about the completed work. The indicator light changed back from green to red and the Cobot moved the finished product into the box. The procedure was repeated until the total time of 30 minutes, for each experiment, was reached.

### 3.2 Experiment design

To test our hypothesis optimal, we decided to design an assembly operation, a collaborative assembly operation, where the Cobot and the worker work sequential. At sequential type, they share the same workspace but at different time intervals. The sequential type of collaboration in our case was ideal because we still provided the contact between them and we could obtain objective results about a relation between the parameters of the robot and the operation time of the worker. In the next phase of experiment planning, we had to determine the structure of the experiment, length of the experiment and Cobot parameters (speed and acceleration). We decided to limit our experiment to 30 minutes and divide it into four phases as seen in Table 1.

The experiment was divided into four phases. In the first phase, the Cobot and the worker worked separately. The worker manually assembled the finished products for 5 minutes. The goal of the first phase for the worker was to get used to such a type of the work and to the proximity of the Cobot. After 5 minutes, phase 2 has begun. Phase 2 lasted 10 minutes and consisted of collaborative work. The worker assembled the finished products with the help of the Cobot. The speed and acceleration of the Cobot were set to 60 %. After phase 2, phase 3 had started, it was set up the same way as phase 1, mainly to relax the worker. The worker and Cobot worked separately for 5 minutes. The goal of phase 3 was to release the pressure from the worker from the previous phase in which the worker collaborated with the Cobot. In the last phase of the experiment, phase 4, the worker worked with the Cobot again. Phase 4 lasted the same amount of time as phase 2, but the parameters of the Cobot were set higher, at 100 %. Cobot parameters (Table 2) were define based on attempted test in laboratory, simulation model presented in Fig. 3 and the specifics of the application type. After the experiment was completed, we obtained the results, describing collaborative workplace efficiency from phase 2 and phase 4.

**Table 1** Structure of the experiment

| Phase No. | Time length (min) | Description |
|---|---|---|
| Phase 1 | 5 | Manual assembly operation |
| Phase 2 | 10 | Collaborative assembly operation (CR speed and acceleration 60 %) |
| Phase 3 | 5 | Manual assembly operation |
| Phase 4 | 10 | Collaborative assembly operation (CR speed and acceleration 100 %) |

**Table 2** Cobot speeds and accelerations

| Linear movements | | | | add | Joint movements | | | |
|---|---|---|---|---|---|---|---|---|
| Speed (%) | (mm/s) | Acceleration (%) | (mm/s$^2$) | | Speed (%) | (°/s) | Acceleration (%) | (°/s$^2$) |
| 60 | 600 | 60 | 1500 | | 60 | 206 | 60 | 310 |
| 100 | 1000 | 100 | 2500 | | 100 | 344 | 100 | 516 |

## 4. Results

The experiment involved nine participants, both men's and women's, aged from 20 to 50 years. Until the end of experiment participants did not know the real goal of the experiment. With unknown, research goal (caning speeds and accelerations of the Cobot), we provided that they could not had an impact on their assembly task. The results in Table 3 show the average assembly time and number of finished products of each participant in two different scenarios corelated to phase 2 and phase 4. In both scenarios, the worker collaborated with the Cobot, but in scenario 1 (S1) the Cobot parameters were set to 60 % meanwhile in scenario 2 (S2) the parameters were set to 100 % of the specified speed and acceleration. Throughout the experiment we focus on next optimization parameters: worker average assembly times, number of finished products and Cobot and worker occupancy. Each worker average assembly times were saved to the time variable of the Cobot data collecting unit. According to the number of finished products and stored assembly times in the time variable, the average assembly time for each scenario was calculated.

### 4.1 Results of average assembly times and number of finished products

From the results seen in Table 3 and Fig. 5, it is clear that with increased Cobot parameters assembly times did shorten. Although the number of participants in our experiment was low, we did not perceive a single longer assembly time while the parameters of the Cobot were increased in comparison with the S1, where Cobot parameters were lower. The average assembly time in S1 was 3.4 s with a standard deviation of 0.81. The number of participants in which the average assembly time was below average was 5 out of 9 participants. In scenario S2, where the speed of the robot was increased to 100 %, the average assembly time decreased to 2.6 s, in this case the standard deviation is lower at 0.66. In S2, 6 out of 9 participants had a shorter average assembly time than the average total time.

Increasing the parameters of the Cobot from 60 % to 100 % contributed to the 23.4 % decrease in average assembly time of the worker. The minimum decrease in average assembly time that occurred in our experiment was 8.70 %, while the maximum decrease was 36.90 %.

The presented results of the experiment confirm our prediction. Higher define parameters of the Cobot had an impact on the worker and resulted in a higher working speed. Due to the higher working speed, the average assembly time is shorter, and we are able to deliver a higher number of finished products. Using the number of finished products parameters, we see that the total number of products produced in S1 is 497 pieces for nine participants in total. On average, each participant assembled 55.2 pieces in 10 minutes, with a standard deviation of 3.9. A significantly higher number of finished products is seen in S2, where participants assembled a total of 761 pieces in 10 minutes, while each worker assembled an average of 85.5 pieces with a standard deviation of 7.6, as shown in Fig. 6.

**Table 3** Average assembly times and Number of finished products per participant in S1 and S2

| Participants | Average assembly time (s) – S1 | Number of finished products (pcs) – S1 | Average assembly time (s) – S2 | Number of finished products (pcs) – S2 |
|---|---|---|---|---|
| 1 | 2.82 | 58 | 2.34 | 87 |
| 2 | 3.00 | 57 | 2.42 | 86 |
| 3 | 2.82 | 58 | 1.97 | 92 |
| 4 | 2.65 | 59 | 2.27 | 88 |
| 5 | 2.48 | 60 | 1.70 | 96 |
| 6 | 3.59 | 54 | 2.27 | 88 |
| 7 | 4.98 | 48 | 3.34 | 76 |
| 8 | 4.24 | 51 | 3.45 | 75 |
| 9 | 4.02 | 52 | 3.67 | 73 |

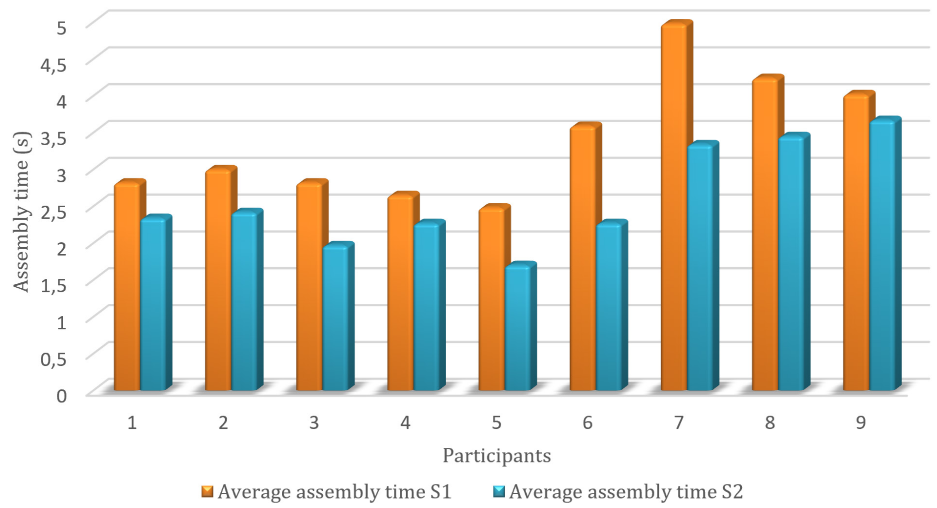


**Fig. 5** Average assembly times, results comparison (S1 vs S2)

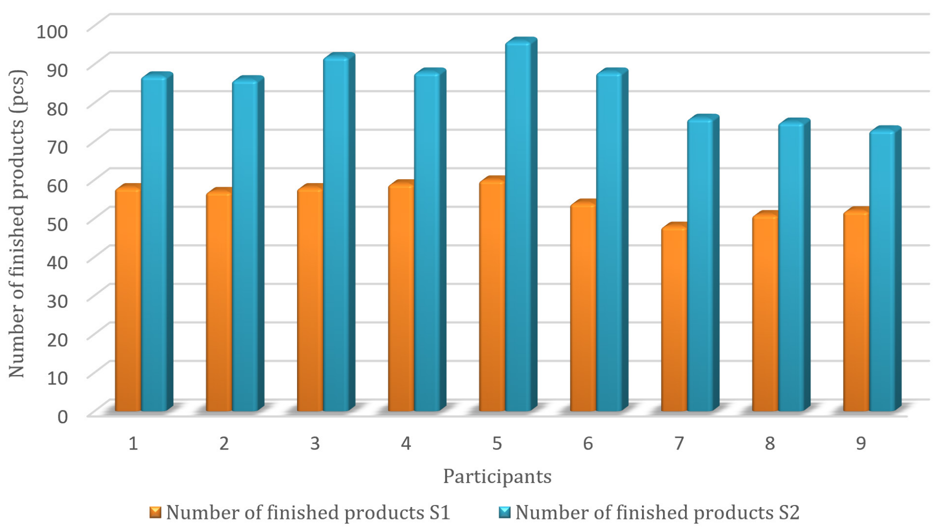


**Fig. 6** Number of finished products, results comparison (S1 vs S2)

## 4.2 Results of Cobot and worker occupancy

Table 4 shows the occupancy of the collaborative workspace (Cobot and worker time occupancy), where the values are evaluated according to the total assembly time, which is in total 10 minutes for the individual scenario. The results show the three optimization parameters, where the Cobot occupancy indicates the total operating time of the Cobot. The worker occupancy is divided into the assembly and setup time parameters. Notice: the worker's assembly setup time is performed when the robot performs its operations.

**Table 4** Cobot and worker occupancy in S1 and S2

| Participants | Cobot occupancy (min) – S1 | Worker occupancy (min) – S1 | | Cobot occupancy (min) – S2 | Worker occupancy (min) – S2 | |
|---|---|---|---|---|---|---|
| | | Assembly time | Setup time | | Assembly time | Setup time |
| 1 | 7.27/10 | 2.73/10 | 1.87/10 | 6.60/10 | 4.40/10 | 3.19/10 |
| 2 | 7.15/10 | 2.85/10 | 1.95/10 | 6.53/10 | 3.47/10 | 2.52/10 |
| 3 | 7.27/10 | 2.73/10 | 1.87/10 | 6.98/10 | 3.02/10 | 2.19/10 |
| 4 | 7.40/10 | 2.60/10 | 1.78/10 | 6.68/10 | 3.32/10 | 2.41/10 |
| 5 | 7.52/10 | 2.48/10 | 1.70/10 | 7.28/10 | 2.72/10 | 1.97/10 |
| 6 | 6.77/10 | 3.23/10 | 2.21/10 | 6.68/10 | 3.32/10 | 2.41/10 |
| 7 | 6.02/10 | 3.98/10 | 2.72/10 | 5.77/10 | 4.43/10 | 3.22/10 |
| 8 | 6.39/10 | 3.61/10 | 2.47/10 | 5.69/10 | 4.31/10 | 3.13/10 |
| 9 | 6.52/10 | 3.48/10 | 2.38/10 | 5.54/10 | 4.46/10 | 3.24/10 |

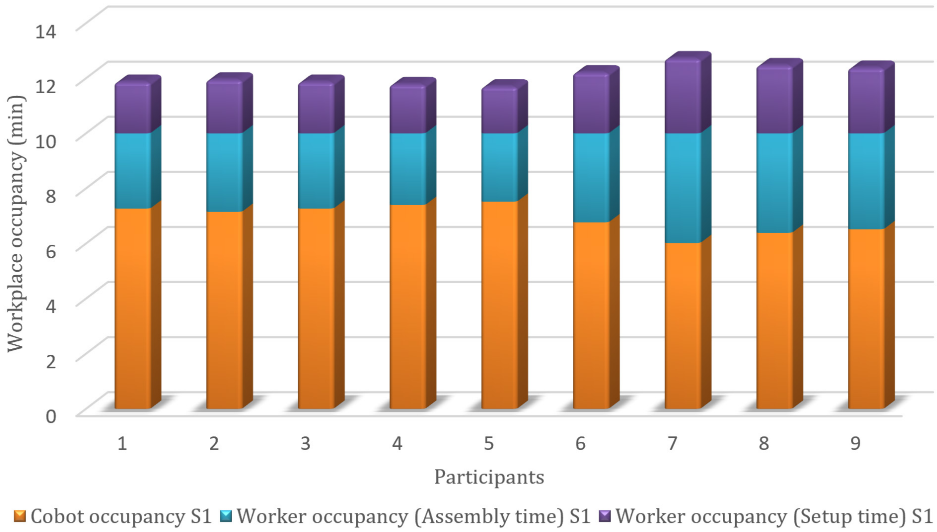


**Fig. 7** Workplace occupancy in S1

Fig. 7 and the results in Table 4 show that in S1, the participating robot is occupied on average 6.92 minutes of the available 10 min total time. The standard deviation of average Cobot occupancy is 4.9. A worker at a collaborative workstation is engaged in assembling operation for an average of 3.08 minutes while spending another 2.11 minutes preparing the parts to be assembled, giving a total time occupancy of 5.18 in the available time of 10 min, where the standard deviation is 4.9.

Results of the S2 in Fig. 8 shows, that the Cobot works an average of 6.42 min of the available 10 min. With the parameters S2, the worker is occupied for 3.71 min for the assembly operation and 2.69 min for the setup time, which totals 6.40 min of the available 10 min workplace operation time. For parameters S2, the standard deviation of the Cobot occupancy is 5.7 and for the worker it is 6.3.

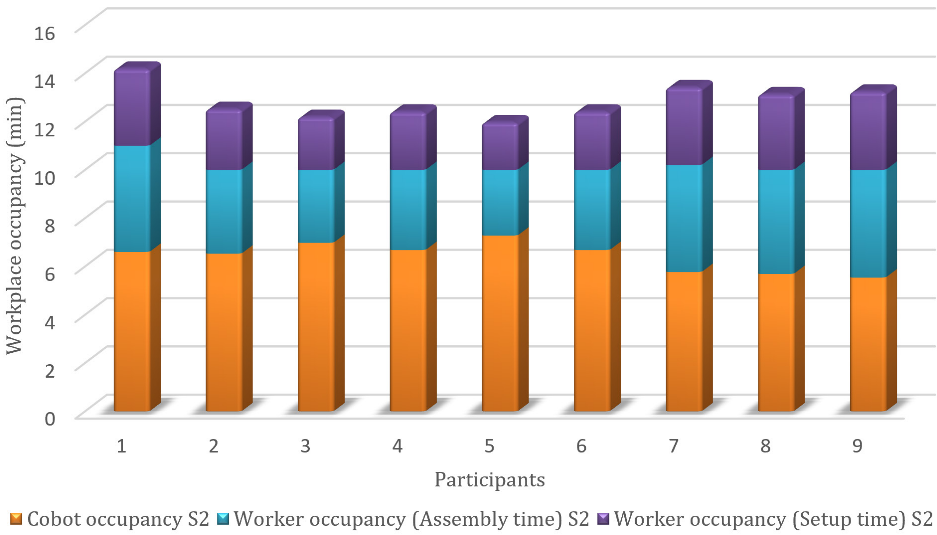


**Fig. 8** Workplace occupancy in S2

## 5. Discussion

Based on the results shown, we conclude that in total 264 more pieces are produced in S2 at the collaborative workplace than with the parameters representing scenario S1. The average number of finished products at the collaborative workplace in scenario S2 increases by 54.9 %, which significantly increases the number of manufactured products. At the same time, the standard deviation results, which are 3.7 higher for S2, indicate a higher probability of non-constant operation of the collaborative workplace assembly operations when repeated operations are performed in several shifts with several different workers. The results presented indicate that worker workload increases at higher speeds and accelerations of the Cobot. Based on the evaluated optimization parameter of the average assembly time, we find that it is 23.5 % shorter in scenario S2, which is an interesting observation from the justifying the collaborative workplace point of view. The worker changed the work speed (assembling operation) when the Cobot mode of operation changed (the transition of the Cobot parameters from S1 to S2). Obviously, the visual and audio effects presences (perception of the Cobot) had a positive effect on the shorter average assembly time, even though the worker had exactly the same time to assemble the product in both evaluated scenarios (S1 and S2).

It is also interesting to analyse the occupancy of the participants (Cobot and worker) in the collaborative workplace. The results show that the occupancy of the Cobot in the S2 scenario decreased by 7.2 % compared to the time occupancy in the S1 scenario. The results prove that the Cobot is able to perform multiple activities simultaneously and possibly participate in more complex activities or collaborate in a workplace with two workers when the operating parameters are increased. In this case, it is useful to study the utilization of the Cobot in detail, because only with a detailed analysis we can ensure the justification for the introduction of such a machine in existing or newly proposed production system. In contrast to the decrease in the time occupancy of the Cobot in S2, the occupancy of the worker in S2 increases, by 23.6 %, the occupancy is higher both during assembly and setup time. With respect to the time occupancy parameter, we find that the importance of consistent collaborative workplace occupancy is critical to the economic and social justification of a collaborative workplace. When introducing new collaborative workstations, the use of simulation techniques is highly justified, assuming that they represent the minimum cost of the initial investment and reduce the risk that the new investment is not justified.

As mentioned in the introduction, usually companies start to increase the parameters (speeds and accelerations) of the Cobot to reduce the cycle time of the machine operations to provide enough collaborative workplace capacity. But as our results show, the integrators probably also affect the worker's working speed unconsciously. It is difficult to fully determine the reason for the increased worker operating speed, but a few options emerged during the experiment that may be important contributors. Different speeds and accelerations of the Cobot provide different volumes of noise. The loudness of electro motors in joints could be a factor for faster movements and greater willingness of the worker. The other aspect that should be considered is visualization. In collaborative operation, the worker is constantly in "contact" with the Cobot, as with assembling the products together as at observing the robot's movements. With defined and constant parameters of the Cobot, workers get to use of work sequence and begin to memorize specific positions of the Cobot at specific time frames. If the remembered positions start to differ from previously remembered start to deviate from previous memorized positions, this could trigger some kind of alarm in the worker, whose spontaneous reaction could be an increased working speed.

According to the existing literature [19, 21], the presented work highlights the importance of a detailed study of the feasibility of introducing collaborative workplaces, where the setting parameters of the collaborative machine can significantly affect the efficiency of such a workplace. Proper integration of a Cobot affects both economic, time and social justification. The main contribution of the presented work is evident in the results that highlight the study of the importance of the visual and acoustic impact on the worker and consequently on its use. Considering the number of participants considered, the trend of results shown allows further work and extension of the experiment, which must be transferred to a real-world environment where the working hours of the collaborative workplace would be longer. With longer working hours and the evaluation of the collaborative workplace efficiency, the speed and acceleration of the Cobot would have a significant impact on the worker's workload, concentration, and therefore on the quality of the work performed.

## 6. Conclusions

In the research paper, the importance of Cobot parameters on worker productivity is presented. The results of the study provide useful and interesting answers to our research question, but new doubts have also been raised. The results show that the parameters of the Cobot have an impact on the assembly times of the workers. Higher speed and acceleration of the Cobot contribute to a higher working speed of the worker, which leads to shorter assembly times in our study. Despite the positive results, the limit of the Cobot parameters must be considered at different collaborative work operations. The speed and acceleration limit should be set in such a way that it does not affect the correct performance of the Cobot and, most importantly, it does not negatively affect the worker (performance, physical health, mental health, etc.).

Future research will focus on the analysis of more participants, different ages, educations and genders. We will focus our research on studying the mental and physical health of workers working with Cobot. Favourable research results will lead to the transfer of the laboratory experiment to a real-world production environment, where the speed and acceleration of the Cobot will have a longer-term effect on the efficiency of the worker and the entire collaborative workplace. When evaluated in a real-world environment, the challenges will enable a more detailed and practical application value of the presented research work, which is crucial in the era of Industry 4.0 and the arrival of new technologies. Cost, time and social justified of the collaborative workplaces certainly represent one of the more attractive research areas from the manufacturing efficiency point of view.

## Acknowledgement

The authors gratefully acknowledge the support of the Slovenian Research Agency (ARRS), Research Core Funding No. P2-0190. The authors acknowledge the use of research equipment system for development and testing cognitive production approaches in industry 4.0: Collaborative robots with equipment and Sensors, hardware and software for ergonomic analysis of a collaborative workplace, procured within the project "Upgrading national research infrastructures - RIUM", which was co-financed by the Republic of Slovenia, the Ministry of Education, Science and Sport and the European Union from the European Regional Development Fund.

## References

[1] Rosin, F., Forget, P., Lamouri, S., Pellerin, R. (2021). Impact of Industry 4.0 on decision-making in an operational context, *Advances in Production Engineering & Management*, Vol. 16, No. 4, 500-514, doi: 10.14743/APEM2021.4.416.

[2] Hall, R.E., Jones, C.I. (1999). Why do some countries produce so much more output per worker than others?, *The Quarterly Journal of Economics*, Vol. 114, No. 1, 83-116, doi: 10.1162/003355399555954.

[3] Iriondo Pascual, A., Högberg, D., Lämkull, D., Perez Luque, E., Syberfeldt, A., Hanson, L. (2021). Optimization of productivity and worker well-being by using a multi-objective optimization framework, *IISE Transactions on Occupational Ergonomics and Human Factors*, Vol. 9, No. 3-4, 143-153, doi: 10.1080/24725838.2021.1997834.

[4] Drucker, P.F. (2013). Implementing the effective management of knowledge: Knowledge-worker productivity: The biggest challenge, In: Woods, J.A., Cortada, J. (eds.), *The Knowledge Management Yearbook 2000-2001*, First Edition, Routledge, London, United Kingdom, 267-283, doi: 10.4324/9780080941042-28.

[5] Mirzapour Al-E-Hashem, S.M.J., Baboli, A., Sadjadi, S.J., Aryanezhad, M.B. (2011). A multiobjective stochastic production-distribution planning problem in an uncertain environment considering risk and workers productivity, *Mathematical Problems in Engineering*, Vol. 2011, Article ID 406398, doi: 10.1155/2011/406398.

[6] Hu, M., Wang, H., Pan, X. (2020). Multi-objective global optimum design of collaborative robots, *Structural and Multidisciplinary Optimization*, Vol. 62, 1547-1561, doi: 10.1007/S00158-020-02563-X.

[7] Gualtieri, L., Palomba, I., Merati, F.A., Rauch, E., Vidoni, R. (2020). Design of human-centered collaborative assembly workstations for the improvement of operators' physical ergonomics and production efficiency: A case study, *Sustainability*, Vol. 12, No. 9, Article No. 3606, doi: 10.3390/SU12093606.

[8] Realyvásquez-Vargas, A., Arredondo-Soto, K.C., García-Alcaraz, J.L., Márquez-Lobato, B.Y., Cruz-García, J.L. (2019). Introduction and configuration of a collaborative robot in an assembly task as a means to decrease occupational risks and increase efficiency in a manufacturing company, *Robotics and Computer-Integrated Manufacturing*, Vol. 57, 315-328, doi: 10.1016/J.RCIM.2018.12.015.

[9] Jiang, H. (2020). Solving multi-robot picking problem in warehouses: A simulation approach, *International Journal of Simulation Modelling*, Vol. 19, No. 4, 701-712, doi: 10.2507/IJSIMM19-4-CO19.

[10] Fager, P., Calzavara, M., Sgarbossa, F. (2020). Modelling time efficiency of Cobot-supported kit preparation, *International Journal of Advanced Manufacturing Technology*, Vol. 106, 2227-2241, doi: 10.1007/S00170-019-04679-X.
[11] El Zaatari, S., Marei, M., Li, W., Usman, Z. (2019). Cobot programming for collaborative industrial tasks: An overview, *Robotics and Autonomous Systems*, Vol. 116, 162-180, doi: 10.1016/j.robot.2019.03.003.
[12] Vidaković, J., Jerbić, B., Švaco, M., Šuligoj, F., Šekoranja, B. (2017). Position planning for collaborating robots and its application in neurosurgery, *Tehnički Vjesnik – Technical Gazette,* Vol. 24, No. 6, 1705-1711, doi: 10.17559/TV-20170213110534.
[13] Kunpeng, Y., Jiafu, S., Hui, H. (2017). Simulation of collaborative product development knowledge diffusion using a new cellular automata approach, *Advances in Production Engineering & Management*, Vol. 12, No. 3, 265-273, doi: 10.14743/APEM2017.3.257.
[14] Himmelsbach, U.B., Wendt, T.M., Hangst, N., Gawron, P., Stiglmeier, L. (2021). Human–machine differentiation in speed and separation monitoring for improved efficiency in human–robot collaboration, *Sensors*, Vol. 21, No. 21, Article No. 7144, doi: 10.3390/S21217144.
[15] Belić, Ž., Majstorović, V., Đurđanović, D., Kirin, S. (2019). Data driven root cause analyses in multistage manufacturing utilising life cycle wide product information, *Tehnički Vjesnik – Technical Gazette,* Vol. 26, No. 4, 920-926, doi: 10.17559/TV-20170922210328.
[16] Janekova, J., Fabianova, J., Fabian, M. (2019). Assessment of economic efficiency and risk of the project using simulation, *International Journal of Simulation Modelling*, Vol. 18, No. 2, 242-253, doi: 10.2507/IJSIMM18(2)467.
[17] Ojstersek, R., Buchmeister, B., Vujica Herzog, N. (2020). Use of data-driven simulation modeling and visual computing methods for workplace evaluation, *Applied Sciences*, Vol. 10, No. 20, Article No. 7037, doi: 10.3390/APP10207037.
[18] Carvalho Alves, A., Ferreira, A.C., Costa Maia, L., Leão, C.P., Carneiro, P. (2019). A symbiotic relationship between lean production and ergonomics: Insights from industrial engineering final year projects, *International Journal of Industrial Engineering and Management*, Vol. 10, No. 4, 243-256, doi: 10.24867/IJIEM-2019-4-244.
[19] Ojstersek, R., Javernik, A., Buchmeister, B. (2021). The impact of the collaborative workplace on the production system capacity: Simulation modelling vs. real-world application approach, *Advances in Production Engineering & Management*, Vol. 16, No. 4, 431-442, doi: 10.14743/apem2021.4.411.
[20] Tomašević, M., Ralević, N., Stević, Ž., Marković, V., Tešić, Z. (2018). Adaptive fuzzy model for determining quality assessment services in the supply chain, *Tehnički Vjesnik – Technical Gazette,* Vol. 25, No. 6, 1690-1698, doi: 10.17559/TV-20170705130711.
[21] Ojstersek, R., Buchmeister, B. (2020). Simulation modeling approach for collaborative workplaces' assessment in sustainable manufacturing, *Sustainability*, Vol. 12, No. 10, Article No. 4103, doi: 10.3390/SU12104103.
[22] Ojstersek, R., Buchmeister, B., Javernik, A. (2022). The importance of Cobot speed and acceleration on the manufacturing system efficiency, *Procedia Computer Science*, In press.
[23] Zhang, A. ABB's Cobot Portfolio – Customer Presentation, from *https://s.sick.com/at-en-robot-roadshow-2022-documents*, accessed November 15, 2022.
[24] International Federation of Robotics (2020). *Demystifying collaborative industrial robots*, IFR International Federation of Robotics, Frankfurt, Germany.

APEM journal
**Advances in Production Engineering & Management** **ISSN 1854-6250**
Volume 17 | Number 4 | December 2022 | pp 505–513 Journal home: apem-journal.org
https://doi.org/10.14743/apem2022.4.452 Original scientific paper

# Study on scheduling and path planning problems of multi-AGVs based on a heuristic algorithm in intelligent manufacturing workshop

**Wang, Y.J.[a,*], Liu, X.Q.[a], Leng, J.Y.[a], Wang, J.J.[a], Meng, Q.N.[a], Zhou, M.J.[a]**

[a]School of Mechanical Engineering, Dalian Polytechnic University, Dalian, P.R. China
[b]School of Management, Dalian University of Technology, Dalian, P.R. China

**A B S T R A C T**

In order to solve the scheduling and path planning problems of multi-AGVs in an intelligent manufacturing workshop, it is necessary to consider loading, unloading, and transporting the workpiece of each AGV at the same time. A step task scheduling and path optimization mode of AGV is proposed. The process is as follows: Firstly, a mathematical model algorithm and a material transportation task allocation algorithm based on the urgency degree of workpiece processing were established for the optimization objective, and all workpiece transportation task sequences between shelves and processing equipment were assigned to the corresponding AGV to generate the initial feasible path of each AGV. Then, the AGV collision detection and anti-collision algorithm are designed to plan the global collision-free walking path of multi-AGVs in the workshop, and the path can be dynamically adjusted according to the delivery task. The model is solved by a heuristic algorithm ant colony algorithm and MATLAB coding. Finally, an example is given to verify the effectiveness of the method, which can effectively solve the task allocation of multi-AGVs and avoid collision path planning based on the transportation task sequence, and improve the work efficiency of AGV. This research can provide a theoretical basis and practical reference for realizing multi AGVs collaborative scheduling by using AGV automated material transport system in an intelligent production workshop.

**A R T I C L E I N F O**

*Keywords:*
Intelligent manufacturing;
Automated guided vehicle(AGV);
Multi-AGVs;
Task sequence;
Task scheduling;
Path planning;
Heuristic algorithm;
Ant colony algorithm;
MATLAB

**Corresponding author:*
wangyj@dlpu.edu.cn
(Wang, Y.J.)

*Article history:*
Received 25 October 2022
Revised 14 December 2022
Accepted 17 December 2022



## 1. Introduction

With the rapid development of artificial intelligence, the Internet of Things, 5G, and other innovative technologies, the main direction of the future development of China's manufacturing industry is intelligent manufacturing. The digital workshop of intelligent manufacturing is highly integrated with mechanical equipment, sensor equipment, and other hardware, control, data acquisition, and data processing systems. Automated Guided Vehicle (AGV) is applied to intelligent production workshops, and with its high flexibility and stability, it can help the workshop to realize flexible automatic production [1]. Automatic call, information sensing, and production tempo control functions of AGV can improve workshop efficiency. However, How to design An optimization algorithm for AGV workpiece transportation task scheduling in an intelligent manufacturing workshop and plan the route of AGV for workpiece transportation in the workplace, and AGV can accurately and timely execute and complete the production material transport task, it is an urgent problem to be solved in AGV work of intelligent manufacturing workshop.

In the intelligent production workshop based on Manufacturing Execution System (MES), the work of AGV is mainly to load, unload and transport the workpiece, and ensure that the workpiece is delivered to the equipment workbench or the finished workpiece is delivered to the shelf in time, and cooperate with the vehicle equipment to avoid idle mechanical equipment or production delay, and ensure the working efficiency of the equipment. The task scheduling of AGV is aimed at minimizing the total AGV workpiece transportation time, determining the task execution sequence and travel path, and preventing conflicts and collisions in the process of multiple AGVs.

There has been much research on AGV scheduling and path planning. Ma *et al*. [2] applied a tabu search algorithm to solve the vehicle slash-and-drop transportation problem and carried out path planning. Yin *et al*. [3] applied a tabu search algorithm to solve the path planning problem and solved the problem of excessive energy consumption in the process of vehicle movement. Wang *et al*. [4] proposed an improved A* algorithm, which solved the problems of redundant points and unsmooth in path planning. Sun *et al*. [5] proposed a neural network algorithm based on directional constraints, which improved the speed of path planning. Li *et al*. [6] applied BP neural network to study the path planning and obstacle avoidance problems of robots. Corpuz *et al*. [7] proposed an improved neural network to solve the problem of slow convergence speed in intelligent vehicle path planning. Sunet *et al.* [8] solved the problem of complex traps in path navigation based on an adaptive fuzzy neural network. S. Hitam *et al*. [9] applied an improved genetic algorithm to improve the quality of path planning solutions. Li *et al*. [10] integrated AGV environmental safety information into a grid map and applied a genetic algorithm to solve the path planning problem. Mousavi *et al*. [11] applied genetic algorithm and particle swarm optimization algorithm to the AGV task scheduling model. Deepak *et al*. [12] combined decision theory with stochastic time path planning to schedule and control the optimal path under dynamic and uncertain conditions. Yue *et al*. [13] proposed a hybrid PSO-GA algorithm to complete the scheduling and planning problem of AGV. Rugalska [14] proposed a new control strategy for cooperative AGVs, in which two AGVs cooperate to achieve specific task objectives. Antakly[15] *et al.* proposed a task scheduling method based on temporal logic, adding appropriate delay to AGV to avoid collisions between multiple vehicles. Yan *et al.* [16] proposed an algorithm based on co-evolution to conduct scheduling research on AGV. Shi *et al.* [17] proposed a multi-objective scheduling model based on total driving distance and waiting time, and used the A* path planning algorithm to search the shortest path of AGV. Zou *et al.* [18] proposed a multi-objective mixed-integer linear programming model to solve a new automatic guided vehicle scheduling problem with pickup and delivery from the goods handling process in a matrix manufacturing workshop with multi-variety and small-batch production. Yin *et al.* [19] proposed a decentralized framework of multi-task allocation with attention (MTAA) in deep reinforcement learning.

To sum up, most of the literature on AGV path planning focuses on planning AGV anti-collision strategies in static environments with known obstacles, which does not apply to intelligent production workshops where multiple AGVs work together. The scheduling algorithm in the existing literature does not apply to intelligent workshops. AGV is necessary equipment for an intelligent workshop to realize intelligent production, but there is little research literature on AGV path planning and collision prevention in an intelligent workshop. Therefore, the problems of workpiece transportation task allocation, task sequencing, path planning, and collision prevention in the multi-AGV system are studied in the intelligent workshop.

The paper is organized as follows. The AGV scheduling and path optimization framework is constructed in Section 2. AGV Initial feasible path and AGV collision detection and anti-collision algorithm are described in this section. The case analysis and discussion are reported in Section 3. Finally, in Section 4, the conclusions are reported.

## 2. AGV scheduling and path optimization framework

In the actual production process of the workshop, multiple stations are requiring multiple AGVs to transport the workpiece to each station at the same time. It is necessary to allocate the AGV delivery sequence and optimize the AGV delivery path to make the AGV perform the task of the total transport path shorter, at the same time, to complete the delivery of workpieces for all stations or shelves. Because of AGV path planning and task allocation problems, combined with the manufacturing production line process, a step optimization algorithm model is proposed, as shown in Fig. 1.

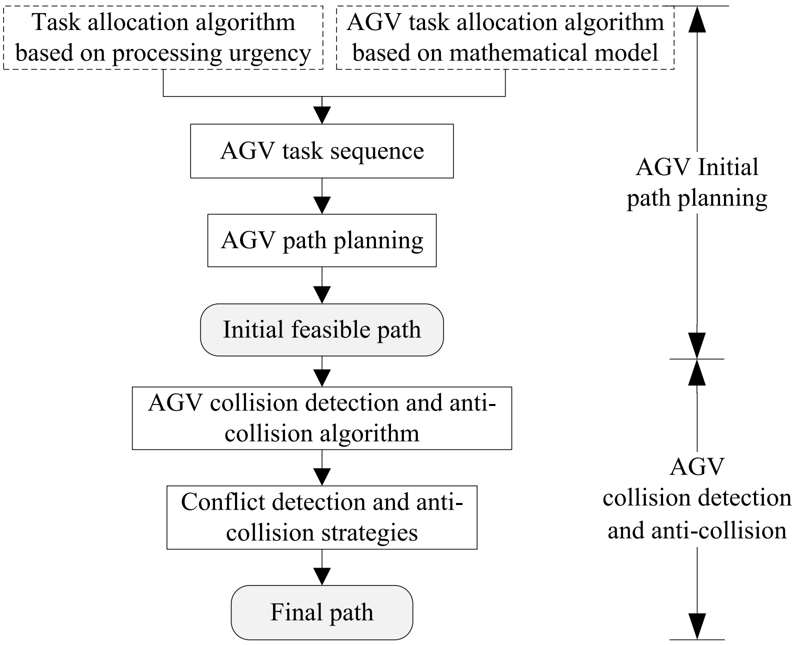


**Fig. 1** AGV scheduling and path step optimization mode

First, using the mathematical model of the algorithm based on minimizing the total delivery time, or the materials transportation task allocation algorithm based on the emergency degree of workpiece processing, all workpiece transport tasks within the planned time between the shelves and the processing equipment shall be assigned to the AGV currently in the idle state according to rules. The current AGV task sequence is dynamically updated, and the initial feasible task transport path for each AGV is generated. Then, the algorithm of AGV collision detection and anti-collision is designed, and the global collision-free walking path of multiple AGVs in the intelligent workshop is planned, and the path can be dynamically adjusted.

### 2.1 AGV initial feasible path

#### 2.1.1 Generation of AGV transportation task sequence

Two algorithms can be used to generate AGV transportation task sequences.

*(1) AGV task allocation algorithm based on time minimization mathematical model*

According to the production plan, the workpiece delivery task is assigned to the appropriate AGV, and the task execution sequence is determined. The mathematical model is established with the goal of the shortest time for the AGV to complete all delivery tasks. The relevant settings and assumptions are as follows:

- All AGVs are the same, and the transport speed is the same and uniform.
- Keep a safe distance during driving, and the waiting time is short and ignored.
- Ignore equipment start time.

- Each AGV can perform one transportation task at a time. Similarly, only one AGV can perform a transportation task.
- No more than two AGVs in each direction on the driving channel to avoid congestion and conflict, and re-plan the route when the capacity exceeds.
- AGV runs along the grid, one grid per second, and the statistical distance is calculated according to the broken line distance travelled
- When the AGV works, it is powered on continuously and will not fail.
- AGV returns to berth after delivery.

The notations used for modelling are described below.

$P$ represents the transportation set of the workpiece to the equipment for processing and is $\{1,2,\dots,n\}$.
$D$ represents the task set of transporting the finished workpiece back to the shelf and is $\{n+1, n+2, \dots, 2n\}$.
$N$ is the set of transporting workpiece, $N = P \cup D$.
$K$ is the set of AGVs, represented as $\{1,2,\dots,m\}$, 0 indicates the docking position.
$A$ is the set of workshop location points, $A = N \cup 0$.
$B_i^k$ and $E_i^k$ are the start time and finish time of AGV $k$, $i \in N, k \in K$.
$(X_i, Y_i)$ represents the position coordinates. The AGV travels one grid per second, so $X_i + Y_i$ can represent the travel time.
$X_{ij}^k$ is the 0-1 variable. When the value is 1, AGV $k$ performs the transport task $i$ and then the task $j$, a value of 0 indicates other cases, $i \in N, j \in N, k \in K$.
$t_i$ is the minimum travel time for task $i$.
$T_{ij}^k$ represents the minimum travel time from the completion position of task $i$ to the start position of task $j$.
$Pt_i$ represents the workpiece processing time.
$e_i$ represents the planned processing time or planned completion time of the workpiece in the production plan.

The mathematical model is constructed to determine the delivery task and execution sequence of AGV.

$$min\, Z = \max_{k \in K, j \in A} E_i^k + (X_i + Y_i) \tag{1}$$

$$\sum_{j \in N} X_{0j}^k = 1, \sum_{i \in N} X_{i0}^k = 1 \qquad \forall k \in K \tag{2}$$

$$\sum_{k \in K} \sum_{j \in A, j \neq i} X_{ij}^k = 1 \qquad \forall i \in N \tag{3}$$

$$\sum_{k \in K} \sum_{i \in A, i \neq j} X_{ij}^k = 1 \qquad \forall j \in N \tag{4}$$

$$E_i^k \geq Z_i^k (B_i^k + t_i) \qquad \forall i \in A, k \in K \tag{5}$$

$$E_i^k \geq e_i \qquad \forall i \in P, k \in K \tag{6}$$

$$B_{n+i}^k \geq E_i^k + Pt_i \qquad i \in P, \forall k \in K \tag{7}$$

$$B_{n+i}^k \geq e_i \qquad \forall i \in D, k \in K \tag{8}$$

$$B_j^k \geq X_{ij}^k (E_i^k + T_{ij}^k) \qquad \forall i, j \in N, k \in K \tag{9}$$

$$X_{ij}^k, Z_{ij}^k \in \{0,1\} \qquad i, j \in A, \forall k \in K \tag{10}$$

$$B_i^k, E_i^k \geq 0 \qquad \forall k \in K, i \in A \tag{11}$$

Eq. 1 is the objective function. The objective is to minimize the maximum AGV transportation time. Others are constraint conditions.

Eq. 2 indicates that AGV starts from the docking position and returns to the docking position after the workpiece arrives. Eqs. 3 and 4 ensure that all delivery tasks are performed. Eqs. 5 and 6 ensure that the execution time of the task is logical, that is, the completion time of task $i$ transporting the workpiece to the machine tool by AGV is later than the sum of the start time and execution time of the task, and cannot be earlier than the planned processing time of the workpiece. In Eqs. 7 and 8, the start time of task $i$ of transporting the finished workpiece to the shelf shall not be earlier than the sum of the processing time and completion time of the task transporting the workpiece to the machine tool, nor shall it be earlier than the planned completion time of the workpiece. Eq. 9 indicates that AGV executes tasks in sequence, and drives to task $j$ by raster after completing task $i$, so the start time of task $j$ cannot be earlier than the time when AGV arrives at the start point of task $j$. Eqs. 10 and 11 represent variable types, which are 0-1 variables and integer variables respectively.

*(2) AGV transportation task assignment based on processing priority*

Aiming at the fastest completion of the workpiece according to the production plan, an AGV task allocation algorithm based on the degree of workpiece processing urgency is proposed. Fig. 2 is the algorithm flow. Based on the workpiece processing plan time and completion time set by the intelligent workshop manufacturing execution system, all delivery tasks are sorted according to the urgency of processing to form the whole task sequence. According to the AGV's idle-as-allotment rule, the workpiece delivery task is assigned to the AGV that has completed the preorder task and is waiting for task assignment, and the task sequence of the AGV is updated. Repeat the above process until all workpiece delivery tasks are assigned to the corresponding AGV, and the task assignment is stopped. Finally, the workpiece delivery task sequence of each AGV is formed.

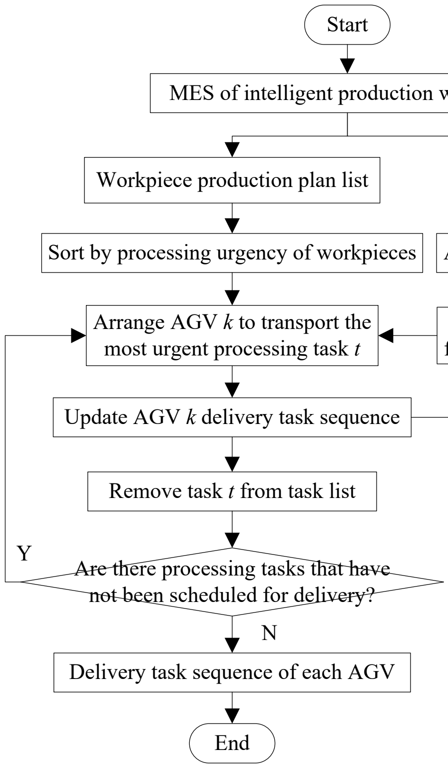


**Fig. 2** AGV transportation task assignment based on processing priority

### 2.1.2 Generation of AGV initial feasible path

In order to facilitate path planning and path expression, the intelligent workshop is rasterized, and each functional area is expressed by grids and coded according to the grid position, as shown in Figure 3. Each grid represents a location node, which can be a device or a driving channel for an AGV or a shelf. The grid in front of the equipment and shelves is the AGV operating station, where the AGV completes the feeding and retaking actions. When the AGV is idle, it stops at the docking position. When the task instruction is received, the AGV will transport the workpiece from the current position to the specified grid position according to the task sequence number, and then carry out the operation of material taking or feeding. The AGV will transport the workpiece in the feasible area of the workshop (grid nodes 1-12 in Fig. 3), and complete the loading, unloading, and transportation of the specified workpiece according to the task sequence. In order to ensure the workshop production process stability, AGV drives in the workspace according to the instructions and follows the principle of driving in the workshop grid channel after the first lateral longitudinal to determine the initial path of AGV to perform each task. According to this path, AGV can reduce the collision probability when driving in the workshop grid channel, and efficiently complete the task of workpiece delivery. Transport such as the current task is to carry a workpiece on shelf 2 to equipment 1 for processing, the initial delivery path of AGV is the grid node 7→8→9→4→3. The AGV picks up the workpiece with the specified number on shelf 2 at the starting node 7, then drives to the end node 3 of the grid according to this path, and puts the workpiece in the designated position in front of the machine of equipment 1. According to the assigned task sequence, each AGV forms the initial transport path of all transport tasks, which is expressed by the grid node number in the sequence.

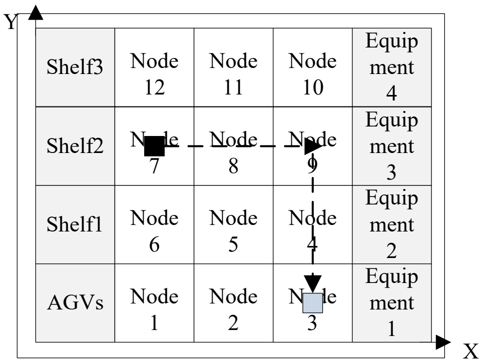


**Fig. 3** Floor plan of raster intelligent production workshop

### 2.2 AGV collision detection and anti-collision algorithm

The purpose of collision detection is to update the initial AGV transport path in real-time so that there are no two AGVs in the same grid position in the workshop AGV driving area. The current grid position and driving time of AGV in the workshop are represented in the form of <position, time>, the variables position and time are non-negative integers. The algorithm of AGV collision detection and anti-collision is shown in Fig. 4.

The heuristic algorithm ant colony algorithm is a probabilistic algorithm used to find the optimal path. It was proposed by Marco Dorigo in his doctoral dissertation in 1992, and its inspiration comes from the behavior of ants in finding a path in the process of searching for food. This algorithm has the characteristics of distributed computing, positive information feedback and heuristic search, and is essentially a heuristic global optimization algorithm in evolutionary algorithms.

The basic idea of applying the ant colony algorithm to solving optimization problems is to use the ant's walking path to represent the feasible solution of the problem to be optimized, and all paths of the entire ant colony constitute the solution space of the problem to be optimized. Ants with short paths release more pheromones. As time goes on, the concentration of pheromones accumulated on the short paths increases gradually, and the number of ants choosing this path also increases. Finally, the whole ant will focus on the best path under the action of positive feedback, and the corresponding is the optimal solution of the problem to be optimized.

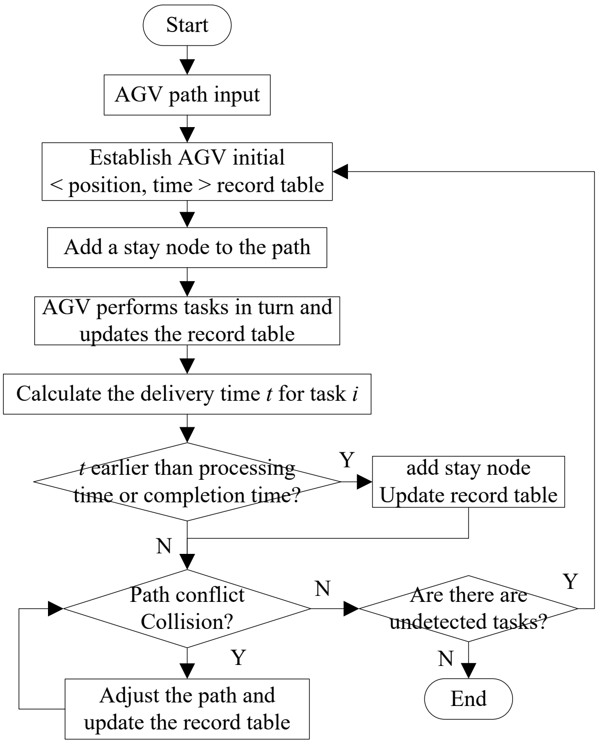


**Fig. 4** AGV collision detection and anti-collision algorithm

## 3. Example verification

The above grid intelligent workshop is still used as the workplace of two AGVs. The model is solved by a heuristic algorithm ant colony algorithm and MATLAB coding. In order to compare the effects of the two task allocation methods in section 2.1, the calculation results are solved and compared respectively, as shown in Table 1. The notation n is the total number of workpiece transportation tasks in the workshop, $p1$ and $p2$ represent the two stages of AGV initial path planning and anti-collision, $t1$ and $t1$ represent the task completion time of each stage, and $d1$ and $d1$ are the corresponding time difference rate. In the AGV initial path generation stage, the total completion time of the AGV initial path calculated by the two task allocation methods is slightly different, and the maximum difference rate is 1.06%. After AGV anti-collision adjustment, the total time calculated by the two scheduling methods is the same.

The operation of multiple AGVs in the intelligent workshop is limited by constraints such as conflict and collision. The completion time of the workpiece transportation task should consider the completion time of the delivery task after constraint detection and path adjustment. In this example, the two scheduling methods have the same results after AGV task scheduling allocation and path step-by-step optimization, which can effectively solve the problem of task scheduling and path planning of multiple AGVs in the workshop, and has good practicability.

To sum up, since multiple AGVs must consider the impact of collision when driving in the same workshop, the actual completion time of the system depends on the delivery time after collision adjustment, that is, the final result of the second stage. For the small-scale example in this paper, the final results of the two methods are consistent, so the two-stage algorithm (time priority) proposed in this paper can effectively solve small-scale problems.

**Table 1** Comparison of calculation results

| $n$ | Minimum time mathematical model | | | Processing urgency | | | Difference rate % | |
|---|---|---|---|---|---|---|---|---|
| | $p1$ | $p2$ | $t1$ | $p1$ | $p2$ | $p2$ | $d1$ | $d2$ |
| 9 | 43 | 52 | 16.68 | 43 | 52 | 6.84 | 0 | 0 |
| 12 | 94 | 96 | 123.57 | 95 | 96 | 9.44 | 1.06 | 0 |
| 15 | 127 | 127 | 34.2 | 127 | 127 | 9.51 | 0 | 0 |
| 18 | 153 | 155 | 216.34 | 154 | 155 | 10.51 | 0.65 | 0 |

## 4. Conclusion

Aiming at the problems of AGV transportation task scheduling and path planning in the intelligent workshop, according to the corresponding mathematical model established to minimize the maximum delivery task completion time and the workpiece processing urgency, the workpiece delivery task sequence of each AGV is determined and the initial delivery path of AGV is generated. Considering conflict prevention and collision avoidance when multiple AGVs are running, conflict detection and anti-collision strategies are proposed. Finally, an example is given to verify the feasibility and effectiveness of multi AGV task allocation and path planning based on transportation task sequence to avoid conflict and collision.

The experiments prove that the multiple collision avoidance strategies proposed in this paper can efficiently complete the delivery tasks according to the production plan while obtaining the collision free path of AGV. In conclusion, this paper schedules the tasks of AGV according to the manufacturing process flow, and plans the path, and avoids collisions of AGV. Finally, the real-time scheduling scheme of the automated material transportation system is obtained, which can provide a reference for intelligent production workshops. In addition, the algorithm proposed in this paper can be extended to other practical application scenarios such as automated terminals and intelligent warehouses using AGV, and has strong practical value. In future research, the non-uniform motion of AGV will be considered.

## Acknowledgment

The research was funded by the Natural Science Foundation of Liaoning province (2019-ZD-0123) and Natural Science Foundation of Liaoning province (No. LJKZ0532).

## References

[1] Li, G., Zeng, B., Liao, W., Li, X., Gao, L. (2018). A new AGV scheduling algorithm based on harmony search for material transfer in a real-world manufacturing system, *Advances in Mechanical Engineering,* Vol. 10, No. 3, Article No. 1687814018765560, doi: 10.1177/1687814018765560.

[2] Ma, H.W., Fan, F.W., Hu, X.X. (2016). Solving the multi-truck and single trailer routing problem based on tabu search algorithm, *Chinese Journal of Management Science,* Vol. 24, No. S1,194-198.

[3] Yin, W.Z., Jiang, W.D., Tao, J. (2017). Strategy of dynamic path planning based on tabu search algorithm for AUV, *Journal of Nanjing University (Natural Sciences),* Vol. 53, No. 1, 144-150.

[4] Wang, Z., Zeng, G., Huang, B., Fang, Z. (2019). Global optimal path planning for robots with improved A * algorithm, *Journal of Computer Applications,* Vol. 39, No. 9, 2517-2522, doi: 10.11772/j.issn.1001-9081.2019020284.

[5] Sun, Y.-B., Yang, H.-Z. (2019). Path planning based on pulse coupled neural networks with directed constraint, *Computer Science,* Vol. 46, No. 11A, 28-32.

[6] Li, W., Sun, J., Chen, W. (2019). Real-time obstacle avoidance algorithm for robots based on BP neural network, *Chinese Journal of Scientific Instrument*, Vol. 40, No. 11, 204-211.

[7] Corpuz, R.S.A. (2019). Characterization of a mobile waste-robot: A heuristic method to path planning using artificial neural networks, *International Journal of Recent Technology and Engineering,* Vol. 8, No. 4, 3902-3910, doi: 10.35940/ijrte.D8324.118419.

[8] Sun, K., Wu, J., Sun, Z., Cao, Z. (2019). Optimal path planning method of marine sailboat based on fuzzy neural network, *Journal of Coastal Research*, Vol. 93, 911-916, doi: 10.2112/SI93-131.1.

[9] Sarkar, R., Barman, D., Chowdhury, N. (2020). Domain knowledge based genetic algorithms for mobile robot path planning having single and multiple targets, *Journal of King Saud University - Computer and Information Sciences,* Vol. 34, No. 7, 4269-4283, doi: 10.1016/j.jksuci.2020.10.010.

[10] Li, T., Ning, P. Niu, P. (2020).Safety path planning of factory AGV based on improved genetic algorithm, *Combined machine tool and automatic processing technology,* Vol. 3, 160-163, doi: 10.13462/j.cnki.mmtamt.2020.03.038.

[11] Mousavi, M., Yap, H.J., Musa, S.N., Tahriri, F., Dawal, S.Z.M. (2017). Multi-objective AGV scheduling in an FMS using a hybrid of genetic algorithm and particle swarm optimization, *Plos One,* Vol. 12, No. 3, Article No. e0169817, doi: 10.1371/journal.pone.0169817.

[12] Subramani, D.N., Lermusiaux, P.F.J. (2019). Risk-optimal path planning in stochastic dynamic environments, *Computer Methods in Applied Mechanics and Engineering*, Vol. 353, 391-415, doi: 10.1016/j.cma.2019.04.033.

[13] Yue, X.-H., Xu, X.-J., Wang, X.-B. (2018). Research on multi AGV scheduling algorithm based on improved hybrid PSO-GA for FMS, *Computer Science,* Vol. 45, No. 11A, 167-171.

[14] Mrugalska, B, Stetter, R. (2019). Health-aware model-predictive control of a cooperative AGV-based production system, *Sensors*, Vol. 19, No. 3, 167-171, doi: 10.3390/s19030532.

[15] Antakly, D., Loiseau, J.J. Abbou, R. (2017). A temporised conflict-free routing policy for AGVs, *IFAC-PapersOnLine,* Vol. 50, No. 1, 11169-11174, doi: 10.1016/j.ifacol.2017.08.1239.

[16] Wang, Y., Jia, Z.-H., Li, K. (2021). A multi-objective co-evolutionary algorithm of scheduling on parallel non-identical batch machines, *Expert Systems with Applications,* Vol. 167, Article No. 114145 doi: 10.1016/j.eswa.2020.114145.

[17] Shi, W., Tang, D.B., Zou, P. (2021). Multi-objective automated guided vehicle scheduling based on MapReduce framework, *Advances in Production Engineering & Management,* Vol. 16, No. 1, 37-46, doi: 10.14743/apem2021.1.383.

[18] Zou, W.-Q., Pan, Q.-K., Wang, L. (2021). An effective multi-objective evolutionary algorithm for solving the AGV scheduling problem with pickup and delivery, *Knowledge-Based Systems*, Vol. 218, Article No. 106881, doi: 10.1016/j.knosys.2021.106881.

[19] Yin, Z., Liu, J., Wang, D. (2022). Multi-AGV task allocation with attention based on deep reinforcement learning, *International Journal of Pattern Recognition and Artificial Intelligence,* Vol. 36, No. 9, Article No. 2252015, doi: 10.1142/S0218001422520152.

## Calendar of events

- 7th International Conference of Computational Methods in Engineering Science, November 24-26, 2022, Zamosc, Poland.
- 14th International Conference on Mechatronics and Manufacturing, February 10-12, 2023, Royal Princess Larn Luang, Bangkok, Thailand.
- 7th International Conference on Material Engineering and Manufacturing, April 7-10, 2023, Chiba University, Japan.
- 51th North American Manufacturing Research Conference, June 12-16, 2023, Rutgers University, New Brunswick, New Jersey, USA.

## Notes for contributors

### General

Articles submitted to the *APEM journal* should be original and unpublished contributions and should not be under consideration for any other publication at the same time. Manuscript should be written in English. Responsibility for the contents of the paper rests upon the authors and not upon the editors or the publisher. The content from published paper in the *APEM journal* may be used under the terms of the Creative Commons Attribution 4.0 International Licence (CC BY 4.0). For most up-to-date information please see the APEM journal homepage *apem-journal.org*.

### Submission of papers

A submission must include the corresponding author's complete name, affiliation, address, phone and fax numbers, and e-mail address. All papers for consideration by *Advances in Production Engineering & Management* should be submitted by e-mail to the journal Editor-in-Chief:

**Miran Brezocnik**, Editor-in-Chief
UNIVERSITY OF MARIBOR
Faculty of Mechanical Engineering
Chair of Production Engineering
Smetanova ulica 17, SI – 2000 Maribor
Slovenia, European Union
E-mail: editor@apem-journal.org

### Manuscript preparation

Manuscript should be prepared in *Microsoft Word 2010* (or higher version) word processor. *Word .docx* format is required. Papers on A4 format, single-spaced, typed in one column, using body text font size of 11 pt, should not exceed 12 pages, including abstract, keywords, body text, figures, tables, acknowledgements (if any), references, and appendices (if any). The title of the paper, authors' names, affiliations and headings of the body text should be in *Calibri* font. Body text, figures and tables captions have to be written in *Cambria* font. Mathematical equations and expressions must be set in *Microsoft Word Equation Editor* and written in *Cambria Math* font. For detail instructions on manuscript preparation please see instruction for authors in the *APEM journal* homepage *apem-journal.org*.

### The review process

Every manuscript submitted for possible publication in the *APEM journal* is first briefly reviewed by the editor for general suitability for the journal. Notification of successful submission is sent. After initial screening, and checking by a special plagiarism detection tool, the manuscript is passed on to at least two referees. A double-blind peer review process ensures the content's validity and relevance. Optionally, authors are invited to suggest up to three well-respected experts in the field discussed in the article who might act as reviewers. The review process can take up to eight weeks on average. Based on the comments of the referees, the editor will take a decision about the paper. The following decisions can be made: accepting the paper, reconsidering the paper after changes, or rejecting the paper. Accepted papers may not be offered elsewhere for publication. The editor may, in some circumstances, vary this process at his discretion.

### Proofs

Proofs will be sent to the corresponding author and should be returned within 3 days of receipt. Corrections should be restricted to typesetting errors and minor changes.

### Offprints

An e-offprint, i.e., a PDF version of the published article, will be sent by e-mail to the corresponding author. Additionally, one complete copy of the journal will be sent free of charge to the corresponding author of the published article.

APEM journal

Advances in Production Engineering & Management

Chair of Production Engineering (CPE)
University of Maribor
APEM homepage: apem-journal.org

Volume 17 | Number 4 | December 2022 | pp 397-516

## Contents



Published by CPE, University of Maribor

ISSN 1854-6250

apem-journal.org